

**Fossil C<sub>4</sub> plant signals in Southeast Atlantic  
Ocean continental margin sediments indicate  
climate-dependent vegetation changes on the  
adjacent continent**

Fossile C<sub>4</sub>-Pflanzensignale in Kontinentalrandsedimenten  
des Südostatlantiks weisen auf klimaabhängige Änderungen in  
der Vegetation auf dem angrenzenden Kontinent hin

Von der  
**Fakultät für Mathematik und Naturwissenschaften**  
der  
**Carl von Ossietzky Universität Oldenburg**  
zur Erlangung des Grades und Titels eines

**Doktors der Naturwissenschaften**

- Dr. rer. nat. -

angenommene  
**Dissertation**

von  
**Florian Rommerskirchen**  
geboren am 30. Mai 1974 in Nordenham

Erstreferent: Prof. Dr. Jürgen Rullkötter  
Korreferent: Prof. Dr. Hans-Jürgen Brumsack  
Korreferent: Prof. Geoffrey Eglinton, FRS

Eingereicht am: 21. Dezember 2005  
Tag der Disputation: 28. Februar 2006

# Contents

**Kurzfassung** (Abstract in German)

**Abstract**

**Contents**

|          |  |           |
|----------|--|-----------|
| <b>1</b> | <b>Introduction</b>  | <b>1</b>  |
| 1.1      | Scope and framework  | 1         |
| 1.2      | C <sub>3</sub> , C <sub>4</sub> and CAM plant characteristics and factors controlling their contribution to the vegetation   | 3         |
| 1.3      | C <sub>3</sub> , C <sub>4</sub> and CAM plant distribution on the southwestern African continent   | 15        |
| 1.4      | Principles of stable carbon isotopic composition of organic plant material, a geochemical tool unravelling the use of the C <sub>3</sub> and C <sub>4</sub> pathways | 17        |
| 1.5      | Motivation, outline and objectives of this project   | 24        |
| 1.6      | Outline of the author's contribution   | 27        |
| <b>2</b> | <b>Chemotaxonomic significance of distribution and stable carbon isotopic composition of long-chain alkanes and alkan-1-ols in C<sub>4</sub> grass waxes</b>         | <b>30</b> |
| 2.1      | Abstract   | 30        |
| 2.2      | Introduction   | 31        |
| 2.3      | Description of sampling area, samples and methods  | 37        |
| 2.3.1    | <i>Description of sampling area: Grass diversity and distribution in southern Africa</i>   | 37        |
| 2.3.2    | <i>Samples</i>   | 38        |
| 2.3.3    | <i>Analytical and evaluation methods</i>   | 41        |

|            |   |           |
|------------|---|-----------|
| <b>2.4</b> | <b>Results</b>  | <b>43</b> |
| 2.4.1      | <i>Contents and carbon number distributions of long-chain n-alkanes of grass waxes</i>  | 43        |
| 2.4.2      | <i>Molecular carbon isotopic signatures of long-chain n-alkanes of grass waxes</i>  | 46        |
| 2.4.3      | <i>Contents and carbon number distributions of long-chain n-alkanols of grass waxes</i>   | 48        |
| 2.4.4      | <i>Molecular carbon isotopic signatures of long-chain n-alkanols of grass waxes</i>   | 49        |
| <b>2.5</b> | <b>Discussion</b>   | <b>49</b> |
| <b>2.6</b> | <b>C<sub>4</sub> grass wax adaptation and implications for palaeoenvironmental studies</b>  | <b>53</b> |
| 2.6.1      | <i>C<sub>4</sub> grass wax adaptation to the climatic conditions of the habitat</i>   | 53        |
| 2.6.2      | <i>Leaf wax n-alkane and n-alkanol homologues as palaeoclimatic proxies</i>   | 55        |
| <b>2.7</b> | <b>Conclusions</b>  | <b>58</b> |
| <b>2.8</b> | <b>Appendix</b>   | <b>59</b> |
| <br>       |   |           |
| <b>3</b>   | <b>A north to south transect of Holocene southeast Atlantic continental margin sediments: Relationship between aerosol transport and compound-specific <math>\delta^{13}\text{C}</math> land plant biomarker and pollen records</b> | <b>65</b> |
| <br>       |   |           |
| 3.1        | <b>Abstract</b>   | <b>65</b> |
| 3.2        | <b>Introduction</b>   | <b>66</b> |
| 3.3        | <b>Materials and methods</b>  | <b>70</b> |
| 3.3.1      | <i>Sediment cores</i>   | 70        |
| 3.3.2      | <i>Mass accumulation rates</i>  | 71        |
| 3.3.3      | <i>Methods for lipid and pollen analysis</i>  | 71        |
| 3.3.4      | <i>Satellite aerosol imaging</i>  | 73        |
| 3.4        | <b>Results and discussion</b>   | <b>73</b> |
| 3.4.1      | <i>Simplified phytogeographical units of southwest Africa</i>   | 73        |
| 3.4.2      | <i>Carbon number distribution and molecular carbon isotopic signatures of long-chain n-alkanes</i>  | 74        |
| 3.4.3      | <i>Carbon number distribution and molecular carbon isotope signatures of long-chain n-alkanols</i>  | 80        |
| 3.4.4      | <i>Pollen distributions</i>   | 83        |
| 3.4.5      | <i>Plant wax components of the transect sediments: biogeochemical and environmental considerations</i>  | 87        |
| 3.4.6      | <i>Synoptic view of the north/south transect: lipid biomarkers and pollen from the African continent</i>  | 94        |
| 3.5        | <b>Conclusions</b>  | <b>95</b> |



|              |   |            |
|--------------|---|------------|
| <b>4</b>     | <b>Glacial/interglacial changes in southern Africa: compound-specific <math>\delta^{13}\text{C}</math> land plant biomarker and pollen records from Southeast Atlantic continental margin sediments</b> | <b>98</b>  |
| <b>4.1</b>   | <b>Abstract</b>   | <b>98</b>  |
| <b>4.2</b>   | <b>Introduction</b>   | <b>99</b>  |
| <b>4.3</b>   | <b>Material and methods</b>   | <b>101</b> |
| <i>4.3.1</i> | <i>Sediment cores</i>   | <i>101</i> |
| <i>4.3.2</i> | <i>Mass accumulation rates</i>  | <i>103</i> |
| <i>4.3.3</i> | <i>Methods for lipid and pollen analysis</i>  | <i>103</i> |
| <b>4.4</b>   | <b>Results</b>  | <b>104</b> |
| <i>4.4.1</i> | <i>Simplified phytogeographical units of southwest Africa</i>   | <i>104</i> |
| <i>4.4.2</i> | <i>Carbon number distributions and molecular carbon isotope signatures of long-chain n-alkanes</i>  | <i>106</i> |
| <i>4.4.3</i> | <i>Carbon number distributions and molecular carbon isotope signatures of long-chain n-alkanols</i>   | <i>112</i> |
| <i>4.4.4</i> | <i>Pollen distributions</i>   | <i>113</i> |
| <b>4.5</b>   | <b>Discussion</b>   | <b>115</b> |
| <i>4.5.1</i> | <i>Temporal and latitudinal changes of aliphatic biomarker distributions and carbon isotope signatures</i>  | <i>115</i> |
| <i>4.5.2</i> | <i>Pollen signals</i>   | <i>120</i> |
| <i>4.5.3</i> | <i>Comparison of biomarker and pollen data</i>  | <i>121</i> |
| <b>4.6</b>   | <b>Conclusions</b>  | <b>125</b> |
| <b>4.7</b>   | <b>Appendix</b>   | <b>127</b> |
| <b>5</b>     | <b>Summary and perspectives</b>   | <b>133</b> |
| <b>6</b>     | <b>References</b>   | <b>138</b> |
| <b>7</b>     | <b>Appendix</b>   | <b>I</b>   |
| <b>7.1</b>   | <b>Supplementary data</b>   | <b>I</b>   |
| <b>7.2</b>   | <b>Photographs</b>  | <b>VI</b>  |

**Acknowledgements (Danksagung)**

**Curriculum vitae (Lebenslauf)**

# Kurzfassung

Die vorliegende Arbeit untersucht die Aussagekraft von langkettigen *n*-Alkanen und *n*-Alkan-1-olen als Paläoumweltbiomarker. Der Schwerpunkt der Analysen liegt auf den Verteilungsmustern und molekularen stabilen Kohlenstoffisotopensignaturen. Es handelt sich hierbei um Proxies, mit denen die klimaabhängigen Änderungen in der Vorherrschaft von C<sub>4</sub>- oder C<sub>3</sub>-Pflanzen in geeigneter Weise nachvollzogen werden können. Gräser (Poaceae) sind eine wichtige Quelle von C<sub>4</sub>-Biomasse in geologischen Archiven sowohl in Böden als auch in lakustrinen und marinen Sedimenten. Auf der ganzen Welt kommen Gräser in Zonen der trocken-subtropischen Grassteppen und Savannen vor, in denen sie sich erfolgreich gegen C<sub>3</sub>-Pflanzen (z.B. C<sub>3</sub>-Gräser, Bäume und Sträucher) durchsetzen. Eine Ausdehnung oder ein Rückzug der grasdominierten Vegetation hängt von den jeweiligen klimatischen Verhältnissen ab. Der geochemische Nachweis der kontinentalen Verbreitung der Grasvegetation aus geologischen Archiven liefert daher wichtige paläoökologische Informationen. Langkettige Blattwachslipide von 35 C<sub>4</sub>-Gräsern und drei C<sub>3</sub>-Gräsern der in Südafrika häufig vorhandenen Arten wurden untersucht. Die analytischen Daten wurden mit der Zugehörigkeit der Gräser zu den drei C<sub>4</sub>-Untertypen (NADP-ME, NAD-ME und PCK) sowie der phylogenetischen Verwandtschaft auf dem Niveau von Unterfamilien verglichen. Die Untersuchungen zeigen, dass sich im Allgemeinen C<sub>4</sub>-Gräser in ihren chemischen Signaturen von den C<sub>3</sub>-Arten durch deutlich höhere molekulare  $\delta^{13}\text{C}$  Werte, hohe Gehalte an *n*-C<sub>31</sub>- und *n*-C<sub>33</sub>-Alkanen und durch die Dominanz des *n*-C<sub>32</sub>-Alkanols unterscheiden. Vor allem die C<sub>4</sub>-Gräser, die zur Unterfamilie Chloridoideae gehören, oder diejenigen, die den NAD-ME- oder PCK-C<sub>4</sub>-Metabolismus nutzen, enthalten länger-kettige Wachshomologe. Diese Arten gedeihen vorzugsweise in Lebensräumen mit besonders trockenen klimatischen Bedingungen. Der Vergleich mit Literaturdaten bestätigt die Befunde.

Die Zuordnung von länger-kettigen Wachshomologen zu C<sub>4</sub>-Pflanzen wurde in südwestafrikanischen Kontinentalrandsedimenten aus neun Bohr- und Kolbenlotkernen auf einem Nord-/Südtransekt vom Kongo-Fächer (4°S) zum Kap-Becken (30°S) überprüft. Vier Zeitscheiben der jüngeren geologischen Geschichte, zwei Glazial- (MIS 2 und 6a) und zwei Interglazialstadien (MIS 1 und 5e), wurden untersucht. An den südlichen Lokationen wird vor allem durch die Atmosphäre transportiertes partikuläres Material eingetragen. Dieses Material stammt vom westlichen und zentralen südafrikanischen Hinterland, das von Wüsten, Halbwüsten und Savannen dominiert wird. Diese Gebiete sind reich an organischem Material von C<sub>4</sub>-Pflanzen. Die nördlichen Positionen des Transekts erhalten im Wesentlichen terrestrisches Material aus dem Kongo-Becken und dem Angola-Hochland, die durch C<sub>3</sub>-Pflanzen beherrscht werden. Hinsichtlich der Glazial/Interglazial-Unterschiede in den phytogeografischen Hauptzonen des angrenzenden Kontinents wurden die Signaturen von langkettigen *n*-Alkanen und *n*-Alkanolen mit den Konzentrationen und Verteilungen von Pollentaxa in den gleichen Sedimenten korreliert. Breitengradabhängig erhöhen sich im Transekt in Richtung Süden die molekularen  $\delta^{13}\text{C}$ -Werte. Diese Tendenz wird von einer Verlagerung der Verteilungsmustermaxima zu länger-kettigen Homologen und einem höheren Anteil von C<sub>4</sub>-Pollen in allen Zeitscheiben begleitet. Lediglich die durchschnittliche Kettenlänge (ACL) der *n*-Alkanole folgt diesem Trend nicht. Die *n*-Alkanolsignaturen stammen mutmaßlich von unterschiedlichen Organismen wie C<sub>3</sub>-, C<sub>4</sub>- und CAM-Pflanzen sowie der Flora und Fauna des Meeres. C<sub>4</sub>-Anteilsabschätzungen, die auf dem gewichteten Mittel der  $\delta^{13}\text{C}$ -Werte von *n*-Alkanen und *n*-Alkanolen basieren, stimmen mit denen der Pollenzählungen überein. Glazial/Interglazial-Änderungen sind durch eine deutliche Verschiebung zu höheren C<sub>4</sub>-Anteilen während der Glazialstadien im nördlichen Bereich des Transekts gekennzeichnet. Dies lässt die Schlussfolgerungen zu, dass sich offene grasartige Vegetation nordwärts verschob und sich Wüsten und Halbwüsten vergrößerten. Südwärts verringert sich der Glazial/Interglazial-Unterschied bis er schließlich unbedeutend wird. An den beiden südlichsten Lokationen deuten ein geringerer Anteil von Graspollen und ein höherer Anteil von C<sub>3</sub>-Pollen während der Glazialstadien auf eine nordwärts gerichtete Verschiebung der südlichen Winterregenvegetation (hauptsächlich C<sub>3</sub>- und CAM-Pflanzen) hin. Die Ergebnisse dieser Studie zeigen, dass die Kombination von Pollendaten und

molekularen geochemischen Proxies effektiv auf die Rekonstruktion von kontinentalen phytogeografischen Entwicklungen angewendet werden kann.

# Abstract

This thesis elucidates the significance of long-chain *n*-alkanes and *n*-alkan-1-ols as palaeoenvironmental indicators. Special emphasis is placed on the distribution patterns and molecular stable carbon isotopic signatures of these biomarkers, because they appear to be suitable proxies to trace climate dependent changes in the predominance of C<sub>4</sub> or C<sub>3</sub> land plants. Grasses (Poaceae) are an important source of C<sub>4</sub> biomass in the geological record of soils as well as lacustrine and marine sediments. Grasses are found across the world in broad latitudinal belts in dry subtropical grasslands and savannas, where the C<sub>4</sub> species successfully outcompete C<sub>3</sub> plants (e.g. C<sub>3</sub> grasses, trees and shrubs). An extension or regression of grassy vegetation depends on the climatic conditions. Thus, the fossil record of indicators of subtropical grass holds important ecological information related to continental vegetation in the geological past. Long-chain leaf wax lipids of 35 C<sub>4</sub> grasses and three C<sub>3</sub> grasses of abundant species in southern Africa were analysed and their molecular signatures compared to the physiological classification in three C<sub>4</sub> subtypes (NADP-ME, NAD-ME and PCK) and phylogenetic systematics of these plants on a subfamily level. These investigations revealed that C<sub>4</sub> grass waxes are distinguishable from those of C<sub>3</sub> species by significantly higher compound-specific  $\delta^{13}\text{C}$  values, high contents of *n*-C<sub>31</sub> and *n*-C<sub>33</sub> alkanes and the abundance of the *n*-C<sub>32</sub> alkanol, which is largely absent in C<sub>3</sub> grasses. Especially species of the subfamily Chloridoideae or of species using the NAD-ME or PCK C<sub>4</sub> metabolism exhibit longer-chain wax homologues. These species preferably thrive in habitats of extremely arid climatic conditions. Comparison with published data substantiated these findings.

The specificity of long-chain aliphatic wax components in C<sub>4</sub> plants for palaeoenvironmental assessment was determined by investigating Southwest African continental margin sediments from nine drill and piston cores on a North to South transect from the Congo Fan (4°S) to the Cape Basin (30°S). Four time slices of the recent geological history were investigated representing two glacial (MIS 2 and 6a) and two interglacial stages (MIS 1 and 5e). Airborne particulate material was deposited in significant amounts at the southern oceanic sampling locations. This material is rich in organic matter from C<sub>4</sub> plants, because it is derived from the western and central southern African hinterland dominated by deserts, semi-deserts and savanna regions. The northern sites of the transect get most of their terrestrial material from the Congo Basin and the Angola highlands dominated by C<sub>3</sub> plants. Signatures of long-chain *n*-alkanes and *n*-alkanols were correlated with those of pollen taxa in the same sediments concerning glacial/interglacial changes in major phytogeographic zones on the adjacent continent. Latitudinal trends southwards in the transect exhibited higher molecular  $\delta^{13}\text{C}$  values accompanied by a shift in the distribution pattern maxima of the wax components to longer-chain homologues and more C<sub>4</sub> pollen contribution in all time slices. Only the average chain length (ACL) of the *n*-alkanols did not follow this trend. The *n*-alkanol signatures appear to be comprised of assemblages from different organisms, i.e. C<sub>3</sub>, C<sub>4</sub> and CAM plants as well as marine biota. C<sub>4</sub> proportion estimates based on weighted mean  $\delta^{13}\text{C}$  values for *n*-alkanes and *n*-alkanols paralleled each other and those afforded by pollen counts. Glacial/interglacial changes were characterised by a significant shift to a higher contribution of C<sub>4</sub> plants in the northern part of the transect during glacial stages. It can be inferred that open grass-rich vegetation shifted northwards and desert and semi-desert areas expanded. Further to the South, the glacial/interglacial differences decrease until they become insignificant. At the two southernmost sites less Poaceae pollen and a higher contribution of C<sub>3</sub> pollen during glacial stages suggest a northward shift of the winter rain vegetation (mostly C<sub>3</sub> and CAM plants). The results of the study demonstrate that this combination of pollen data and compound-specific geochemical proxies can be effectively applied in the reconstruction of past continental phytogeographic developments.

# 1 Introduction

## 1.1 Scope and framework

The largest fluxes of the global carbon cycle are those that link atmospheric carbon dioxide ( $\text{CO}_2$ ) to land vegetation and to the ocean. Continental vegetation plays an important role in the primary production of organic carbon in the world. Primary production varies widely over the land surface. Deserts and continental ice masses have little or no net production, whereas tropical rainforests show an annual production, which ranges between 1000 and 3500  $\text{g C m}^{-2}$  and is, thus, much higher than the oceanic highly productive areas like continental shelf upwelling zones (200 to 1000  $\text{g C m}^{-2}$ ; Whittaker, 1975). Savannas and grasslands are widespread ecosystems which also have major impacts on the carbon cycle (primary production: 200 to 2000  $\text{g C m}^{-2}$ ; Whittaker, 1975; Schlesinger, 1997). Generally, the distribution of major continental vegetation zones is closely linked to global and regional climate conditions, which vary geographically as well as with geological time. For example, the spreading of grasslands as a function of climatic changes in the earth history is especially favoured by decreasing temperatures and increasing aridity and seasonality (Jacobs et al., 1999).

Climate-dependent vegetation changes can be monitored by plant-specific organic signatures, such as microscopically recognisable spores, pollen and various kinds of plant fragments as well as geochemical fossils (biomarkers), i.e. lipids in geological samples which are related to biogenic precursors. The ocean is an important sink of terrigenous organic matter transported offshore by rivers and winds and preserves a continuous record of geographic and secular changes of continental climate and vegetation in its sediments. Preservation of organic material in continental margin sediments is supported by an increase in upwelling-induced marine production and, thereby, the development of an oxygen minimum zone beneath the oceanic high-productivity areas. Furthermore, high sedimentation rates and shallow water depths enhance lipid preservation in sediments. Thus, marine sediments contain a geological archive of the terrestrial and marine biosphere.

The most recent geological past, i.e. the Quaternary covering the last 2.5 million years, is characterised by the periodic build-up of major continental ice sheets in the northern

and southern hemispheres due to recurring global climatic variations. Imbrie et al. (1984) detected climatic variations termed marine oxygen isotopic stages (MIS) by analysing the carbonate remnants of planktonic foraminifera. High and low isotopic  $^{18}\text{O}/^{16}\text{O}$  ratios revealed periodical cycles, which are linked to the ice sheet volume. They are indicators of the global nature of climatic variations and can be used as a dating tool. Odd-numbered stages represent warm periods (interglacials) and even-numbered stages cold periods (glacials). The occurrence of these periodical changes between glacial and interglacial periods has a 100 kyr cyclicity during the Late Quaternary which can be explained by astronomical variations in the Earth's orbit, changing the incoming solar radiation (Milankovitch, 1930). The variations are related to the eccentricity of the Earth's elliptical orbit around the sun. The short axis of this ellipse varies over time, changing the mean distance between Earth and Sun. Therefore, the insolation changes by eccentricity variations have a symmetrical global impact and equally affect all latitudes (Berger, 1978). Low-latitude regions are very sensitive to these changes since the differences in solar heating drive variations in the seasonal atmospheric circulation. The biosphere responds to these cycles by increasing or decreasing the size of certain biomes (distinctive plant and animal communities) during the climatic cycles. Glacial/interglacial cycles initiate climatic variations in precipitation and temperature as well as  $\text{CO}_2$  concentrations in the atmosphere, which govern the distribution of the major vegetation zones. For example, in low latitudes (today's tropical areas) the colder glacials are characterised by a more arid climate as well as lower  $\text{CO}_2$  concentrations. It is thought that these conditions led to an expansion of biomes, such as grasslands and savannas, which are generally adapted to dryer climates (e.g. Anhuf, 1997; Ehleringer et al., 1997; Collatz et al., 1998; Partridge et al., 1999; Ray and Adams, 2001).

Classification of vegetation zones into functional groups for reconstruction of past vegetation changes is a goal of this study. Distinguishing these groups is important for palaeoclimatic assessments or the development of vegetation models. The majority of palaeo-vegetation studies are primarily focussed on reconstructions inferred from fossil pollen assemblages. Some aspects of vegetation may not be registered in those records. The main targets of this study are subtropical grasses ( $\text{C}_4$  grasses), which cannot be easily distinguished from grasses in temperate regions ( $\text{C}_3$  grasses) by pollen analysis. Especially the geographical distribution of  $\text{C}_4$  grasses holds important ecological information. Recognition of the subtropical grass distribution in the geological past is an important step forward for the palaeoclimate research in terms of palaeoenvironmental reconstructions. Their distinct metabolic pathways allow separation of these two types of grasses by means of stable carbon isotopes, thus providing a powerful tool to reconstruct the ecotones of  $\text{C}_3$  and  $\text{C}_4$  vegetation (Schwartz et al., 1986). This project elucidates geographical changes during glacial/interglacial cycles in subtropical to tropical major

vegetation zones of southern Africa by using distribution patterns and compound-specific isotopic compositions of land plant biomarker together with pollen records. For that purpose, two glacial times, the Last Glacial Maximum (LGM; MIS 2, 26-13 ka before present, BP) and the penultimate glacial (MIS 6, 190-129 ka BP), as well as two interglacial times, the Holocene (MIS 1, 13-0 ka BP) and the penultimate interglacial (MIS 5, 129-70 ka BP), were evaluated for land plant signatures in marine sediments.

## 1.2 C<sub>3</sub>, C<sub>4</sub> and CAM plant characteristics and factors controlling their contribution to the vegetation

### *C<sub>3</sub> photosynthetic mechanism*

In general, plants can be divided into distinctive physiological groups according to the CO<sub>2</sub> fixation pathway which occurs in the chlorophyll-bearing leaf cells of plants. The majority of higher plant species (about 85 to 90%; according to Sage, 2001, 2004) use the photosynthetic pathway, which fixes CO<sub>2</sub> during all-day open stomata into a three carbon atom molecular storage product, phosphoglycerate (usually referred to as PGA), by using the enzyme ribulose biphosphate carboxykinase/oxygenase (RuBisCO; Leegood, 1999a; Sage et al., 1999a). Hence, these plants use the so-called C<sub>3</sub> photosynthetic pathway (cf. Fig. 1.1a) which in textbooks is often referred to as the Benson-Calvin cycle. Besides aquatic photosynthetic organisms, most higher land plants utilise this method of carbon fixation, e.g. almost all trees and shrubs, most herbs as well as generally grasses preferring wet, cool growing seasons.

It is generally assumed that the C<sub>3</sub> pathway is the oldest way of photosynthesis among higher plants since their advent some 450 million years ago occurred at a time of relatively high concentrations of atmospheric CO<sub>2</sub> (Sage 1999, 2004). In the long course of Earth's history, there were also periods when the environmental conditions for C<sub>3</sub> plants were less favourable. For example, relatively high oxygen (O<sub>2</sub>) concentrations like in the Carboniferous around 360 to 286 million years BP (Berner, 1993) and in the past 35 million years cause photorespiration in green plants. Photorespiration is an energy-wasting process by which CO<sub>2</sub> assimilation is inhibited by O<sub>2</sub> and CO<sub>2</sub> is re-released. This process originates in the bifunctional nature of RuBisCO and the generation of glycolate biphosphate in the oxygenase reaction of ribulose biphosphate (RuBP; Leegood, 1999a). The rate of photorespiration is promoted by an increase in temperature and irradiance and by an increase in the O<sub>2</sub>/CO<sub>2</sub> ratio. Up to 40% of newly fixed carbon

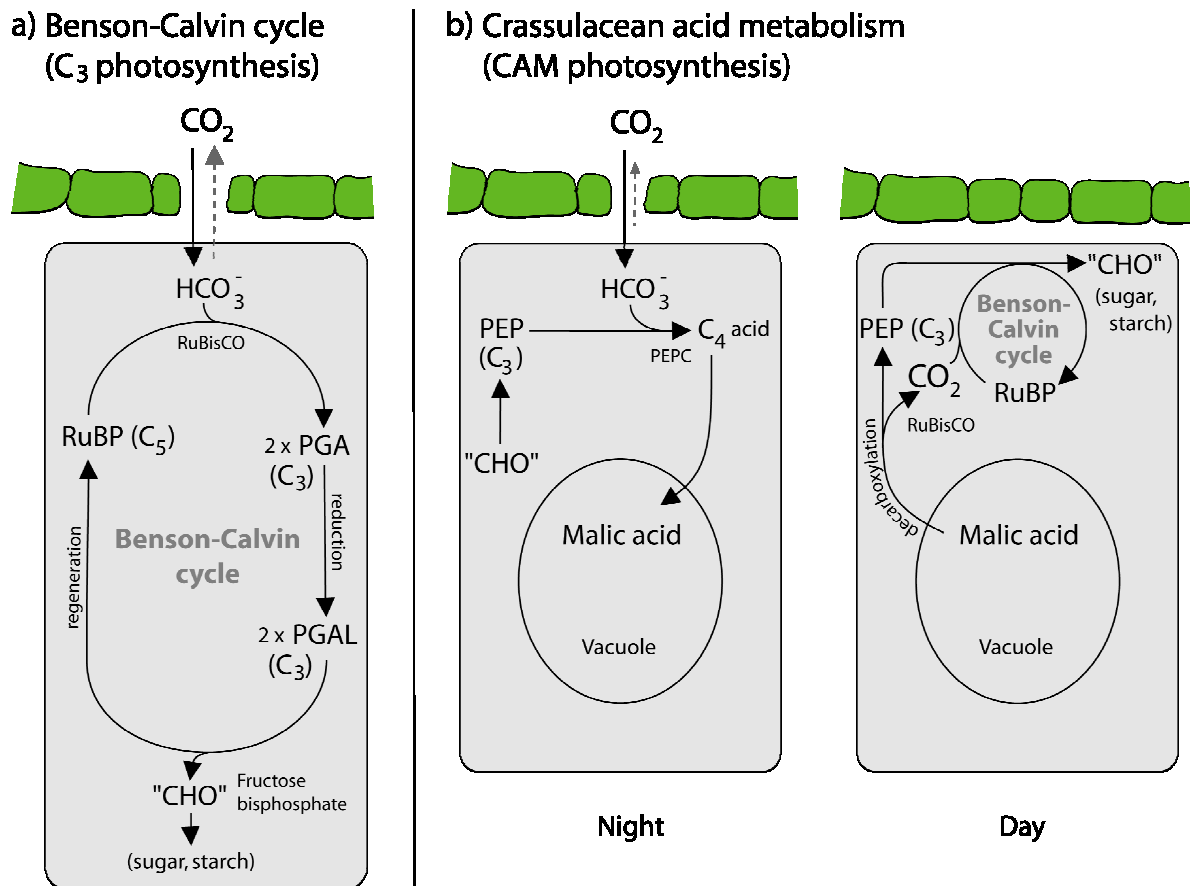


**Fig. 1.1.** a) Simplified scheme of the Benson-Calvin cycle (C<sub>3</sub> photosynthesis) and b) of the Crassulacean acid metabolism (CAM photosynthesis) according to Libbert (1991) and Leegood (1999a; 1999b). The Benson-Calvin cycle can be divided into three phases: (1) carboxylation catalysed by RuBisCO, (2) reductive phase by which PGA is converted into PGAL, and (3) regeneration of the CO<sub>2</sub> acceptor RuBP. The CAM photosynthesis shows the temporal separation of assimilation of CO<sub>2</sub> by PEPC prior to fixation in the Benson-Calvin cycle. Nocturnal CO<sub>2</sub> assimilation leads to malate storage in the vacuols. During the day, malate is decarboxylated to provide CO<sub>2</sub> for fixation in the Benson-Calvin cycle.

may be re-released as CO<sub>2</sub> under environmental conditions of high light intensity and high temperatures like in tropical and subtropical climates, or at the low atmospheric concentration of CO<sub>2</sub> in the past. To counteract the loss of CO<sub>2</sub> under these conditions, C<sub>3</sub> plants operate with widely open stomata which dramatically lower the water use efficiency (WUE) by evaporation loss.

### *CAM photosynthetic mechanism*

A significant part of plant evolution was the development of mechanisms for inhibiting photorespiration by concentrating CO<sub>2</sub> around RuBisCO. One of these mechanisms is the oldest alternative way to photosynthesis following the C<sub>3</sub> pathway, the Crassulacean acid mechanism (CAM), which is named after the plant family in which this physiological system was first observed. The use of a dual carboxylation pathway, i.e. initial CO<sub>2</sub> fixation



with phosphoenolpyruvate carboxylase (commonly referred to as PEPC) and then by RuBisCO, is separated temporally in the same tissue (Fig. 1.1b; Leegood 1999b; Keeley and Rundel, 2003). Stomata are open at night to take in and fix CO<sub>2</sub> using PEPC. The CO<sub>2</sub> is temporarily stored subcellularly in the vacuole, primarily as malic acid (Fig. 1.1b). During the day, closure of stomata in terrestrial plants reduces water loss to a minimum and inhibits CO<sub>2</sub> leakage due to the prevented photorespiration. It results in an internal carbon deficit which is overcome by decarboxylation of the stored malic acid. The process concentrates CO<sub>2</sub> around RuBisCO resulting in daytime internal inorganic carbon levels two to 60 times ambient levels (Lüttge, 2002) before the CO<sub>2</sub> enters the subsequent Benson-Calvin cycle (Fig. 1.1b). However, if the stored acid is used up at daytime, the stomata open to use fresh CO<sub>2</sub> in the normal C<sub>3</sub> pathway.

The CAM pathway is rather uncommon in the plant kingdom. It is used by only 20,000 to 30,000 species of the estimated 250,000 land plant species (according to Sage, 2001, 2004) and specifically by highly specialised plants adapted to survive in extreme conditions. These plants often experience periods of drought with extreme water shortage during the day. They have particular morphological features such as large vacuoles for carbon and water storage, which give the tissues a succulent appearance. However, this adaptation is an expensive process. Compared to CAM plants the C<sub>3</sub> plants just let CO<sub>2</sub> diffuse to the RuBisCO enzyme. Many CAM plants grow slowly and can become very old. The CAM mechanism is best known from modern-day desert succulents but also many epiphytes, like bromeliads and orchids. As a curiosity, some submerged aquatic plants have been found to use this pathway. Typical dry-subtropical vegetation consists of xerophytic (adapted to dry conditions) shrubs and CAM plants.

### *C<sub>4</sub> photosynthetic mechanism*

The other mechanism for inhibiting photorespiration by concentrating CO<sub>2</sub> around RuBisCO is the Hatch-Slack cycle, in which CO<sub>2</sub> is initially fixed in a C<sub>4</sub> acid (Hatch and Slack, 1966). This mechanism is often referred to as the C<sub>4</sub> photosynthetic pathway. The C<sub>4</sub> photosynthesis is fundamentally different from the more common C<sub>3</sub> pathway: first, CO<sub>2</sub> is actively fixed by a light-regulated PEPC instead of RuBisCO, like in CAM plants. Unlike in CAM plants, PEPC in C<sub>4</sub> plants is active in the light. Stomata are less open during the day. CO<sub>2</sub> is fixed preliminarily in the form of a dicarboxylic C<sub>4</sub> acid, oxaloacetate (OA), which can be converted into aspartate and/or malate. C<sub>4</sub> plants create an internal pool of C<sub>4</sub> acid which releases CO<sub>2</sub> inside the bundle sheath tissue, where RuBisCO is located which in turn supplies the CO<sub>2</sub> to the subsequent Benson-Calvin cycle (Fig. 1.2). C<sub>4</sub> plants

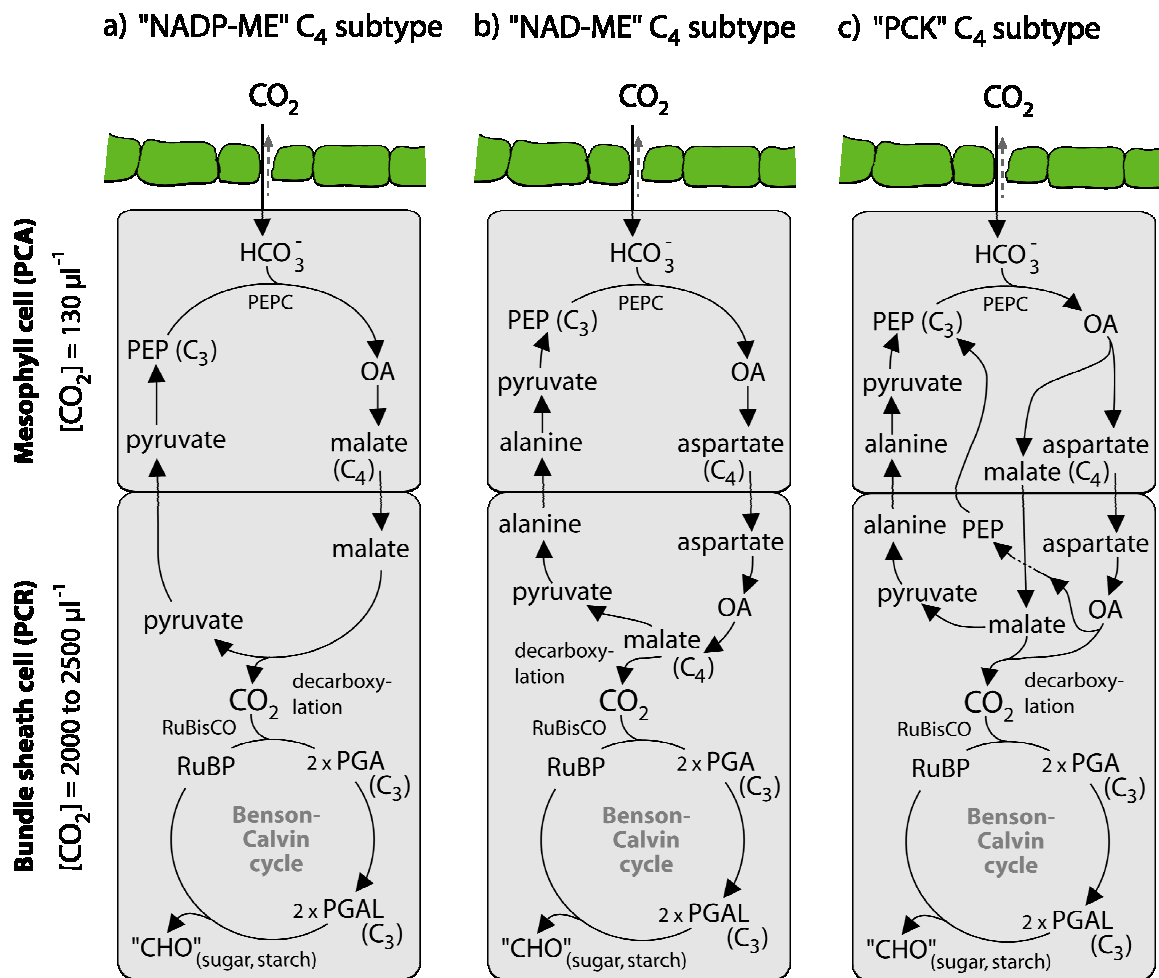


**Fig. 1.2.** Simplified pathways of the three carbon dioxide assimilation variations of the Hatch-Slack cycle ( $C_4$  photosynthesis): a) "NADP-ME", b) "NAD-ME", and c) "PCK"; according to Hatch et al. (1975), Hattersley (1987) and Leegood (1999b). Generally, atmospheric  $CO_2$  is initially fixed inside leaf mesophyll cells in a reaction catalysed by PEPC. The resulting  $C_4$  acids are decarboxylated inside the bundle sheath cells, providing a source of  $CO_2$  for RuBisCO and the normal Benson-Calvin cycle. Values of the  $CO_2$  concentration inside the bundle sheaths and the leaf mesophyll cells are from Ehleringer et al. (1991).

have a strategy which is different from that of the specialised CAM plants, in which the two processes are separated in time allowing the plant to minimise daytime water loss due to evaporation. The  $C_4$  pathway involves a separation in space. The leaf tissue is divided into two separated specialised compartments, the photosynthetic assimilation in the mesophyll cells (PCA) and the adjacent photosynthetic reduction tissue of thick-walled bundle sheaths which surround the vascular bundles (PCR; Laetsch, 1969). This is called the "Kranz" anatomy (the german word "Kranz" means wreath) and can be found in almost all  $C_4$  plants. The designation "Kranz" and non-"Kranz" is thus synonymous with  $C_4$  and  $C_3$ /CAM. Due to this space separation in photosynthesis,  $C_4$  plants are able to control the supply of  $CO_2$  to the RuBisCO enzyme without interference by the competing  $O_2$ . Furthermore, the  $CO_2$  concentrating mechanism leads to a 10- to 20-fold higher  $CO_2$  concentration around RuBisCO than in the mesophyll cell (Fig. 1.2; Ehleringer et al.,

1991). This prevents photorespiration and evaporation and results in a high WUE in growth areas of high temperature, high irradiance, limited water supply and low atmospheric CO<sub>2</sub> concentration (Björkmann, 1976; Ehleringer et al., 1997; Collatz et al., 1998; Winslow et al., 2003; Sage, 2004).

It is believed that the physiological adaptation of the C<sub>4</sub> mechanism evolved independently many times within the last 7 to 30 million years in response to a decline in concentration of CO<sub>2</sub>. This led to its distribution among a wide range of phylogenetically unrelated plants. The C<sub>4</sub> mechanism is predominantly found in tropical grasses, followed by sedges and dicotyledons (Kellogg, 1999; Leegood 1999b; Sage et al., 1999b; Giussani et al., 2001; Sage, 2001; Keeley and Rundel, 2003; Sage, 2004). Three different C<sub>4</sub> subgroups evolved which possess enzymes responsible for decarboxylation of the internal carbon pool: (1) Those using the nicotinamide adenine dinucleotide phosphate malate dehydrogenase enzyme (NADP-ME; malate as CO<sub>2</sub> supplier), (2) those using the nicotinamide adenine dinucleotide malate dehydrogenase enzyme (NAD-ME; aspartate), and (3) those using the phosphoenolpyruvate carboxykinase enzyme (PCK; aspartate; Hatch et al., 1975). In Fig. 1.2a-c these different mechanisms are shown in a simplified manner, and it is clear that the biochemistry of these three C<sub>4</sub> subtypes is quite different. The “Kranz” leaf morphology typical for C<sub>4</sub> plants is slightly different in all of the three C<sub>4</sub> subtypes, and it is thus possible to identify the subtypes by investigating the leaf morphology (Dengler and Nelson, 1999). It is of interest to note that the subtypes occupy

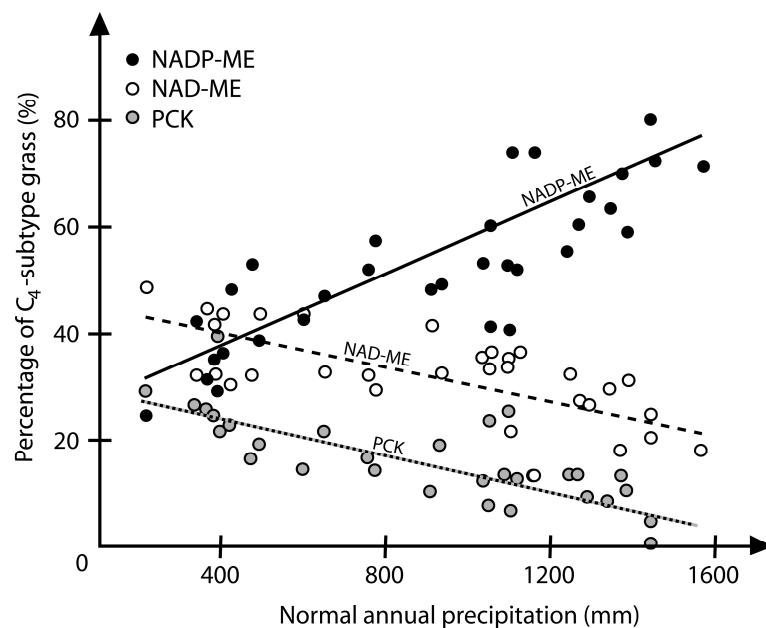


**Fig. 1.3.** Relationship between annual precipitation and the percentage of the C<sub>4</sub> grass flora that uses the NAD-ME, NADP-ME, and PCK biochemical variations of C<sub>4</sub> photosynthesis for 32 sites in the USA (after Taub, 2000).

different ecological niches and that the distribution of different  $C_4$  grasses holds important climatic information. For example, in subtropical and tropical grasslands, there is a consistent transition from a dominance of PCK- and NAD-ME-type grasses in drier regions to mainly NADP-ME-type grasses in regions of higher precipitation (cf. Fig. 1.3; Vogel et al., 1978; Schulze et al., 1996; Taub, 2000).

### *Factors controlling $C_4$ versus $C_3$ contribution to the vegetation*

Compared to CAM plants, generally, the  $C_4$  plants are not represented in a high species number (about 7,500 to 10,000 species, or about 3% of the approx. 250,000 land plant species; Sage 2004). However, their environmental importance across the world is great because they provide the principal vegetation cover of the tropical and subtropical areas. This is due to several advantages over the more widespread  $C_3$  pathway. Most  $C_4$  plants are confined to warm climates, where they are more efficient than  $C_3$  grasses. However, the strategy of  $C_4$  plants is not like that of CAM plants to merely survive in niches where  $C_3$  plants cannot thrive. Their strategy is to grow and out-compete  $C_3$  plants in places where the climate is warm enough to give them an advantage over the  $C_3$  plants. In Fig. 1.4a-d it is shown that the response to temperature,  $CO_2$  as well as  $O_2$  concentration, and light is different in  $C_3$  and  $C_4$  plants. In  $C_3$  plants, the quantum yield of  $CO_2$  uptake in normal air falls as the temperature rises (Fig. 1.4a). In contrast, the cost of fixing  $CO_2$  in a  $C_4$  plant remains constant in relation to changes in temperature and  $CO_2$  concentration (cf. Fig. 1.4a and b). In the absence of possible photorespiration (at low  $O_2$  concentration in the air) and at low light,  $C_3$  plants are more efficient than  $C_4$  plants and exhibit the same constancy in the  $CO_2$  uptake (cf. Fig. 1.4a and b). With respect to light intensity  $C_3$  and  $C_4$  species perform photosynthesis at nearly the same rate at low illumination (Fig. 1.4c). With increasing light intensity both photosynthetic types increase their photosynthesis rate, but rates for the  $C_4$  species are higher than for the  $C_3$  species at full light intensity (Björkman and Berry, 1973; Björkman, 1976).  $CO_2$  assimilation has an optimum at 20-30°C in  $C_3$  leaves and at 30-40°C in  $C_4$  leaves (Fig. 1.4d). However, the temperature dependency of  $C_3$  photosynthesis is a function of the concentration of  $CO_2$  or  $O_2$  which increases or suppresses photorespiration, just as the light intensity dependence is altered. At high concentration of  $CO_2$  the temperature response of a  $C_3$  leaf becomes similar to that of a  $C_4$  leaf and the decline in carbon uptake in a  $C_3$  leaf can be attributed to an accelerated rate of photorespiratory loss (Leegood, 1999b).

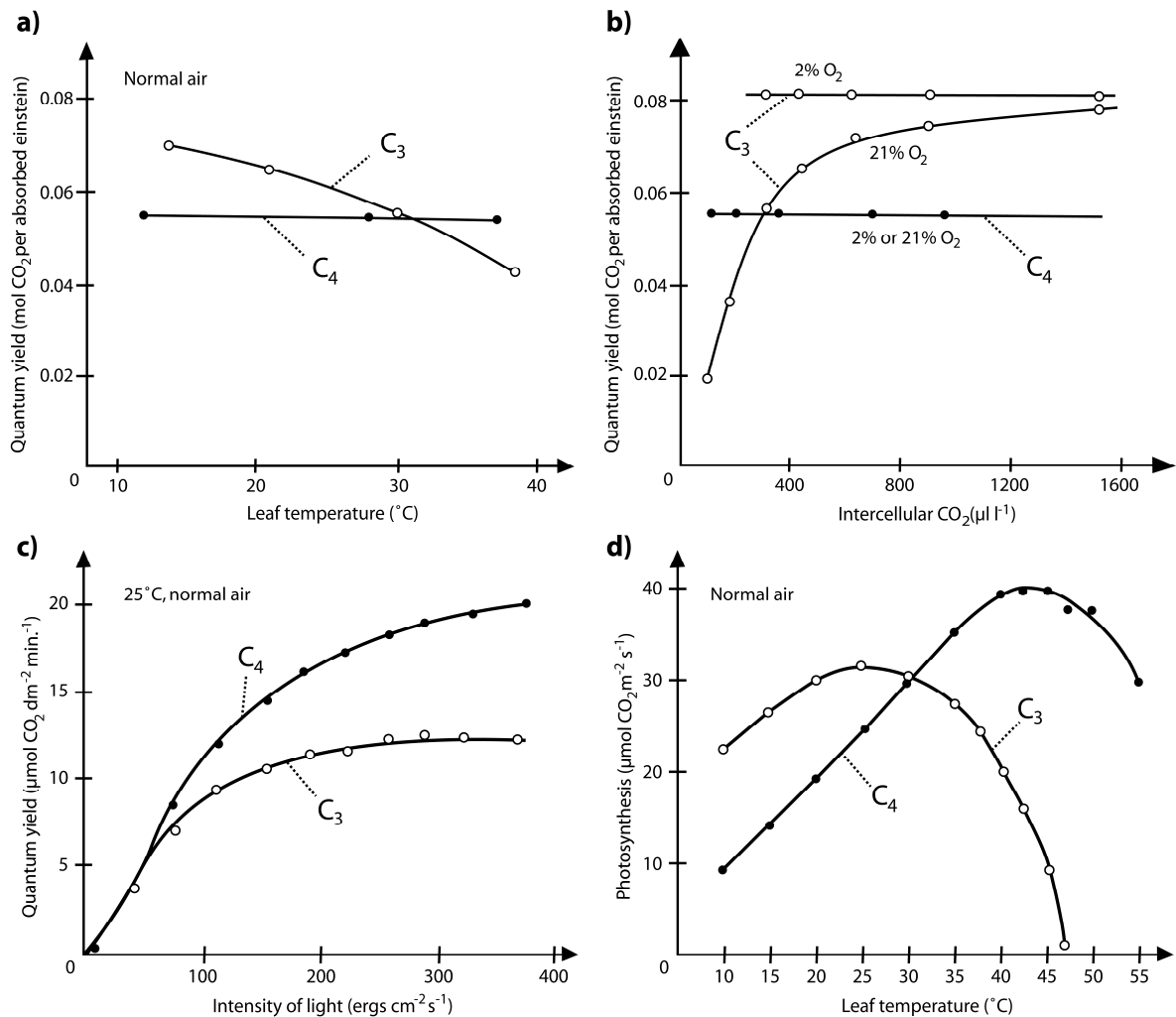


**Fig. 1.4.** The diagrams show the quantum yield for net CO<sub>2</sub> uptake of *Encelia californica* (C<sub>3</sub>) and *Atriplex rosea* (C<sub>4</sub>) as a function of a) temperature in the air, b) CO<sub>2</sub> and O<sub>2</sub> concentration (after Osmond et al., 1980), c) the quantum yield of the closely related plants *Atriplex patula* (C<sub>3</sub>) and *Atriplex rosea* (C<sub>4</sub>) as a function of light intensity (after Björkman and Berry, 1973), and d) the temperature dependence of photosynthesis in the prairie grasses *Agropyron smithii* (C<sub>3</sub>) and *Bouteloua gracilis* (C<sub>4</sub>; after Edwards et al., 1985).

The C<sub>4</sub> plants can significantly reduce photorespiration by their typical “CO<sub>2</sub> concentrating mechanism”. They are more efficient than C<sub>3</sub> plants in open, sunny habitats, but if the light is dimmed by the shade of other plants or by clouds, the superiority of one species over the other would be insignificant. The C<sub>4</sub> plants are superior photosynthesisers under combined circumstances of intense solar radiation and high temperature characteristic of an arid habitat on clear warm days. As a consequence, C<sub>4</sub> plants also have a higher WUE allowing them to grow in climates with low precipitation or in slightly saline environments. However, improved WUE is sometimes over-interpreted and leads to the erroneous conclusion that C<sub>4</sub> plants thrive in arid environments. C<sub>4</sub> plants have no morphological modification to avoid water loss like CAM plants. An illustrative example for the fact that the occurrence of C<sub>4</sub> plants does not necessarily mean aridity are the tropical sedges such as the C<sub>4</sub> plant *Cyperus papyrus* (papyrus), which grows in

tropical Africa and is a swamp plant (Jones, 1987). It can dominate African swamps because the high temperatures enable C<sub>4</sub> Cyperaceae to perform better than their C<sub>3</sub> relatives. In fact, the C<sub>4</sub> type is more common among monocotyledons than among dicotyledons, and it is thought that the C<sub>4</sub> photosynthesis is limited to angiosperms. 79% of all C<sub>4</sub> plant species are monocotyledons, most of them being grasses (about 60% of all C<sub>4</sub> species; Sage, 2001, 2004). For example, competing C<sub>3</sub> and C<sub>4</sub> grasses occurring in grasslands have two distinct growing seasons: C<sub>3</sub> grasses mostly grow in cooler, moist months whereas the C<sub>4</sub> grasses grow in hotter, dryer months (Williams, 1974; Winslow et al., 2003). In temperate latitudes, C<sub>3</sub> grasses start growing early and have sole access to the water stored in the soil from melting snow and spring rain. C<sub>4</sub> grasses start later when temperatures are higher, and both grasses will have access to the available water, predominantly from rainfall. Finally, when temperatures increase, C<sub>3</sub> grasses undergo senescence so that C<sub>4</sub> grasses will have sole access to the available water from rainfall (Winslow et al., 2003). Ehleringer et al. (1997) and Collatz et al. (1998) developed an ecophysiological model equation (Equation 1.1) depending on atmospheric CO<sub>2</sub> partial pressure ( $p\text{CO}_2$ ). The model predicts the temperature at which C<sub>4</sub> monocotyledons and dicotyledons start to gain importance at the expense of C<sub>3</sub> plants (Fig. 1.5).

$$T_{50\%} = \frac{10}{\ln Q_{10}} \cdot \ln \left( \frac{pO_2}{p s_{25}} \cdot \frac{1 + 0.5 \cdot \frac{\alpha_{C_3}}{\alpha_{C_4}}}{\frac{\alpha_{C_3}}{\alpha_{C_4}} - 1} \right) + 25$$

#### Equation 1.1

$T_{50\%}$ : Crossover temperature

$Q_{10}$ : Relative change in  $s_{25}$  due to 10°C temperature change

$p_i$ : Internal leaf partial CO<sub>2</sub> pressure

$pO_2$ : Partial atmospheric O<sub>2</sub> pressure

$s_{25}$ : Specificity of RuBisCO for CO<sub>2</sub> relative to O<sub>2</sub> at 25°C

$\alpha_{C_3}$ : Intrinsic quantum efficiency of C<sub>3</sub>

$\alpha_{C_4}$ : Intrinsic quantum efficiency of C<sub>4</sub>

For more details see Collatz et al. (1998)

$T_{50\%}$  mathematically describes the crossover temperature at which both C<sub>3</sub> and C<sub>4</sub> plant types are equally important at a defined  $p\text{CO}_2$  level and the transition of C<sub>3</sub>- to C<sub>4</sub>-favoured vegetation occurs. The  $p\text{CO}_2$  at the site of fixation during active C<sub>3</sub> photosynthesis due to diffusion across stomata, intercellular air space, cell wall, and membranes, is always lower than the ambient atmospheric  $p\text{CO}_2$  (Collatz et al., 1998). At current  $p\text{CO}_2$  and 25°C, the maximum rate of net CO<sub>2</sub> fixation by C<sub>3</sub> plants is only about 20% of the maximum capacity of RuBisCO in leaves, and about 20% of the photosynthetic light reaction products are used for the unproductive photorespiration reaction (Laing et al., 1974; Collatz et al., 1977). Therefore C<sub>3</sub> plants are less competitive relative to C<sub>4</sub> plants at low atmospheric  $p\text{CO}_2$ . C<sub>4</sub> plants will be able to dominate over the C<sub>3</sub> species except for colder

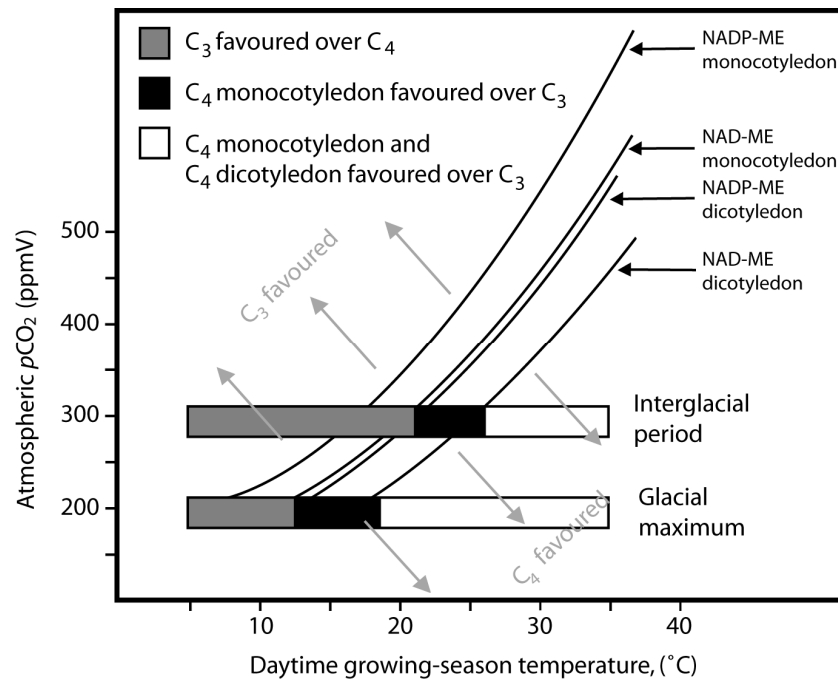


**Fig. 1.5.** Predicted superiority of favoured C<sub>3</sub> plants and C<sub>4</sub> plants (monocotyledons and dicotyledons) as a function of temperature and atmospheric pCO<sub>2</sub> (after Ehleringer et al., 1997 and Collatz et al., 1998). The modeled crossover temperatures (after Equation 1.1) are displayed, at which the quantum yield for CO<sub>2</sub> uptake is equal for C<sub>3</sub> plants and for the respective C<sub>4</sub> plant type (lines). The conditions for both monocotyledons and dicotyledons are shown for NADP-ME C<sub>4</sub> plants (upper boundaries) and NADP-ME C<sub>4</sub> plants (lower boundaries). Atmospheric CO<sub>2</sub> concentrations are also displayed as values for glacial maximum (lower bar) and interglacial periods (upper bar; values after Jouzel et al., 1987).

areas where, under current pCO<sub>2</sub> conditions, C<sub>4</sub> grasses have only minor importance compared to C<sub>3</sub> species (cf. Fig. 1.5). Collatz et al. (1998) successfully predicted that today's global C<sub>4</sub> plant distribution is determined by temperature. In areas where growing season temperature exceeds 22°C, C<sub>4</sub> monocots (mainly grasses) dominate over C<sub>3</sub> plants (Fig. 1.5).

Ehleringer et al. (1997) used this model to demonstrate that the evolution of C<sub>4</sub> grasslands was coupled to a gradual decline in atmospheric CO<sub>2</sub> during the Palaeogene (65.5 to 1.8 million years BP). Thus, this model is also competent to explain vegetation changes in the younger Earth history, e.g. in the Pleistocene (1.8 million years BP to 11.5 kyr BP) and the Holocene (11.5 kyr BP to present). These geological times are characterised by an alternation between glacial and interglacials. The ice core record from many cores shows that glacial maximum CO<sub>2</sub> concentrations were between 180 and 200 ppmV during glacial periods and reached 270 to 290 ppmV during interglacial periods (Jouzel et al., 1987; Neftel et al., 1988; Leuenberger et al., 1992; Petit et al., 1999). Numerous sites in the world also provide evidence for a more extensive distribution of C<sub>4</sub> ecosystems (especially grasslands) in glacial periods than in the recent interglacial period (e.g. Street-Perrott and Perrott, 1993; Jolly and Haxeltine, 1997; Street-Perrott et al.,

1997). Thus, lowered atmospheric  $p\text{CO}_2$  levels in glacials may have resulted in the appearance of  $\text{C}_4$ -dominated grasslands (Cerling et al., 1993, 1997; Ehleringer et al., 1997). BIOME3 and BIOME4 models (Prentice et al., 1992; Haxeltine and Prentice, 1996, 2003) show that under lower atmospheric  $p\text{CO}_2$  global vegetation patterns change. In a single simulation of BIOME3 Jolly and Haxeltin (1997) showed that in tropical Africa, at high elevation, scrub vegetation replaces montane forests when  $p\text{CO}_2$  is reduced. A  $\text{C}_4$  grassland was also simulated, when both  $p\text{CO}_2$  and precipitation were reduced.

Although there is no doubt that  $\text{C}_4$  plants occupy ecological niches, such as areas with drier climatic conditions, the main factor controlling their distribution is temperature, which in turn is a function of atmospheric  $\text{CO}_2$ . The model of Ehleringer et al. (1997) and Collatz et al. (1998) is able to predict the distribution of  $\text{C}_4$  plants (especially tropical grasses) in time and space. Usually,  $\text{C}_4$  grasses are always more effective under warm conditions than  $\text{C}_3$  grasses. Principally, the productivity of grasses is determined by light and water. Grasses are extraordinarily versatile. They have an enormous significance of biotic factors in moderating the competitiveness and relaxing the influence of climate as a controlling factor (Clayton and Renvoiz, 1986). They are found in places world-wide, where a marked seasonality in the rainfall provides adequate moisture during limited growing seasons. In dry places, the shallow-rooted grasses, especially those species using the  $\text{C}_4$  pathway, receive sufficient moisture to grow which leads to a dominance of grasslands and savannas. Under current  $p\text{CO}_2$  most of the  $\text{C}_4$  grasses are found in places where, during the growing season, average monthly temperatures exceed  $22^\circ\text{C}$  and rainfall is more than 25 mm per month (Ehleringer et al., 1997; Collatz et al., 1998). However, in terms of vegetation dynamics, not only grasses and herbs should be taken into account. A forest which is dominated by  $\text{C}_3$  trees will shade  $\text{C}_4$  grassland no matter how prolific and remove the advantage the  $\text{C}_4$  plant might have in full light. Thus, a far more important issue in terms of competition is light.

Several simple models have been developed that describe today's environmental conditions defining and limiting global terrestrial ecosystems. For example, one of the earliest models (Whittaker, 1975) used annual rainfall patterns and annual temperatures (Fig. 1.6a). Generally, six major physiognomic types were described: forest, grassland, woodland (small trees, generally in open spacing), shrubland (dominated by shrubs above 50%), semidesert scrubland (semiarid communities with shrub and other plants forming a sparse vegetation cover), and desert (plant cover very sparse, often much below 10%). Each of the six types occurs in a wide range of environments. In Whittaker's (1975) model savannas are described as subtropical grasslands, with or without scattered trees or shrubs. However, commonly they are described as biomes with continuous



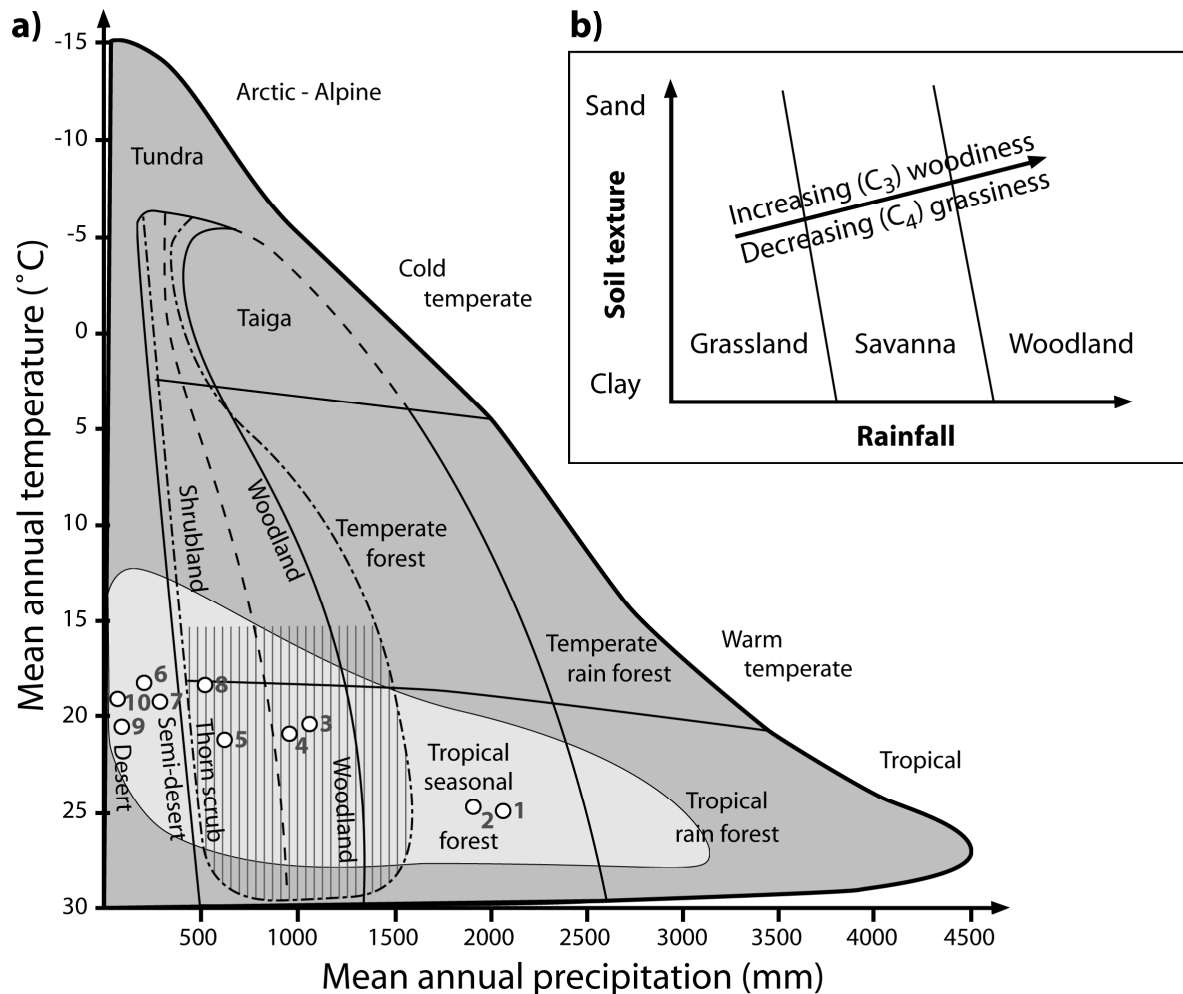


**Fig. 1.6.** a) Pattern of world major terrestrial biome types in relation to climatic rainfall gradients and temperature (modified from Whittaker, 1975). Boundaries between types are approximate. Humid and arid climates, maritime versus continental climates, soil effects, herbivore activity, and fire effects can shift the balance between woodland, shrubland, and grassland. The dot-and-dash line encloses a wide range of environments in which either grassland, or one of the vegetation types dominated by woody plants, may form the prevailing vegetation. Tropical savannas and grassland are displayed in the hatched area. Numbers and white dots refer to mean annual data of climatograms of stations in southwest Africa presented in Fig. 1.7 (page 16) from North (1) to South (10; cf. appendix, Chapter 7, Table 7.1, page I). The light-grey area represents the southwest African continental variation in mean annual temperature and precipitation (according to data of climatograms presented by Walter et al., 1975). b) Modified Walter/Walker model of southwest African tropical savanna vegetation showing the transition from grassy to woody vegetation, which depends on soil texture and rainfall abundance (after Walker and Noy-Meir, 1982).

grass strata and discontinuous tree or shrub strata, whereas grasslands are separated from the savanna biome and represent the opposite of forest (Huntley and Walker, 1982; Bourliere, 1983; Werner, 1991). Savannas represent a transition biome which occurs in climates too dry for forest. Soil conditions or fire, or both, rather than climate cause their appearance also in less arid to temperate climates. Tropical savannas are replaced by woodlands and forests at higher rainfall regimes, by thorn-scrublands and desert at lower rainfall regimes (cf. hatched area in Fig. 1.6a). In areas where the amount of rainfall would normally lead to the development of woodlands, high grazing activity of herbivores and

fires control seedling establishment and prevent savanna from evolving into woodland (Norton-Griffiths, 1979; Gillon, 1983; Frost and Robertson, 1987; Bond and van Wilgen, 1996; Bond, et al., 2003). Tree dominated tropical rainforest occurs in the humid and warm tropics where rainfall is abundant and well distributed over the year. Trees are often tall (up to 30 to 40 m) and of numerous species.

Not only climatic factors like temperature and precipitation limit vegetation types. Also edaphic characteristics, soil moisture and available nutrients govern the vegetation type. For example, an essential aspect of a savanna is the alternating wet and dry soil phase. The soil moisture dynamics vary with depth. The upper layers, to which grass roots are restricted, dry out first. The lower layers, sometime in weathered broken bedrock, remain above the wilting point much longer and are accessible by woody vegetation roots only. A simple regional model for the transition biomes between deserts and forests is the Walter/Walker model (Fig. 1.6b). Walter (1971) identified rainfall as the major factor governing savanna physiognomy in African savannas. His description of savanna function was developed and expanded into a series of models by Walker et al. (1981) and Walker and Noy-Meir (1982). The simplest model is based on two environmental gradients, rainfall and soil texture (Fig. 1.6b). In low-rainfall areas only grass species received sufficient moisture to grow and grasslands dominate. In higher-rainfall areas water percolates to lower soil horizons, allowing the more deeply rooted trees to survive periods of drought. Trees and grasses coexist in a typical savanna vegetation. Woodlands dominate in areas of high rainfall since soil moisture is sufficient to support a closed canopy, which shade out the grasses (cf. Fig. 1.6b). The proportion of trees and grasses is inherently unstable, and small changes in climate or land-use practice can lead to rapid changes in biomass and soil properties. Increasing ( $C_3$ ) woodiness is associated with increasing rainfall and with the possibility for water-storing in deeper soil layers. Hence, the distribution of  $C_4$  grasses holds important ecological information in the tropics.

Overall, based on the knowledge of distribution of the photosynthesis types within plant species, the environmental conditions determine the type of photosynthesis preferred by plants and the representation of  $C_3$  and  $C_4$  plants in typical ecosystems across the world. The  $C_3$  versus  $C_4$  competition may be simplified and reduced to a two-component ecosystem valid in tropical and subtropical environments: tree- and shrub- dominated vegetation is mainly  $C_3$  vegetation, and grass-dominated vegetation is mainly  $C_4$  vegetation.

### 1.3 C<sub>3</sub>, C<sub>4</sub> and CAM plant distribution on the southwestern African continent

Today's climatic conditions as well as edaphic characteristics lead to a vegetation of southern Africa which ranges from equatorial lowland rain forest, dry forests, woodlands and savannas to grasslands and deserts as well as finally to Afroalpine vegetation as represented in Figure 1.7 in a simplified way (cf. biomes in the light grey area of Fig. 1.6). The climatic gradients govern the distribution of C<sub>3</sub> versus C<sub>4</sub> (and CAM) plant contribution to the vegetation. Figure 1.7 displays a few climatograms which present a decrease in annual precipitation from North to South, accompanied by a decrease in annual temperatures. The southern African climate is mainly influenced by a subtropical high-pressure system, which controls the air mass along the southwestern African coast. The cold oceanic upwelling water, induced by the wind-regulated "Ekman-Drift" at western oceanic continental margins (Shannon and Nelson, 1996; Lutjeharms and Meeuwis, 1987; Lutjeharms and Stockton, 1987), reduces the evaporation and causes a temperature reversal, which reduces the convection and leads to a decrease in precipitation in the coastal zones. Fogs, which originate from the sea surface of the cold upwelling waters, inhibit a landward moisture transport in the air masses. Based on these climatic conditions the world's oldest desert, the Namib Desert, evolved 55 million years ago. It extends in a strip along the African west coast (exceeding 2000 km in length; cf. Fig. 1.7; Lancaster, 1984). The northern boundary of the Namib Desert is accompanied by the northernmost upwelling area of the ocean (cf. Fig. 1.7). Eastwards of the Namib Desert, in the African hinterland with a height above 1000 m, the vegetation is mainly represented by a transition from grasslands and savannas to dry woodlands and forests. These are the largest biomes in southern Africa. The woody species are C<sub>3</sub> and the grass species mostly C<sub>4</sub> plants. They are found in a climatic zone, which exhibits an increase in annual precipitation from 100 mm to over 1000 mm. Southwards, an inactive system of shifting sand dunes is covered by grass-, scrub-, and woodland (dry savanna). This area, the Kalahari-Plateau, has an annual precipitation of 250 mm to 500 mm (Fig. 1.7). Further south, the Succulent and Nama Karoo semi-deserts exhibit thorn-bush and scrub vegetation, which is bordered by the southernmost Cape Fynbos vegetation zone (White, 1993; Cowling et al., 1997). The semi-desert and desert regions are dominated by C<sub>4</sub> plants (grasses and weeds), but CAM plants are also abundant. The Succulent Karoo is rich in CAM plants but poor in C<sub>4</sub> plants. C<sub>4</sub> plants are also almost absent

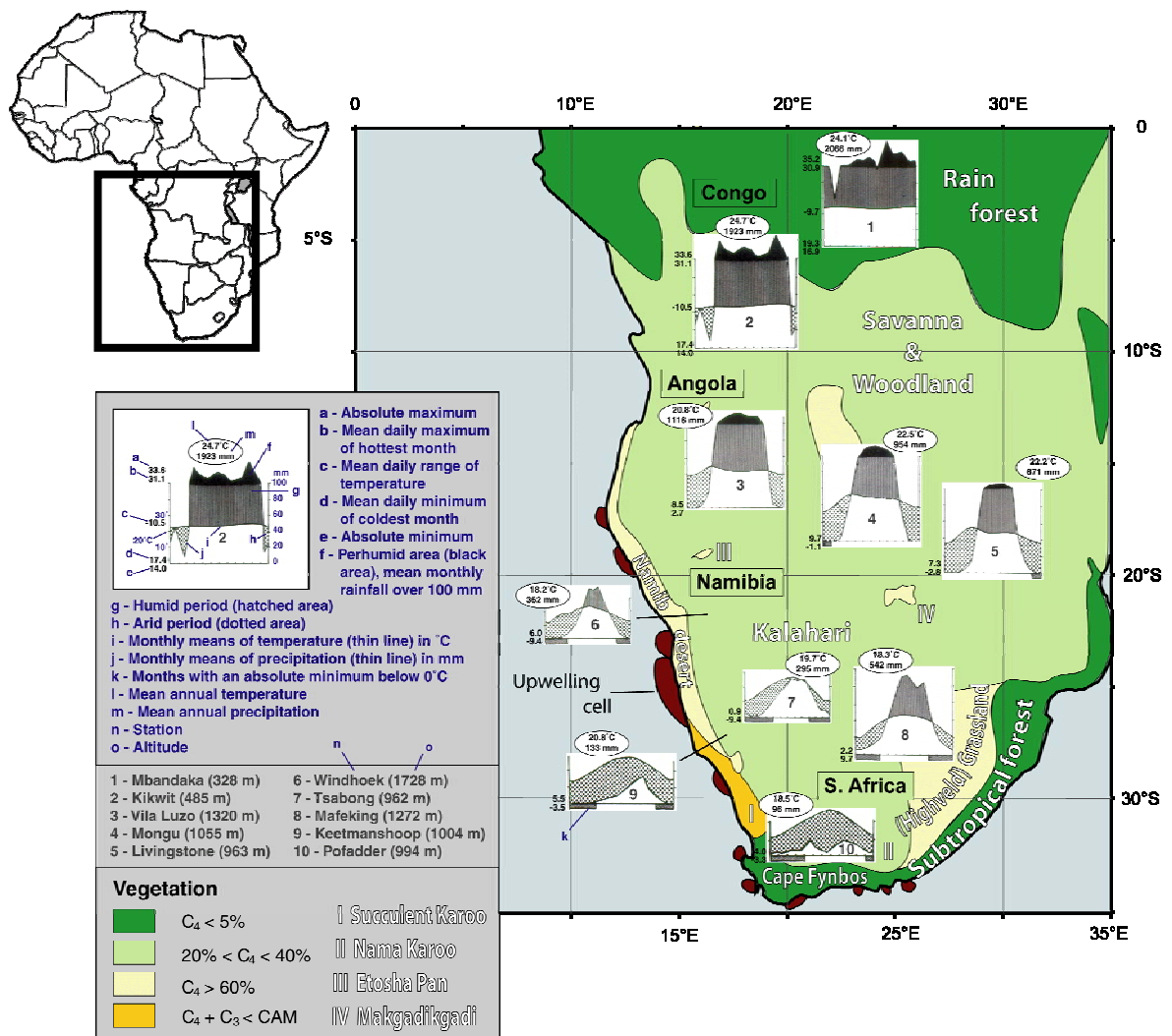


**Fig. 1.7.** Climatic classification and simplified phytogeographical units of today in southwest Africa (continental colour codes according to C<sub>4</sub> plant occurrence). Also shown are main upwelling cells along the southwest African coast (dark red areas; according to Shannon and Nelson, 1996). The figure is based on a broad brush assessment of the distribution of C<sub>3</sub>, C<sub>4</sub> and CAM plants by using maps of White (1983), Cowling et al. (1997) and of the satellite images of the Africa Land Cover Characteristics Database 2.0 (Loveland et al., 2000; <http://edcdaac.usgs.gov>) as well as lists of C<sub>4</sub> plants of Downton (1975), Raghavendra and Das (1978), Elmore and Paul (1983), and Smith and Winter (1996). Climatograms are according to Walter and Lieth (1960-1967) and Walter et al. (1975). For more details see White (1983) and Chapter 3.

in the winter rainfall area of Cape Fynbos. The only regions, where C<sub>3</sub> plants are abundant, are Cape Fynbos, the southeastern coastal subtropical forest as well as the equatorial rainforest and its adjacent biomes. In equatorial swamp forest and lowland rainforest, C<sub>4</sub> plants form a small minority. The C<sub>4</sub> contribution is fairly high in swamp regions without closed canopy (e.g. *Cyperus papyrus*; Fig. 1.7; White, 1983).

## 1.4 Principles of stable carbon isotopic composition of organic plant material, a geochemical tool unravelling the use of the C<sub>3</sub> and C<sub>4</sub> pathways

Various proxies have been used in palaeoenvironmental studies to deduce relative contributions of C<sub>3</sub> and C<sub>4</sub> land plant material to the sediments. Palynological analyses can determine the contribution of grass pollen and pollen of woody plants, and are thus useful to distinguish between tree- or grass-dominated vegetation, but are not suited to clearly differentiate between C<sub>3</sub> and C<sub>4</sub> grasses (Moore et al., 1991). Grass phytoliths (biogene opaline silica bodies present in plant cells) can be identified at a more precise taxonomic level than grass pollen, relating them to subfamilies with specific environmental requirements, including C<sub>3</sub> and C<sub>4</sub> types (McLean and Scott, 1999). Phytoliths are usually better preserved in sediments and soils than pollen. On the other hand, phytoliths are not very suitable for biomass estimation, since they are almost entirely limited to grass species. There are strong differences in the phytolith production among grasses (Fredlund and Tieszen, 1997). Geochemically the stable carbon isotopic ratio is the most widely accepted tool to determine the C<sub>3</sub> or C<sub>4</sub> pathway of biogenic organic matter in sediments.

The carbon component of most naturally occurring carbon-containing materials exhibit 98.9% of <sup>12</sup>C, 1.1% of <sup>13</sup>C and about 10<sup>-10</sup>% of the unstable radionuclide <sup>14</sup>C. The ratio of the stable isotopes <sup>13</sup>C over <sup>12</sup>C in atmospheric CO<sub>2</sub> has been rather constant over time since the formation of the earth. This ratio, thus, is a powerful tracer for geoscientists, who can study geological processes using <sup>13</sup>C as a natural label. The <sup>13</sup>C/<sup>12</sup>C ratios are measured with isotope ratio mass spectrometers. The stable carbon isotopic composition is expressed as delta values (δ<sup>13</sup>C; Equation 1.2) in units of per mil (‰) relative to the Vienna-“Pee Dee Belemnite” standard (V-PDB, refers to the Pee Dee carbonate formation in North America).

$$\delta^{13}\text{C} = \left( \frac{\left( \frac{^{13}\text{C}}{^{12}\text{C}} \right)_{\text{sample}}}{\left( \frac{^{13}\text{C}}{^{12}\text{C}} \right)_{\text{V-PDB}}} - 1 \right) \cdot 1000 \text{ (‰)} \quad \text{Equation 1.2}$$

Chemically <sup>13</sup>C and <sup>12</sup>C are indistinguishable, but the physical difference in atomic radii causes reactions or processes to require slightly more energy if a <sup>13</sup>C atom is involved, which will behave slightly different from <sup>12</sup>C. Fractionation between the heavy and the light carbon isotopes can occur in two ways. Dissolution of atmospheric carbon dioxide in

seawater, for example, will slightly enrich  $^{13}\text{CO}_2$  relative to  $^{12}\text{CO}_2$  in the seawater by an equilibrium isotope effect. In biological systems, kinetic isotope effects during chemical transformation will enrich the  $^{12}\text{C}$  isotope in the products. The production of biomass proceeds in two steps; the assimilation of carbon and the biosynthesis of cell components. As a consequence, the amount of  $^{13}\text{C}$  in biological molecules mainly depends on (1) the  $^{13}\text{C}$  content of the carbon source, (2) isotopic effects during the assimilation of carbon, and (3) isotopic effects during metabolism and biosynthesis (Hayes, 1993).

Bender (1968) was the first to recognise that higher plants fall into distinct groups on the basis of the  $^{13}\text{C}/^{12}\text{C}$  ratio in their organic carbon and that this was related to the operation of  $\text{C}_4$  and  $\text{C}_3$  photosynthesis. This discovery arose through an interest in  $^{14}\text{C}$  dating for archaeological purposes and early observations that corn cobs and kernels of a wide variety of plant species have a higher  $^{13}\text{C}/^{12}\text{C}$  ratio than tissues. Bender went on to survey a number of grass species and showed the clear link between higher  $\delta^{13}\text{C}$  ratios and the taxonomic position of grasses which Hatch et al. (1967) previously had identified as plants using the  $\text{C}_4$  pathway. Numerous studies confirmed that biomass of  $\text{C}_3$  and  $\text{C}_4$  plants exhibit distinctive  $\delta^{13}\text{C}$  values (Fig. 1.8). The  $\text{C}_3$  photosynthetic pathway produces organic matter with  $\delta^{13}\text{C}$  values ranging from -23‰ to -34‰ (Schidlowski, 1987), whereas the organic matter of  $\text{C}_4$  plants is significantly enriched in  $^{13}\text{C}$  and generally ranges from -12‰ to -14‰ (cf. Fig. 1.8; Schidlowski, 1987). CAM plants are more difficult to

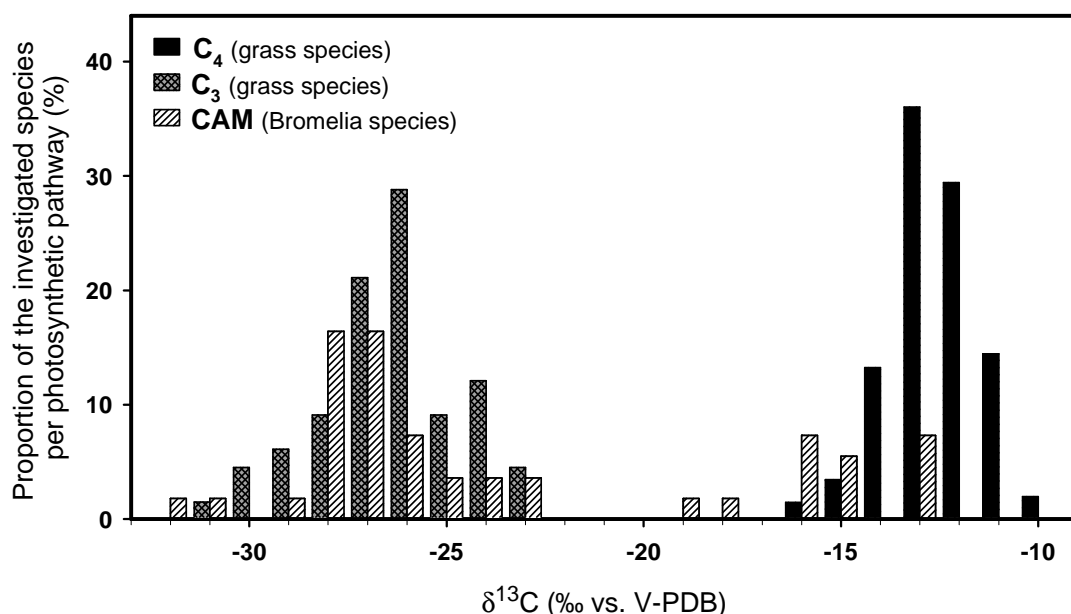


**Fig. 1.8.**  $\delta^{13}\text{C}$  values of 474 grass species and of 55 Bromelia species, demonstrating the distinct difference in isotopic composition between  $\text{C}_3$ ,  $\text{C}_4$  and CAM plants. Values collected from Smith and Epstein (1971), De La Harpe et al. (1981), Hattersley (1982), Koch et al. (1991), Lichtfouse et al. (1994), Schulze et al. (1996), Muzuka (1999), Pierce et al. (2002), and Boom (2004).

distinguish, since CAM plants are able to use the  $C_3$  pathway. When the full CAM pathway is engaged, the isotopic signature is more like that of  $C_4$  plants. Therefore, in general, CAM plants show  $\delta^{13}C$  values in-between those of  $C_3$  and  $C_4$  plants (Fig. 1.8) depending on the climatic conditions of the habitat. They approximately range from -10‰ to -33‰ (Schidlowski, 1987).

The fixation of atmospheric carbon ( $CO_2$ , inorganic carbon) as well as the storage of carbon in the form of organic matter in plants passes through several equilibrium and kinetic reaction steps, which cause  $^{13}C/^{12}C$  fractionation and affect the  $\delta^{13}C$  values. At the  $CO_2$  level only a fraction of the source carbon will enter the pathway. In all the fixation processes the heavier  $^{13}C$  isotope will react slightly more slowly than the lighter isotope  $^{12}C$ . This results in a relative enrichment of  $^{12}C$  and a depletion of  $^{13}C$  in the product at the end of the process and an enrichment in  $^{13}C$  in the remaining fraction (which in the case of plants is the left-over  $CO_2$ ). The route of fractionation in higher land plants starts with the diffusion of  $CO_2$  from the atmosphere through the stomata. The  $CO_2$  dissolves and is converted into  $HCO_3^-$  in the lumen of the leaf. This causes a fractionation of about 4.4‰ in  $C_3$  plants. The second fractionation step in the  $C_3$  pathway is the enzymatic fixation of  $CO_2$ . The carboxylation mediated by RuBisCO results in about 30‰ fractionation. The overall carbon isotopic composition is related to that of atmospheric  $CO_2$  by the simplified model relationship for  $C_3$  plants in Equation 1.3 (Farquhar et al., 1982, 1989).

$$\delta^{13}C_{C_3\text{plant}} = \delta^{13}C_{CO_2} - a - (b_1 - a) \frac{C_i}{C_a} \quad \text{Equation 1.3}$$

$$\delta^{13}C_{C_4\text{plant}} = \delta^{13}C_{CO_2} - a - (b_2 + b_3 \Phi - a) \frac{C_i}{C_a} \quad \text{Equation 1.4}$$

$$\delta^{13}C_{CAM\text{plant}} = \delta^{13}C_{CO_2} - a - \frac{\int^D A(b_2 - a) \frac{C_i}{C_a} dt + \int^L A(b_4 - a) \frac{C_i}{C_a} dt}{\int^D A dt + \int^L A dt} \quad \text{Equation 1.5}$$

$\delta^{13}C_{C_3\text{plant}}$ ,  $\delta^{13}C_{C_4\text{plant}}$ ,  $\delta^{13}C_{CAM\text{plant}}$ : Isotopic composition of the biosynthetic carbon of the  $C_3$ ,  $C_4$ , and CAM plant

$\delta^{13}C_{CO_2}$ : Isotopic composition of the ambient  $CO_2$

a: Variable describes the discrimination by the diffusion of  $CO_2$  into the leaf

$b_1$ ,  $b_2$ ,  $b_3$ ,  $b_4$ : Variable describes the discrimination against  $^{13}CO_2$  by RuBisCO in  $C_3$  plants ( $b_1$ ), by PEPC in  $C_4$  and CAM plants ( $b_2$ ), by RuBisCO in  $C_4$  plants ( $b_3$ ) and during the light period in CAM plants ( $b_4$ )

$C_i$ :  $CO_2$  concentration in the intercellular space of leaves

$C_a$ : Ambient  $CO_2$  concentration in the air

$\Phi$ : Extent of leakiness

$\int^D dt$  and  $\int^L dt$ : Denotes the time integral in the dark ( $\int^D dt$ ), and that in the light ( $\int^L dt$ )

A: Assimilation rate

In  $C_4$  plants, discrimination against  $^{13}\text{C}$  is more complex. The overall fractionation is described by the model in Equation 1.4.  $\text{CO}_2$  diffuses through stomata, dissolves, is converted into  $\text{HCO}_3^-$  and fixed by PEPC into oxaloacetate (OA; cf. Fig. 1.2, page 6). Then various transformations occur which are different for the various  $C_4$  types (cf. Chapter 1.2). At equilibrium, the heavier isotope concentration in  $\text{HCO}_3^-$  is similar to that in  $C_3$  plants. This discrimination depends on temperature, being 8.5‰ at 20°C, 7.9‰ at 25°C, and 7.4‰ at 30°C (Mook et al., 1974). PEPC discriminates against  $\text{H}^{13}\text{CO}_3^-$  by about 2.2‰ (O’Leary, 1981). No further discrimination would occur if the bundle sheath cells would be gas tight but some  $\text{CO}_2$  and  $\text{HCO}_3^-$  is likely to leak into the mesophyll cells. The isotopic fractionation by RuBisCO cannot be fully expressed due to the internal carbon concentration mechanism and the dependence on the tightness of the bundle-sheaths (in which the RuBisCO is located). The extent of leakiness of the bundle sheath is given by  $\Phi$  in the Equation 1.4 and determines to which extent fractionation occurs by RuBisCO (Farquhar, 1983; Farquhar et al., 1989).

Plants in the full CAM mode take up  $\text{CO}_2$  and synthesize OA using PEPC; the OA is then reduced and stored as malate (cf. Fig. 1.2, page 6). At dawn the plants close their stomata and decarboxylate the malate, refixing the released  $\text{CO}_2$  using RuBisCO. The malate that is stored at night will show the same discrimination as for  $C_4$  species with zero leakage. In the simplest case of  $C_4$  fixation in the dark and possible  $C_3$  fixation in the light, the average discrimination over a 24 h period is modelled by Equation 1.5 (Farquhar et al., 1989).

The important controls on  $\delta^{13}\text{C}$  values of plants are the isotopic composition of the atmosphere and those environmental and physiological variables that influence the  $c_i/c_a$  ratios in Equations 1.3, 1.4, and 1.5. The  $^{13}\text{C}/^{12}\text{C}$  ratio of the global atmospheric  $\text{CO}_2$  is largely constant over time. It has only slightly changed over the last glacial/interglacial cycles with lower  $\delta^{13}\text{C}$  values occurring during the glacial stage (about -6.8‰ during LGM) compared to the interglacial (about -6.6‰, early Holocene; Friedli et al., 1986; Leuenberger et al., 1992; Smith et al., 1999).  $\delta^{13}\text{C}$  values have declined since the industrial revolution due to fossil fuel burning to about -7.2‰ to -7.6‰ (Keeling et al., 1979).  $\delta^{13}\text{CO}_2$  values varied by about 1.5‰ during the Pleistocene glacial/interglacial cycles (Marino et al., 1992). The causes of the glacial/interglacial changes in  $\delta^{13}\text{C}$  values as well as the variations in atmospheric  $\text{CO}_2$  concentration (cf. Chapter 1.2; Fig. 1.5, page 11) are unclear. Shackleton (1977) interpreted these changes as the result of a decreased forest cover during glacial time. However, it is thought that the process of the “biological pump” regulates the concentration of dissolved  $\text{CO}_2$  in the surface waters of the oceans. It transports carbon to deep waters. Then the higher alkalinity in the oceans during glacial times is a consequence of changes in carbonate dissolution or sedimentation. Changes in



the sea surface temperature affect both  $p\text{CO}_2$  and  $\delta^{13}\text{CO}_2$  by approximately 4.2% per °C (Takahashi et al., 1993) and 0.11‰ to 0.13‰ per °C (Mook et al., 1974), respectively, whereas changes in salinity (S) alter  $p\text{CO}_2$  by 10 ppmV per ‰S without affecting the  $\delta^{13}\text{C}$  value (Weiss, 1974). From the last glacial maximum to the early Holocene the sea surface temperature measured on tropical corals increased by 5 to 6°C (Guilderson et al., 1994), whereas ocean salinity, estimated from sea level change, was approximately -1.4‰S (Fairbanks, 1989). Both may have resulted in an increase in the  $\text{CO}_2$  concentration and  $\delta^{13}\text{CO}_2$  of about 30 ppmV and 0.6‰, respectively. However, these facts alone can not explain the changes in  $p\text{CO}_2$  and  $\delta^{13}\text{CO}_2$  (after Leuenberger et al., 1992, and Smith et al., 1999) and point to additional unknown factors. Anyway, the global  $\delta^{13}\text{CO}_2$  is not thought to have changed much during the Pleistocene. It has certainly changed significantly on longer time scales and has apparently been recorded in the carbon isotopic composition of fossil plants (Faure et al., 1995; Gröcke et al., 2003). Pliocene-Pleistocene variations of up to 3‰ were reported in marine sediments (Shackleton and Hall, 1984; Grazzini et al., 1990; Whitman and Berger, 1994). For example, very high variations in the  $\delta^{13}\text{CO}_2$  value of up to 8‰ have been inferred for the Devonian and Carboniferous (416 to 286 million years BP; Tajika, 1998).

Long-term variations in  $\delta^{13}\text{CO}_2$  on a geological time scale are one feature. On a regional level several studies showed that large changes in  $\delta^{13}\text{CO}_2$  occur in different altitudinal layers in forests (e.g. Vogel, 1978; Medina and Minchin, 1980; Schleser and Jayasekera, 1985; van der Merwe and Medina, 1989). They noted a  $\delta^{13}\text{C}$  gradient of 3‰ to 5.6‰ towards lighter values between upper (>20 m) and lower canopy leaves (or understory plants; <5 m) and attributed this to recycled  $\text{CO}_2$  of soil respiration. Within closed canopies or in ecosystems where soil outgassing is high, soil  $\text{CO}_2$  exhibits a lower  $\delta^{13}\text{C}$  value than that from air in an open space, because it results from the oxidation of litter material already depleted in  $^{13}\text{C}$  and also from root respiration, i.e. oxidation of sugars with  $\delta^{13}\text{C}$  values similar to that of the organic matter of the  $\text{C}_3$  trees which synthesized them (Vogel, 1978). This is a reasonable explanation why differences in leaf isotopic composition should be expected between open and closed habitats. This will mainly affect  $\text{C}_3$  plants, because  $\text{C}_4$  plants (mainly grasses) are most abundant in open habitats due to their affinity to higher light intensities as well as their drought resistance by the carbon concentrating mechanism. Among the  $\text{C}_3$  species, which are represented in all habitats (i.e. ferns, grasses, shrubs and trees), the changes in average  $\delta^{13}\text{C}$  values tend to become more negative (exceeding 3.3‰) when going from open to closed canopy habitats. This may be an effect of recycled  $\text{CO}_2$  as well as of irradiance accompanied by warmer temperatures in the direct sunlight (Ehleringer et al., 1987; Ehleringer and Monson, 1993).

Especially the  $\delta^{13}\text{C}$  values of  $\text{C}_3$  plants are affected by several factors causing wider range in  $\delta^{13}\text{C}$  values compared to  $\text{C}_4$  plants (cf. Fig. 1.8). Arens et al. (2000) collected factors from the literature that have been cited to influence carbon isotopic discrimination in  $\text{C}_3$  plants and are shown in Table 1.1. Environmental factors, such as water stress, can influence the  $\delta^{13}\text{C}$  value of the leaf tissue. The water use efficiency of a plant, which is regulated by stomatal conductance, becomes particularly important in arid habitats. The discrimination against  $^{13}\text{CO}_2$  during photosynthesis is greatest when stomatal conductance is high. When stomata are partially or completely closed, nearly all of the  $\text{CO}_2$  inside the leaf reacts with RuBisCO or PEPC, respectively, and there is little fractionation of isotopes. Thus, the isotopic ratio is directly related to the averaged stomatal conductance during its growth (DeLucia et al., 1988). The same is evident when photorespiration is avoided during geological periods of high atmospheric  $\text{O}_2/\text{CO}_2$  ratios. Whereas the  $p\text{CO}_2$  variation examined by Arens et al. (2000) apparently did not exert a strong control on plant  $\delta^{13}\text{C}$  values, the large changes in  $\text{O}_2/\text{CO}_2$  ratios over geological time scales likely do (Beerling and Royer, 2002). Beerling and Royer (2002) examined previously reported  $\delta^{13}\text{C}$  values for fossil plant material and noted that atmospheric  $\text{O}_2/\text{CO}_2$  ratios and atmospheric  $\delta^{13}\text{C}$  values exert significant controls on fossil plant  $\delta^{13}\text{C}$  values. However, environmental factors explained only a relatively small proportion of

**Table 1.1** Factors that influence the carbon isotopic discrimination in  $\text{C}_3$  plants (adopted from Arens et al., 2000). For more details see Arens et al. (2000).

| Factor                               | Effect on $\text{C}_i/\text{C}_a$ | Effect on $\delta^{13}\text{C}_{\text{C}_3 \text{ plant}}$ |                      |  |
|--------------------------------------|-----------------------------------|--|----------------------|--|
|                                      |                                   | Range  | Direction            | Ecological conditions  |
| Recycled $\text{CO}_2$               | little                            | 1-5‰   | negative             | within closed canopies or in ecosystems where soil outgassing is high                    |
| Low light                            | increase                          | 5-6‰   | negative             | forest understory  |
| Water stress, low relative humidity  | decrease                          | 3-6‰   | positive             | arid and semiarid climate  |
| Osmotic stress                       | decrease                          | 3-10‰  | positive             | high-salinity soils, extreme at high $p\text{CO}_2$                                      |
| Low nutrients                        | increase                          | 4‰   | negative             | nutrient-poor soils  |
| Low temperature                      | increase                          | 3‰   | negative             | polar regions during ice house times, high altitude                                      |
| Reduced $p\text{CO}_2$ with altitude | decrease                          | 3-7‰   | positive             | high mountains   |
| Growth form and deciduousness        | increase/decrease                 | 1-3‰   | negative/positive    | variation between trees, forbs, and grasses, and between evergreen and deciduous species |
| Age (juvenile versus adult)          | increase in juvenile              | 2‰   | negative in juvenile | seedling or sapling versus reproductive individual                                       |
| Sun versus shade leaves              | increase in sun                   | 1-3‰   | negative in sun      | variation due to positive in the canopy relative to direction of sun                     |
| Seasonal variation                   | increase/decrease                 | 1-2‰   | negative/positive    | strongest effect in semiarid and arid climate  |

variation in the  $\delta^{13}\text{C}$  value. In contrast, over 90% of the variation of the carbon isotopic composition of plant tissue was explained by variation in  $\delta^{13}\text{CO}_2$  of the atmosphere under which it was fixed (Arens et al., 2000).

Using stable carbon isotope measurements of terrestrial organic material  $\text{C}_3$  and  $\text{C}_4$  plants can be distinguished through their  $\delta^{13}\text{C}$  values, which is of great use in the investigation of palaeovegetation. We do not know much yet on the palaeoecological aspect of CAM plants. Possibly, CAM plants disturb the reliability of the assessments, but, looking at the present-day CAM plants, it seems unlikely that CAM plants would have ever been a large portion of plant biomass, since they usually occupy small ecological niches.  $\text{C}_4$  and  $\text{C}_3$  plants are in the focus of attention of palaeo-orientated scientists working with stable isotopes to reconstruct palaeoenvironments, especially the palaeoclimatic conditions, by determining the proportion of representatives of the photosynthetic pathways in the vegetation. Features such as Kranz anatomy are seldom preserved in fossil material. The leaf itself is often not preserved as such and simply does not allow investigation at all. The only material omnipresent in geological archives is morphologically degraded organic material. Bulk marine sediments typically contain at least some marine-derived organic matter and typically cannot be used easily to determine the carbon-isotopic composition of terrestrial plants on the adjacent continent on a bulk level. In contrast, specific biomarkers, derived solely from higher plants are useful for such investigations (Pancost and Boot, 2004). In general, all aerially exposed organs of higher land plants are covered by wax lipids. Waxes can easily be dispersed by wind and rivers, can be associated with plant detritus (dead plant parts) or adhered to dust particles and can thus end up in soils as well as lake and ocean sediments. They function as molecular isotopic biomarkers for plants. Long-chain *n*-alkanes ( $n\text{-C}_{27}$  to  $n\text{-C}_{35}$ ) with an odd-over-even carbon number predominance and long-chain *n*-alkan-1-ols ( $n\text{-C}_{20}$  to  $n\text{-C}_{34}$ ) with an even-over-odd carbon number predominance are major components of leaf waxes (Eglinton and Hamilton, 1967; Tulloch, 1976; Baker, 1982; Bianchi, 1995). During their biosynthesis, they become more depleted in  $^{13}\text{C}$  than the total biomass (by about 10‰ in the case of *n*-alkanes; Collister et al., 1994), so that their  $\delta^{13}\text{C}$  ratios vary between -32‰ and -39‰ in  $\text{C}_3$  plants and between -18‰ and -25‰ in  $\text{C}_4$  plants (Rieley et al., 1991, 1993; Collister et al., 1994). Neglecting the CAM plant contribution to the biomass and their contribution to preserved wax biomarkers in soils and sediments, a simple two-component equation, the bimodal mixture model (Equation 1.6), can be used to estimate the contribution of the  $\text{C}_3$  or  $\text{C}_4$  photosynthetic pathway by using compound-specific stable carbon isotopic compositions.

$$\delta^{13}\text{C}_{\text{SWB}} = (1 - n_{\text{C}_4}) \cdot \delta^{13}\text{C}_{\text{WB-C}_3\text{plant}} + n_{\text{C}_4} \cdot \delta^{13}\text{C}_{\text{WB-C}_4\text{plant}} \quad \text{Equation 1.6}$$

$\delta^{13}\text{C}_{\text{SWB}}$ : measured  $\delta^{13}\text{C}$  value of sedimented leaf wax biomarker

$\delta^{13}\text{C}_{\text{WB-C}_3\text{plant}}$ :  $\delta^{13}\text{C}$  value of the biomarker in  $\text{C}_3$  plant leaf waxes

$\delta^{13}\text{C}_{\text{WB-C}_4\text{plant}}$ :  $\delta^{13}\text{C}$  value of the biomarker in  $\text{C}_4$  plant leaf waxes

$n_{\text{C}_4}$ : proportion of the  $\text{C}_4$  plant wax signal to the total biomarker

Thus, records of plant signatures may hold important climatic information. A combination of molecular stable isotopes and pollen analyses (as well as that of phytoliths) will provide a wealth of ecological information that will be a powerful tool to the ecophysiological and to the palaeo-orientated scientist.

## 1.5 Motivation, outline and objectives of this project

The aim of this project arose from geochemical assessments of marine versus terrigenous organic matter in marine sediments by using carbon isotopic data of bulk organic matter to calculate their respective proportion. Marine autochthonous carbon (phytoplankton) is  $^{13}\text{C}$ -enriched (-18‰ to -24‰) compared to the carbon delivered to the ocean from a typical terrestrial environment (-26‰ to -28‰; Fontugne and Duplessy, 1981; Jansen et al., 1984; Sackett, 1989; Mariotti et al., 1991; Schneider et al., 1996). This simple two-component marine/terrestrial assessment was frequently performed because the contribution of  $\text{C}_4$  terrestrial plants to marine sediments was considered negligible (e.g. Jansen et al., 1984; Mariotti et al., 1991; Schneider et al., 1996). Recent studies, however, indicated the supply of a significant amount of organic matter from  $\text{C}_4$  plants to sediments in the North Atlantic off the West African coast (Huang et al., 2000) and in the equatorial Atlantic (Wagner, 1998, 1999; Wagner and Dupont, 1999; Wagner, 2000). The highest ever recorded bulk isotopic value of organic matter exceeding -18‰ was found in marine sediments from an area off the East African coast (Muzuka, 1999). This  $\delta^{13}\text{C}$  value indicates an abundant terrigenous  $\text{C}_4$  plant component and implies that previous studies may have significantly overestimated the proportion of marine organic matter in certain sedimentary areas. Since  $\text{C}_4$  plants are characteristic of savanna-type vegetation (grasses), variations of  $\text{C}_4$  plant proportion in continental margin sediments will provide information on vegetation changes on the adjacent continent as a function of time (glacial/interglacial) and space (geographic latitude). An extension or regression of savanna areas depends on the respective climatic conditions.

In a study of sediments from Ocean Drilling Program (ODP) cores from the Congo Fan and the Angola Basin, evidence for the presence of terrestrial  $C_4$  plant material was obtained from the molecular and isotopic analysis of *n*-alkanes (Güntner, 2000). It was suggested that plants of warmer tropical climates biosynthesise longer-chain wax components than plants in habitats of the temperate regions (e.g. Gagosian and Peltzer, 1986; Poynter et al., 1989). This concept has been used to reconstruct continental climate development in studies of marine sediments, in which contents of longer-chain-length alkane homologues covaried with higher sea-surface temperature estimates (Hinrichs et al., 1997; Rinna et al., 2000), although, Schefuß et al. (2003b) did not find the same relationship in dust collected along a North-South transect off the African continent.

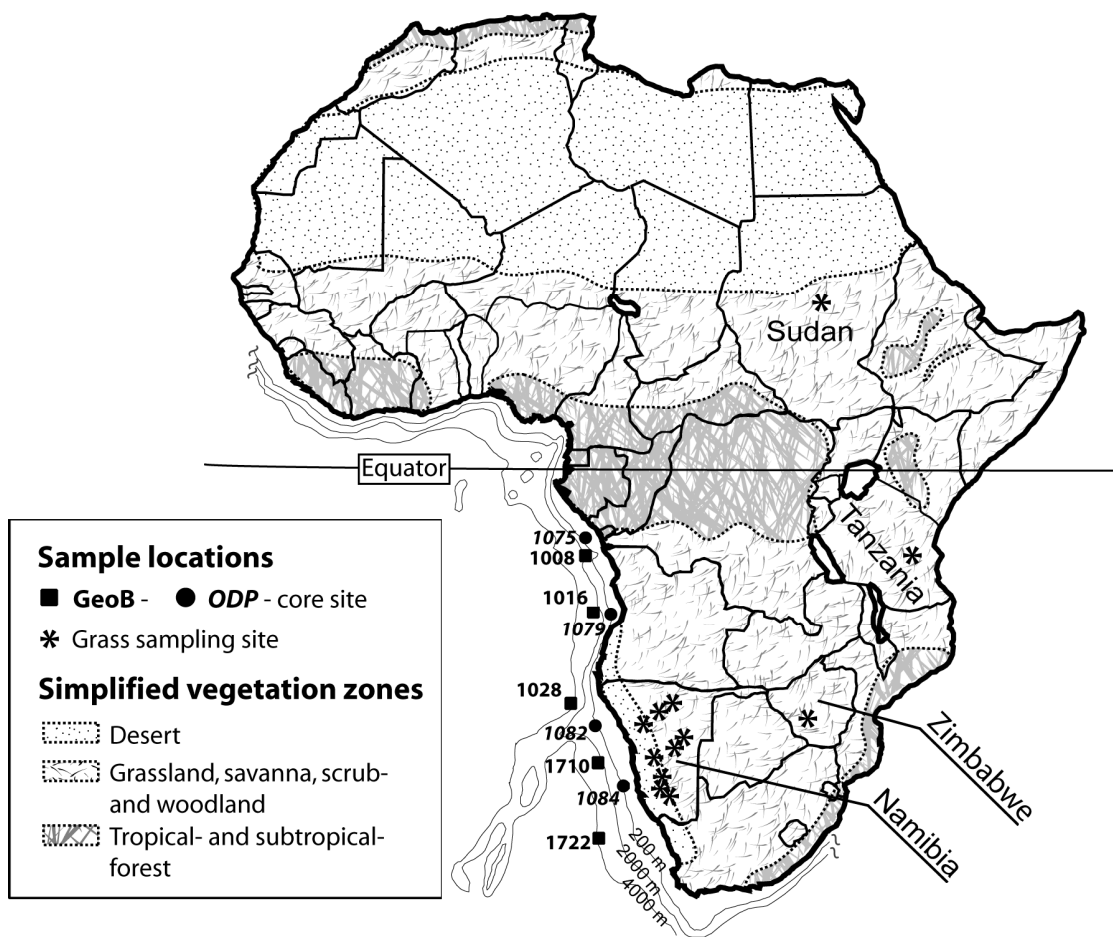


**Fig. 1.9.** Map of Africa with an overview of sampling sites of continental margin sediments, comprising holes drilled by the Ocean Drilling Program (ODP; Leg 175) as well as piston core locations of the Geosciences Department of the University of Bremen, Germany (GeoB, cruises M 6/6 and M 20/2 with RV METEOR), and grass plants, which were collected on different field trips at the African continent (not included on this map are the sampling sites of grasses in Peru and Australia). Also shown are political boundaries on the continent (countries where grass samples were collected are labelled) as well as simplified phytogeographical units of today (based on maps of White, 1983, and of the Global Land Cover Characteristics Database 2.0, Loveland et al., 2000; <http://edcdaac.usgs.gov>). For more details see Fig. 1.7 (page 16) as well as chapters 2, 3 and 4.

They argued that precipitation (aridity) is more important in governing higher plant *n*-alkane distributions. Many other palaeoenvironmental studies found a shift to longer-chain homologues with heavier compound-specific  $\delta^{13}\text{C}$  values and attributed these findings to an increase in abundance of  $\text{C}_4$  vegetation (e.g. Ficken et al., 1998; Huang et al., 2000; Zhao et al., 2000; Boom et al., 2001, 2002; Conte and Weber, 2002a, 2002b; Schefuß et al., 2003a; Zhang et al., 2003). However, analytical data for leaf waxes of  $\text{C}_4$  plants (especially grasses) are only sparsely available in the literature (e.g. Rieley et al., 1991, 1993; Collister et al., 1994; Smith et al., 2001; Boom et al., 2002; Chikaraishi and Naraoka, 2003).

The above mentioned overestimation of marine organic matter as well as the lack in data of biomarker signatures of  $\text{C}_4$  plants was the motivation to conduct the present work. The focus of this project is a general assessment of the organic geochemical methodology in a testing area: the vegetation of the southwest African continent and sediment samples which were recovered in a North-South transect of borehole and piston coring locations along the southwest African continental margin (Fig. 1.9). Latitudinal changes as well as the changes in the  $\text{C}_3$  versus  $\text{C}_4$  land plant vegetation with geological time should be reflected in the organic inventory of marine sediments. This study deals with a molecular-level estimation of the proportion of  $\text{C}_4$  plants on the continent by using specific land plant wax biomarkers (long-chain *n*-alkanes and *n*-alkanols), which were preserved in marine sediments. To validate this approach leaves of grasses were collected during different field trips mainly in southern Africa (cf. Fig. 1.9) and their leaf waxes were analysed. The key questions of the project are summarised as follow:

- Are long-chain wax *n*-alkane and *n*-alkanol carbon number distribution patterns and compound-specific isotopic compositions valid parameters to elucidate the molecular  $\text{C}_4$  plants signature of savanna vegetation, which may be reflected and preserved in marine sediments?
- How does the geochemical assessment based on molecular distributions of key compounds and bulk and molecular isotopic data compare with the pollen record in the same samples of southwest African continental margin sediments?
- How can the combined geochemical and pollen data be translated into vegetational changes on the South African continent taking into consideration climate-related changes of the wind patterns in the study area?
- How does the molecular information based on wax *n*-alkanes compare with that of wax *n*-alkanols?

- ➔ Can wax *n*-alkanol distributions substitute *n*-alkane distributions in cases where the *n*-alkane pattern is obscured by petroleum hydrocarbons from oil seeps as previously observed in some southwest African continental margin sediments?
- ➔ What is the glacial/interglacial variation of the C<sub>4</sub> plant fraction in southwest African continental margin sediments along a North to South transect?

## 1.6 Outline of the author's contribution

This thesis presents published material and material submitted for publication from two interdependent study areas within organic geochemistry. The first category deals with the chemotaxonomic significance of carbon number distributions and of molecular stable carbon isotopic compositions of long-chain *n*-alkanes and *n*-alkan-1-ols in leaf waxes of African C<sub>4</sub> grasses. The second category deals with the relationship between evidence for latitudinal aerosol transport pathways and lipid and pollen compositions in southeast Atlantic continental margin sediments. The recovery sites of the sediment samples are located along a North to South transect on the African continental margin south of the equator (Fig. 1.9). They follow the major phytogeographic zonations. Vegetation changes on the adjacent African continent during the Holocene as well as additional three major glacial/interglacial time slices during the past 140 kyr are recorded. These results of the studies are compiled in three separate publications, which are presented as individual chapters (Chapters 2, 3, and 4). As all publications bear the names of several co-authors, it is clarified below which parts of the individual publications were contributed by the author himself. A short overview on the individual chapters is also given.

### **Chapter 2: *Chemotaxonomic significance of distribution and stable carbon isotopic composition of long-chain alkanes and alkan-1-ols in C<sub>4</sub> grass waxes***

For the first manuscript molecular stable carbon isotopic compositions of long-chain wax *n*-alkanes and *n*-alkanols as well as their distribution patterns in waxes of 38 grasses, abundant in southern Africa, were determined. The author investigated 14 grasses and Anna Plader analysed additional 24 grasses for her diploma thesis, supervised by the author. Yoshito Chikaraishi made available analytical data of leaf wax *n*-alkanes of 17 trees and 12 grasses collected in Japan and Thailand. The evaluation and interpretation of the results as well as the development of the concept, the writing and editorial handling of the publication was mainly done by the author himself, supported by suggestions from Geoffrey Eglinton (University of Bristol, UK) and Jürgen Rullkötter (ICBM, University of Oldenburg, Germany).

This first manuscript aims at a characterisation of the major C<sub>4</sub> signatures of tropical and subtropical savannas, which can be reduced to a C<sub>4</sub> grass contribution to the vegetation. Contents, distribution patterns and molecular isotopic compositions of long-chain *n*-alkanes and *n*-alkanols in the waxes of 35 C<sub>4</sub> and three C<sub>3</sub> grasses were evaluated for the chemotaxonomic relevance of wax signatures of whole plants and their parts. The selected grasses belong to different subfamilies and C<sub>4</sub>-subtypes (NADP-ME, NAD-ME and PCK). It is shown that the wax signatures of C<sub>4</sub> grasses are generally distinguishable from those of C<sub>3</sub> species by higher carbon isotopic values, higher contents of longer-chain *n*-alkanes and *n*-alkanols. By reviewing relevant botanical and phytogeographic background information of the tropical grasses studied, it arose that especially the NAD-ME and PCK C<sub>4</sub>-subtype grasses, which thrive in extremely arid areas, contain longer-chain wax homologues. The agreement between the chemical classification of the grass wax components on a subfamilial level and the previously reported phylogeny of grasses implies an evolutionary wax adaptation to warm and arid habitats. The results confirm the validity of these wax signatures as indirect proxies of continental climate conditions in environmental studies of the tropics and subtropics.

**Chapter 3: *A north to south transect of Holocene southeast Atlantic continental margin sediments: Relationship between aerosol transport and compound-specific  $\delta^{13}\text{C}$  land plant biomarker and pollen records***

For the second manuscript molecular stable carbon isotopic compositions of long-chain *n*-alkanes and *n*-alkanols as well as their distribution patterns in lipid fractions of deep sea sediment samples were analysed, evaluated and interpreted by the author. The integrated results of pollen analyses and their evaluation as well as interpretation were obtained by Lydie Dupont (University of Bremen, Germany). Selected geochemical data were taken from the unpublished theses of Ute Güntner and Claudia Wenzel (both ICBM). The concept of the publication as well as the discussion of the results were jointly elaborated during several meetings of the co-authors, and the manuscript was drafted by the author; Geoffrey Eglinton, Lydie Dupont, Jürgen Rullkötter contributed to it and particularly improved the language.

In the second manuscript distribution patterns and molecular stable carbon isotopic signatures of long-chain *n*-alkanes and *n*-alkanols of lipid fractions of Holocene sediment samples were correlated with concentrations and taxonomic distributions of pollen in the same sediments. The sediment samples were taken from nine cores drilled along the southwest African continental margin. This multidisciplinary approach provides clear evidence of latitudinal differences in lipid and pollen composition paralleling the major phytogeographic zonations on the adjacent continent. The interpretation of the analytical



data was substantiated by using published information from modelled clusters of wind trajectories and satellite Aerosol Index imagery (dust and smoke) providing information on the source areas. Furthermore, published information on present phytogeographic zones with their known or estimated C<sub>3</sub> and C<sub>4</sub> plant population and climatic information (annual temperature and rainfall profiles) were used to interpret the analytical data. The results of this study demonstrate that the combination of pollen data and compound-specific isotope geochemical proxies can be effectively applied in the reconstruction of the continental phytogeographic development in the past.

**Chapter 4: *Glacial/interglacial changes in southern Africa: Compound specific  $\delta^{13}\text{C}$  land plant biomarker and pollen records from southeast Atlantic continental margin sediments***

The third manuscript extends the results compiled in the second manuscript (Chapter 3) to glacial/interglacial variations by using the same proxies, i.e. molecular stable carbon isotopic compositions of long-chain *n*-alkanes and *n*-alkanols as well as their distribution patterns and pollen analyses of the same samples. Analyses, evaluation and interpretation were done in the same way like mentioned for Chapter 3 (see above). Additionally, Jung-Hyun Kim, Thorsten Bickert and Barbara Donner (all at University of Bremen) provided data of high resolution age models of some of the cores. The concept of the publication and the discussion of the results were jointly elaborated during several meetings of the co-authors and the manuscript was drafted by the author; Jürgen Rullkötter, Lydie Dupont and Geoffrey Eglinton contributed to the manuscript and polished the language.

The third manuscript evaluates glacial/interglacial changes by analysing two interglacial periods, the Holocene (MIS 1) and the penultimate interglacial period (Eemian, MIS 5e), and two glacial periods, the LGM (MIS 2) and the penultimate glacial (MIS 6a). Sediment samples from the same core sites like those described for Chapter 3 were taken for the three additional time slices. Data of long-chain *n*-alkanes and *n*-alkanols, of pollen analyses, calculated clusters of wind trajectories for the Holocene and LGM afford evidence of glacial/interglacial changes of major phytogeography zonations in the source areas on the adjacent continent. The multiproxy results illustrate vegetation changes on the continent, which are discussed on the basis of previously known glacial/interglacial changes in southern African vegetation as well as climatic conditions. The results of the study confirm the results of Chapter 3, i.e. the validity of the combination of pollen data and compound-specific isotope geochemical proxies for the reconstruction of past continental phytogeographic developments.

## 2 Chemotaxonomic significance of distribution and stable carbon isotopic composition of long-chain alkanes and alkan-1-ols in C<sub>4</sub> grass waxes

Florian Rommerskirchen, Anna Plader, Geoffrey Eglinton, Yoshito Chikaraishi, Jürgen Rullkötter

This chapter was accepted for publication: Rommerskirchen, F., Plader, A., Eglinton, G., Chikaraishi, Y., Rullkötter, J., 2005. Chemotaxonomic significance of distribution and stable carbon isotopic composition of long-chain alkanes and alkan-1-ols in C<sub>4</sub> grass waxes. *Organic Geochemistry*, in press.

### 2.1 Abstract

Grasses (Poaceae) are distributed across the world in broad latitudinal belts and are an important source of C<sub>4</sub> biomass in the geological record of soils as well as lake and marine sediments. We examined long-chain leaf wax components of 35 C<sub>4</sub> grasses of the subfamilies Aristidoideae, Chloridoideae and Panicoideae from the southern African grasslands and savannas and three C<sub>3</sub> grasses of the subfamily Pooideae from Peru and Australia and review the relevant botanical, phytogeographic and leaf wax compositional background information. Contents, distribution patterns and molecular stable carbon isotopic compositions of long-chain *n*-alkanes (*n*-C<sub>27</sub> to *n*-C<sub>35</sub>) and *n*-alkan-1-ols (*n*-C<sub>22</sub> to *n*-C<sub>32</sub>) were used to estimate the chemotaxonomic relevance of wax signatures of whole plants, separately for different subfamilies and for members of the three C<sub>4</sub> subtypes (NADP-ME, NAD-ME and PCK). Two grass species were separated into flower heads, leaves and stems and the parts analysed separately. Grass flowers contain remarkable amounts of short-chain *n*-alkanes, which may have a significant influence on the chemical signature of the whole plant, whereas *n*-alkanol distribution patterns exhibit no systematics. The stable carbon isotopic composition of both biomarker types in different plant parts is remarkably uniform. Chemotaxonomic differentiation was not possible on a species level based on whole plant samples, but was more successful for averages of subfamily and photosynthetic subtype data. Wax signatures of C<sub>4</sub> grasses are generally distinguishable from those of C<sub>3</sub> species by heavier isotopic values, higher contents of *n*-C<sub>31</sub> and *n*-C<sub>33</sub> alkanes and the abundance of the *n*-C<sub>32</sub> *n*-alkanol, which is largely absent in C<sub>3</sub> grass waxes. Especially the waxes of the NAD-ME and PCK C<sub>4</sub>-subtype grasses, which thrive in extremely arid tropical and subtropical areas, contain high relative amounts

of longer-chain *n*-alkane homologues. The chemical classification on a subfamily level, which is in agreement with previously reported subfamilial phylogeny of grasses, implies an evolutionary wax adaptation of C<sub>4</sub> grasses to warm and arid habitats. Our results confirm the validity of the contents, distribution patterns and molecular stable carbon isotopic compositions of long-chain *n*-alkanes and alkan-1-ols as indirect proxies of continental climate conditions in environmental studies of the tropics.

## 2.2 Introduction

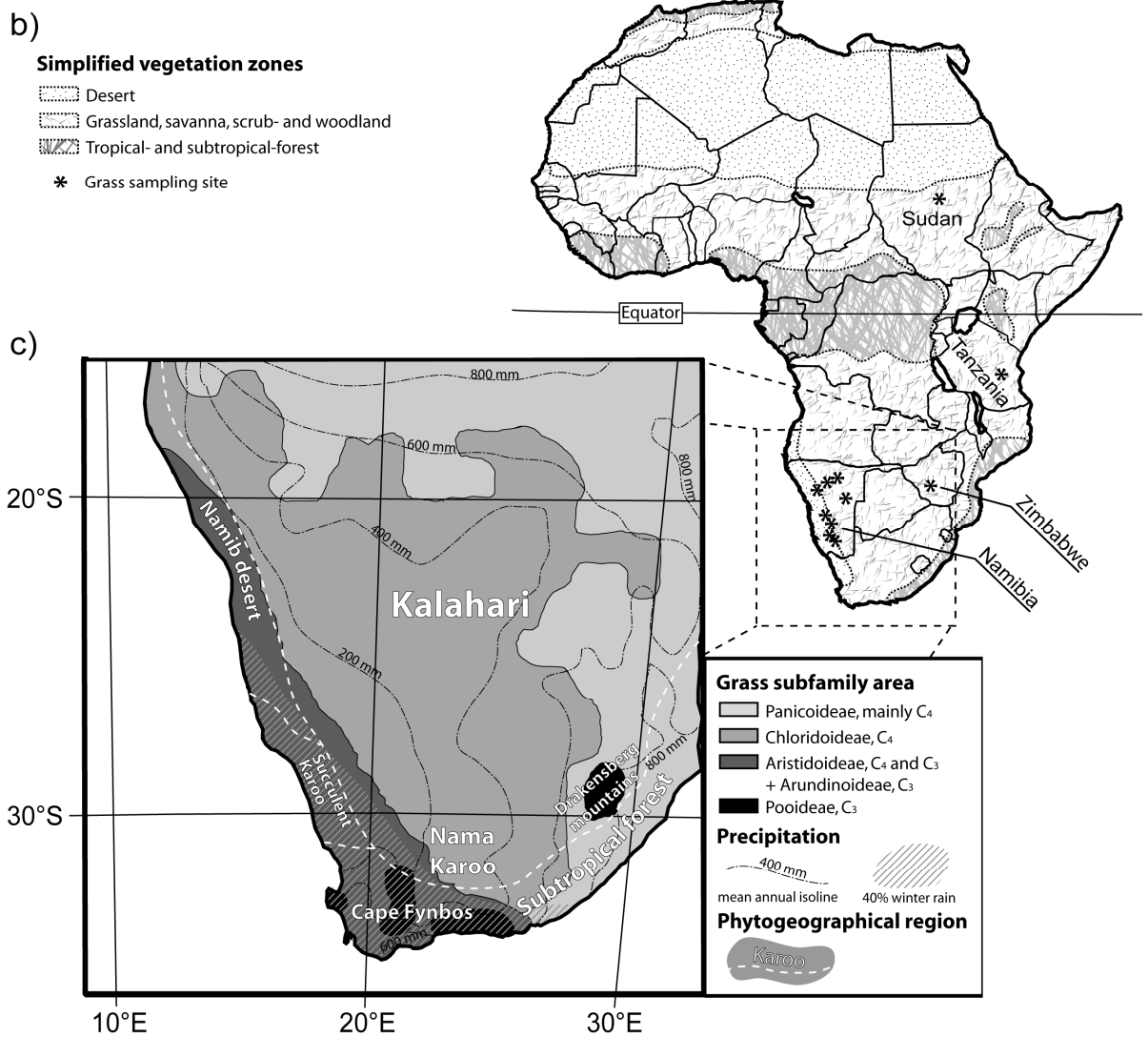
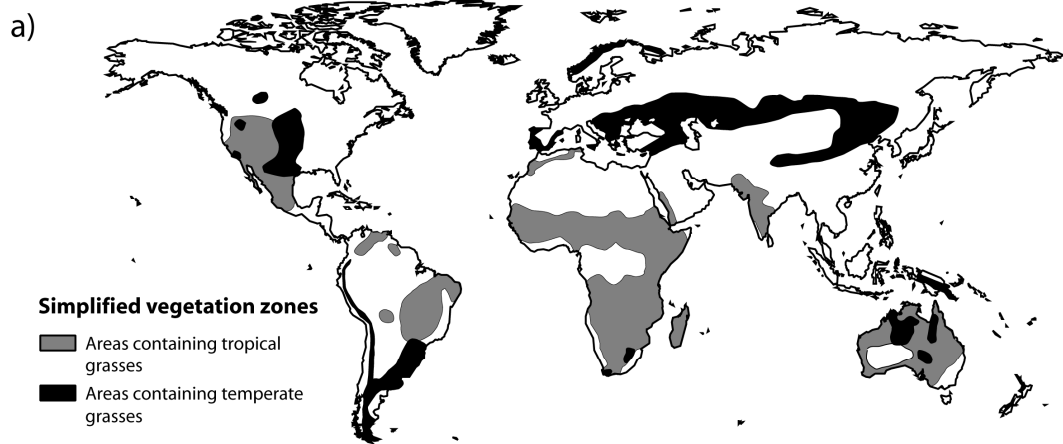
Plants use two principal types of carbon fixation pathways during photosynthesis. The first is the so-called C<sub>3</sub> pathway (Benson-Calvin Cycle), which is thought to have been used by higher land plants since their advent some 450 million years ago at relatively high concentrations of atmospheric CO<sub>2</sub> (Sage, 1999, 2004). Of the estimated 250,000 species of land plants, about 85-89% use the C<sub>3</sub> photosynthetic pathway, e.g. almost all trees, shrubs, as well as grasses preferring wet, cool growing seasons (Leegood, 1999a; Sage et al., 1999a). The other principal way, the C<sub>4</sub> pathway (Hatch-Slack-Cycle), requires a cell anatomy which differs substantially from that of the C<sub>3</sub> plants (Hatch and Slack, 1966). It is believed that the physiological adaptation of the C<sub>4</sub> mechanism evolved independently many times between 7 and 30 million years ago in response to a decline in concentration of CO<sub>2</sub>, conditions that would have favoured photorespiration (Kellogg, 1999; Leegood, 1999b; Sage et al., 1999b; Giussani et al., 2001; Keeley and Rundel, 2003; Sage, 2004). This has resulted in three C<sub>4</sub> sub-groups: Those using the NADP-malic enzyme (NADP-ME; malate as CO<sub>2</sub> supplier), those using the NAD-malic enzyme (NAD-ME; aspartate), and those using the PCK enzyme (aspartate) to release CO<sub>2</sub> from their internally stored carbon pools (Hatch et al., 1975). These mechanisms of CO<sub>2</sub> concentration lead to an improved water use efficiency (Downes, 1969) and prevent ineffective photorespiration at locations of high temperature, high light intensity, high salinities, limited water supply and/or low CO<sub>2</sub> concentrations (Björkman, 1976; Ehleringer et al., 1997; Collatz et al., 1998; Winslow et al., 2003; Sage, 2004). Under these conditions, which prevail in certain subtropical and tropical areas, C<sub>4</sub> plants successfully outcompete C<sub>3</sub> plants (e.g. Björkman and Berry, 1973; Osmond et al., 1980; Edwards et al., 1985).

The independent evolutionary events in the history of the C<sub>4</sub> photosynthetic mechanism led to its distribution among a wide range of unrelated plants, and it is represented in 8,000 to 10,000 species in 19 diverse taxonomic families (Sage, 1999, 2004). About 60% of C<sub>4</sub> land plant species belong to the grass family (Poaceae), followed by sedges (about 20%) and dicotyledons (about 16%; according to Sage, 2004). Within the grass family,

one half of the around 10,000 species use the C<sub>4</sub> pathway (Hattersley, 1987; Hattersley and Watson, 1992). The grass family is not the largest in term of species and genera, but its environmental importance is great for it provides the principal ground cover of the grasslands and savannas. In savannas, woody species are significant but do not form a closed canopy or a continuous cover (Bourliere, 1983). Thereby, the importance of C<sub>4</sub> plants (predominantly tropical grasses) decreases with increasing abundance of woody (C<sub>3</sub>) species, which is governed by edaphic characteristics and the climate, especially the mean annual rainfall (Walter, 1971; Whittaker, 1975). Where grasslands exhibit two distinct growing seasons, C<sub>3</sub> grasses mostly grow in the cooler, moist months (Williams, 1974; Winslow et al., 2003). Grassy vegetation occupies a third of the land surface (Clayton and Renvoize, 1986; Werner, 1991) and is distributed across the world in broad latitudinal belts (Fig. 2.1a; Hartly, 1950; Cross, 1980). Savannas and grasslands cover 50% of Africa and Australia, about 45% of South America and 10% of India and Southeast Asia (Fig. 2.1a,b; Werner, 1991).

Grasses may be divided into the major subfamilies Bambusoideae, Chloridoideae, Panicoideae, and Pooideae (Clayton and Renvoize, 1986; Gibbs Russell et al., 1991; Watson and Dallwitz, 1992a,b; Grass Phylogeny Working Group, 2001). Pooideae (C<sub>3</sub>) reaches their maximum diversity in the temperate zone and Bambusoideae (C<sub>3</sub>), though mostly tropical, are mainly confined to humid forest shade. Chloridoids (C<sub>4</sub>) and panicoids (mainly C<sub>4</sub>), on the other hand, are concentrated in the tropics and subtropics (cf. Fig. 2.2b; Gibbs Russell et al., 1991). They can be found in savanna zones between deserts and forests (cf. Fig. 2.1a,b; Clayton and Renvoize, 1986), although the chloridoids in particular grow in extremely arid areas. The subfamilial classification of grass species undergoes frequent reorganisation due to ongoing reevaluation of phylogeny. The current phylogenetic tree of grasses, which was elaborated by the Grass Phylogeny Working Group (2001), consists of 12 subfamilies (Fig. 2.2a). The C<sub>4</sub> carbon fixation pathway is generally found in three subfamilies: Aristidoideae, Chloridoideae and Panicoideae (Fig. 2.2a).

The geographical distribution of the C<sub>4</sub>-containing subfamilies is linked to the abundance of C<sub>4</sub> subtypes within them, because they prefer different habitats of annual rainfall patterns compared to the rest of the subfamily members (cf. Fig. 2.2b; Schulze et al., 1996; Taub, 2000; Ghannoum et al., 2001; Wan and Sage, 2001). The NADP-ME grass species (mainly in the Panicoideae and Aristidoideae subfamilies) predominate in all regions where C<sub>4</sub> grasses occur, but they reach their maximum abundance in areas of moderate moisture with more than 500 mm/a precipitation (e.g. Fig. 2.1c). NAD-ME and PCK species have their maximum diversity in relatively arid regions with less than 500 mm



annual precipitation and are concentrated in the subfamily Chloridoideae, where the NADP-ME subtype is unknown (Fig. 2.1c; according to Ellis et al., 1980; Gibbs Russell et al., 1991; Renvoize and Clayton, 1992; Watson and Dallwitz, 1992a; Schulze et al., 1996; Wan and Sage, 2001).

The distinctions in carbon isotopic composition of land plant biomass due to different carbon fixation pathways can be used to assign plants to the C<sub>3</sub>/C<sub>4</sub> photosynthetic pathways. The  $\delta^{13}\text{C}_{\text{TOC}}$  of total organic carbon (TOC) has characteristic ranges from -23‰ to -34‰ and from -12‰ to -14‰ in C<sub>3</sub> and C<sub>4</sub> plants, respectively (Schidlowski, 1987). Leaf wax lipids during biosynthesis become more depleted in <sup>13</sup>C than the total biomass, e.g. by about 10‰ in *n*-alkanes (Collister et al., 1994), so that their  $\delta^{13}\text{C}$  values vary between -32‰ and -39‰ in C<sub>3</sub> and between -18‰ and -25‰ in C<sub>4</sub> plants (Rieley et al., 1991, 1993; Collister et al., 1994).

Wax lipids cover all aerially exposed organs of higher land plants to control the water balance and protect against mechanical damage to leaf cells, weathering, water stress, and attack by microbes, fungi and insects (Chibnall et al., 1934; Eglinton and Hamilton, 1967; Kolattukudy, 1976, 1980, 1996; Tulloch, 1976; Baker, 1982; Bianchi, 1995; Riederer and Schreiber, 1995). Their development was a prerequisite for the evolutionary step of aquatic to terrestrial plants (Gülz, 1994). The thickness of the wax layer is variable and difficult to evaluate. It depends on many stimulatory effects on wax production like increase in energy flux, decrease in humidity or soil moisture content (Whitecross and Armstrong, 1972; Baker, 1974; Baker and Procopiou, 1980). Exceptionally thick layers are found on leaves of plants which grow under arid conditions (Baker and Procopiou, 1980) with their particular needs for regulating transpiration (Riederer and Schreiber, 1995).

Long-chain *n*-alkanes and *n*-alkan-1-ols are major components of leaf waxes (Tulloch, 1976; Bianchi, 1995); *n*-Alkanes typically occur in the *n*-C<sub>27</sub> to *n*-C<sub>35</sub> range with characteristic odd-over-even (Eglinton and Hamilton, 1967) and *n*-alkanols in the *n*-C<sub>20</sub> to *n*-C<sub>34</sub> range with even-over-odd carbon number predominance (Baker, 1982; Bianchi,

---

**Fig. 2.1.** (opposite) a) World map showing a simplified assessment of the global distribution of areas with typical tropical and temperate grasses including grasslands, savannas, wood- and scrublands. The assessment is based on maps of Whittaker (1975), Cross (1980), Bourlière (1983), Coupland (1992), of the Global Land Cover Characteristics Database 2.0 (Loveland et al., 2000; <http://edcdaac.usgs.gov>) as well as Sala et al. (2001). b) Map of Africa showing political boundaries as well as simplified phytogeographical units of today, based on maps of White (1983) and of the Global Land Cover Characteristics Database 2.0 (Loveland et al., 2000; <http://edcdaac.usgs.gov>). Countries where grass samples for this study were collected are labelled. c) Partial map of Africa showing generalised units of dominating subfamilies of the grass vegetation (grey codes according to grass subfamily superiority; after Gibbs Russell, 1988), of phytogeographical regions (white text and broken boundaries) and of mean annual rainfall based on the 1961-1990 mean monthly climatology of New et al. (1999; alternately dotted and dashed grey lines). Areas of precipitation where more than 40% of rainfall occurs during the winter season are diagonally striped. All other areas are summer rainfall areas.

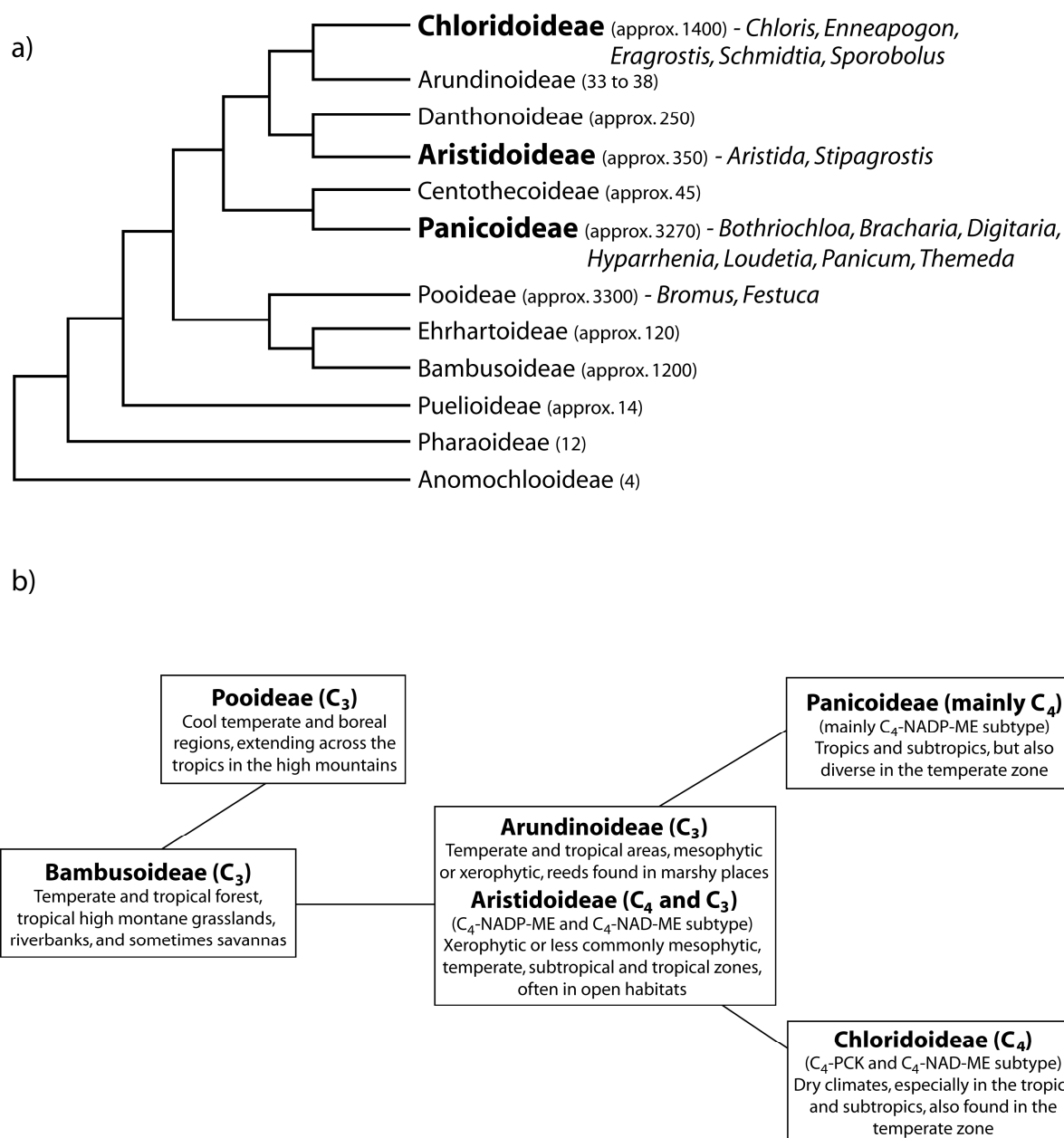


**Fig. 2.2.** a) Phylogeny of the grass family based on the grass subfamily classification of the Grass Phylogeny Working Group (2001). Taxa that contain the C<sub>4</sub> photosynthetic mechanism are boldfaced. Number of species of the whole subfamily (bracketed; gathered from the Grass Phylogeny Working Group, 2001) as well as grass species used for chemical classification, are noted next to the subfamily. b) Simplified evolutionary sequence of grass embryo types (based on the postulated sequence of Clayton and Renvoize, 1986). Displayed are the four species-richest subfamilies Bambusoideae, Chloridoideae, Panicoideae and Pooideae as well as the potentially crossing subfamilies Arundinoideae and Aristidoideae. Preferred habitat description of the subfamilies was gathered from the Grass Phylogeny Working Group (2001). C<sub>4</sub>-containing subfamilies exhibit further information about the major C<sub>4</sub> physiology within the subfamily (according to Ellis, 1977, Watson and Dallwitz, 1992a,b onwards, and Schulze et al., 1996).

1995). These compounds are relatively resistant against degradation after the decay of plants, although the stability decreases from *n*-alkanes to *n*-alkanols (Cranwell, 1981). Epicuticular wax components can easily be dispersed by wind and rivers; they can be associated with plant detritus or adhere to dust particles and can thus end up in soils, lake and ocean sediments, which makes them useful higher-plant biomarkers in palaeoenvironmental studies.

It has been suggested that plants of warmer tropical climates biosynthesise longer-chain wax components than do plants in habitats of the temperate regions (e.g. Cranwell, 1973; Gagosian and Peltzer, 1986; Poynter et al., 1989). This concept has been used as a proxy for continental climate development in studies of marine sediments, where contents of longer-chain length alkane homologues covaried with higher sea-surface temperature estimates based on long-chain alkenones (Hinrichs et al., 1997; Rinna et al., 2000). Schefuß et al. (2003b), however, did not find the same relationship in dusts collected off the African continent in a north-south transect. They argued that precipitation (aridity) is more important in governing higher plant *n*-alkane distributions. Other palaeoenvironmental studies found a shift to longer-chain homologues with heavier  $\delta^{13}\text{C}$  values and attributed these findings to an increase in abundance of C<sub>4</sub> vegetation (e.g. Ficken et al., 1998; Huang et al., 2000; Zhao et al., 2000; Boom et al., 2001, 2002; Conte and Weber, 2002a, 2002b; Eglinton et al., 2002; Conte et al., 2003; Rommerskirchen et al., 2003, Chapter 3; Schefuß et al., 2003a, 2003b; Zhang et al., 2003; Zhao et al. 2003; McDuffee et al., 2004; Zhang et al., in press). The waxes of C<sub>4</sub> grasses are cited in several recent sediment studies as representing important fossil C<sub>4</sub> plant material (e.g. Boom et al., 2002; Rommerskirchen et al., 2003, Chapter 3; Zhang et al., 2003; Zhao et al., 2003; Zhang et al., in press). However, analytical data for *n*-alkanes and *n*-alkanols in the leaf waxes of extant C<sub>4</sub> grasses are only sparsely available (e.g. Tulloch, 1981, 1984; Dove and Mayes, 1991; Dove et al., 1996; Chen et al., 1998; Smith et al., 2001). A chemotaxonomic approach to grass waxes on a subfamilial level by Maffei (1996) was mainly based on C<sub>3</sub> grasses.

The present study provides significant background information relevant to the emerging use of long-chain aliphatic biomarkers in environmental studies. We focused our grass wax lipid investigation on the southern African tropical and subtropical savannas and deserts. On a subfamilial and photosynthetic level we evaluate the chemotaxonomic significance of wax *n*-alkane and free wax *n*-alkanol carbon number distribution patterns as well as molecular stable carbon isotopic compositions of thirty-five C<sub>4</sub> and three C<sub>3</sub> grasses. We also make a preliminary assessment of the reliability of wax homologues as proxy parameters by evaluating the contribution of different plant parts of two grass species to the whole plant wax signal. By reviewing the botanical background information



and using the analytical data of the present study together with previously published analytical data, we elucidate the significance of C<sub>4</sub> grass waxes for palaeoenvironmental studies of the tropics and subtropics.

## 2.3 Description of sampling area, samples and methods

### 2.3.1 Description of sampling area: Grass diversity and distribution in southern Africa

The vegetation types of Africa grade south- and northwards from the equatorial lowland rain forest to dry forest, wood-, scrub- and grassland, different types of savannas and deserts, and finally to Afroalpine vegetation, southern subtropical and northern Mediterranean forest. For a broad-brush assessment in Fig. 2.1b we combined grasslands, savannas, wood- and scrublands into a grass vegetation zone, tropical and subtropical forest into a tree-dominated vegetation and defined deserts as sparse vegetation zones. A large part of the African continent is covered by grass-dominated ecosystems (White, 1983).

The predominance of C<sub>4</sub> grass species (Fig. 2.1c) ranges south and eastward from the central arid desert over the cool temperate highvelds to the humid subtropical east coast (Vogel et al., 1978). Chloridoideae (Ch), Panicoideae (Pa) and Aristidoideae (Ari) are common subfamilies (Fig. 2.1c) and grass species of *Aristida* (Ari, C<sub>4</sub>), *Chloris* (Ch, C<sub>4</sub>), *Cynodon* (Ch, C<sub>4</sub>), *Eragrostis* (Ch, C<sub>4</sub>), *Panicum* (Pa, C<sub>4</sub>), *Sporobolus* (Ch, C<sub>4</sub>), *Stipagrostis* (Ari, C<sub>4</sub>) or the subspecies *Themeda triandra* (Pa, C<sub>4</sub>) are dominant (Bayer, 1959; White, 1983; O'Connor and Bredenkamp, 1997). Aristidoideae and Arundinoideae (Aru) are mostly found in areas with more than 40% of rainfall occurring in winter, like at the southwest coast of Africa (cf. Fig. 2.1c; according to Ellis et al., 1980; Gibbs Russell et al., 1988, 1991). Up to 86% of all plant species in the hot dry environment of the southern Kalahari use the C<sub>4</sub> photosynthetic pathway (Leistner, 1967), and 95% of the grass species are C<sub>4</sub> plants (Ellis et al., 1980). C<sub>3</sub> grasses are sparse, occupying moist places on river banks, in lakes and swamps, where the ubiquitous *Phragmites* species (Aru, C<sub>3</sub>) are dominant (White, 1983). The mountain grasslands are characterised by moist and relatively cool conditions so that temperate grasses of Pooideae (Po), like *Festuca* (Po, C<sub>3</sub>) and *Bromus* (Po, C<sub>3</sub>) become dominant (Bayer, 1959; White, 1983). Thus, the only regions where C<sub>3</sub> grass is more abundant than the C<sub>4</sub> species are the highest parts of the Drakensberg mountains and the winter rainfall areas on the west and south coast of Cape

Fynbos, with outliers on the mountains (Fig. 2.1c; Vogel et al., 1978; Ellis et al., 1980; Werger and Ellis, 1981).

### 2.3.2 Samples

For this study we selected thirty-five C<sub>4</sub> and three C<sub>3</sub> grass samples of the most abundant types in southern Africa. Nine grasses belong to the Aristidoideae, 15 to the Chloridoideae, 11 to the Panicoideae and 3 to the Pooideae subfamilies. Grass samples were made available by Dr. R.W. Mayes of the Macaulay Institute in Aberdeen (United Kingdom), Prof. E.-D. Schulze of the Max-Planck Institute of Biogeochemistry in Jena (Germany) and A. Gerecht of the University of Oldenburg (Germany). They collected grasses on different field trips for similar lipid and stable carbon isotopic investigations. Where typical African grass species were not available, we used species of other tropical or subtropical sampling sites in the world. Grasses from R.W. Mayes were collected by D. Smith, R.W. Mayes, H. Ali, M. Daniels and their colleagues during wet seasons on different field trips in Zimbabwe, Tanzania, Sudan, Peru and Australia. Species assignment was performed by using the field guides of Clayton and Renvoize (1986) and Gibbs Russell et al. (1991). The samples were dried at 65°C, ground and stored in annealed glasses. E.-D. Schulze collected plants on a field trip in Namibia in the dry season of 1964. Prof. O. Volk, University of Würzburg (Germany), determined the species. After drying the samples were stored between pieces of paper in a herbarium. A. Gerecht collected grasses in Namibia during the dry season of 2004. The grass species were determined by using the field guide of van Oudtshoorn (1999).

Information about the analysed species, sampling locality and season is compiled in Table 2.1 (page 39). Of *Aristida meridionalis*, *Chloris virgata*, *Enneapogon cenchroides*, *Panicum maximum* and *Festuca orthophylla* we used duplicate samples collected during different field trips. Grasses collected during the dry seasons were mainly strawy. Three of the grasses had lost their reproductive parts (cf. Table 2.1). In general, however, complete grass plants were analysed. Sufficient material of *Sporobolus* sp. and *Brachiaria* sp. (Table 2.1) was available to separate them into flower heads, stems and leaves and, thus, to estimate the contribution of different plant parts to the whole wax signal of these species.

To extend the significance of our results by comparison, we collected analytical data of odd-carbon-numbered *n*-C<sub>27</sub> to *n*-C<sub>33</sub> *n*-alkanes and even-carbon-numbered free *n*-alkanols of grass waxes from the literature. Data of 291 grasses from different sampling sites in the world were used to evaluate the general characteristics in wax lipid distribution

**Table 2.1.** Grass species studied: Subfamily, tribus, subtribus, species and photosynthetic group membership of analysed subspecies as well as C<sub>4</sub> physiology, sample locality and sampling season. Taxonomical classification after Clayton and Renvoise (1986), Watson and Dallwitz (1992a,b onwards) and Grass Phylogeny Working Group (2001); photosynthetic pathway, habitat and dispersal areas in southwest Africa after Watson and Dallwitz (1992a,b onwards) as well as C<sub>4</sub> physiology according to Ellis (1977), Watson and Dallwitz (1992a,b onwards) and Schulze et al. (1996).

| Subfamily     | Tribus        | Subtribus    | Species                     | Photosynthetic pathway | Preferred habitat and climate  | SW African Dispersal    |             |                       |          | Analysed subspecies          | C <sub>4</sub> physiology | Locality <sup>a</sup> (sampling season)                 |
|---------------|---------------|--------------|-----------------------------|------------------------|--|-------------------------|-------------|-----------------------|----------|------------------------------|---------------------------|---|
|               |               |              |                             |                        |  | West African rainforest | Namib-Karoo | South tropical Africa | Kalahari |                              |                           |   |
| Aristidoideae | Aristideae    |              | <i>Aristida</i> L.          | C <sub>4</sub>         | temperate and subtropical  | x                       | x           | x                     | x        | <i>A. adscensionis</i> *     | NADP-ME                   | Namibia <sup>2</sup> (dry)                              |
|               |               |              |                             |                        |  |                         |             |                       |          | <i>A. barbicollis</i>        | NADP-ME                   | Zimbabwe <sup>1</sup> (wet)                             |
|               |               |              |                             |                        |  |                         |             |                       |          | <i>A. congesta</i>           | NADP-ME                   | Namibia <sup>2</sup> (dry)                              |
|               |               |              |                             |                        |  |                         |             |                       |          | <i>A. graciliflora</i>       | NADP-ME                   | Zimbabwe <sup>1</sup> (wet)                             |
|               |               |              |                             |                        |  |                         |             |                       |          | <i>A. meridionalis</i>       | NADP-ME                   | Zimbabwe <sup>1</sup> (wet), Namibia <sup>2</sup> (dry) |
|               |               |              | <i>Stipagrostis</i> Nees    | C <sub>4</sub>         | desert and semidesert, sometimes dunes ( <i>S. ciliate</i> , a sandbinder)                                 |                         | x           | x                     | x        | <i>S. ciliate</i>            | NAD-ME                    | Namibia <sup>2</sup> (dry)                              |
|               |               |              |                             |                        |  |                         |             |                       |          | <i>S. hirtigluma</i>         | NAD-ME                    | Namibia <sup>2</sup> (dry)                              |
|               |               |              |                             |                        |  |                         |             |                       |          | <i>S. uniplumis</i>          | NAD-ME                    | Namibia <sup>2</sup> (dry)                              |
| Chloridoideae | Cynodonteae   | Chloridinae  | <i>Chloris</i> O. Swartz    | C <sub>4</sub>         | tropical and warm temperate, diverse habitats, mostly in short grassland on poor soils or disturbed ground | x                       | x           | x                     | x        | <i>C. gayana</i>             | PCK                       | Zimbabwe <sup>1</sup> (wet)                             |
|               |               |              |                             |                        |  |                         |             |                       |          | <i>C. virgata</i>            | PCK                       | Zimbabwe <sup>1</sup> (wet), Namibia <sup>2</sup> (dry) |
|               | Eragrostideae | Eleusiminae  | <i>Eragrostis</i> N.M. Wolf | C <sub>4</sub>         | cosmopolitan, subtropical, mostly open habitats, often on poor or sandy soils or disturbed ground          | x                       | x           | x                     | x        | <i>E. nindensis</i>          | NAD-ME                    | Namibia <sup>2</sup> (dry)                              |
|               |               |              |                             |                        |  |                         |             |                       |          | <i>E. superba</i>            | NAD-ME                    | Zimbabwe <sup>1</sup> (wet)                             |
|               |               |              |                             |                        |  |                         |             |                       |          | <i>E. tremula</i>            | NAD-ME                    | Sudan <sup>1</sup> (wet)                                |
|               |               |              |                             |                        |  |                         |             |                       |          | <i>E. violacea de winter</i> | NAD-ME                    | Zimbabwe <sup>1</sup> (wet)                             |
|               |               |              |                             |                        |  |                         |             |                       |          | <i>E. viscosa</i>            | NAD-ME                    | Zimbabwe <sup>1</sup> (wet)                             |
|               |               |              |                             |                        |  |                         |             |                       |          |                              |                           |   |
|               |               | Sporobolinae | <i>Sporobolus</i> R.Br.     | C <sub>4</sub>         | tropical and warm temperate, diverse habitats including coastal sand dunes                                 | x                       | x           | x                     | x        | <i>S. ioclados</i>           | NAD-ME                    | Zimbabwe <sup>1</sup> (wet)                             |
|               |               |              |                             |                        |  |                         |             |                       |          | <i>S. pyramidalis</i>        | PCK                       | Zimbabwe <sup>1</sup> (wet)                             |
|               |               |              |                             |                        |  |                         |             |                       |          | <i>Sporobolus</i> sp.        | (?)                       | Tanzania <sup>1</sup> (wet)                             |
|               |               |              |                             |                        |  |                         |             |                       |          |                              |                           |   |
|               | Pappophoreae  |              | <i>Enneapogon</i> Desv.     | C <sub>4</sub>         | in warm regions, open habitats, bushland and semidesert  |                         | x           | x                     | x        | <i>E. cenchroides</i>        | NAD-ME                    | Zimbabwe <sup>1</sup> (wet), Namibia <sup>2</sup> (dry) |
|               |               |              | Ex P. Beauv.                |                        |  |                         |             |                       |          | <i>Enneapogon</i> sp.        | NAD-ME                    | Namibia <sup>3</sup> (dry)                              |
|               |               |              | <i>Schmidtia</i> Steud.     | C <sub>4</sub>         | tropical and dry, open habitats, woods and bushland, on dry sandy soils                                    |                         | x           | x                     | x        | <i>S. kalahariensis</i> *    | PCK                       | Namibia <sup>2</sup> (dry)                              |

cont. Table 2.1. Grass species studied.

| Subfamily   | Tribus        | Subtribus      | Species                           | Preferred habitat and climate  | SW African Dispersal    |             |                       |          | Analysed subspecies    | C <sub>4</sub> physiology | Locality <sup>a</sup><br>(sampling season) |
|-------------|---------------|----------------|-----------------------------------|--|-------------------------|-------------|-----------------------|----------|------------------------|---------------------------|--|
|             |               |                |                                   |  | West African rainforest | Namib-Karoo | South tropical Africa | Kalahari |                        |                           |  |
| Panicoideae | Andropogoneae | Andropogoninae | <i>Bothriochloa</i> Kuntze        | C <sub>4</sub> warm regions, open habitats, grassy places  | x                       | x           | x                     | x        | <i>B. insculpta</i>    | NADP-ME                   | Zimbabwe (wet)                             |
|             |               |                | <i>Hyparrhenia</i> Anderss.       | C <sub>4</sub> commonly adventive, open habitats, savannah   | x                       | x           | x                     | x        | <i>H. filipendula</i>  | NADP-ME                   | Zimbabwe (wet)                             |
|             |               |                | <i>Themeda</i> Forssk.            | C <sub>4</sub> commonly adventive, open habitats, warm   | x                       | x           |                       |          | <i>T. triandra</i>     | NADP-ME                   | Zimbabwe (wet)                             |
|             |               |                | <i>Loudetia</i> Hochst.           | C <sub>4</sub> tropical, open habitats, in savannah, woodland, often on poor shallow soils                     | x                       | x           | x                     | x        | <i>L. simplex</i>      | NADP-ME                   | Zimbabwe (wet)                             |
|             |               |                | <i>Digitaria</i> Haller           | C <sub>4</sub> mainly warm regions, mostly open habitats including weedy ground and sandy beaches              | x                       | x           | x                     | x        | <i>D. milaniana</i>    | NADP-ME                   | Zimbabwe (wet)                             |
| Poaceae     | Digitariinae  | Setariinae     | <i>Bracharia</i> (trin.) Gribseb. | C <sub>4</sub> shade species or of open habitats   | x                       | x           | x                     | x        | <i>B. eruciformis</i>  | PCK                       | Zimbabwe (wet)                             |
|             |               |                | <i>Panicum</i> L.                 | C <sub>4</sub> tropical, subtropical and warm temperate, commonly adventive, shade and open habitats           | x                       | x           | x                     | x        | <i>Bracharia</i> sp.   | PCK                       | Tanzania <sup>1</sup> (wet)                |
|             |               |                |                                   |  |                         |             |                       |          | <i>P. arbusculum</i> * | NAD-ME                    | Namibia <sup>2</sup> (dry)                 |
|             |               |                |                                   |  |                         |             |                       |          | <i>P. maximum</i>      | PCK                       | Zimbabwe (wet), Namibia <sup>2</sup> (dry) |
|             |               |                |                                   |  |                         |             |                       |          | <i>Panicum</i> sp.     | (?)                       | Namibia <sup>3</sup> (dry)                 |
| Poideae     | Bromeae       | Poeae          | <i>Bromus</i> L.                  | C <sub>3</sub> temperate and tropical mountains, commonly adventive, shade and open habitats                   | x                       |             | x                     |          | <i>Bromus</i> sp.      |                           | Australia (wet)                            |
|             |               |                | <i>Festuca</i> L.                 | C <sub>3</sub> worldwide temperate and mountains, commonly adventive, hillsides, mountains, plains and meadows | x                       |             | x                     |          | <i>F. orthophylla</i>  |                           | Peru (wet)                                 |

\* Sample without inflorescence part

<sup>a</sup> Grasses were made available by: <sup>1</sup> = R.W. Mayes, <sup>2</sup> = E.-D. Schulze, <sup>3</sup> = A. Gerech.

patterns of a given subfamily as well as averages of the three C<sub>4</sub> subtypes (cf. Figs. 2.4, 2.5, and 2.6, and their legends).

### 2.3.3 Analytical and evaluation methods

The analytical procedures were similar to those previously described by Mangelsdorf et al. (2000) apart from the details noted below. For lipid analyses grass aliquots of 0.5 to 2 g were extracted. Two different extraction methods, optimized to ascertain comparability with respect to efficiency and selectivity, were used. E.-D. Schulze's and A. Gerecht's non-ground grass samples were extracted ultrasonically using a mixture of dichloromethane and methanol (99/1, v/v; 5 times 60 mL, each 60 s). R.W. Mayes' ground grass samples were extracted in an Accelerated Solvent Extractor (ASE) using dichloromethane and methanol (99/1, v/v; three times 70 bar and 100°C, each 5 min.). Squalane, erucic acid (*n*-C<sub>22:1</sub>), 5 $\alpha$ -androstan-17-one and 5 $\alpha$ -androstan-3 $\beta$ -ol were added to the extracts as internal standards. The *n*-hexane-soluble plant lipids were separated by medium-pressure liquid chromatography (Radke et al., 1980) into fractions of aliphatic/alicyclic hydrocarbons, aromatic hydrocarbons and polar heterocomponents (NSO). Carboxylic acids were separated from the NSO fraction by using a column with potassium hydroxide-impregnated silica gel.

*n*-Alkanols were isolated by urea adduction. The lipid fraction was dissolved in 1 mL *n*-hexane. To facilitate crystallisation, 3  $\mu$ g of *n*-dotetracontane (*n*-C<sub>42</sub>H<sub>86</sub>) were added. While shaking, 1.0 mL of acetone and 1.5 mL of a saturated methanolic urea solution was added. Crystallisation of the urea adduct started immediately. During a short heating period the crystals redissolved and then recrystallised slowly by cooling over night. The crystals were dried under a stream of nitrogen without heating. The nonadduct fraction was extracted four times with 8 mL of *n*-hexane. After each addition of *n*-hexane, the sample was dispersed ultrasonically (30 s) and centrifuged (10 min at 3000 min<sup>-1</sup>). The solution above the crystals was removed each time using a pipette. The entire adduction procedure was repeated with the resulting crude nonadduct. Both adduct fractions were then dissolved in 2 mL water, combined and extracted 5 times with 4 mL *n*-hexane. The solution was dried with sodium sulphate (1 h) and filtered. The solvent was removed under reduced pressure. Urea adduction was repeated once with this adduct fraction. *n*-Alkanols were converted to their trimethylsilyl ether derivatives before analysis by gas chromatography (GC).

The wax lipids were analysed by gas chromatography with a flame ionisation detector (GC-FID), gas chromatography-mass spectrometry (GC-MS), and a GC coupled to a Finnigan MAT 252 isotope mass spectrometer for compound-specific stable carbon

isotope ratios (GC-irm-MS). The purity of lipid fractions for isotopic measurements was checked by GC-MS. GC-irm-MS analyses were run in duplicate or triplicate with standard deviations better than 0.5‰. Isotopic ratios are expressed as  $\delta^{13}\text{C}$  values in per mil relative to the V-PDB standard. Contents as well as  $\delta^{13}\text{C}$  values of *n*-alkanols are corrected for the contribution of the trimethylsilyl group from derivatisation. The  $\delta^{13}\text{C}$  values are expressed as single weighted mean averages for the odd-carbon-numbered *n*-C<sub>27</sub> to *n*-C<sub>35</sub> alkanes ( $\delta^{13}\text{C}_{\text{WMA27-35}}$ ) as well as for the even-carbon-numbered *n*-C<sub>22</sub> to *n*-C<sub>32</sub> alkanols ( $\delta^{13}\text{C}_{\text{WMA22-32}}$ ) in order to encompass the variability of data for individual homologues.

Plant wax biomarker contents were calculated as  $\mu\text{g g}^{-1}$  dry plant material (DM) based on signal intensities of biomarkers and internal standards in the GC-FID traces. For an assessment of systematics in the distribution patterns of biomarkers, contents of individual homologues were converted into percentage of that biomarker within the homologous series to allow comparison of samples after averaging. In order to find systematic patterns of chemical composition, we performed an agglomerate hierarchical cluster analysis by using the SYSTAT 11 software for Windows and the minimum variance Ward linkage (squared Euclidean distances; for more details see Kaufmann and Rousseeuw, 1990, as well as Legendre and Legendre, 1998).

Seven aliphatic/alicyclic fractions of grass lipid samples were contaminated by fossil fuel refinery products (Tables 2.3a and 2.4 page 59 and 63, respectively), albeit in a small proportion relative to the main *n*-alkane homologues. For a correction of the distribution patterns and  $\delta^{13}\text{C}$  values we applied the mass balance approach of Huang et al. (2000). Generally, the odd-carbon-number predominance of wax *n*-alkanes of terrestrial higher plants is expressed as a high carbon preference index (CPI >5; e.g. Collister et al., 1994), whereas oil-derived *n*-alkanes have no significant odd-over-even carbon number predominance and, thus, a CPI close to 1 (Bray and Evans, 1961). In our slightly contaminated samples we detected a decrease in CPI values and a shift to lighter  $\delta^{13}\text{C}$  values in the range of the *n*-C<sub>19</sub> to *n*-C<sub>29</sub> alkanes. The contamination maximised at the *n*-C<sub>23</sub> alkane. For correction, we assumed that (a) due to significant variations in CPI of higher land plants the averaged CPI of our unpolluted grass samples ( $\text{CPI}_{\text{av}} = 15.6$ ) represents the typical grass wax CPI, (b) the *n*-alkanes of the fossil fuel have a CPI of 1, and (c) the averaged  $\delta^{13}\text{C}$  values of the *n*-C<sub>20</sub> to *n*-C<sub>24</sub> alkanes in each polluted sample represent the stable carbon isotopic composition of the fossil fuel *n*-alkanes. Assuming that the relative contribution of contamination to the *n*-C<sub>n</sub> and *n*-C<sub>n+1</sub> alkanes ( $n = 25, 27, 29$ ) is equal, we can write:

$$\text{CPI}_{\text{av}} = \frac{A_{\text{W},n}}{A_{\text{W},n+1}} = \frac{A_n - A_{\text{x},n}}{A_{n+1} - A_{\text{x},n}} \quad \text{or} \quad A_{\text{x},n} = \frac{\text{CPI}_{\text{av}} \times A_{n+1} - A_n}{\text{CPI}_{\text{av}} - 1}$$

where  $n$  and  $n+1$  refer to  $n$ -C <sub>$n$</sub>  and  $n$ -C <sub>$n+1$</sub>  alkanes,  $A$  = abundance,  $w$  = grass wax  $n$ -alkane,  $x$  = contamination.  $A_n$  and  $A_{n+1}$  are the measured abundances of  $n$ -C <sub>$n$</sub>  and  $n$ -C <sub>$n+1$</sub>  alkanes in grass waxes and  $A_{x,n}$  is the abundance of the  $n$ -C <sub>$n$</sub>  alkane in the fossil fuel (after Huang et al., 2000). Simple subtraction of  $A_{x,n}$  from  $A_n$  leads to  $A_{w,n}$ . By using  $A_{x,n}$  and a bimodal mixture model we corrected the molecular  $\delta^{13}\text{C}$  values in the following way:

$$\delta^{13}\text{C}_n \times A_n = \delta^{13}\text{C}_{w,n} \times (A_n - A_{x,n}) + \delta^{13}\text{C}_x \times A_{x,n}$$

where  $\delta^{13}\text{C}_n$  refers to the measured  $\delta^{13}\text{C}$  value of the  $n$ -C <sub>$n$</sub>  alkane and  $\delta^{13}\text{C}_x$  refers to the averaged  $\delta^{13}\text{C}$  values of the  $n$ -C<sub>20</sub> to  $n$ -C<sub>24</sub> alkanes in the same sample.

## 2.4 Results

### 2.4.1 Contents and carbon number distributions of long-chain $n$ -alkanes of grass waxes

Lipids in the fractions of the aliphatic/alicyclic hydrocarbons of the organic solvent extracts of grass samples are dominated by homologous series of  $n$ -alkanes. They have 27 to 35 carbon atoms in the long-chain range. Shorter- and longer-chain  $n$ -alkanes were detected, but they are present in small quantities and, thus, have less chemotaxonomic significance. The  $\text{CPI}_{27-35}$  values are high and range from 6.7 to 30.2 (Table 2.3a).

The total content of odd-carbon-numbered  $n$ -C<sub>27</sub> to  $n$ -C<sub>35</sub> alkanes ( $\text{TCOC}_{27-35}$ ) of whole grass samples varies significantly between  $85.5 \mu\text{g g}^{-1}$  DM and  $1,295 \mu\text{g g}^{-1}$  DM. Of the plant parts studied separately, the flower heads of *Brachiaria* sp. and *Sporobolus* sp. have the highest  $\text{TCOC}_{27-35}$  values ( $860$  and  $610 \mu\text{g g}^{-1}$  DM, respectively), followed by leaves ( $226$  and  $80 \mu\text{g g}^{-1}$  DM), whereas stems have less of these alkanes ( $76.1$  and  $34.8 \mu\text{g g}^{-1}$  DM; Table 2.3a). The total  $n$ -alkane contents of grasses may be affected by different contributions of flowers, leaves and stems. In the present study, limited to two species, analysis reveals that flower heads contain markedly higher amounts of the  $n$ -C<sub>27</sub> and  $n$ -C<sub>29</sub> alkanes compared to leaves and stems of the same species (Fig. 2.3). Especially in the *Brachiaria* sp. sample the distribution pattern maxima differ significantly, i.e. they shift from  $n$ -C<sub>33</sub> in the leaves and stems to the  $n$ -C<sub>27</sub> alkane in the flowers. In addition, the flowers contain significant amounts of shorter-chain  $n$ -alkanes (an additional 16% of the  $n$ -C<sub>25</sub> and 1% of the  $n$ -C<sub>23</sub> alkane; cf. Fig. 2.3). The overall chain length distribution, best expressed by the average chain length parameter in the odd-carbon-number range 27 to 35 ( $\text{ACL}_{27-35}$ ; Poynter et al., 1989), is more or less the same in leaves

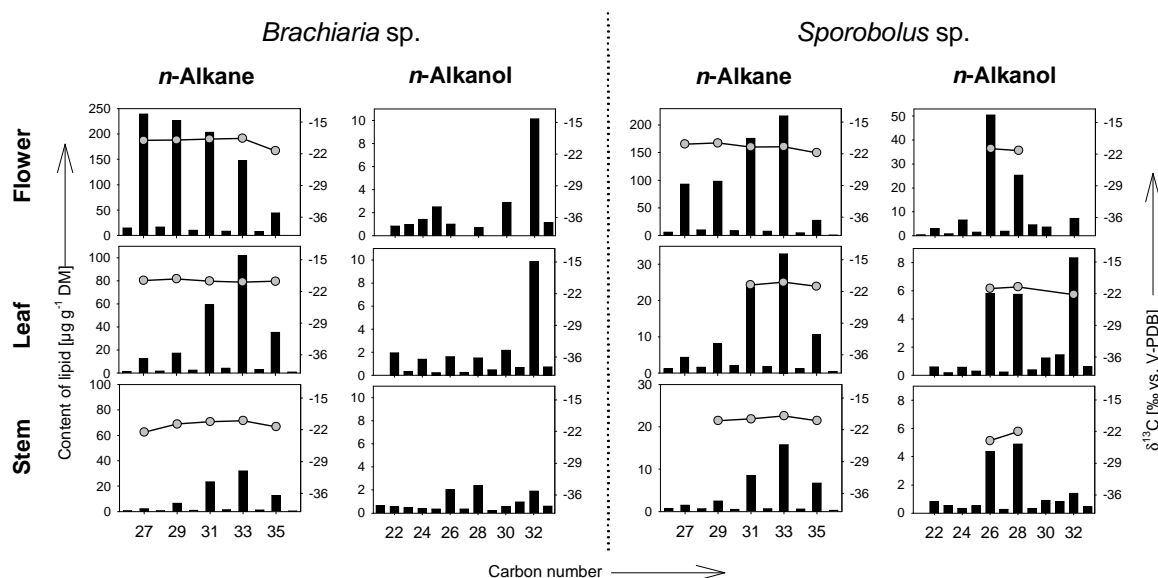


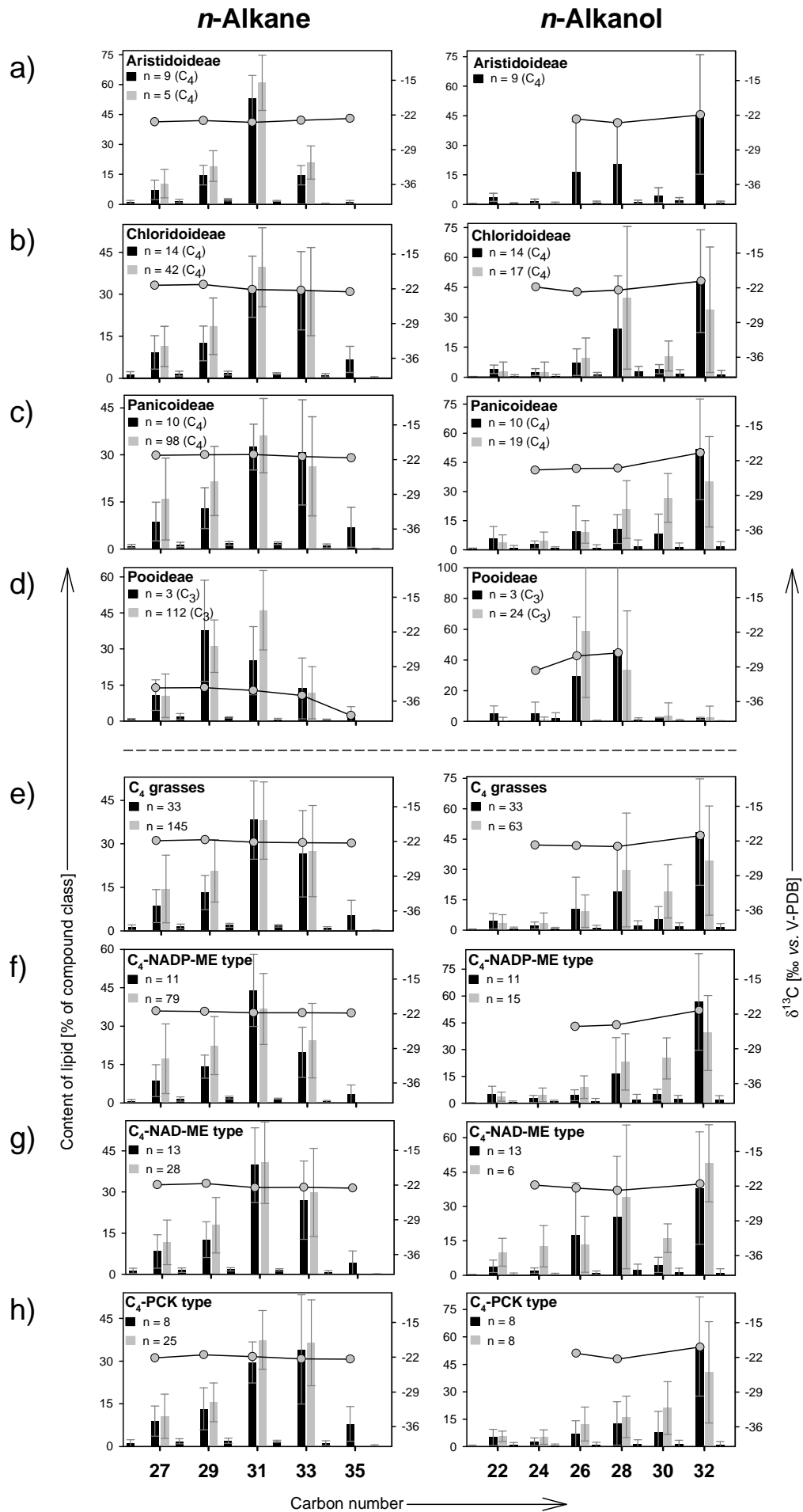
**Fig. 2.3** Histogram representations of long-chain *n*-alkane and *n*-alkanol contents (in  $\mu\text{g g}^{-1}$  DM, left Y-axis), overlain by molecular stable carbon isotope data ( $\circ$ ;  $\delta^{13}\text{C}$  in ‰ versus V-PDB, right Y-axis) of individual homologues in waxes of grass flowers, leaves and stems of one species each of *Brachiaria* (Panicoideae, C<sub>4</sub>) and *Sporobolus* (Chloridoideae, C<sub>4</sub>). The histograms of the compounds in the flowers are individually normalised to the most abundant homologue, whereas each leaf and stem pair are normalised together to the most abundant homologue.

and stems. The  $\text{ACL}_{27-35}$  values decrease from around 32.17 for stem and leaf *n*-alkanes in *Brachiaria* sp. and *Sporobolus* sp. to 29.91 and 30.96 for flower head *n*-alkanes (Table 2.3a). Thus, the amount of shorter-chain *n*-alkane homologues outside the main long-chain range of the whole plant wax *n*-alkane distribution can be described by the flower/leaf alkane ratio.

The *n*-alkane distribution patterns of whole grass plant waxes maximise either at the *n*-C<sub>29</sub>, *n*-C<sub>31</sub> or *n*-C<sub>33</sub> alkane (Table 2.3a). The subspecies of *Aristida*, *Stipagrostis* and *Sporobolus*, as well as the duplicate samples of *Aristida meridionalis*, *Festuca orthophylla* and *Panicum maximum* exhibit consistent *n*-alkane patterns. The members of other subspecies have *n*-alkane distribution patterns which resemble each other, but are not constant. Variations on the species level are difficult to evaluate due to inconsistent flower/leaf ratios and different habitats and sampling seasons of the grasses. However, on a subfamily level the distribution patterns are more systematic, e.g. the C<sub>4</sub> species of Aristidoideae always show a distribution maximum at the *n*-C<sub>31</sub> alkane. The *n*-alkanes of grasses from the other C<sub>4</sub> subfamilies (Chloridoideae and Panicoideae) have a maximum either at the *n*-C<sub>31</sub> or the *n*-C<sub>33</sub> homologue. On the other hand, the two different C<sub>3</sub> species of the Pooideae subfamily contain more abundant shorter-chain *n*-alkanes, and the long-chain homologues maximise at *n*-C<sub>29</sub> or *n*-C<sub>31</sub> (Table 2.3a).

Averaged *n*-alkane distribution patterns of subfamilies and plants having the same photosynthetic pathway or physiology are shown in Fig. 2.4; numerical data of





averaged proxies are compiled in Table 2.2 (page 47). The subfamilies have averaged ACL<sub>27-35</sub> values, which increase from 30.10 for Pooideae to 30.74 for Aristidoideae, 31.24 for Chloridoideae and 31.27 for Panicoideae (Table 2.2). Generally, the averaged distribution patterns separate the Pooideae from the subfamilies comprising the C<sub>4</sub> grasses. Thus, distributions maximising at slightly shorter-chain *n*-alkanes are typical of C<sub>3</sub> grasses, whereas longer-chain maxima characterise C<sub>4</sub> grasses (Fig. 2.4d-e). A further separation was observed between the aristidoid C<sub>4</sub> species and the remaining C<sub>4</sub> containing subfamilies. The chloridoids and panicoids are similar in averaged *n*-alkane distribution patterns (Fig. 2.4a-c). Within the three C<sub>4</sub> subtypes the *n*-C<sub>33</sub> alkane contents increase from the NADP-ME to the NAD-ME and PCK subtypes (Fig. 2.4f-h). Accordingly, the average ACL<sub>27-35</sub> values increase from 30.87 (NADP-ME) to 31.09 (NAD-ME) and 31.37 (PCK; Table 2.2).

#### 2.4.2 Molecular carbon isotope signatures of long-chain *n*-alkanes of grass waxes

The compound-specific  $\delta^{13}\text{C}$  values of the individual odd-carbon-numbered *n*-alkanes (Table 2.4, Figs. 2.3 and 2.4) are consistent with their origins in waxes of C<sub>3</sub> and C<sub>4</sub> higher land plants. The weighted mean average of  $\delta^{13}\text{C}$  values ranges from -18.7‰ to -25.8‰ and centres at -21.7‰ for C<sub>4</sub> grasses, compared to a range of -30.4‰ to -36.4‰ and a centre at -33.8‰ for the few C<sub>3</sub> grasses examined (Tables 2.4 and 2.2). The wax *n*-alkanes of individual plant parts exhibit no significant distinctions in the  $\delta^{13}\text{C}_{\text{WMA27-35}}$  values for the two species (*Bracharia* sp. and *Sporobolus* sp.) sampled (Table 2.4, Fig. 2.3).

Three characteristic  $\delta^{13}\text{C}_{\text{WMA27-35}}$  ranges occur within the subfamilies. As expected, the lightest values belong to the C<sub>3</sub> pooid grasses. The  $\delta^{13}\text{C}_{\text{WMA27-35}}$  values of the C<sub>4</sub> species separate the aristidoid grasses from the other C<sub>4</sub> subfamilies by the former having about 2‰ lighter  $\delta^{13}\text{C}$  values (Table 2.2). The variations of  $\delta^{13}\text{C}_{\text{WMA27-35}}$  within the C<sub>4</sub> subtypes spread from -21.3‰ for NADP-ME subtype species to -21.7‰ for NAD-ME subtypes and to -22.0‰ for PCK-subtypes (Table 2.2). This trend differs slightly from that of bulk  $\delta^{13}\text{C}$

**Fig. 2.4.** (opposite) Averaged histogram representations of long-chain *n*-alkane and *n*-alkanol content (content in % of compound class, left Y-axis) based on data for odd *n*-C<sub>27</sub> to *n*-C<sub>35</sub> alkanes and even *n*-C<sub>22</sub> to *n*-C<sub>32</sub> alkanols (black bars), overlain by molecular stable carbon isotope data ( $\delta^{13}\text{C}$  in ‰ versus V-PDB, right Y-axis) of individual homologues (this study) as well as averaged histogram representation of published data of odd *n*-C<sub>27</sub> to *n*-C<sub>33</sub> alkanes and even *n*-C<sub>22</sub> to *n*-C<sub>32</sub> alkanols (grey bars; from Smith and Martin-Smith, 1978; Tulloch, 1981, 1982, 1984; Spencer and Champman, 1985; Mayes et al., 1986; Dove et al., 1990; Malossini et al., 1990; Dove and Mayes, 1991; Laredo et al., 1991; Dove, 1992; Mayes et al., 1994; Dove et al., 1996; Maffei, 1996; Chen et al., 1998; Dawson et al., 2000; Delgado et al., 2000; Smith et al., 2001; Boadi et al., 2002; Ali, 2003; Chikaraishi and Naraoka, 2003). Displayed are averages of four grass subfamilies (a-d) and different types of C<sub>4</sub> photosynthesis (e-h). Data of duplicate samples are averaged. The diagrams are individually normalised to the most abundant homologue. n: number of species used for the averaging of data from this study (■) and from published data (▒).

Table 2.2. Averaged biomarker and isotope data.

|                                 | <i>n</i> -Alkane                          |   |   | <i>n</i> -Alkanol                         |   |   |
|---------------------------------|---|---|---|---|---|---|
|                                 | CPI <sub>27-35</sub> <sup>a</sup><br>(SD) | ACL <sub>27-35</sub> <sup>b</sup><br>(SD) | ACL <sub>LIT-27-33</sub> <sup>c</sup><br>(SD)           | CPI <sub>22-32</sub> <sup>a</sup><br>(SD) | ACL <sub>22-32</sub> <sup>b</sup><br>(SD) | ACL <sub>LIT-22-32</sub> <sup>c</sup><br>(SD)           |
|                                 |   |   | δ <sup>13</sup> C <sub>WMA27-35</sub> <sup>d</sup><br>‰ |   |   | δ <sup>13</sup> C <sub>WMA22-32</sub> <sup>d</sup><br>‰ |
| Aristidoideae (C <sub>4</sub> ) | 16.2<br>(± 6.3)                           | 30.74<br>(± 0.40)                         | 30.67<br>(± 0.68)                                       | 16.1<br>(± 10.4)                          | 29.43<br>(± 1.68)                         | -<br>(± 2.8)  |
| Chloridoideae (C <sub>4</sub> ) | 15.3<br>(± 5.4)                           | 31.24<br>(± 0.68)                         | 30.79<br>(± 0.66)                                       | 19.1<br>(± 23.2)                          | 29.64<br>(± 1.10)                         | 29.08<br>(± 1.62)                                       |
| Panicoideae (C <sub>4</sub> )   | 14.0<br>(± 2.2)                           | 31.27<br>(± 0.90)                         | 30.46<br>(± 0.88)                                       | 28.0<br>(± 34.0)                          | 29.71<br>(± 1.29)                         | 29.34<br>(± 1.09)                                       |
| Pooideae (C <sub>3</sub> )      | 21.2<br>(± 4.0)                           | 30.10<br>(± 1.18)                         | 30.19<br>(± 0.51)                                       | 54.0<br>(± 52.3)                          | 26.84<br>(± 1.31)                         | 26.92<br>(± 1.05)                                       |
| C <sub>4</sub> grasses          | 15.2<br>(± 4.9)                           | 31.11<br>(± 0.71)                         | 30.52<br>(± 0.81)                                       | 22.3<br>(± 26.7)                          | 29.37<br>(± 1.55)                         | 28.98<br>(± 1.52)                                       |
| C <sub>4</sub> -NADP-ME type    | 14.7<br>(± 3.4)                           | 30.87<br>(± 0.61)                         | 30.35<br>(± 0.86)                                       | 12.6<br>(± 8.6)                           | 30.04<br>(± 1.32)                         | 29.49<br>(± 1.01)                                       |
| C <sub>4</sub> -NAD-ME type     | 16.6<br>(± 6.4)                           | 31.09<br>(± 0.69)                         | 30.77<br>(± 0.71)                                       | 18.7<br>(± 12.1)                          | 29.04<br>(± 1.26)                         | 28.78<br>(± 2.06)                                       |
| C <sub>4</sub> -PCK type        | 13.6<br>(± 3.8)                           | 31.37<br>(± 0.82)                         | 30.99<br>(± 0.65)                                       | 35.9<br>(± 42.5)                          | 29.90<br>(± 1.21)                         | 29.32<br>(± 1.26)                                       |

SD: Standard deviation

<sup>a</sup>CPI<sub>27-35</sub>: Carbon preference index of *n*-alkanes (carbon number 27 - 35); CPI<sub>22-32</sub>: Carbon preference index of *n*-alkanols (carbon number 22 - 32)<sup>b</sup>ACL<sub>27-35</sub>: Averaged chain length of odd-carbon-numbered *n*-alkanes (carbon number 27 - 35); ACL<sub>22-32</sub>: Averaged chain length of even-carbon-numbered *n*-alkanols (carbon number 22 - 32)<sup>c</sup>ACL<sub>LIT-27-33</sub>: Averaged chain length of odd-carbon numbered *n*-alkanes (carbon number 27 - 33) from bibliographic data; ACL<sub>LIT-22-32</sub>: Averaged chain length of even-carbon numbered *n*-alkanols (carbon number 22 - 32) from bibliographic data (cf. Fig. 2.4);<sup>d</sup>δ<sup>13</sup>C<sub>WMA27-35</sub>: Weighted mean average of molecular stable carbon isotopic composition of odd-carbon-numbered *n*-alkanes (carbon number 27 - 35) [‰ versus V-PDB]; δ<sup>13</sup>C<sub>WMA22-32</sub>: Weighted mean average of measured molecular stable carbon isotopic composition of even-carbon-numbered *n*-alkanols (carbon number 22 to 32) [‰ versus V-PDB] (note that mean average values for given sample were only calculated of the alkane and alkanol homologues for which carbon isotopic ratios were available)

values of grasses of the three C<sub>4</sub> subtypes determined by Hattersley (1982) and Schulze et al. (1996). The differences among the  $\delta^{13}\text{C}_{\text{WMA27-35}}$  values of the subtypes are within the standard deviation of molecular  $\delta^{13}\text{C}$  values of 0.5‰, i.e. significantly smaller than the standard deviation of 1.3‰ and 2.0‰ of the averaged values (Table 2.2), which suggests that carbon isotope values cannot be used reliably for chemotaxonomic classification at this level.

#### 2.4.3 Contents and carbon number distributions of long-chain *n*-alkanols of grass waxes

Free wax *n*-alkanols exhibit a pronounced even-over-odd carbon number predominance of long-chain components, which mainly comprise the *n*-C<sub>22</sub> to *n*-C<sub>32</sub> homologues. The *n*-alkanol CPI<sub>22-32</sub> values range from 2.3 to 112.2 and centre at about 22.3 (Table 2.3b, page 61). The total content of even-carbon-numbered *n*-alkanols (TCEC<sub>22-32</sub>) varies significantly from 10.5 to 777 µg g<sup>-1</sup> DM, whereas in general the *n*-C<sub>22</sub> to *n*-C<sub>31</sub> alkanols are less abundant than the *n*-C<sub>27</sub> to *n*-C<sub>35</sub> alkanes in the same species (cf. Tables 2.3b and 2.3a). TCEC<sub>22-32</sub> values of individual parts of the two grass species examined exhibit a trend similar to that found for the *n*-alkanes and are highest in flower heads followed by leaves and are lowest in stems (Table 2.3b). The corresponding carbon number distributions do not reveal relationships with plant classification similar to those found for the *n*-alkanes (Fig. 2.3). The *n*-alkanol pattern of *Sporobolus* sp. flower heads is dominated by *n*-C<sub>26</sub> and *n*-C<sub>28</sub> alkanols, whereas in the leaves the *n*-C<sub>32</sub> compound appears as an additional major homologue. The *n*-alkanol pattern in the stem is similar to that in flower heads. In flower heads and leaves of *Brachiaria* sp. the *n*-C<sub>32</sub> homologue is the principal *n*-alkanol, whereas stems are dominated by the *n*-C<sub>28</sub> alkanol.

In most samples studied, the *n*-alkanol distribution patterns are not unimodal or in a bell-shaped curve as found for the *n*-alkanes. Generally, one or two *n*-alkanols, mainly *n*-C<sub>26</sub>, *n*-C<sub>28</sub> or *n*-C<sub>32</sub>, dominate (Table 2.3b). The *n*-C<sub>30</sub> alkanol is not a prominent homologue, as it is typically for higher plant waxes (Bianchi, 1995). The C<sub>30</sub> alkanol has been reported to have hormonal activity as a plant growth regulator (Ries et al., 1977) and, thus, may be partly retained in the interior of the cell.

The waxes of the few C<sub>3</sub> grasses included in this study mainly contain *n*-C<sub>26</sub> and *n*-C<sub>28</sub> alkanols (Fig. 2.4d), with either one dominating (Table 2.3b). In contrast to this, in C<sub>4</sub> grass waxes (Fig. 2.4e) the *n*-C<sub>32</sub> alkanol generally appears as the major homologue. The *n*-C<sub>32</sub> alkanol is almost totally absent in the C<sub>3</sub> grasses (cf. Fig. 2.4d,e). This separates the Pooideae from those subfamilies using C<sub>4</sub> photosynthesis (cf. Fig. 2.4a-d). The averaged ACL<sub>22-32</sub> values increase from Pooideae (26.84) to Aristidoideae (29.43), Chloridoideae

(29.64) and finally Panicoideae (29.71; Table 2.2). This trend is similar to that found for *n*-alkane patterns. The alkanol distribution patterns of the C<sub>4</sub> subtypes (Fig. 2.4f-h) generally exhibit the *n*-C<sub>32</sub> compound as the major homologue, whereas the NAD-ME subtype additionally has a higher content of the shorter-chain *n*-C<sub>26</sub> and *n*-C<sub>28</sub> alkanols; this property separates it from the PCK and NADP-ME subtypes (Fig. 2.4f-h).

#### 2.4.4 Molecular carbon isotope signatures of long-chain *n*-alkanols of grass waxes

The  $\delta^{13}\text{C}$  values of the *n*-alkanols of the C<sub>4</sub> grasses are in the range of those found for the *n*-alkanes. The  $\delta^{13}\text{C}_{\text{WMA22-32}}$  values vary from -18.6‰ to -25.5‰ and centre at about -21.4‰. However, the C<sub>3</sub> grass wax *n*-alkanols are markedly less <sup>13</sup>C-depleted than the associated *n*-alkanes, and their  $\delta^{13}\text{C}_{\text{WMA}}$  values range from -26.1‰ to 28.4‰, centring at about -26.7‰ (Tables 2.4 and 2.2), although the few data points limit the significance of this remarkable observation. More extensive study of C<sub>3</sub> grasses is desirable if this unexpected inconsistency between the *n*-alkane and *n*-alkanol  $\delta^{13}\text{C}$  data is to be resolved. The *n*-alkanols of individual plant parts of *Sporobolus* sp. show decreasing  $\delta^{13}\text{C}_{\text{WMA22-32}}$  values from the flower head and leaves (about -21.1‰) to the stem (-23.0‰; Table 2.4). Due to low *n*-alkanol contents in the plant parts of *Brachiaria* sp. no reliable  $\delta^{13}\text{C}$  values are available. On the subfamilial level the averaged  $\delta^{13}\text{C}_{\text{WMA22-32}}$  values separate the C<sub>4</sub> aristidoids from the other C<sub>4</sub> subfamilies by having about 1‰ lighter  $\delta^{13}\text{C}_{\text{WMA22-32}}$  values. This offset is consistent with that found for the *n*-alkane  $\delta^{13}\text{C}_{\text{WMA27-35}}$  values (Table 2.2). However, the alkanols of the three C<sub>4</sub> subtypes exhibit a trend opposite to that of their *n*-alkanes. The  $\delta^{13}\text{C}_{\text{WMA22-32}}$  values range from -20.3‰ (PCK) to about -21.8‰ (NADP-ME and NAD-ME) and have no correlation with the  $\text{ACL}_{22-32}$  values (Table 2.2).

## 2.5 Discussion

The fully developed grass plants we analysed (Table 2.1) grew in the wild in a variety of habitats and were collected in different seasons. The total contents of the most significant wax *n*-alkanes and *n*-alkan-1-ols in these grasses, expressed by their  $\text{TCOC}_{27-35}$  and  $\text{TCEC}_{22-32}$  values (Table 2.3a and 2.3b), do not reveal any systematics on a species or subfamily level. Variations of *n*-alkane contents of grass waxes as a function of different climatic conditions at the respective sampling sites were also described by Malossini et al. (1990) and Zhang et al. (2004). In three-fourths of our grass samples we observed lower  $\text{TCEC}_{22-32}$  values compared to the  $\text{TCOC}_{27-35}$  values of the same plants (cf. Table 2.3a,b).

It has been reported that the amount of free *n*-alkanols decreases during maturation of the plant (Tulloch, 1973; Bianchi et al., 1989; Avato et al., 1990). Normally, they are classified as major components of plant waxes with yields exceeding 60% (Baker, 1982; Avato et al., 1987), whereas *n*-alkanes are usually considered subordinate components (3-40%; Tulloch, 1976; Tulloch et al., 1980). Whereas the content of free *n*-alkanols decreases after full development of the plant, wax esters rapidly gain in relative importance. Shrivelling and loss of old leaf blades reduce the *n*-alkanol content of the total plant wax and increasing ester contents indicate new wax production (Tulloch, 1973). Lower *n*-alkanol than *n*-alkane contents may possibly be explained by the degree of senescence of the plants at the time of collection.

The total wax content of an entire plant depends on the different contributions by the different parts of the plants. Generally, the *n*-alkane contents decrease from flowers to leaves and finally to stems (Dove et al., 1996; Smith et al., 2001; Zhang et al., 2004). These findings are confirmed in this study by the TCOC<sub>27-35</sub> and TCEC<sub>22-32</sub> values of individual parts, although this type of analysis was performed for two grasses only, *Brachiaria* sp. and *Sporobolus* sp. The total *n*-alkane and *n*-alkanol contents of flower heads were about three times larger than in leaves and six times larger than in stems (Table 2.3a,b). Different wax quantity contributions by different parts of a plant may lead to significant seasonal variations of the whole-plant wax content. The flower/leaf wax ratio of a plant is thus an important factor for its characterisation. Loss of flower heads and leaves during senescence reduces the total wax biomarker contents of a plant (Smith et al., 2001).

The processes controlling the carbon number distributions of aliphatic wax components have not been clearly described in the literature. The variations observed in this study concerning different parts of the grass plant exhibit a tendency to higher contents of shorter-chain homologues in flowers (Fig. 2.3; cf. Dove et al., 1996; Smith et al., 2001). Nishimoto (1974a), Smith et al. (2001) and Zhang et al. (2004) found that the dominant alkane of plant waxes moves to shorter-chain-length homologues as soon as the plant enters the reproductive phase. Smith et al. (2001) also concluded that the difference in distribution patterns of wax *n*-alkanes of the same grass species, sampled during wet and dry seasons, respectively, may be attributed to the presence or absence of flower heads. Furthermore, they did not find any significant seasonal changes of individual *n*-alkane contents of stem and leaf samples, and there was also no change in the ranking of the more abundant alkanes. However, Tulloch's (1973) findings point to an additional influence on the *n*-alkane distribution pattern of different leaf parts. He found high contents of the *n*-C<sub>29</sub> alkane in grass sheath and flag leaf waxes, whereas the third-last leaf generation contained high amounts of the *n*-C<sub>31</sub> alkane. Changes in composition are

related to the stage of development, particularly to completion of the development of flag leaf and sheath. A similar effect on *n*-alkanes was noted by Laredo et al. (1991). However, the wax biomarker distribution patterns of the same grass species from different habitats and collecting seasons or within the same subspecies are not generally consistent (Table 2.3a,b), at least not in this limited survey.

Tulloch and Hoffman (1976) and Tulloch et al. (1980) did not observe changes in *n*-alkanol distribution patterns due to the effects described before and also saw no variations in repeated analyses of a number of perennial species. In contrast to this, Sauvaire et al. (1987) found evidence for lipid profile changes during the development of a leaf. We conclude that chemical classification of grass wax lipids based on homologue distribution patterns of individual subspecies or related species is not suitable to establish a phylogenetic influence on wax homologue distribution patterns.

Averaging the *n*-alkane and *n*-alkanol distributions and carbon isotope patterns on a subfamilial level (Table 2.2 and Fig. 2.4, black bars) exhibits a clearer systematics and allows the grasses to be divided chemotaxonometrically into two main groups: In the first group, the C<sub>3</sub> grasses of the Pooideae subfamily (Fig. 2.4d) have shorter-chain-length aliphatic compounds, mainly the *n*-C<sub>29</sub> and *n*-C<sub>31</sub> alkanes and the *n*-C<sub>26</sub> and *n*-C<sub>28</sub> alkanols. They also have lighter  $\delta^{13}\text{C}_{\text{WMA}}$  values. In the second group, the C<sub>4</sub> grasses of the Chloridoideae and Panicoideae subfamilies are generally characterised by their dominant *n*-C<sub>31</sub> and *n*-C<sub>33</sub> alkanes and the prominent *n*-C<sub>32</sub> alkanol, as well as heavier  $\delta^{13}\text{C}_{\text{WMA}}$  values (Fig. 2.4 and Table 2.2). In this comparison, the distribution patterns of Aristidoideae (Fig. 2.4a) are intermediate. In addition, the isotopic  $\delta^{13}\text{C}$  values of the aristidoid C<sub>4</sub> species exhibit, on average, 1‰ to 2‰ lighter values compared to the remaining C<sub>4</sub> grass subfamilies (Table 2.2). Possibly, this may be attributed to a specific property of *Aristida* having an uncommon triple layer C<sub>4</sub> anatomy: a mesophyll cell, inner bundle sheath and outer bundle sheath (Voznesenskaya et al., 2005). Anyway, it appears from the present analytical study of more than 30 subspecies that the *n*-C<sub>33</sub> alkane and *n*-C<sub>32</sub> alkanol are rather characteristic of C<sub>4</sub> grasses overall (Fig. 2.4e), whereas the *n*-C<sub>29</sub> alkane and the *n*-C<sub>26</sub> and *n*-C<sub>28</sub> alkanols are prominent in the pooid C<sub>3</sub> grasses (Fig. 2.4d).

Contents and distribution patterns of *n*-alkanes and *n*-alkanols in the leaf waxes of grasses have been reported in a number of studies scattered widely throughout the literature (Fig. 2.4; legend). Sampling, extraction and analysis procedures varied considerably but a useful collection of data exists for 257 grass subspecies in the case of the *n*-alkanes; data sets are less numerous for *n*-alkanols (69 subspecies). These literature data were used to compile the average histograms shown in Fig. 2.4 (grey bars; numerical data compiled in Table 2.2) where they are displayed in parallel with the limited but more uniformly generated data from the present study (black bars). Literature data for

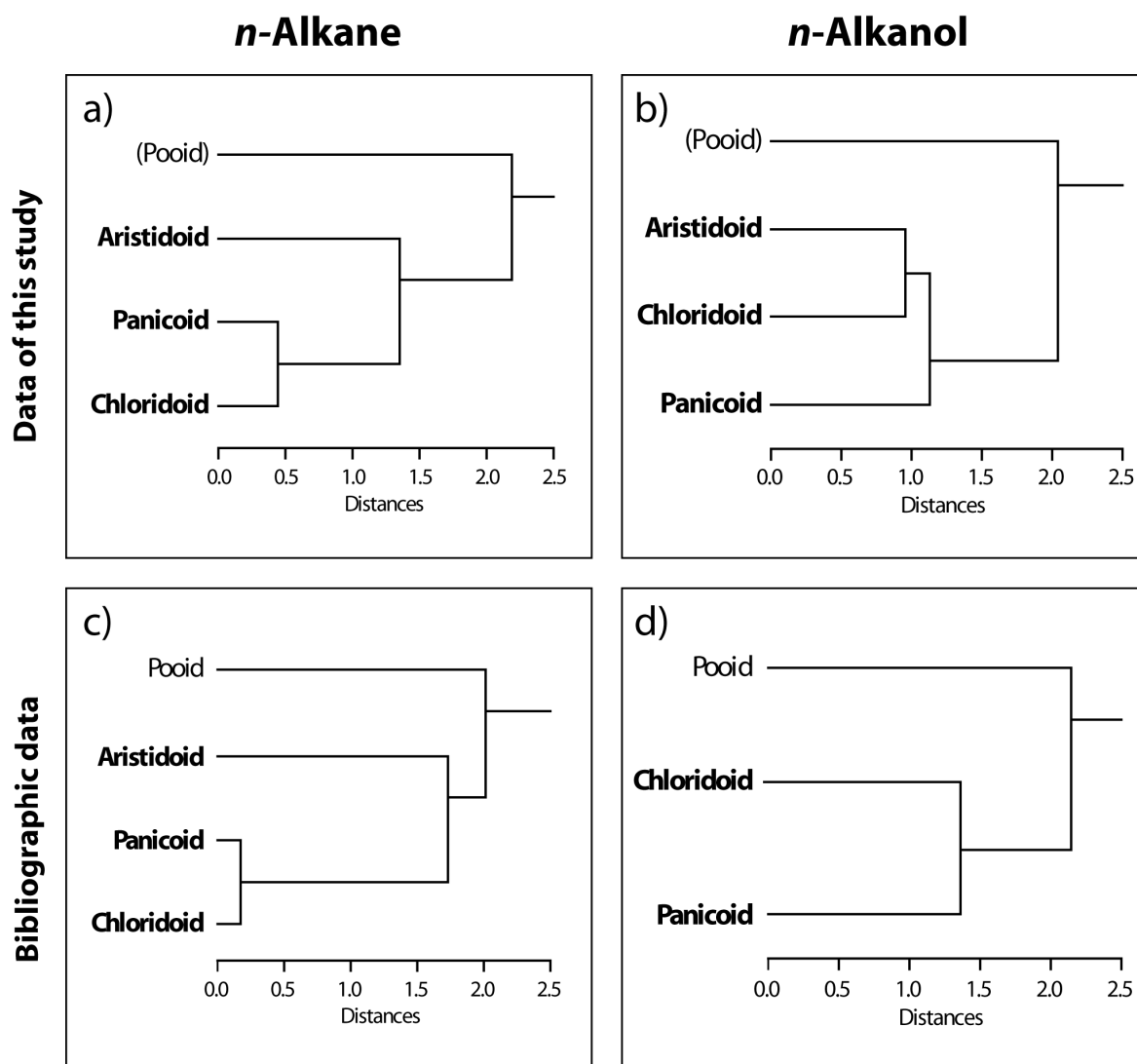


**Fig. 2.5.** Results of agglomerate hierarchical cluster analysis using averaged subfamilial a) *n*-alkane and b) *n*-alkanol data of contents and stable molecular carbon isotopic compositions of individual homologues based on analytical data of this study as well as c) *n*-alkane and d) *n*-alkanol data of contents of individual homologues based on bibliographic data (cf. Fig. 2.4) in poooid, aristidoid, chloridoid and panicoid waxes. Taxa that contain the C<sub>4</sub> photosynthetic mechanism are boldfaced. In Fig. 2.5d the aristidoid data are missing due to lacking bibliographic data.

compound-specific  $\delta^{13}\text{C}$  values are extremely sparse and are not presented in Fig. 2.4. Agreement between the average histograms for the subfamilies examined in the present study and those of the literature survey is generally good for the Aristidoideae, Chloridoideae and Panicoideae (Fig. 2.4a-c) which all comprise C<sub>4</sub> species. Hence, the use of the average histograms (Fig. 2.4e) for the *n*-alkanes and *n*-alkanols as being characteristic of the C<sub>4</sub> grasses appears justified. The situation for the Pooideae, however, is in a much more preliminary state, since only two grass species were analysed in the present study. However, the bibliographic data (of 112 subspecies for *n*-alkanes and of 24 subspecies for *n*-alkanols; cf. Fig. 2.4d) are sufficient to give confidence in the average histograms (grey bars) for this C<sub>3</sub> grass subfamily.



Cluster analysis of our data illustrates the chemical affinity of the waxes of the grass subfamilies. Fig. 2.5a,b displays cluster trees based on the averaged *n*-alkane and *n*-alkanol distribution patterns and on averaged compound-specific stable carbon isotopic compositions of the grass species studied. Fig 2.5c,d is based on the averaged *n*-alkane and *n*-alkanol distribution patterns of bibliographic data. The distance length exhibits the affinity of the nearest cluster. The *n*-alkane cluster tree (Fig. 2.5a) is similar to the evolutionary sequence (Fig. 2.2b) and exhibits a separation in the subfamilies comprising C<sub>4</sub> plants that is slightly different from that in the *n*-alkanol tree (Fig. 2.5b), which in turn matches the phylogenetic tree of the subfamilies (Fig. 2.2a). The same is evident for the bibliographic data (Fig 2.5c,d). Thus, the aristidoids in the *n*-alkane tree are completely separated from the panicoids and chloridoids (cf. Fig. 2.5a,c), the other C<sub>4</sub> subfamilies, whereas in the *n*-alkanol tree the chloridoids as well as the aristidoids are connected to each other in one cluster arm (cf. Fig. 2.5b,d). This confirms the ambivalent position of aristidoid waxes. Maffei (1996) observed a similar separation of *n*-alkane distribution patterns between Pooideae and the C<sub>4</sub>-plant-containing subfamilies based on the *n*-C<sub>33</sub> alkane content. However, his cluster analysis used *n*-alkane and *iso*-alkane data and was limited mainly to pooid (C<sub>3</sub>) species.

Averaged C<sub>4</sub> grass subtype distribution patterns of wax components, both in the literature and in the our study, exhibit an increase in *n*-C<sub>33</sub> alkane content from the NADP-ME to the NAD-ME and finally the PCK subtype, but there is no such trend in the averaged *n*-alkanol data. All subtype members generally contain the *n*-C<sub>32</sub> alkanol as the major homologue (Fig. 2.4f-h). Nine out of thirteen NAD-ME and five out of eight PCK subtype grasses belong to the Chloridoideae subfamily, whereas twelve NADP-ME subtype grasses are almost equally from the Aristidoideae and Panicoideae (Table 2.4).

## 2.6 C<sub>4</sub> grass wax adaptation and implications for palaeoenvironmental studies

### 2.6.1 C<sub>4</sub> grass wax adaptation to the climatic conditions of the habitat

Mean annual temperatures (about 25°C) and precipitation (2000 mm/a) in the northern part of our sampling area, the equatorial tropical rainforest, are relatively high, whereas southwards, the annual temperatures and precipitation decrease to about 19°C and 300 mm/a, respectively, in the grass-dominated Kalahari savanna and finally to 15°C and

15 mm/a, respectively, in the Walvis Bay area (cf. Fig. 2.1b,c; data from climatograms published by Walter et al., 1975). The rainforest has a closed canopy and humid overcast climate, which reduces direct sunlight irradiation of the vegetation and inhibits grass growth. The absolute maximum temperatures are at about 35°C. In contrast, the sparse vegetation of the Namib Desert is exposed to much higher absolute maximum temperatures of 40-50°C (according to van der Merwe, 1983) with the plants growing in the direct sunlight. Generally, tropical C<sub>4</sub> grasses occur in open environments, where temperature at the leaf surface may rise to extreme maximum temperatures eventually exceeding even those cited for the Namib Desert.

Kawamura et al. (2003) remarked that higher plants growing in tropical regions biosynthesise higher-molecular-weight waxes in response to higher ambient temperatures to maintain the hardness of their leaf surfaces. Leaf waxes occur as carpets of microcrystallites in the micrometer range, varying greatly in size, shape and cuticular distribution from species to species (Martin and Juniper, 1970; Juniper and Southwood, 1986). Loss of microstructure due to melting at elevated temperatures is deleterious to the protective role and transpiration control of leaf waxes. Lipid melting results in increased permeability (Gibbs, 2002). The melting points of the pure *n*-alkane homologues are reported as follows: *n*-C<sub>27</sub>, 59.2°C; *n*-C<sub>29</sub>, 63.7°C; *n*-C<sub>31</sub>, 67.9°C; *n*-C<sub>33</sub>, 71.2°C and *n*-C<sub>35</sub>, 74.6°C. Those of the *n*-alkanol homologues are: *n*-C<sub>22</sub>, 72.5°C; *n*-C<sub>24</sub>, 77.0°C; *n*-C<sub>26</sub>, 80.0°C; *n*-C<sub>28</sub>, 83.4°C and *n*-C<sub>30</sub>, 88.0°C (Lide, 2004), i.e. with an ACL increase of 2 the melting point rises by approximately 4°C. Little is known about the actual effect of increased ACL values on the melting points of leaf waxes. Furthermore, waxes contain a wide range of aliphatic and other compounds. The mixing ratio of straight-chain, branched, saturated or unsaturated, as well as cyclic and heterocompounds will affect the melting point of an epicuticular wax. Chain length has a relatively small effect on the melting point compared to differences in lipid class (alkenes, methylalkanes etc.; Gibbs, 2002). For example, Patel et al. (2001) found that a mixture of synthetic wax esters with *n*-alkanes melted 3-5°C lower than predicted from the melting points of the individual lipids. Gibbs (1995) examined two-component mixtures of long-chain cuticular hydrocarbons as a model for lipid interactions. Pure *n*-alkanes melted abruptly over a 2-3°C range, whereas mixtures melted over a range of 5-20°C. In addition, for *n*-alkane/*n*-alkene mixtures the melting temperatures were higher than the calculated weighted average temperatures by as much as 17°C.

Gülz (1994) described fundamental differences between leaf wax compositions of gymnosperms and angiosperms and attributed them to fundamental evolutionary developments. Dodd and Afzal-Rafii (2000) analysed waxes of plant species of the family Cupressaceae and proposed that the hydrocarbon composition displays a strong genetic

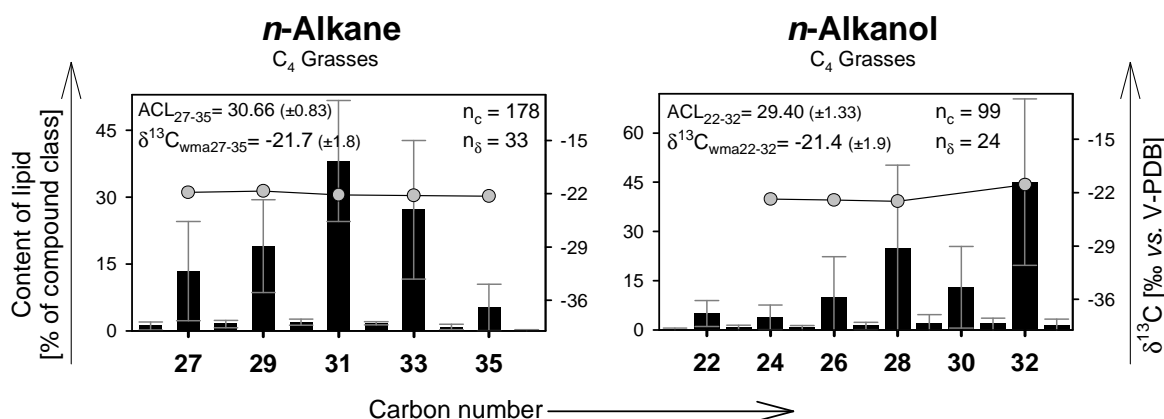
influence of adaptation to environmental conditions. As yet, little attention has been given to the evolutionary pathways which must underlie the current plant phylogeny and the chemotaxonomic distribution of the lipid biomarkers.

The postulated evolutionary sequence of the major grass subfamilies is shown in Fig. 2.2b. The original grasses were plants of forest margins or deep shade, characteristics that are retained today in the bamboos and the basal pooid grasses (Kellogg, 2001). Members of the subfamily Bambusoideae traditionally have been speculated to be the most primitive members of the grass family (Soderstrom, 1981). Their adaptation to forest habitats precluded them from the main evolutionary line of the whole family. C<sub>3</sub> grasses of the subfamily Arundinoideae appear to be the descendants of an ancestral line closest to the earliest true grasses and members of this subfamily may have been the first to move to open “savanna ecosystems” from savanna/forest ecotone. Chloridoideae and Panicoideae have come to dominate the open environments of the tropical and subtropical zones. They are the descendants of the early arundinoid grasses which, through the evolution of the C<sub>4</sub> photosynthetic pathway, gained a competitive edge over their C<sub>3</sub> grass ancestors (Fig. 2.2b; Renvoize and Clayton, 1992). The close relationship of the chloridoid and panicoid grasses, along with other C<sub>4</sub> species, suggests the possibility of underlying physiological similarities (Kellogg, 2001).

The results of our cluster analysis of the distribution patterns of aliphatic wax components (Fig. 2.5a-d), combined with the known grass subfamilial phylogeny and preferred habitat of subfamilies or C<sub>4</sub> subtypes (e.g. Fig. 2.2b) suggest that plant wax compositions reflect adaptation to the climate of the habitat. This adaptation may have developed as a secondary effect during the evolutionary succession of the grasses, especially of C<sub>4</sub> grasses during their adaptation to low concentrations of atmospheric CO<sub>2</sub>. The carbon number distributions of the *n*-alkanes of the panicoids and chloridoids and the NAD-ME and PCK C<sub>4</sub>-subtype species may have evolved to give the increased content of the *n*-C<sub>33</sub> alkane and the *n*-C<sub>32</sub> alkanol with their higher melting points. Presumably, C<sub>4</sub> grasses acquired an advantage over C<sub>3</sub> plants in hot and arid regions by having higher-melting-point waxes as a result of increased content of longer-chain wax components. An evolutionary adaptive role of plant waxes seems certain but requires further investigation.

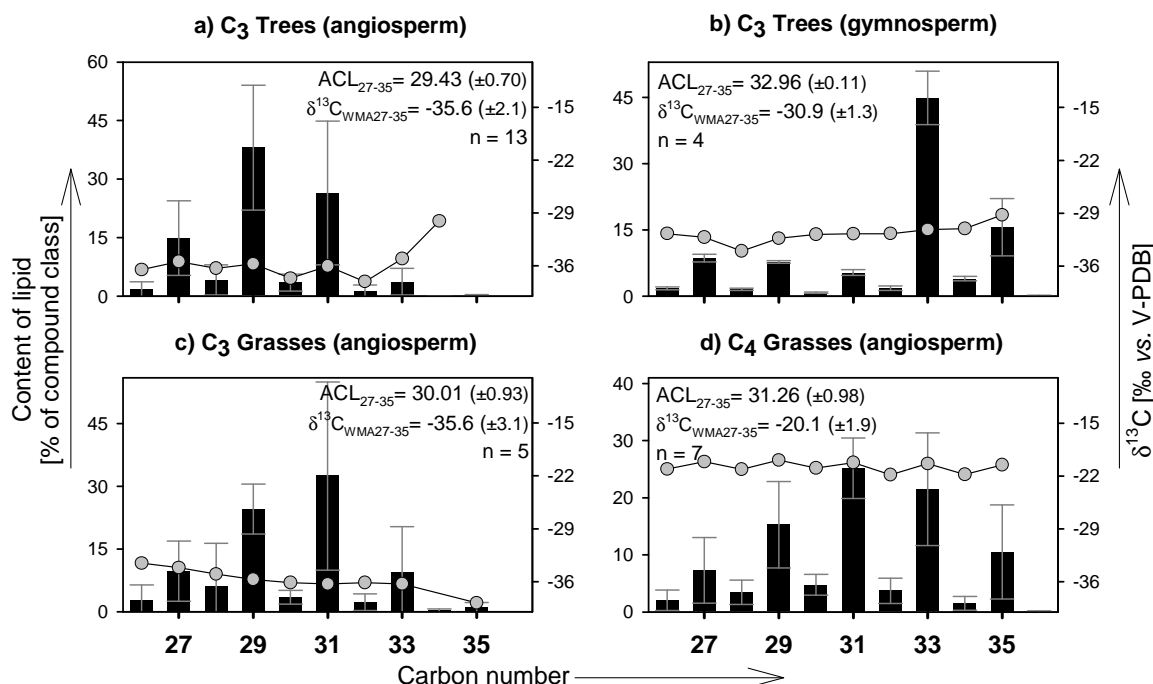
### 2.6.2 Leaf wax *n*-alkane and *n*-alkanol homologues as palaeoclimatic proxies

The potential for chemical adaptation of C<sub>3</sub> and C<sub>4</sub> plants to habitat occupancy has implications for the use of wax compositions in fossil records as biomarker proxies. Thus, palaeoenvironmental studies use chain-length distributions and stable carbon isotopic measurements of aliphatic biomarkers to deduce the C<sub>3</sub> and C<sub>4</sub> plant contribution to



**Fig. 2.6.** Averaged histogram representation for C<sub>4</sub> grasses of *n*-alkane and *n*-alkanol homologue contents (in % of compound class, left Y-axis) of leaf waxes, based on combined bibliographic data and data of this study, for odd *n*-C<sub>27</sub> to *n*-C<sub>35</sub> alkanes as well as even *n*-C<sub>22</sub> to *n*-C<sub>32</sub> alkanols (black bars), overlain by molecular stable carbon isotope data of this study (○;  $\delta^{13}C$  in ‰ versus V-PDB, right Y-axis; cf. Fig. 2.4). The diagrams are individually normalised to the most abundant homologue. ACL: Mean average chain length of odd-carbon-numbered *n*-alkanes (*n*-C<sub>27</sub> to *n*-C<sub>35</sub>; ACL<sub>27-35</sub>) as well as even-carbon-numbered *n*-alkanols (*n*-C<sub>22</sub> to *n*-C<sub>32</sub>; ACL<sub>22-32</sub>) including the standard deviation (in brackets).  $\delta^{13}C_{WMA}$ : Mean weighted mean average of carbon isotopic values of odd-carbon-numbered *n*-C<sub>27</sub> to *n*-C<sub>35</sub> alkanes ( $\delta^{13}C_{WMA27-35}$ ) as well as of even-carbon-numbered *n*-C<sub>22</sub> to *n*-C<sub>32</sub> alkanols ( $\delta^{13}C_{WMA22-32}$ ) including the standard deviation (in brackets).  $n_c$ : number of species used for the averaging of content data.  $n_\delta$ : number of species used for the averaging of isotopic data.

sediments from continental vegetation. The averaged C<sub>4</sub> grass wax signatures (Fig. 2.6), based on the bibliographic data in Fig. 2.4 as well as on data of this study, may be representative of the world's tropical grasslands and savannas, and as the most important group of plants they may dominate the fossil signatures related to the proportions of C<sub>3</sub> and C<sub>4</sub> vegetation. Chikaraishi and Naraoka (2003) analysed wax *n*-alkanes of higher land plants which were collected in Japan and Thailand. Histograms and molecular isotopic data of *n*-alkanes as well as averaged numerical data are shown in Fig. 2.7a-d. The C<sub>3</sub> and C<sub>4</sub> grasses mainly contain the *n*-C<sub>31</sub> alkane, whereas the C<sub>4</sub> grasses have also a higher relative content of the *n*-C<sub>33</sub> alkane (cf. Fig. 2.7c,d). The angiosperm trees (C<sub>3</sub>, Fig. 2.7a), which represent the second-most important group in the C<sub>3</sub> versus C<sub>4</sub> competition in tropical vegetation, contain mainly the *n*-C<sub>29</sub> alkane. This supports the findings in palaeoenvironmental studies, which deduce the C<sub>3</sub> and C<sub>4</sub> plant contribution to sediments from continental vegetation by using chain-length distributions of aliphatic biomarkers and isotopic measurements. For example, Eglinton et al. (2002), Schefuß et al. (2003b) and Rommerskirchen et al. (2003, Chapter 3) found high relative amounts of the *n*-C<sub>29</sub> and *n*-C<sub>31</sub> alkanes combined with lighter  $\delta^{13}C$  values in those marine sediments on the West African continental margin off the Congo river which received terrestrial organic matter from the predominantly C<sub>3</sub> tropical rainforest in the hinterland. On the other hand, their samples from marine settings near the adjacent African savannas and deserts

*n*-Alkane

**Fig. 2.7.** Averaged histogram representation for a) C<sub>3</sub> angiosperm and b) C<sub>3</sub> gymnosperm trees as well as c) C<sub>3</sub> and d) C<sub>4</sub> grasses of contents of *n*-C<sub>26</sub> to *n*-C<sub>36</sub> alkanes in leaf waxes (in % of compound class, left Y-axis; black bars), overlain by averaged molecular stable carbon isotope data (○;  $\delta^{13}\text{C}$  in ‰ versus V-PDB, right Y-axis). *n*-Alkane isotopic values based on data of Chikaraishi and Naraoka (2003). The diagrams are individually normalised to the most abundant homologue. ACL: Mean average chain length of odd-carbon-number *n*-alkanes (*n*-C<sub>27</sub> to *n*-C<sub>35</sub>;  $\text{ACL}_{27-35}$ ) including the standard deviation (in brackets).  $\delta^{13}\text{C}_{\text{WMA}}$ : Mean weighted mean average of carbon isotopic values of odd-carbon-numbered *n*-C<sub>27</sub> to *n*-C<sub>35</sub> alkanes ( $\delta^{13}\text{C}_{\text{WMA}27-35}$ ) including the standard deviation (in brackets). n: number of species used for the averaging of content data as well as of isotopic data.

mainly exhibited the *n*-C<sub>31</sub> and *n*-C<sub>33</sub> alkane homologues, which were isotopically enriched in  $^{13}\text{C}$  relative to the *n*-C<sub>29</sub> alkane. The molecular isotope signatures determined in these sediment studies are not as uniform within the homologous series as found for the C<sub>4</sub> and C<sub>3</sub> grasses in this study (Figs. 2.4 and 2.6). This underlines, as expected, the occurrence of complex mixtures of C<sub>3</sub> and C<sub>4</sub> plant wax components in geological samples.

As a result of the present study, we propose, as a working paradigm, that the carbon number histograms of the C<sub>4</sub> grasses (Fig. 2.6) have the *n*-C<sub>31</sub> and *n*-C<sub>33</sub> alkanes and the *n*-C<sub>32</sub> alkanol as dominant homologues with each carrying a  $\delta^{13}\text{C}$  value of approximately -22‰. We thus have an experimentally derived proxy for the C<sub>4</sub> tropical and subtropical grasslands of the continents as registered in aquatic sediments. While the expansions and contractions of these grassland zones can serve as indirect measures of continental climate change, the actual assessment and modelling of such phenomena can now – in addition to mineral composition, pollen and plant fossil records and estimates of  $p\text{CO}_2$ , temperature and precipitation – be based upon lipid biomarker distributions and compound-specific stable carbon isotope data.

## 2.7 Conclusions

In this paper we have attempted to establish a reliable biomarker proxy for tropical and subtropical grasslands, based on molecular characteristics of C<sub>4</sub> grasses which are predominant in these biomes. The analytical data are for the long chain *n*-alkanes and *n*-alkanols in the epicuticular waxes extracted from more than thirty grass species native to the African grasslands. These lipid distributions have allowed a chemotaxonomic survey which has been extended by a detailed assessment of the respective literature data. The combined findings may be summarized as follows:

- C<sub>4</sub> grasses display considerable variation in the content and distribution of their lipids at the subspecies and species level. At this level the data reveal little in the way of useful chemotaxonomic systematics.
- The C<sub>4</sub> grasses do display characteristic lipid distributions at the subfamily level. The dominant *n*-alkanes are *n*-C<sub>31</sub> and *n*-C<sub>33</sub> homologues and the dominant *n*-alkanol is the *n*-C<sub>32</sub> compound. The ACL values are higher than those of the C<sub>3</sub> grasses and also those reported for many C<sub>3</sub> plants of the temperate zones. The carbon number distribution patterns found in this study are broadly substantiated by the data recorded in the literature for more than 200 species of C<sub>3</sub> and C<sub>4</sub> grasses.
- The dominant *n*-C<sub>31</sub> and *n*-C<sub>33</sub> alkanes and *n*-C<sub>32</sub> alkanol in the C<sub>4</sub> grasses are also each characterised by consistently heavy  $\delta^{13}\text{C}$  values of circa. -22‰.
- The higher ACL values shown by the C<sub>4</sub> grasses may reflect evolutionary adaptation to high-temperature arid habitats. If so, the explanation may be a need for retention of crystallinity and hence micromorphology of leaf surface waxes at high temperatures, as in plants exposed to high-intensity insolation in deserts and other exposed and sparsely vegetated areas.
- In terms of palaeoenvironmental studies, the distributions and isotopic characteristics of the *n*-alkanes and *n*-alkanols constitute useful biomarker proxies for the C<sub>4</sub>-dominated tropical and subtropical grasslands. These proxies may afford estimates of the areal extent of these biomes and hence the palaeoclimatic conditions.

## 2.8 Appendix

**Table 2.3. a)** *n*-Alkane data of grass subspecies studied: Subfamily, subspecies, sampling location, individual *n*-alkane content in µg g<sup>-1</sup> dry matter (DM), TCOC<sub>27-35</sub>, CPI<sub>27-35</sub> and ACL<sub>27-35</sub> values. Boldface content values of individual *n*-alkanes refer to distribution pattern maxima.

| Subfamily/<br><i>subspecies</i> | Sampling<br>location                         | <i>n</i> -Alkane content <sup>a</sup> (µg g <sup>-1</sup> DM) |      |             |      |              |      |              |      |              |      |       |      | TCOC <sub>27-35</sub> <sup>b</sup> | CPI <sub>27-35</sub> <sup>c</sup> | ACL <sub>27-35</sub> <sup>d</sup> |
|---------------------------------|--|---|------|-------------|------|--------------|------|--------------|------|--------------|------|-------|------|------------------------------------|-----------------------------------|-----------------------------------|
|                                 |  | 26  | 27   | 28          | 29   | 30           | 31   | 32           | 33   | 34           | 35   | 36    |      |                                    |                                   |                                   |
| Whole plant samples             | <b>Aristidoideae</b>                         |   |      |             |      |              |      |              |      |              |      |       |      |                                    |                                   |                                   |
|                                 | <i>Aristida adscensionis</i> <sup>#*</sup>   | Namibia   | 7.4  | 17.8        | 8.6  | 63.3         | 16.9 | <b>411.1</b> | 12.4 | 80.4         | 2.6  | 5.3   | n.d. | 577.9                              | 14.1                              | 30.97                             |
|                                 | <i>Aristida barbicollis</i>                  | Zimbabwe  | 0.6  | 13.0        | 2.1  | 30.3         | 4.4  | <b>112.2</b> | 4.5  | 49.4         | 1.5  | 6.9   | n.d. | 211.8                              | 16.2                              | 31.07                             |
|                                 | <i>Aristida congesta</i>                     | Namibia   | 3.1  | 19.4        | 3.9  | 50.5         | 7.8  | <b>225.5</b> | 6.2  | 62.8         | 2.3  | 6.8   | n.d. | 365.0                              | 17.1                              | 30.93                             |
|                                 | <i>Aristida graciliflora</i>                 | Zimbabwe  | 0.6  | 4.6         | 1.5  | 45.1         | 7.8  | <b>230.6</b> | 5.6  | 44.2         | 0.6  | 3.4   | n.d. | 327.8                              | 20.9                              | 30.98                             |
|                                 | <i>Aristida meridionalis</i>                 | Zimbabwe  | 1.2  | 17.2        | 3.1  | 27.4         | 3.4  | <b>44.9</b>  | 2.0  | 12.4         | 0.4  | 1.0   | n.d. | 103.0                              | 10.6                              | 30.08                             |
|                                 | <i>Aristida meridionalis</i>                 | Namibia   | 3.7  | 26.9        | 4.4  | 31.7         | 4.0  | <b>62.3</b>  | 2.8  | 21.4         | 0.5  | 1.3   | n.d. | 143.6                              | 11.3                              | 30.14                             |
|                                 | <i>Stipagrostis ciliata</i> <sup>#</sup>     | Namibia   | 2.0  | 4.3         | 0.9  | 8.1          | 1.3  | <b>69.3</b>  | 1.2  | 25.2         | 0.1  | 1.0   | n.d. | 107.9                              | 30.2                              | 31.19                             |
|                                 | <i>Stipagrostis hirtigluma</i> <sup>#</sup>  | Namibia   | 14.1 | 87.2        | 29.9 | 156.1        | 32.8 | <b>593.9</b> | 23.5 | 162.3        | 5.9  | 11.3  | n.d. | 1010.8                             | 10.5                              | 30.71                             |
|                                 | <i>Stipagrostis uniplumis</i>                | Namibia   | 4.7  | 18.7        | 3.5  | 41.4         | 4.7  | <b>100.8</b> | 2.6  | 16.5         | 0.5  | 1.5   | n.d. | 178.8                              | 14.9                              | 30.63                             |
|                                 | <b>Chloridoideae</b>                         |   |      |             |      |              |      |              |      |              |      |       |      |                                    |                                   |                                   |
|                                 | <i>Chloris gayana</i>                        | Zimbabwe  | 1.5  | 20.6        | 4.2  | 35.3         | 6.3  | 188.3        | 10.4 | <b>287.6</b> | 8.9  | 63.4  | n.d. | 595.2                              | 18.5                              | 32.14                             |
|                                 | <i>Chloris virgata</i>                       | Zimbabwe  | 2.0  | 17.8        | 3.5  | 27.5         | 3.6  | 42.2         | 2.8  | <b>51.9</b>  | 3.3  | 22.1  | n.d. | 161.5                              | 10.7                              | 31.41                             |
|                                 | <i>Chloris virgata</i> <sup>#</sup>          | Namibia   | 3.2  | 13.8        | 3.2  | 15.1         | 3.1  | <b>26.4</b>  | 2.2  | 16.2         | 2.3  | 14.0  | 0.9  | 85.5                               | 6.7                               | 31.03                             |
|                                 | <i>Enneapogon sp.</i>                        | Namibia   | 3.1  | 30.5        | 5.3  | 69.8         | 11.0 | 352.4        | 13.7 | <b>407.9</b> | 7.9  | 79.8  | 1.4  | 940.4                              | 23.7                              | 31.93                             |
|                                 | <i>Enneapogon cenchroides</i>                | Zimbabwe  | 0.7  | 9.4         | 2.2  | 30.4         | 5.0  | <b>215.4</b> | 6.9  | 200.1        | 3.2  | 21.2  | 0.6  | 476.6                              | 26.7                              | 31.81                             |
|                                 | <i>Enneapogon cenchroides</i> <sup>#</sup>   | Namibia   | 4.3  | 14.9        | 2.9  | 21.9         | 3.7  | <b>103.6</b> | 2.3  | 32.7         | 1.0  | 3.1   | n.d. | 176.2                              | 16.8                              | 30.85                             |
|                                 | <i>Eragrostis nindensis</i>                  | Namibia   | 3.7  | 12.1        | 2.7  | 14.9         | 2.1  | <b>33.7</b>  | 2.3  | 29.3         | 1.2  | 5.2   | n.d. | 95.2                               | 10.2                              | 31.01                             |
|                                 | <i>Eragrostis superba</i>                    | Zimbabwe  | 2.8  | <b>60.2</b> | 6.1  | 44.7         | 3.4  | 42.1         | 3.1  | 54.7         | 2.4  | 14.5  | 0.2  | 216.2                              | 11.8                              | 30.25                             |
|                                 | <i>Eragrostis tremula</i>                    | Sudan   | 2.2  | 17.1        | 3.5  | 41.8         | 7.4  | <b>178.4</b> | 5.6  | 78.2         | 1.6  | 8.0   | n.d. | 323.3                              | 17.1                              | 31.11                             |
|                                 | <i>Eragrostis violacea de winter</i>         | Zimbabwe  | 1.5  | 25.5        | 4.7  | 31.7         | 7.3  | <b>104.0</b> | 4.8  | 76.8         | 1.9  | 8.4   | 0.4  | 246.5                              | 12.3                              | 31.09                             |
|                                 | <i>Eragrostis viscosa</i>                    | Zimbabwe  | 7.1  | 79.5        | 11.5 | <b>149.1</b> | 12.8 | 139.4        | 7.5  | 77.7         | 2.3  | 7.1   | 0.3  | 452.7                              | 12.0                              | 30.05                             |
|                                 | <i>Schmidtia kalahariensis</i> <sup>#*</sup> | Namibia   | 1.4  | 61.6        | 18.6 | 35.6         | 13.6 | 225.6        | 19.8 | <b>805.6</b> | 16.2 | 166.9 | 1.3  | 1295.3                             | 17.0                              | 32.51                             |
|                                 | <i>Sporobolus ioclados</i>                   | Zimbabwe  | 2.1  | 28.0        | 3.4  | 41.3         | 5.9  | 116.5        | 6.5  | <b>119.6</b> | 3.4  | 16.8  | 1.0  | 322.2                              | 15.5                              | 30.90                             |
|                                 | <i>Sporobolus pyramidalis</i>                | Zimbabwe  | 2.8  | 66.6        | 9.0  | 95.8         | 11.1 | 185.2        | 10.2 | <b>222.4</b> | 6.0  | 41.1  | 1.3  | 611.1                              | 15.4                              | 31.25                             |

Whole plant samples

cont. Table 2.3. a) *n*-Alkane data of grass subspecies studied.

|                     | Subfamily/<br>subspecies                 | Sampling<br>location | <i>n</i> -Alkane content <sup>a</sup> (µg g <sup>-1</sup> DM) |              |      |             |      |             |      |              |      |       |      | TCOC <sub>27-35</sub> <sup>b</sup> | CPI <sub>27-35</sub> <sup>c</sup> | ACL <sub>27-35</sub> <sup>d</sup> |
|---------------------|--|----------------------|---|--------------|------|-------------|------|-------------|------|--------------|------|-------|------|------------------------------------|-----------------------------------|-----------------------------------|
|                     |  |                      | 26  | 27           | 28   | 29          | 30   | 31          | 32   | 33           | 34   | 35    | 36   |                                    |                                   |                                   |
| Whole plant samples | <b>Panicoideae</b>                       |                      |   |              |      |             |      |             |      |              |      |       |      |                                    |                                   |                                   |
|                     | <i>Bothriochloa insculpta</i>            | Zimbabwe             | 1.9   | 20.7         | 3.8  | 24.5        | 3.5  | <b>39.5</b> | 1.7  | 18.5         | 0.5  | 2.4   | n.d. | 105.6                              | 9.8                               | 30.19                             |
|                     | <i>Brachiaria erucitormis</i>            | Zimbabwe             | 1.1   | 3.9          | 1.4  | 8.1         | 1.8  | 34.1        | 3.1  | <b>64.2</b>  | 1.0  | 2.9   | n.d. | 113.1                              | 15.1                              | 31.96                             |
|                     | <i>Digitaria milaniana</i>               | Zimbabwe             | 0.8   | 18.4         | 3.9  | 44.2        | 6.3  | 102.6       | 6.3  | <b>113.9</b> | 4.4  | 36.1  | 0.9  | 315.1                              | 13.8                              | 31.67                             |
|                     | <i>Hyparrhenia filipendula</i>           | Zimbabwe             | 2.7   | 37.7         | 5.5  | 43.6        | 6.6  | 183.1       | 13.3 | <b>265.6</b> | 8.1  | 59.4  | n.d. | 589.4                              | 16.2                              | 31.90                             |
|                     | <i>Loudetia simplex</i>                  | Zimbabwe             | 0.8   | 8.6          | 1.7  | 23.2        | 2.8  | <b>76.1</b> | 2.4  | 41.3         | 1.4  | 9.9   | n.d. | 159.0                              | 18.1                              | 31.26                             |
|                     | <i>Panicum sp.</i>                       | Namibia              | 5.3   | 39.7         | 6.5  | 68.2        | 9.7  | 145.1       | 11.2 | <b>236.1</b> | 10.4 | 117.2 | 0.8  | 606.2                              | 13.9                              | 32.06                             |
|                     | <i>Panicum arbusculum</i> <sup>#</sup> * | Namibia              | 5.3   | 12.1         | 5.2  | 20.7        | 6.8  | 146.3       | 15.4 | <b>357.0</b> | 13.9 | 95.7  | 1.0  | 631.8                              | 14.0                              | 32.59                             |
|                     | <i>Panicum maximum</i>                   | Zimbabwe             | 2.1   | 36.2         | 4.3  | 51.1        | 5.2  | <b>81.9</b> | 2.8  | 24.5         | 0.6  | 2.4   | n.d. | 196.0                              | 13.7                              | 30.04                             |
|                     | <i>Panicum maximum</i>                   | Namibia              | 3.2   | 15.1         | 3.5  | 40.5        | 5.3  | <b>84.4</b> | 4.1  | 34.4         | 0.9  | 2.4   | 0.3  | 176.8                              | 12.0                              | 30.64                             |
|                     | <i>Themeda triandra</i>                  | Zimbabwe             | 1.8   | 35.2         | 2.9  | 25.2        | 3.9  | <b>69.2</b> | 3.2  | 33.6         | 1.2  | 4.8   | n.d. | 168.1                              | 13.2                              | 30.38                             |
|                     | <b>Pooideae</b>                          |                      |   |              |      |             |      |             |      |              |      |       |      |                                    |                                   |                                   |
|                     | <i>Bromus sp.</i>                        | Australia            | 1.1   | 14.6         | 2.1  | 49.9        | 3.6  | <b>95.3</b> | 2.5  | 63.3         | 0.9  | 14.5  | n.d. | 237.6                              | 24.6                              | 31.11                             |
|                     | <i>Festuca orthophylla</i>               | Peru                 | 1.6   | 29.1         | 4.6  | <b>89.4</b> | 1.9  | 14.7        | n.d. | 3.8          | n.d. | 1.4   | n.d. | 138.5                              | 18.9                              | 28.96                             |
|                     | <i>Festuca orthophylla</i>               | Peru                 | 1.6   | 21.6         | 4.8  | <b>88.6</b> | 3.0  | 28.3        | n.d. | 4.3          | n.d. | n.d.  | n.d. | 142.9                              | 16.9                              | 29.21                             |
| Plant part samples  | <b>Chloridoideae</b>                     |                      |   |              |      |             |      |             |      |              |      |       |      |                                    |                                   |                                   |
|                     | <i>Sporobolus sp.</i> (flowers)          | Tanzania             | 5.7   | 92.7         | 9.7  | 98.1        | 8.8  | 176.0       | 7.8  | <b>216.3</b> | 4.3  | 27.4  | 0.6  | 610.4                              | 17.9                              | 30.96                             |
|                     | <i>Sporobolus sp.</i> (leaves)           | Tanzania             | 1.1   | 4.4          | 1.6  | 8.2         | 2.1  | 23.7        | 1.8  | <b>32.9</b>  | 1.1  | 10.6  | 0.5  | 79.6                               | 11.0                              | 31.93                             |
|                     | <i>Sporobolus sp.</i> (stems)            | Tanzania             | 0.7   | 1.4          | 0.6  | 2.5         | 0.5  | 8.5         | 0.6  | <b>15.8</b>  | 0.5  | 6.7   | 0.3  | 34.8                               | 13.4                              | 32.37                             |
|                     | <b>Panicoideae</b>                       |                      |   |              |      |             |      |             |      |              |      |       |      |                                    |                                   |                                   |
|                     | <i>Brachiaria sp.</i> (flowers)          | Tanzania             | 14.7  | <b>238.7</b> | 16.3 | 226.5       | 10.1 | 202.9       | 8.2  | 147.7        | 7.2  | 43.9  | 0.0  | 859.8                              | 17.2                              | 29.91                             |
|                     | <i>Brachiaria sp.</i> (leaves)           | Tanzania             | 1.5   | 12.5         | 1.8  | 17.3        | 2.6  | 59.1        | 4.2  | <b>101.8</b> | 3.1  | 35.2  | 0.9  | 226.0                              | 17.4                              | 32.15                             |
|                     | <i>Brachiaria sp.</i> (stems)            | Tanzania             | 0.5   | 2.1          | 0.5  | 6.4         | 0.9  | 23.2        | 1.4  | <b>31.9</b>  | 1.1  | 12.5  | 0.4  | 76.1                               | 17.5                              | 32.21                             |

n.d. : not determined

<sup>#</sup>: After Huang et al. (2000) corrected *n*-alkane contents (see text for details)

\*: Sample without inflorescence part

<sup>a</sup> Numbers according to individual *n*-alkane carbon numbers<sup>b</sup>TCOC<sub>27-35</sub>: Total content of odd- carbon-numbered *n*-C<sub>27</sub> to *n*-C<sub>35</sub> alkanes in µg/g DM<sup>c</sup>CPI<sub>27-35</sub>: Carbon preference index of *n*-alkanes (carbon number 27 - 35)<sup>d</sup>ACL<sub>27-35</sub>: Averaged chain length of odd-carbon-numbered *n*-alkanes (carbon number 27 - 35)



**Table 2.3. b)** *n*-Alkanol data of grass subspecies studied: Subfamily, subspecies, sampling location, individual *n*-alkanol content in  $\mu\text{g g}^{-1}$  dry matter (DM); TCEC<sub>22-32</sub>, CPI<sub>22-32</sub>, and ACL<sub>22-32</sub> values. Boldface content values of individual *n*-alkanols refer to distribution pattern maxima.

|                     | Subfamily/<br>subspecies             | Sampling<br>location | <i>n</i> -Alkanol content <sup>a</sup> ( $\mu\text{g g}^{-1}$ DM) |      |      |     |      |              |      |              |      |      |      |              |      | TCEC <sub>22-32</sub> <sup>b</sup> | CPI <sub>22-32</sub> <sup>c</sup> | ACL <sub>22-32</sub> <sup>d</sup> |
|---------------------|--------------------------------------|----------------------|---|------|------|-----|------|--------------|------|--------------|------|------|------|--------------|------|------------------------------------|-----------------------------------|-----------------------------------|
|                     |                                      |                      | 21  | 22   | 23   | 24  | 25   | 26           | 27   | 28           | 29   | 30   | 31   | 32           | 33   |                                    |                                   |                                   |
| Whole plant samples | <b>Aristidoideae</b>                 |                      |   |      |      |     |      |              |      |              |      |      |      |              |      |                                    |                                   |                                   |
|                     | <i>Aristida adscensionis</i> *       | Namibia              | 0.2   | 1.1  | 0.3  | 0.8 | 0.4  | 1.1          | 0.4  | 3.1          | 0.3  | 1.9  | 0.9  | <b>12.8</b>  | 0.2  | 20.8                               | 5.9                               | 30.07                             |
|                     | <i>Aristida barbicollis</i>          | Zimbabwe             | n.d.  | 16.3 | 2.7  | 9.3 | 3.1  | 23.7         | n.d. | 12.4         | 2.8  | 7.7  | 6.4  | <b>257.9</b> | 7.6  | 327.4                              | 12.7                              | 30.64                             |
|                     | <i>Aristida congesta</i>             | Namibia              | 0.2   | 2.1  | 0.3  | 0.6 | 0.6  | 3.3          | 0.8  | 25.4         | 0.4  | 4.4  | 0.9  | <b>45.3</b>  | 0.5  | 81.1                               | 19.9                              | 30.08                             |
|                     | <i>Aristida graciliflora</i>         | Zimbabwe             | 0.3   | 4.9  | 0.3  | 1.8 | n.d. | 10.1         | 3.7  | <b>119.8</b> | 5.6  | 4.9  | 2.0  | 8.8          | n.d. | 150.4                              | 12.5                              | 27.92                             |
|                     | <i>Aristida meridionalis</i>         | Zimbabwe             | 0.8   | 11.6 | 0.8  | 2.2 | 2.1  | 6.2          | 1.3  | 38.7         | 4.7  | 41.6 | 15.9 | <b>676.3</b> | 6.6  | 776.6                              | 17.5                              | 31.47                             |
|                     | <i>Aristida meridionalis</i>         | Namibia              | n.d.  | 1.3  | 0.1  | 0.3 | 0.2  | 1.0          | 0.2  | 2.7          | 0.4  | 0.2  | 1.6  | <b>29.3</b>  | 0.3  | 34.8                               | 7.9                               | 31.06                             |
|                     | <i>Stipagrostis ciliata</i>          | Namibia              | n.d.  | 0.6  | n.d. | 2.1 | 1.3  | <b>139.3</b> | 1.3  | 18.6         | 1.3  | 0.4  | n.d. | 4.3          | 0.5  | 165.2                              | 41.4                              | 26.35                             |
|                     | <i>Stipagrostis hirtigluma</i>       | Namibia              | n.d.  | 6.6  | n.d. | 2.1 | 0.4  | 18.6         | 0.5  | 12.5         | 1.4  | 5.1  | 2.9  | <b>39.9</b>  | 0.1  | 84.8                               | 11.9                              | 29.00                             |
|                     | <i>Stipagrostis uniplumis</i>        | Namibia              | 0.1   | 0.8  | 0.1  | 0.4 | 0.1  | 3.5          | 0.1  | <b>5.2</b>   | 0.3  | 2.0  | 0.3  | 3.3          | 0.4  | 15.2                               | 15.6                              | 28.24                             |
|                     | <b>Chloridoideae</b>                 |                      |   |      |      |     |      |              |      |              |      |      |      |              |      |                                    |                                   |                                   |
|                     | <i>Chloris gayana</i>                | Zimbabwe             | n.d.  | 3.3  | 0.9  | 2.7 | 1.2  | 4.4          | 1.6  | 15.9         | 4.2  | 3.6  | 2.7  | <b>21.9</b>  | 2.7  | 51.8                               | 3.8                               | 29.07                             |
|                     | <i>Chloris virgata</i>               | Zimbabwe             | n.d.  | 8.6  | 2.5  | 9.0 | 1.2  | 15.8         | 6.7  | <b>86.7</b>  | 9.3  | 12.8 | 4.1  | 82.0         | 6.8  | 215.0                              | 7.1                               | 29.09                             |
|                     | <i>Chloris virgata</i>               | Namibia              | n.d.  | 2.1  | 0.1  | 0.4 | 0.1  | 1.2          | 0.9  | 3.3          | 0.7  | 3.8  | 1.4  | <b>95.9</b>  | 0.3  | 106.6                              | 18.1                              | 31.52                             |
|                     | <i>Enneapogon sp.</i>                | Namibia              | 0.7   | 3.9  | 0.4  | 3.4 | 0.2  | 15.3         | 0.7  | 6.0          | 0.9  | 1.8  | 0.6  | <b>38.5</b>  | 0.9  | 68.8                               | 17.1                              | 29.31                             |
|                     | <i>Enneapogon cenchroides</i>        | Zimbabwe             | 0.8   | 20.2 | 1.1  | 6.5 | 0.9  | 16.8         | 3.0  | 14.1         | 8.8  | 11.1 | n.d. | <b>174.5</b> | n.d. | 243.2                              | 10.6                              | 30.22                             |
|                     | <i>Enneapogon cenchroides</i>        | Namibia              | 0.1   | 1.0  | 0.2  | 0.4 | 0.3  | 3.1          | 1.1  | <b>62.7</b>  | 0.5  | 0.5  | 0.5  | 25.4         | n.d. | 93.0                               | 31.4                              | 28.95                             |
|                     | <i>Eragrostis nindensis</i>          | Namibia              | 0.1   | 1.3  | n.d. | 0.4 | n.d. | 1.5          | 0.1  | 5.7          | 0.1  | 4.0  | 0.8  | <b>31.3</b>  | 0.1  | 44.3                               | 26.4                              | 30.72                             |
|                     | <i>Eragrostis superba</i>            | Zimbabwe             | 0.2   | 3.7  | 0.4  | 3.0 | n.d. | 5.0          | n.d. | <b>146.0</b> | 15.8 | 4.6  | n.d. | 20.0         | n.d. | 182.4                              | 10.5                              | 28.24                             |
|                     | <i>Eragrostis tremula</i>            | Sudan                | n.d.  | 2.7  | 1.0  | 1.6 | n.d. | 2.0          | 0.4  | 1.4          | n.d. | 3.0  | n.d. | <b>46.3</b>  | n.d. | 56.9                               | 23.2                              | 30.89                             |
|                     | <i>Eragrostis violacea de winter</i> | Zimbabwe             | n.d.  | 1.9  | 0.3  | 0.9 | 0.3  | 2.4          | 0.3  | 2.6          | 1.3  | 1.3  | 1.3  | <b>9.9</b>   | 1.6  | 19.0                               | 3.7                               | 29.18                             |
|                     | <i>Eragrostis viscosa</i>            | Zimbabwe             | 0.3   | 3.8  | 0.4  | 3.2 | n.d. | 17.3         | 8.1  | <b>209.0</b> | 11.4 | 9.6  | 3.4  | 15.4         | n.d. | 258.4                              | 10.6                              | 28.04                             |
|                     | <i>Schmidtia kalahariensis</i> *     | Namibia              | n.d.  | 3.2  | 0.1  | 1.9 | 0.2  | 6.2          | 0.3  | 4.9          | n.d. | 0.5  | n.d. | <b>87.4</b>  | 0.6  | 104.1                              | 93.8                              | 30.99                             |
|                     | <i>Sporobolus ioclados</i>           | Zimbabwe             | n.d.  | 4.7  | 0.9  | 1.9 | 1.2  | 4.3          | 1.9  | 7.7          | 3.8  | 5.6  | 3.2  | <b>44.8</b>  | 1.6  | 69.0                               | 4.0                               | 30.12                             |
|                     | <i>Sporobolus pyramidalis</i>        | Zimbabwe             | n.d.  | 1.5  | 0.3  | 2.4 | 0.7  | 9.1          | 0.9  | 5.5          | n.d. | 1.1  | 1.9  | <b>13.8</b>  | 0.7  | 33.4                               | 6.8                               | 28.62                             |

cont. Table 2.3. b) *n*-Alkanol data of grass subspecies studied.

| Subfamily/<br><i>subspecies</i> |                                 |          | <i>n</i> -Alkanol content <sup>a</sup> (μg g <sup>-1</sup> DM) |      |      |      |       |       |       |      |      |      |      |       | TCEC <sub>22-32</sub> <sup>b</sup> | CPI <sub>22-32</sub> <sup>c</sup> | ACL <sub>22-32</sub> <sup>d</sup> |       |
|---------------------------------|---------------------------------|----------|--|------|------|------|-------|-------|-------|------|------|------|------|-------|------------------------------------|-----------------------------------|-----------------------------------|-------|
|                                 |                                 |          | 21   | 22   | 23   | 24   | 25    | 26    | 27    | 28   | 29   | 30   | 31   | 32    |                                    |                                   |                                   | 33    |
| Whole plant samples             | Panicoideae                     |          |  |      |      |      |       |       |       |      |      |      |      |       |                                    |                                   |                                   |       |
|                                 | <i>Bothriochloa insculpta</i>   | Zimbabwe | n.d.   | 3.7  | n.d. | 1.9  | n.d.  | 2.4   | n.d.  | 5.7  | n.d. | n.d. | n.d. | 412.7 | n.d.                               | 426.3                             | n.d.                              | 31.79 |
|                                 | <i>Brachiaria erucitormis</i>   | Zimbabwe | n.d.   | 10.6 | 1.1  | 3.3  | 0.7   | 8.3   | 1.2   | 4.5  | 1.1  | 2.6  | 2.4  | 92.4  | 2.5                                | 121.7                             | 30.5                              | 30.31 |
|                                 | <i>Digitaria milanijana</i>     | Zimbabwe | n.d.   | 2.6  | 2.8  | 2.4  | 2.9   | 2.6   | 2.0   | 3.2  | 5.5  | 2.8  | 2.9  | 12.5  | 2.6                                | 26.1                              | 10.3                              | 28.15 |
|                                 | <i>Hyparrhenia filipendula</i>  | Zimbabwe | n.d.   | 3.0  | 0.9  | 2.4  | 1.5   | 2.8   | 2.1   | 15.8 | 4.4  | 6.8  | n.d. | 38.1  | 2.1                                | 69.0                              | 5.4                               | 29.92 |
|                                 | <i>Loudetia simplex</i>         | Zimbabwe | n.d.   | 0.9  | 0.3  | 0.8  | 0.3   | 1.6   | 0.7   | 2.3  | 1.4  | 1.3  | 0.9  | 3.7   | 1.1                                | 10.5                              | 2.3                               | 28.57 |
|                                 | <i>Panicum sp.</i>              | Namibia  | 0.5  | 2.3  | 0.6  | 2.1  | 1.3   | 12.5  | 1.8   | 21.0 | 3.3  | 7.8  | 1.5  | 44.6  | 0.3                                | 90.4                              | 7.9                               | 29.63 |
|                                 | <i>Panicum arbusculum*</i>      | Namibia  | 0.1  | 0.9  | 0.2  | 2.5  | 1.3   | 101.0 | 2.8   | 38.7 | n.d. | 5.4  | 0.7  | 66.8  | n.d.                               | 215.4                             | 36.3                              | 28.28 |
|                                 | <i>Panicum maximum</i>          | Zimbabwe | 3.2  | 3.4  | 4.5  | 5.4  | 3.3   | 14.4  | 4.4   | 9.3  | 11.1 | 18.7 | 4.7  | n.d.  | n.d.                               | 51.2                              | 15.3                              | 28.52 |
|                                 | <i>Panicum maximum</i>          | Namibia  | 0.1  | 1.9  | n.d. | 0.6  | n.d.  | 5.9   | n.d.  | 34.1 | n.d. | 19.1 | 1.4  | 201.5 | n.d.                               | 263.1                             | 112.2                             | 31.11 |
|                                 | <i>Themeda triandra</i>         | Zimbabwe | 0.3  | 1.7  | 0.4  | 1.4  | 0.2   | 0.9   | n.d.  | 1.7  | n.d. | 1.7  | n.d. | 28.4  | n.d.                               | 35.8                              | 31.6                              | 30.79 |
|                                 | Pooideae                        |          |  |      |      |      |       |       |       |      |      |      |      |       |                                    |                                   |                                   |       |
| <i>Bromus sp.</i>               | Australia                       | 0.9      | 7.2  | n.d. | 1.9  | n.d. | 7.9   | 2.8   | 430.0 | 1.9  | 11.2 | n.d. | 7.1  | n.d.  | 465.3                              | 99.2                              | 27.97                             |       |
| <i>Festuca orthophylla</i>      | Peru                            | n.d.     | 20.1   | 3.6  | 49.6 | 20.4 | 232.0 | n.d.  | 13.3  | 5.4  | 18.3 | 11.5 | 24.9 | 3.1   | 358.2                              | 8.5                               | 25.83                             |       |
| <i>Festuca orthophylla</i>      | Peru                            | n.d.     | 10.3   | 2.5  | 29.8 | 19.3 | 224.0 | 2.7   | 10.8  | n.d. | 8.8  | n.d. | 5.9  | n.d.  | 280.6                              | 8.9                               | 25.60                             |       |
| Plant part samples              | Chloridoideae                   |          |  |      |      |      |       |       |       |      |      |      |      |       |                                    |                                   |                                   |       |
|                                 | <i>Sporobolus</i> sp. (flowers) | Tanzania | 0.4  | 3.0  | 0.9  | 6.6  | 1.4   | 50.4  | 1.9   | 25.2 | 4.6  | 3.7  | 0.0  | 7.2   | 0.0                                | 96.2                              | 10.4                              | 26.87 |
|                                 | <i>Sporobolus</i> sp. (leaves)  | Tanzania | 0.0  | 0.6  | 0.2  | 0.6  | 0.3   | 5.8   | 0.2   | 5.7  | 0.4  | 1.2  | 1.5  | 8.3   | 0.6                                | 22.2                              | 6.9                               | 28.83 |
|                                 | <i>Sporobolus</i> sp. (stems)   | Tanzania | 0.0  | 0.8  | 0.5  | 0.3  | 0.5   | 4.4   | 0.3   | 4.9  | 0.3  | 0.9  | 0.8  | 1.4   | 0.4                                | 12.7                              | 4.7                               | 27.4  |
|                                 | Panicoideae                     |          |  |      |      |      |       |       |       |      |      |      |      |       |                                    |                                   |                                   |       |
|                                 | <i>Brachiaria</i> sp. (flowers) | Tanzania | 0.0  | 0.8  | 1.0  | 1.4  | 2.5   | 1.0   | 0.0   | 0.7  | 0.0  | 2.9  | 0.0  | 10.1  | 1.1                                | 17.0                              | 3.3                               | 29.98 |
|                                 | <i>Brachiaria</i> sp. (leaves)  | Tanzania | 0.0  | 1.9  | 0.3  | 1.4  | 0.2   | 1.6   | 0.3   | 1.5  | 0.5  | 2.2  | 0.7  | 9.8   | 0.7                                | 18.4                              | 6.4                               | 29.27 |
|                                 | <i>Brachiaria</i> sp. (stems)   | Tanzania | 0.6  | 0.6  | 0.5  | 0.4  | 0.3   | 2.0   | 0.3   | 2.4  | 0.2  | 0.6  | 0.9  | 1.9   | 0.6                                | 7.7                               | 2.8                               | 27.97 |

n.d. : not determined

\* Sample without inflorescence part

<sup>a</sup> Numbers according to individual *n*-alkanol carbon numbers<sup>b</sup>TCEC<sub>22-32</sub>: Total content of even-carbon-numbered *n*-C<sub>22</sub> to *n*-C<sub>32</sub> alkanols in µg/g DM<sup>c</sup>CPI<sub>27-33</sub>: Carbon preference index of *n*-alkanes (carbon number 22 - 32)<sup>d</sup>ACL<sub>22-32</sub>: Averaged chain length of even-carbon-numbered *n*-alkanol (carbon number 22 - 32)

**Table 2.4.** Isotopic data for grass subspecies studied: Subfamily, subspecies, photosynthetic pathway, physiology (according to Ellis, 1977; Watson and Dallwitz, 1992a,b onwards; Schulze et al., 1996), sampling location, and molecular stable isotopic composition of *n*-alkanes and *n*-alkanols.

| Subfamily/<br><i>subspecies</i>             | Photosynthetic<br>pathway                   | Physiology     | Sampling<br>location | $\delta^{13}\text{C}$ of <i>n</i> -alkanes <sup>a</sup> (‰ vs. V-PDB) |       |       |       |       | $\delta^{13}\text{C}_{\text{WMA-27-35}}$ <sup>b</sup> | $\delta^{13}\text{C}$ of <i>n</i> -alkanols <sup>a</sup> (‰ vs. V-PDB) |      |       |       |       |       | $\delta^{13}\text{C}_{\text{WMA-22-32}}$ <sup>b</sup> |       |
|---|---|----------------|----------------------|---|-------|-------|-------|-------|---|--|------|-------|-------|-------|-------|---|-------|
|   |   |                |                      | 27  | 29    | 31    | 33    | 35    |   | 22   | 24   | 26    | 28    | 30    | 32    |   |       |
|   |   |                |                      |   |       |       |       |       |   |  |      |       |       |       |       |   |       |
| Whole plant samples                         | Aristidoideae                               |                |                      |   |       |       |       |       |   |  |      |       |       |       |       |   |       |
|   | <i>Aristida adscensionis</i> <sup>#</sup>   | C <sub>4</sub> | NADP-ME              | Namibia   | -29.0 | -24.9 | -25.3 | -23.8 | n.d.  | -25.2  | n.d. | n.d.  | n.d.  | -24.4 | n.d.  | -24.1   | -24.1 |
|   | <i>Aristida barbicollis</i>                 | C <sub>4</sub> | NADP-ME              | Zimbabwe  | -20.0 | -21.4 | -23.9 | -22.1 | -21.2   | -22.8  | n.d. | n.d.  | n.d.  | n.d.  | n.d.  | n.d.  | n.d.  |
|   | <i>Aristida congesta</i>                    | C <sub>4</sub> | NADP-ME              | Namibia   | -20.4 | -22.9 | -24.3 | -24.0 | -24.2   | -23.9  | n.d. | n.d.  | -24.7 | -22.3 | n.d.  | -18.0   | -19.7 |
|   | <i>Aristida graciliflora</i>                | C <sub>4</sub> | NADP-ME              | Zimbabwe  | -25.6 | -23.9 | -24.1 | -23.9 | n.d.  | -24.1  | n.d. | n.d.  | n.d.  | n.d.  | n.d.  | n.d.  | n.d.  |
|   | <i>Aristida meridionalis</i>                | C <sub>4</sub> | NADP-ME              | Zimbabwe  | -21.4 | -22.4 | -22.8 | -22.4 | n.d.  | -22.4  | n.d. | n.d.  | n.d.  | n.d.  | n.d.  | -19.5   | -19.5 |
|   | <i>Aristida meridionalis</i>                | C <sub>4</sub> | NADP-ME              | Namibia   | -20.8 | -21.4 | -21.9 | -22.7 | n.d.  | -21.7  | n.d. | n.d.  | -24.3 | -24.7 | n.d.  | -22.2   | -22.4 |
|   | <i>Stipagrostis ciliata</i> <sup>#</sup>    | C <sub>4</sub> | NAD-ME               | Namibia   | -24.7 | -21.7 | -19.8 | -20.7 | n.d.  | -20.4  | n.d. | n.d.  | -25.1 | -25.3 | n.d.  | n.d.  | -25.1 |
|   | <i>Stipagrostis hirtigluma</i> <sup>#</sup> | C <sub>4</sub> | NAD-ME               | Namibia   | -25.3 | -25.0 | -23.2 | -24.0 | n.d.  | -23.9  | n.d. | n.d.  | -16.7 | -19.1 | n.d.  | -20.2   | -19.1 |
|   | <i>Stipagrostis uniplumis</i>               | C <sub>4</sub> | NAD-ME               | Namibia   | -23.2 | -24.5 | -25.9 | -24.0 | n.d.  | -25.1  | n.d. | n.d.  | -23.1 | -25.7 | n.d.  | -27.8   | -25.5 |
|   | Chloridoideae                               |                |                      |   |       |       |       |       |   |  |      |       |       |       |       |   |       |
|   | <i>Chloris gayana</i>                       | C <sub>4</sub> | PCK                  | Zimbabwe  | -23.0 | -22.5 | -23.4 | -24.9 | -24.0   | -24.1  | n.d. | n.d.  | n.d.  | n.d.  | n.d.  | n.d.  | n.d.  |
|   | <i>Chloris virgata</i>                      | C <sub>4</sub> | PCK                  | Zimbabwe  | -20.3 | -19.6 | -20.2 | -21.1 | -21.9   | -20.6  | n.d. | n.d.  | n.d.  | -23.4 | n.d.  | -19.8   | -21.6 |
|   | <i>Chloris virgata</i> <sup>#</sup>         | C <sub>4</sub> | PCK                  | Namibia   | -24.2 | -20.6 | -21.7 | -21.1 | -20.9   | -21.7  | n.d. | n.d.  | n.d.  | n.d.  | n.d.  | -20.2   | -20.2 |
|   | <i>Enneapogon sp.</i>                       | C <sub>4</sub> | NAD-ME               | Namibia   | -22.3 | -23.0 | -22.7 | -22.5 | -23.2   | -22.7  | n.d. | -21.8 | -24.5 | -23.7 | n.d.  | -21.5   | -22.5 |
|   | <i>Enneapogon cenchroides</i>               | C <sub>4</sub> | NAD-ME               | Zimbabwe  | -19.5 | -19.4 | -20.9 | -22.7 | -23.7   | -21.6  | n.d. | n.d.  | n.d.  | n.d.  | n.d.  | -19.7   | -19.7 |
|   | <i>Enneapogon cenchroides</i> <sup>#</sup>  | C <sub>4</sub> | NAD-ME               | Namibia   | -19.5 | -18.3 | -20.1 | -20.1 | n.d.  | -19.8  | n.d. | n.d.  | n.d.  | -20.3 | n.d.  | -20.6   | -20.4 |
|   | <i>Eragrostis nindensis</i>                 | C <sub>4</sub> | NAD-ME               | Namibia   | -24.4 | -22.7 | -24.6 | -24.0 | n.d.  | -24.0  | n.d. | n.d.  | n.d.  | -25.2 | n.d.  | -20.6   | -21.3 |
|   | <i>Eragrostis superba</i>                   | C <sub>4</sub> | NAD-ME               | Zimbabwe  | -20.4 | -20.8 | -21.8 | -22.7 | -23.0   | -21.5  | n.d. | n.d.  | n.d.  | -21.8 | n.d.  | n.d.  | -21.8 |
|   | <i>Eragrostis tremula</i>                   | C <sub>4</sub> | NAD-ME               | Sudan   | -24.0 | -25.1 | -25.9 | -26.3 | -26.4   | -25.8  | n.d. | n.d.  | n.d.  | n.d.  | n.d.  | -21.5   | -21.5 |
| <i>Eragrostis violacea de winter</i>        | C <sub>4</sub>                              | NAD-ME         | Zimbabwe             | -18.0   | -18.1 | -19.6 | -19.2 | -19.3 | -19.1   | n.d.   | n.d. | n.d.  | n.d.  | n.d.  | n.d.  | n.d.  |       |
| <i>Eragrostis viscosa</i>                   | C <sub>4</sub>                              | NAD-ME         | Zimbabwe             | -20.0   | -19.6 | -21.8 | -22.4 | -21.8 | -20.8   | n.d.   | n.d. | n.d.  | -20.1 | n.d.  | n.d.  | -20.1   |       |
| <i>Schmidtia kalahariensis</i> <sup>#</sup> | C <sub>4</sub>                              | PCK            | Namibia              | -21.8   | -22.0 | -22.9 | -20.5 | -21.3 | -21.2   | n.d.   | n.d. | n.d.  | n.d.  | n.d.  | -21.6 | -21.6   |       |
| <i>Sporobolus ioclados</i>                  | C <sub>4</sub>                              | NAD-ME         | Zimbabwe             | -19.9   | -21.8 | -22.4 | -22.0 | -21.8 | -19.6   | n.d.   | n.d. | n.d.  | n.d.  | n.d.  | -20.6 | -20.6   |       |
| <i>Sporobolus pyramidalis</i>               | C <sub>4</sub>                              | PCK            | Zimbabwe             | -21.2   | -22.0 | -22.1 | -22.7 | -23.8 | -22.3   | n.d.   | n.d. | -21.2 | n.d.  | n.d.  | -20.4 | -20.7   |       |

Whole plant samples

cont. **Table 2.4.** Isotopic data for grass subspecies studied.

|                     | Subfamily/<br>subspecies               | Photosynthetic<br>pathway | Physiology | Sampling<br>location | $\delta^{13}\text{C}$ of <i>n</i> -alkanols <sup>a</sup> (‰ vs. V-PDB) |       |       |       |       | $\delta^{13}\text{C}_{\text{WMA-27-35}}$ <sup>b</sup> | $\delta^{13}\text{C}$ of <i>n</i> -alkanols <sup>a</sup> (‰ vs. V-PDB) |       |       |       |      |       | $\delta^{13}\text{C}_{\text{WMA-22-32}}$ <sup>b</sup> |
|---------------------|--|---------------------------|------------|----------------------|--|-------|-------|-------|-------|---|--|-------|-------|-------|------|-------|---|
|                     |  |                           |            |                      | 27   | 29    | 31    | 33    | 35    |   | 22   | 24    | 26    | 28    | 30   | 32    |   |
| Whole plant samples | <b>Panicoideae</b>                     |                           |            |                      |  |       |       |       |       |   |  |       |       |       |      |       |   |
|                     | <i>Bothriochloa insculpta</i>          | C <sub>4</sub>            | NADP-ME    | Zimbabwe             | -18.0  | -19.2 | -18.7 | -18.6 | n.d.  | -18.7   | n.d.   | n.d.  | n.d.  | n.d.  | n.d. | n.d.  | n.d.  |
|                     | <i>Brachiaria erucitormis</i>          | C <sub>4</sub>            | PCK        | Zimbabwe             | -21.9  | -20.4 | -20.9 | -20.3 | n.d.  | -20.6   | n.d.   | n.d.  | n.d.  | n.d.  | n.d. | -18.6 | -18.6   |
|                     | <i>Digitaria milanijana</i>            | C <sub>4</sub>            | NADP-ME    | Zimbabwe             | -20.5  | -18.9 | -19.5 | -19.7 | -20.4 | -19.7   | n.d.   | n.d.  | n.d.  | n.d.  | n.d. | n.d.  | n.d.  |
|                     | <i>Hyparrhenia filipendula</i>         | C <sub>4</sub>            | NADP-ME    | Zimbabwe             | -21.5  | -21.9 | -21.9 | -22.8 | -23.0 | -22.4   | n.d.   | n.d.  | n.d.  | -25.4 | n.d. | -22.7 | -23.5   |
|                     | <i>Loudetia simplex</i>                | C <sub>4</sub>            | NADP-ME    | Zimbabwe             | -19.8  | -18.6 | -18.2 | -20.0 | -22.0 | -19.1   | n.d.   | n.d.  | n.d.  | n.d.  | n.d. | n.d.  | n.d.  |
|                     | <i>Panicum sp.</i>                     | C <sub>4</sub>            | ?          | Namibia              | -22.2  | -22.6 | -23.0 | -22.7 | -22.3 | -22.7   | n.d.   | -23.9 | -24.4 | -22.6 | n.d. | -20.0 | -21.5   |
|                     | <i>Panicum arbusculum</i> <sup>#</sup> | C <sub>4</sub>            | NAD-ME     | Namibia              | -24.1  | -22.0 | -24.0 | -21.4 | -21.6 | -22.2   | n.d.   | n.d.  | -22.8 | -24.8 | n.d. | -21.8 | -22.8   |
|                     | <i>Panicum maximum</i>                 | C <sub>4</sub>            | PCK        | Zimbabwe             | -20.0  | -20.8 | -19.4 | -23.3 | n.d.  | -20.4   | n.d.   | n.d.  | n.d.  | n.d.  | n.d. | n.d.  | n.d.  |
|                     | <i>Panicum maximum</i>                 | C <sub>4</sub>            | PCK        | Namibia              | -24.7  | -24.2 | -24.5 | -24.8 | n.d.  | -24.5   | n.d.   | n.d.  | n.d.  | -21.3 | n.d. | -19.0 | -19.3   |
|                     | <i>Themeda triandra</i>                | C <sub>4</sub>            | NADP-ME    | Zimbabwe             | -18.7  | -21.3 | -19.6 | -20.0 | -20.5 | -19.8   | n.d.   | n.d.  | n.d.  | n.d.  | n.d. | n.d.  | n.d.  |
|                     | <b>Pooideae</b>                        |                           |            |                      |  |       |       |       |       |   |  |       |       |       |      |       |   |
|                     | <i>Bromus sp.</i>                      | C <sub>3</sub>            |            | Australia            | -36.0  | -35.7 | -36.0 | -37.5 | -38.9 | -36.4   | n.d.   | n.d.  | n.d.  | -26.2 | n.d. | n.d.  | -26.2   |
|                     | <i>Festuca orthophylla</i>             | C <sub>3</sub>            |            | Peru                 | -30.2  | -30.3 | -31.3 | -31.2 | n.d.  | -30.4   | n.d.   | -29.8 | -25.2 | n.d.  | n.d. | n.d.  | -26.1   |
|                     | <i>Festuca orthophylla</i>             | C <sub>3</sub>            |            | Peru                 | -31.0  | -31.2 | -32.2 | -33.1 | n.d.  | -31.4   | n.d.   | n.d.  | -28.4 | n.d.  | n.d. | n.d.  | -28.4   |
| Plant part samples  | <b>Chloridoideae</b>                   |                           |            |                      |  |       |       |       |       |   |  |       |       |       |      |       |   |
|                     | <i>Sporobolus sp.</i> (flowers)        | C <sub>4</sub>            | ?          | Tanzania             | -19.9  | -19.6 | -20.5 | -20.4 | -21.8 | -20.3   | n.d.   | n.d.  | -20.8 | -21.2 | n.d. | n.d.  | -20.9   |
|                     | <i>Sporobolus sp.</i> (leaves)         | C <sub>4</sub>            | ?          | Tanzania             | n.d.   | n.d.  | -20.6 | -20.0 | -20.9 | -20.3   | n.d.   | n.d.  | -20.9 | -20.5 | n.d. | -22.2 | -21.3   |
|                     | <i>Sporobolus sp.</i> (stems)          | C <sub>4</sub>            | ?          | Tanzania             | n.d.   | -20.0 | -19.6 | -18.9 | -20.0 | -19.4   | n.d.   | n.d.  | -24.0 | -22.0 | n.d. | n.d.  | -23.0   |
|                     | <b>Panicoideae</b>                     |                           |            |                      |  |       |       |       |       |   |  |       |       |       |      |       |   |
|                     | <i>Brachiaria sp.</i> (flowers)        | C <sub>4</sub>            | PCK        | Tanzania             | -19.1  | -19.0 | -18.8 | -18.6 | -21.4 | -19.0   | n.d.   | n.d.  | n.d.  | n.d.  | n.d. | n.d.  | n.d.  |
|                     | <i>Brachiaria sp.</i> (leaves)         | C <sub>4</sub>            | PCK        | Tanzania             | -19.6  | -19.2 | -19.7 | -19.9 | -19.8 | -19.8   | n.d.   | n.d.  | n.d.  | n.d.  | n.d. | n.d.  | n.d.  |
|                     | <i>Brachiaria sp.</i> (stems)          | C <sub>4</sub>            | PCK        | Tanzania             | -22.5  | -20.7 | -20.2 | -20.0 | -21.3 | -20.4   | n.d.   | n.d.  | n.d.  | n.d.  | n.d. | n.d.  | n.d.  |

n.d. : not determined

<sup>#</sup> *n*-Alkane stable carbon isotopic values corrected after Huang et al. (2000) (see text for details)<sup>a</sup>  $\delta^{13}\text{C}$ : Molecular stable carbon isotopic composition of *n*-alkanes and *n*-alkanols (numbers according to individual carbon numbers)<sup>b</sup>  $\delta^{13}\text{C}_{\text{WMA-27-35}}$ : Weighted mean average of molecular stable carbon isotopic composition of odd-carbon-numbered *n*-alkanes (carbon number 27 - 35) [‰ versus V-PDB]; $\delta^{13}\text{C}_{\text{WMA-22-32}}$ : Weighted mean average of measured molecular stable carbon isotopic composition of even-carbon-numbered *n*-alkanols (carbon number 22 to 32) [‰ versus V-PDB] (note that mean average values for given sample were only calculated of the alkane and alkanol homologues for which carbon isotopic ratios were available).

### 3 A North to South transect of Holocene southeast Atlantic continental margin sediments: relationship between aerosol transport and compound-specific $\delta^{13}\text{C}$ land plant biomarker and pollen records

Florian Rommerskirchen, Geoffrey Eglinton, Lydie Dupont, Ute Güntner, Claudia Wenzel, Jürgen Rullkötter

This chapter was published: Rommerskirchen, F., Eglinton, G., Dupont, L., Güntner, U., Wenzel, C., Rullkötter, J., 2003. A north to south transect of Holocene southeast Atlantic continental margin sediments: Relationship between aerosol transport and compound-specific  $\delta^{13}\text{C}$  plant biomarker and pollen records. *Geochemistry, Geophysics, Geosystems* 4 (12), 1101, doi:10.1029/2003GC000541.

#### 3.1 Abstract

We examined near-surface, late Holocene deep-sea sediments at nine sites on a North-South transect from the Congo Fan (4°S) to the Cape Basin (30°S) along the Southwest African continental margin. Contents, distribution patterns and molecular stable carbon isotope signatures of long-chain *n*-alkanes (*n*-C<sub>27</sub> to *n*-C<sub>33</sub>) and *n*-alkanols (*n*-C<sub>22</sub> to *n*-C<sub>32</sub>) are indicators of land plant vegetation of different biosynthetic types, which can be correlated with concentrations and distributions of pollen taxa in the same sediments. Calculated clusters of wind trajectories and satellite Aerosol Index imagery afford information on the source areas for the lipids and pollen on land and their transport pathways to the ocean sites. This multidisciplinary approach on an almost continental scale provides clear evidence of latitudinal differences in lipid and pollen composition paralleling the major phytogeographic zonations on the adjacent continent. Dust and smoke aerosols are mainly derived from the western and central South African hinterland dominated by deserts, semi-deserts and savanna regions rich in C<sub>4</sub> and CAM plants. The northern sites (Congo Fan area and northern Angola Basin), which get most of their terrestrial material from the Congo Basin and the Angolan highlands, may also receive some material from the Chad region. Very little aerosol from the African continent is transported to the most southerly sites in the Cape Basin. As can be expected from the present position of the phytogeographic zones, the carbon isotopic signatures of the *n*-alkanes and *n*-alkanols both become isotopically more enriched in <sup>13</sup>C from North to South. The results of the study suggest that this combination of pollen data and

compound-specific isotope geochemical proxies can be effectively applied in the reconstruction of past continental phytogeographic developments.

## 3.2 Introduction

In the global organic carbon cycle the ocean is an important sink for terrigenous organic matter transported off shore by rivers and winds. Through this mechanism, marine sediments preserve a record of geographic and secular changes of continental climate and vegetation. Land-plant-derived organic particles may consist of microscopically recognisable spores, pollen and various kinds of plant fragments (e.g., Taylor et al., 1998). Land plants signatures are also displayed by specific biomarkers, such as long-chain *n*-alkanes and *n*-alkanols, and in bulk and molecular carbon isotopic signatures (e.g., Eglinton and Hamilton, 1967; Rieley et al., 1993).

Recent studies examined aeolian dusts, surface sediments and cores from continental margins for allochthonous terrigenous organic matter, using a combination of aliphatic biomarkers, carbon isotopic compositions and pollen distributions (e.g., Huang et al., 2000; Zhao et al., 2000, 2003; Eglinton et al., 2002; Schefuß et al., 2003a,b, 2004). The results comprise qualitative information concerning the phytogeography, soil conditions and the erosion and transport processes from land to ocean. The hinterland areas may be extensive, but the data provide an informative, integrated signal of the vegetation over a large, but broadly definable continental region.

This multiproxy study assesses the transport of terrestrial material from Southern Africa into the late Holocene Southeastern Atlantic Ocean. The study brings together biomarker abundances,  $\delta^{13}\text{C}$  values and pollen concentrations in ca. 1 cm near-surface sediment layers from nine sites over a 3000 km N-S transect (4°S to 30°S; Fig. 3.1), using material from Ocean Drilling Project (ODP) and RV Meteor cruise cores (Table 3.1). It relates these data to the present-day wind systems and to model transport path calculations, satellite aerosol maps and the continental phytogeography in terms of  $\text{C}_3$ ,  $\text{C}_4$  and CAM plants (cf. Fig. 3.2 and 3.3). We particularly address the question of how the approximately known geographic distribution of  $\text{C}_3$  and  $\text{C}_4$  plants on the continent is reflected in the marine sediments. We are testing out this recently introduced approach (Huang et al., 2000) to the characterisation of epicontinental sedimentation of organic matter in order to lay a basis for the extension of this technique to longer geological records in the Late Pleistocene.

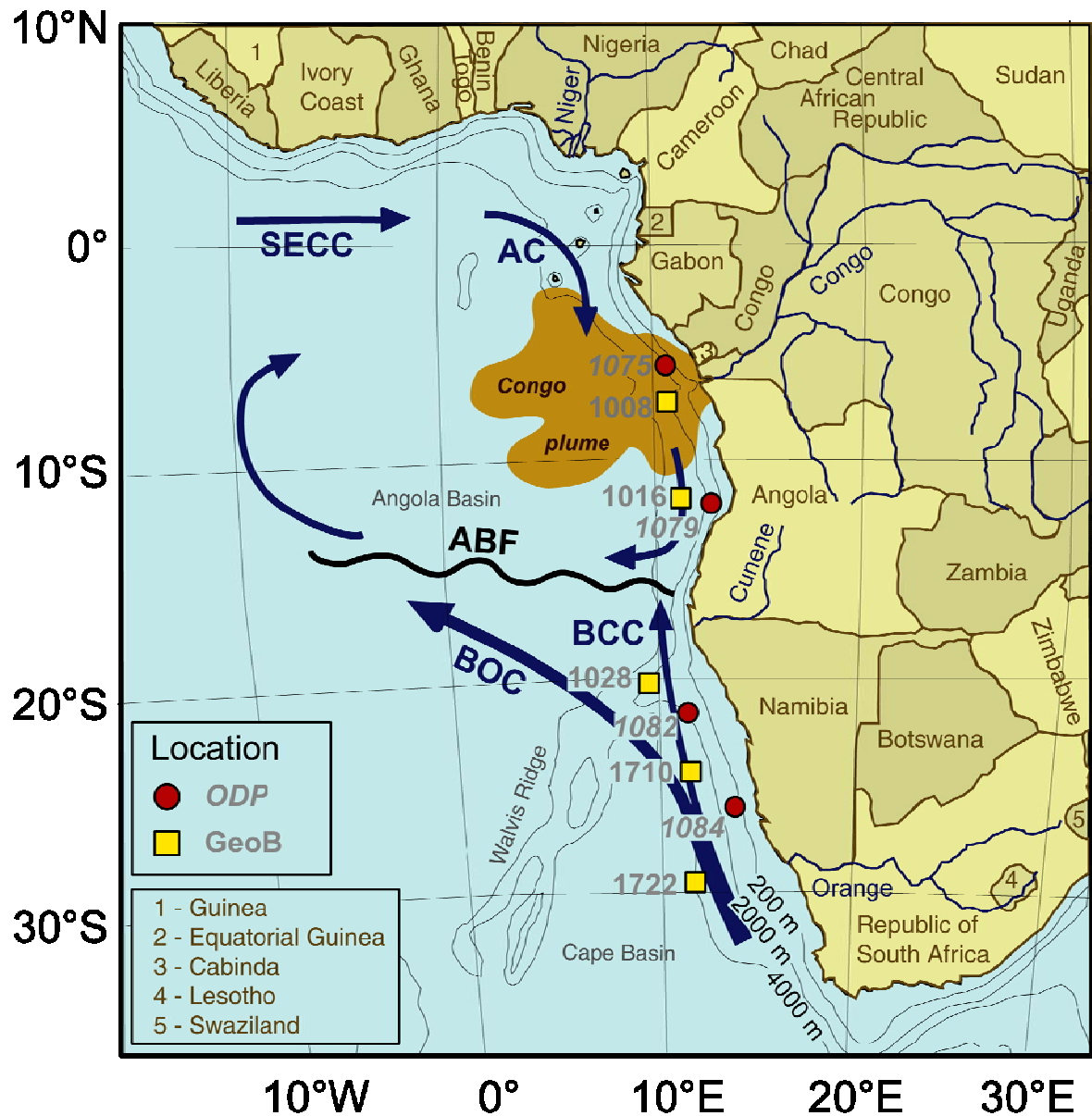


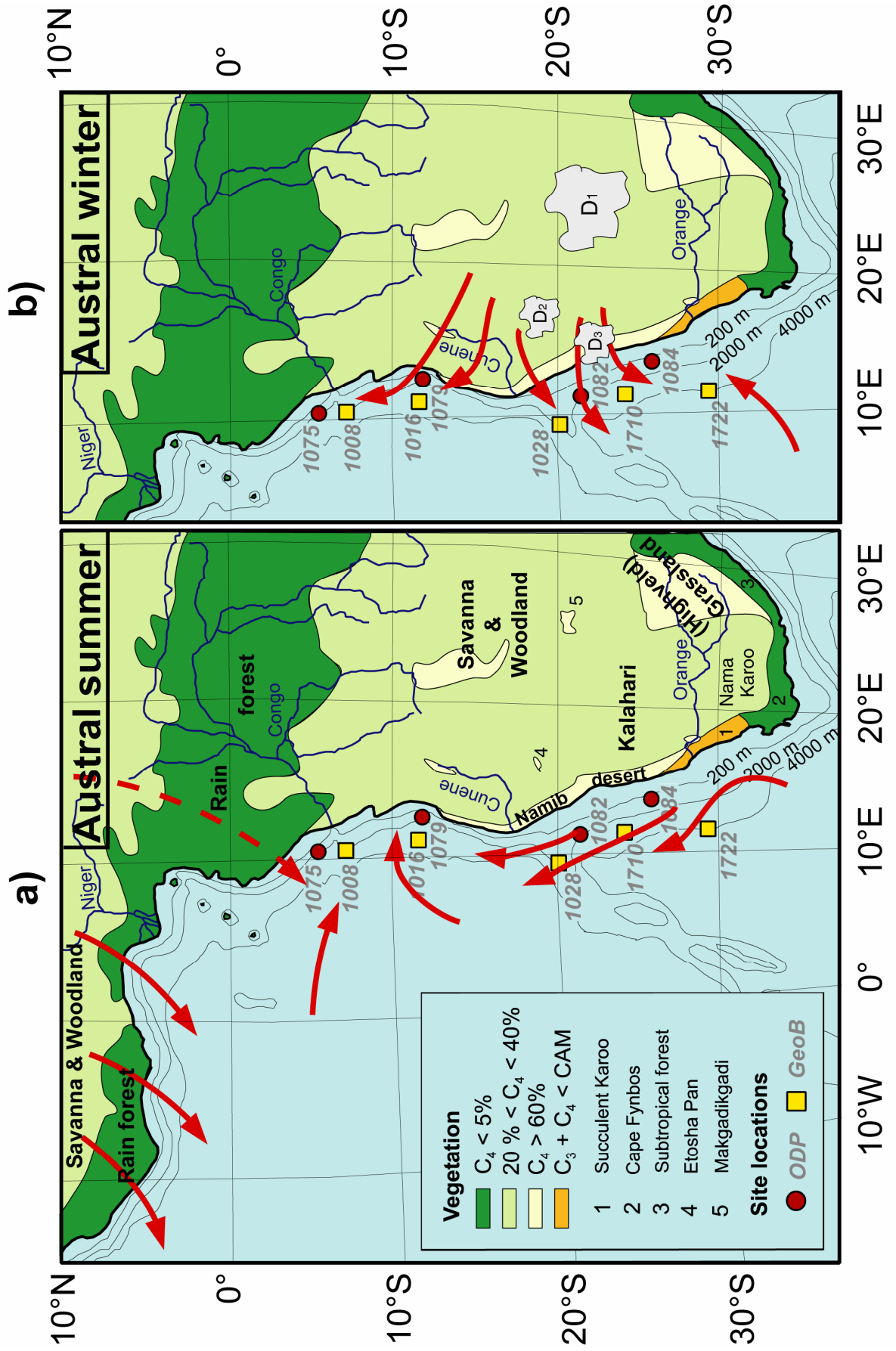
**Fig. 3.1.** Partial map of Africa showing site locations, major oceanic basins and currents in the Southeast Atlantic Ocean as well as political boundaries. The main three rivers in Southern Africa are the Congo (draining tropical rain forest, drainage area  $3.7 \times 10^6 \text{ km}^2$ , total suspension load  $40 \times 10^6 \text{ t yr}^{-1}$ , particulate organic carbon load  $2.8 \times 10^6 \text{ t yr}^{-1}$ , main clay mineral is kaolinite), the Cunene (draining semi-arid, semi-humid regions of Central to Southern Africa, drainage area  $0.12 \times 10^6 \text{ km}^2$ , total suspension load about  $15 \times 10^6 \text{ t}$ , low organic matter load, clay minerals rich in smectite) and the Orange (savannah river, but also drains desert and sub-desert with high proportion of  $C_4$  and CAM plants; drainage basin  $1.0 \times 10^6 \text{ km}^2$ , organic carbon load  $0.01 \times 10^6 \text{ t yr}^{-1}$ , minor clay mineral load of mainly illite). ABF = Angola-Benguela Front, AC = Angola Current, BCC = Benguela Coastal Current, BOC = Benguela Ocean Current, SECC = South Equatorial Countercurrent; Congo Plume after van Bennekom and Berger (1984).

**Table 3.1.** Cores studied. Locations, lithology, sedimentation rates and age models.

| Core        | Location              | Latitude (°S) | Longitude (°E) | Water depth (m) | Distance to shore (km) | Distance to major river mouth (km) | Lithology (clay province <sup>a</sup> )             | Sedimentation rate (cm ka <sup>-1</sup> ) | Age model  |
|-------------|-----------------------|---------------|----------------|-----------------|------------------------|------------------------------------|---|---|--|
| ODP 1075A   | Congo Fan             | 4°47'         | 10°04'         | 2995            | 150                    | 280 (Congo)                        | diatomaceous clay (kaolinite)                       | 9   | Wefer et al. (1998), Dupont et al. (2001)              |
| GeoB 1008-3 | Northern Angola Basin | 6°35'         | 10°19'         | 3124            | 270                    | 310 (Congo)                        | diatomaceous foraminiferal mud (kaolinite)          | 7   | Schneider et al. (1995, 1996)                          |
| GeoB 1016-3 | Southern Angola Basin | 11°46'        | 11°41'         | 3411            | 170                    | 630 (Cunene)                       | foraminiferal hemipelagic mud (smectite)            | 5   | Schneider et al. (1995, 1996)                          |
| ODP 1079A   | Southern Angola Basin | 11°56'        | 13°19'         | 738             | 60                     | 580 (Cunene)                       | foraminiferal and nannofossil silty clay (smectite) | 43  | Wefer et al. (1998)                                    |
| GeoB 1028-5 | Southern Angola Basin | 20°06'        | 9°11'          | 2209            | 320                    | 380 (Cunene)                       | hemipelagic mud (illite)                            | 6   | Schneider et al. (1995, 1996)                          |
| ODP 1082A   | Walvis Ridge          | 21°05'        | 11°49'         | 1279            | 150                    | 1000 (Orange)                      | nannofossil- and foraminifer-rich clay (illite)     | 10  | Wefer et al. (1998)<br>B. Donner (pers. commun., 2002) |
| GeoB 1710-3 | Walvis Basin          | 23°26'        | 11°42'         | 2987            | 270                    | 770 (Orange)                       | hemipelagic mud (illite)                            | 4   | Kirst et al. (1999)                                    |
| ODP 1084A   | Northern Cape Basin   | 25°30'        | 13°01'         | 1992            | 175                    | 480 (Orange)                       | foraminifer- and diatom-bearing clay                | 22  | B. Donner (pers. commun., 2002)                        |
| GeoB 1722-1 | Cape Basin            | 29°27'        | 11°45'         | 3973            | 380                    | 450 (Orange)                       | hemipelagic mud (illite)                            | 2   | T. Bickert (pers. commun., 2000)                       |

<sup>a</sup>Clay mineral provinces according to Petschick et al. (1996)





With the exception of the two northernmost sites, located in front of the Congo River, coring occurred at distances from the coast where aeolian (not riverine) contributions would be the dominant terrigenous sources. The length of the N-S transect, paralleled by a wide phytogeographic diversity on the continent, is an excellent test range for this type of multiproxy assessment. As with all proxies, pollen counts are biased records due to the differential effects of seasonal flowering, varying winds, amounts of pollen produced, transportability, different stabilities of pollen varieties, and ambiguities in the recognition of pollen species. However, wax components also have their problems, such as compositional variation with species in terms of compound and carbon isotope distributions and factors such as ease of abrasion, adsorption to soil particles and transport with dust.

### 3.3 Materials and methods

#### 3.3.1 *Sediment cores*

Material for analysis was selected from five gravity cores collected during Meteor cruises M 6/6 (GeoB 1008, 1016 and 1028; February 1988) and M 20/2 (GeoB 1710 and 1722; January 1992; Wefer et al., 1988; Schulz et al., 1992) and four drill cores from ODP Leg 175 (ODP 1075, 1079, 1082 and 1084; Wefer et al., 1998) (Table 3.1). From each core, 5 to 10 mL sediment was taken representing the late Holocene. Stratigraphy and age models for Meteor cores are after Schneider et al. (1995, 1996), Shi et al. (1998) and Kirst et al. (1999), for ODP Site 1075 after Dupont et al. (2001), for ODP Site 1079 after Pérez

**Fig. 3.2.** (opposite) Simplified phytogeographical units of today in Southwest Africa (colour codes according to  $C_4$  plant occurrence) and generalised wind directions of a) the austral summer (December, January, February) and b) the austral winter season (June, July, August). The broken arrow indicates mid-tropospheric wind from Central Africa, solid arrows indicate lower tropospheric winds. For more details see Dupont and Wyputta (2003). D = main dust storm source areas according to Prospero et al. (2002).  $D_1$  = Makgadikgadi Pans (Kalahari [Botswana], centred near  $21^\circ\text{S}$  to  $26^\circ\text{E}$ , year-long dust activity at a low level, increasing strongly in June-July and maximising in August to October; main pans consist of shallow pools, sandy alkaline clays and islands of grass with other large areas of salt flats to the East; vegetation is mainly  $C_4$ -plant-dominant edaphic grassland, whereas to the Northwest of the Okavango Swamp the vegetation has  $C_3$  and  $C_4$  plants, both between 40 and 60%),  $D_2$  = Etosha Pan (Namibia, centred at  $16^\circ\text{E}$  and  $18^\circ\text{S}$ , large salt pan associated with ephemeral lakes and swamps to its West; seasonal dust generation timing is said to follow that of the Makgadikgadi Depression across the Kalahari to the Southeast; dominant vegetation is  $C_4$  grassland),  $D_3$  = Namib desert.  $C_4$  plants are abundant in Southern Africa, although their occurrence is patchy and difficult to generalise in terms of proportions relative to  $C_3$  plant abundance. A tentative classification in four different areas is made (see legend in the figure). More than 50%  $C_4$  plant coverage is probably only found in the Namib desert, around salt pans, in swamps without canopy and in the Highveld Grassland, but Southern Africa is nevertheless an important source of  $C_4$  plant material transported to the Southeast Atlantic Ocean.

and Berger (2000), for ODP Site 1082 after Bickert (pers. commun., 2000) and for ODP Site 1084 after Donner (pers. commun., 2002). For information on the oceanography of the Southeast Atlantic and the sedimentology and geochemistry of the sediments see Wefer et al. (1998, 2002).

A complete set of analytical data of this study will be made available through the PANGAEA database (<http://www.pangaea.de>).

#### *3.3.2 Mass accumulation rates*

Organic carbon and biomarker mass accumulation rates (MAR,  $\text{mg cm}^{-2} \text{ kyr}^{-1}$ , total organic carbon, or  $\mu\text{g cm}^{-2} \text{ kyr}^{-1}$ , biomarkers) were calculated to eliminate any dilution effects by using the equation  $\text{MAR} = X * \rho * S_A$ , (van Andel et al., 1975; Lyle, 1988), where  $X$  = total organic carbon content ( $\text{mg g sed}^{-1}$ ) or content of a specific biomarker or group of biomarkers ( $\mu\text{g g sed}^{-1}$ ),  $\rho$  = dry bulk density ( $\text{g cm}^{-3}$ ; Wefer et al., 1998) and  $S_A$  = average sedimentation rate ( $\text{cm kyr}^{-1}$ ; Table 3.1).

#### *3.3.3 Methods for lipid and pollen analysis*

The analytical procedures were described by Mangelsdorf et al. (2000) apart from the details noted below. Briefly, organic carbon was calculated as the difference between total carbon and carbonate carbon contents determined by combustion of freeze-dried and ground sediment (at least two measurements each).

For lipid analysis, sample aliquots of 2-15 g were extracted. Squalane, erucic acid ( $n\text{-C}_{22:1}$ ),  $5\alpha$ -androstan-17-one and  $5\alpha$ -androstan-3 $\beta$ -ol were added to the extracts as internal standards. The  $n$ -hexane-soluble fraction was separated by medium-pressure liquid chromatography (Radke et al., 1980) into fractions of aliphatic/alicyclic hydrocarbons, aromatic hydrocarbons and polar heterocomponents (NSO). Carboxylic acids were separated from the NSO fraction using a column with KOH-impregnated silica.  $n$ -Alkanols were isolated by urea adduction.

The compounds of interest were analysed by gas chromatography (GC) and gas chromatography-mass spectrometry (GC-MS). Bulk carbon isotopic measurements of total organic matter were done using a Carlo Erba CHNS 1108 analyser attached to a Finnigan MAT 252 isotope mass spectrometer. The compound-specific carbon isotope analysis (GC-irm-MS) of individual fractions was carried out with a GC coupled to the Finnigan MAT 252 isotope mass spectrometer via a GCC-II combustion interface. GC conditions

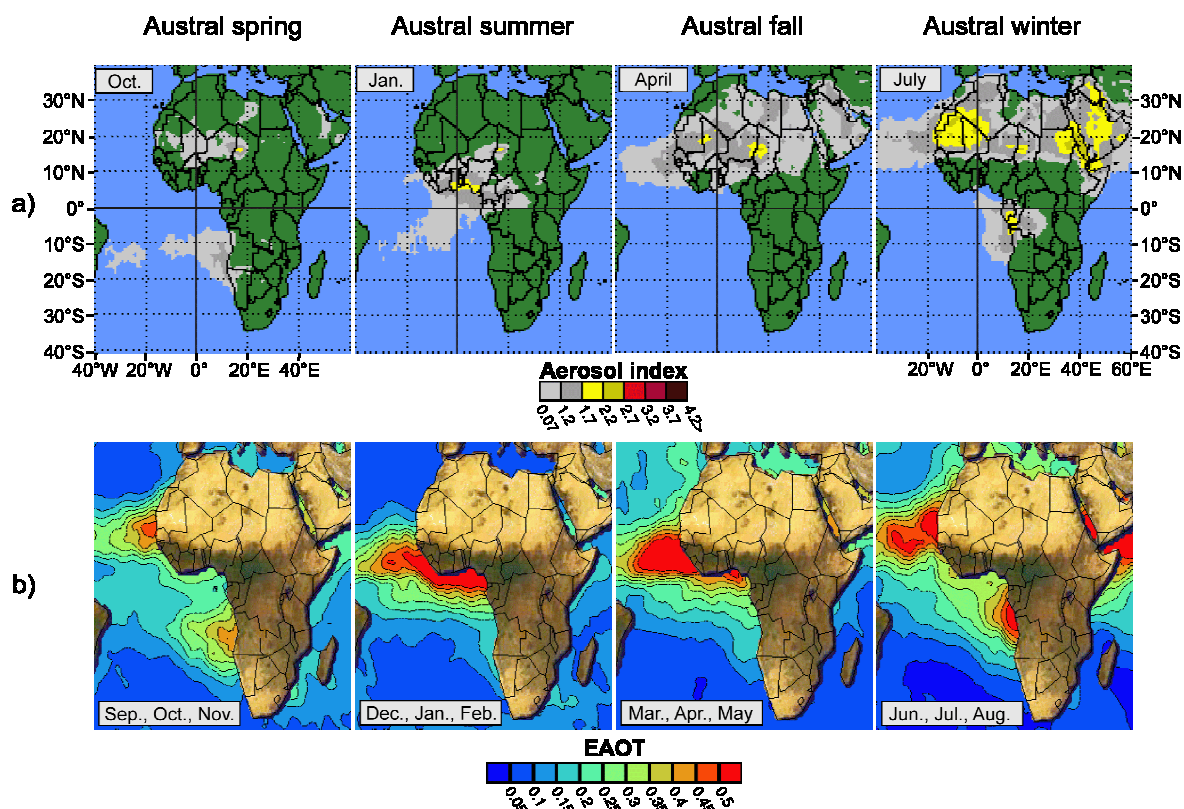


**Fig. 3.3.** Satellite imagery of aerosol (dust and smoke) distributions above the African continent and the Southeast Atlantic Ocean. a) Earth Probe TOMS aerosol images of monthly averages for representative months of each of the four seasons in the year 2000. Data are for the austral spring (October), summer (January), fall (April) and winter (July; [ftp://toms.gsfc.nasa.gov/pub/eptoms/images/monthly\\_averages/aerosol/eam000x.gif](ftp://toms.gsfc.nasa.gov/pub/eptoms/images/monthly_averages/aerosol/eam000x.gif) with  $x=10, 1, 4$  and  $7$ , respectively). The January aerosol cloud from Central Africa (including the Chad region) marginally affects the Congo fan sites. b) Radiatively Equivalent Aerosol Optical Thickness (EAOT  $\times 1000$ ), also expressed as Aerosol Optical Depth (AOD) over oceans, derived from NOAA AVHRR satellites for the four seasons. The figure incorporates data for the period July 1989 to June 1991. The gridded data and the images can be viewed and down-loaded from the website <http://capita.wustl.edu/CAPITA/CapitaReports/TropoAerosolRevised/AVHRR96l.htm> (from Husar et al., 1997). The smoke and dust plume which moves out over the Atlantic Ocean is at its most marked in the austral winter season but weakens and moves south somewhat in the austral spring. The NW to SE elongation of the axis of the lobe in the austral spring is suggestive of some of the dust being transported from the Namib desert and the arid savannah of the Kalahari. However, these regions are not reported to be good sources of fine dust, and their vegetation is too sparse for the occurrence of major biomass burning.

were the same as for GC analysis with the exception that a high-temperature column was used (J&W DB-5HT, 30 m length, 0.25 mm i.d., 0.1  $\mu\text{m}$  film thickness). Calibration was performed by injecting several pulses of  $\text{CO}_2$  of known  $\delta^{13}\text{C}$  value at the beginning and the end of each GC run and by using squalane ( $n$ -alkanes) and  $n$ -hexadecane ( $n$ -alkanols) as internal standards. Isotopic ratios are expressed as  $\delta^{13}\text{C}$  values in per mil relative to the V-PDB standard.  $\delta^{13}\text{C}$  values of alkanols are corrected for the contribution of the trimethylsilyl group from derivatisation.

Procedures and palynological methods for the analysis of pollen and spores are described in Dupont and Wyputta (2003). Data here are given for total pollen, fern spores, sum of pollen from C<sub>3</sub> plants (mainly woody plants), and the pollen taxa Restionaceae (cape reeds), Asteraceae (composites), Poaceae (grasses), Cyperaceae (sedges, rushes, papyrus, etc.) and *Tribulus*.

#### 3.3.4 *Satellite aerosol imaging*

NASA's Nimbus-7 and Earth Probe Total Ozone Mapping Spectrometer (TOMS) data have provided daily global images of the distribution of an Aerosol Index (AI) for a number of years. These can be displayed as monthly averages (<http://toms.gsfc.nasa.gov/index.html>; cf. Fig. 2.3a). The AI registers mineral dust, volcanic ash and smoke distributions in the atmosphere over both continental and oceanic regions (Hsu et al., 1996; Herman et al., 1997; Chiapello et al., 1999). The TOMS detects UV-absorbing aerosols using spectral contrast between 340/380 nm and 331/360 nm. Boundary layer absorbing aerosols are not readily detected with this technique, nor the difference between soil dust and smoke (Husar et al., 1997). Thus, the appearance of areas of enhanced AI in the satellite imagery corresponds to the deflation of dust and/or burning of biomass on the ground beneath (cf. Justice et al., 1996; Swap et al., 1996a,b), followed by the formation of dust or smoke clouds in the middle troposphere. Lateral transport and fallout from these aerosol clouds mostly account for their dispersal over the days following their appearance.

Independent assessments of global aerosol distributions are also available in the form of equivalent aerosol optical thickness (EAOT) data from the National Oceanic and Atmospheric Administration's (NOAA) Advanced Very High Resolution Radiometer (AVHRR), which is on a polar orbiting satellite (cf. Fig. 2.3b). The remote sensing algorithm is based on measurements of back-scattered solar radiation at 0.63  $\mu\text{m}$  (Husar et al., 1997).

### 3.4 Results and discussion

#### 3.4.1 *Simplified phytogeographical units of southwest Africa*

The vegetation of Africa south of the equator ranges from lowland rainforest to desert and to Afroalpine vegetation as represented in Fig. 3.2 in a simplified way. Based on the

maps of White (1983) and Cowling et al. (1997), and the satellite images of the Africa Land Cover Characteristics Database (Sellers et al., 1996; Loveland et al., 1999; [http://edcdaac.usgs.gov/glcc/af\\_int.html](http://edcdaac.usgs.gov/glcc/af_int.html)), we have made a broad brush assessment of the distribution of C<sub>3</sub>, C<sub>4</sub> and CAM plants over this area using lists of C<sub>4</sub> plants of Dowton (1975), Raghavendra and Das (1978), Elmore and Paul (1983), and Smith and Winter (1996).

In swamp forest and lowland rain forest, C<sub>4</sub> plants, notably among the grass species, form a small minority, usually along river banks and in coastal areas. The C<sub>4</sub> plant proportion is high in swamp regions without a closed canopy (e.g., papyrus). The largest biome in southern Africa is the savanna consisting of trees, shrubs and grasses, whereby the woody species are C<sub>3</sub> and the grass species mostly C<sub>4</sub> plants. The relative amounts of grasses and woody species, however, vary considerably. Thus, the importance of C<sub>4</sub> plants increases with the decrease of woody species abundance. The desert regions are dominated by C<sub>4</sub> plants (grasses and weeds), but CAM plants are also abundant. Along the west and south coast of South Africa, the winter rain areas are rich in CAM plants but poor in C<sub>4</sub> plants. C<sub>4</sub> plants are almost absent in the Fynbos of the Cape.

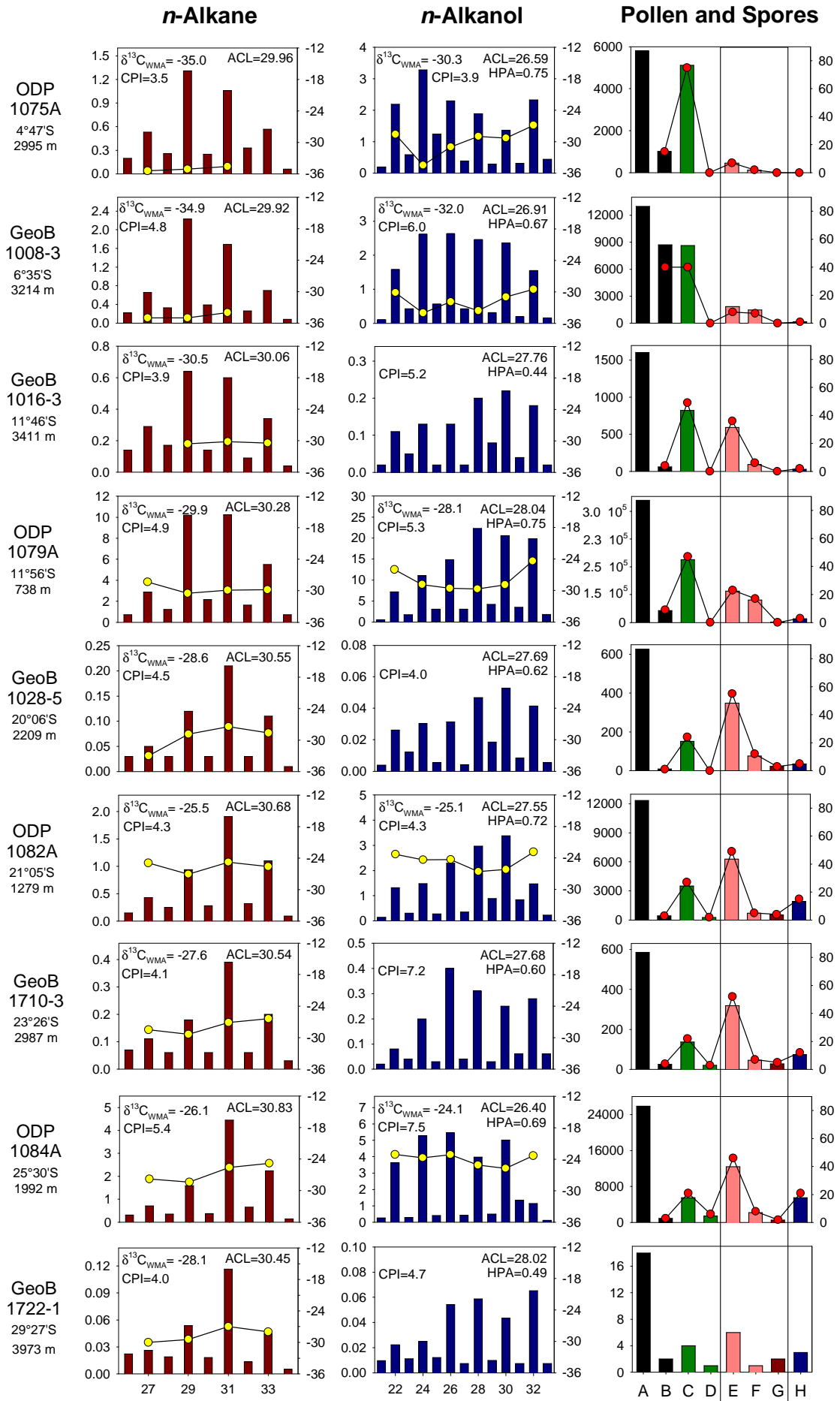
In terms of pollen distribution along the transect, Dupont and Wyputta (2003) concluded that a good latitudinal correspondence exists between the distribution patterns in the marine sediments and the occurrence of the source plants on the continent (Table 3.2).

#### 3.4.2 Carbon number distributions and molecular carbon isotope signatures of long-chain *n*-alkanes

Fig. 3.4 shows the distribution patterns of the long-chain *n*-alkanes (*n*-C<sub>26</sub> to *n*-C<sub>34</sub>) in the extractable lipids of late Holocene sediments from the nine sites. The diagrams are individually normalised to the most abundant homologue for each site. The y axes show the mass accumulation rates (MAR) of the *n*-alkanes; numerical data are compiled in Table 3.3. The Angola Basin ODP Site 1079 exhibits the highest MAR values (29 µg cm<sup>-2</sup> kyr<sup>-1</sup>, sum of *n*-C<sub>27</sub> to *n*-C<sub>33</sub> odd-carbon-number homologues). This site is close to the coast (60 km off shore) and has the shallowest water depth (738 m). Nevertheless, it is distant from the Congo river mouth (Table 3.1). The sediments from the other three ODP sites, which are all in shallower water and closer to the coast than the adjacent GeoB sites, have MAR values for the odd-carbon-number *n*-alkanes lower by a factor of about three to eight. With the exception of Site GeoB 1008, which is close to ODP Site 1075 on the other side of the Congo deep-sea canyon, all other GeoB sites exhibit low *n*-alkane accumulation rates in the order of 0.2 to 2 µg cm<sup>-2</sup> kyr<sup>-1</sup>.

**Table 3.2.** Proposed source areas of pollen, dust and smoke aerosol reaching Southeast Atlantic Ocean sites (and their relative strength; cf. Fig. 3.2). The estimates of the strengths are very tentative and make some allowance for the distance travelled from the coast, with fluxes expected to be less the further from land. The transport is assumed to be aeolian, unless specified as fluvial. The dust and smoke estimates are based on satellite imagery where values of AI below 0.7 are considered minor (Earth TOMS, monthly averages per year - 2000; [ftp://toms.gsfc.nasa.gov/pub/eptoms/images/monthly\\_averages/aerosol/eam000x.gif](ftp://toms.gsfc.nasa.gov/pub/eptoms/images/monthly_averages/aerosol/eam000x.gif) with x=10, 1, 4 and 7, respectively; cf. Fig. 3.3).

| Sites (approx. latitude)  | Pollen abundance  | Dust strength   | Smoke aerosol strength   |
|---|---|---|--|
| ODP 1075 (5°S)<br>Congo Fan<br>GeoB 1008 (7°S)<br>North Angola Basin      | <b><u>Abundant</u></b><br>Fluvial from Congo rainforest and swamp forest<br>Forest and woodland (Southern Congo and Angola) | <b><u>Moderate</u></b><br>Alluvial plains of Chad Basin and Sahel, to North of equator<br>North fringe of plume from Central and Southwest sources (see below)                            | <b><u>Strong</u></b><br>Dry forest to North and South of Congo tropical forest<br>Woodland and savanna (Angola and Botswana) |
| GeoB 1016 (12°S)<br>Angola Basin<br>ODP 1079 (12°S)<br>Angola Basin       | <b><u>Moderate to abundant</u></b><br>Woodland and savanna (Angola)<br>North Namib desert                                   | <b><u>Very strong</u></b><br>Plume from Southeast moving Northwest from Central Kalahari savanna (Botswana) - the Makgadikgadi pans<br>Southwestern Etosha pan (Namibia) and Namib desert | <b><u>Strong</u></b><br>Woodland and savanna (Angola and Botswana)   |
| GeoB 1028 (20°S)<br>South Angola Basin<br>ODP 1082 (21°S)<br>Walvis Ridge | <b><u>Weak to abundant</u></b><br>Kalahari savanna<br>Namib desert  | <b><u>Strong</u></b><br>Southwestern edge of above plume  | <b><u>Strong</u></b><br>Kalahari savanna (Botswana, Kalahari)<br>Northern Nama-Karoo semi-desert (Namibia and South Africa)  |
| GeoB 1710 (23°S)<br>Walvis Basin  | <b><u>Weak</u></b><br>Kalahari savanna<br>Namib desert and succulent Karoo, Nama-Karoo semi-desert                          | <b><u>Moderate</u></b><br>Southern extreme of plume<br>Kalahari savanna<br>Namib desert   | <b><u>Moderate</u></b><br>As for GeoB 1028 and ODP 1082  |
| ODP 1084 (25°S)<br>North Cape Basin                                       | <b><u>Abundant</u></b><br>As for 1710 and Cape Fynbos   | <b><u>Weak</u></b><br>Namib desert<br>Succulent desert  | <b><u>Weak</u></b>   |
| GeoB 1722 (29°S)<br>Cape Basin  | <b><u>Rare</u></b><br>Namib desert<br>Succulent Karoo<br>Cape Fynbos  | <b><u>Very weak</u></b>   | <b><u>Very weak</u></b>  |





The carbon number maximum of the alkanes moves from  $n\text{-C}_{29}$  at the northernmost sites to  $n\text{-C}_{31}$  at ODP Site 1079 and further south. In addition, the overall chain length distribution, best expressed by the Average Chain Length (ACL) parameter (Poynter, 1989), first increases southwards to ODP Site 1084 and then decreases slightly further south ( $\text{ACL}_{27-33}$ ; Fig. 3.5). The  $\text{ACL}_{27-33}$  values for the odd-carbon-number  $n\text{-C}_{27}$  to  $n\text{-C}_{33}$  homologues thus increase down the transect from 29.92 to 30.83 before decreasing again to 30.45 (Table 3.3, Fig. 3.4 and 3.5). A similar latitudinal trend in ACL values of  $n$ -alkanes was not observed by Schefuß et al. (2003b) in the dust samples they collected along the west coast of Africa, despite a shift in the carbon number maximum from  $n\text{-C}_{29}$  to  $n\text{-C}_{31}$  from low to higher latitudes. This shift is also pronounced in our data set and illustrated by the  $n\text{-C}_{31}/(n\text{-C}_{29}+n\text{-C}_{31})$  ratio (Fig. 3.5) which increases from 0.45 to 0.7 in the N-S transect. The triangular plots in Fig. 3.6 clearly show that the N-S distinction among the alkane homologues is brought about only by the  $n\text{-C}_{29}$  and  $n\text{-C}_{31}$  compounds, whereas the  $n\text{-C}_{27}$  and  $n\text{-C}_{33}$  homologues do not contribute (nor does the  $n\text{-C}_{35}$  homologue; not shown). Along the  $n\text{-C}_{29}$  to  $n\text{-C}_{31}$  axis in the diagrams, the latitudinal succession from the northernmost to the southernmost sites is nearly perfect. The offset between the group of the four northernmost sites and the southern localities corresponds to the latitudinal gap in sampling sites between ODP 1079 and ODP 1082 (e.g., Fig. 3.5).

The long-chain  $n$ -alkanes of all the samples in this study exhibit significantly high odd-over-even carbon number preferences ( $\text{CPI}_{27-33}$ ,  $\text{CPI}_{27-33}$  ranging from 3.5 to 5.4; Table 3.3, Fig. 3.4 and 3.5). This is typical for sedimentary hydrocarbons derived from higher plant waxes. On the other hand, it is evident from many studies of organic matter in ancient sediments that enormous quantities of thermally mature hydrocarbons were generated in the past and then liberated into the environment. Two submarine seeps on the Southwest African continental margin were documented by Hovland and Judd (1988,

**Fig. 3.4.** (opposite) N-S transect of histogram representations of long-chain  $n$ -alkane and  $n$ -alkanol accumulation rates (MAR:  $\mu\text{g cm}^{-2} \text{ kyr}^{-1}$ ), overlain by molecular stable carbon isotope data ( $\delta^{13}\text{C}$  in ‰ versus V-PDB) for individual homologues, as well as pollen and spores accumulation rates (counts  $\text{cm}^{-2} \text{ kyr}^{-1}$ ; note very low abundance at Site GeoB 1722) and percentages in deep sea sediments from nine sampling locations in the Southeast Atlantic Ocean (cf. Fig. 3.1). Gaps in the data coverage of molecular isotope values are due to too low concentrations for reliable analysis or evaluation of raw data. Abbreviations and explanations: Left and middle:  $Y_1$ : MAR ( $\mu\text{g cm}^{-2} \text{ ka}^{-1}$ );  $Y_2$ :  $\delta^{13}\text{C}$  (‰ vs. V-PDB);  $\delta^{13}\text{C}_{\text{WMA}}$ : Weighted mean average of carbon isotope values of odd-carbon-numbered  $n\text{-C}_{27}$  to  $n\text{-C}_{33}$  alkanes and even-carbon-numbered  $n\text{-C}_{22}$  to  $n\text{-C}_{32}$  alkanols (‰ versus V-PDB), respectively; ACL: Average chain length (Poynter, 1989;  $n$ -alkanes: odd-carbon-number  $n\text{-C}_{27}$  to  $n\text{-C}_{33}$  alkanes;  $n$ -alkanols: even-carbon-number  $n\text{-C}_{22}$  to  $n\text{-C}_{32}$  alkanols); CPI: Carbon preference index (Bray and Evans, 1962;  $n$ -alkanes:  $n\text{-C}_{27}$  to  $n\text{-C}_{33}$  alkanes;  $n$ -alkanols:  $n\text{-C}_{22}$  to  $n\text{-C}_{32}$  alkanols); HPA: Higher plant  $n$ -alkanol index (Poynter and Eglinton, 1991). Right:  $Y_1$  (bars): Accumulation rate (counts/( $\text{cm}^2 \text{ ka}^{-1}$ ));  $Y_2$ : % (pollen + spores); A: pollen; B: fern spores; C:  $\text{C}_3$  species (mainly woody plants); D: Cape reeds ( $\text{C}_3$ ); H: composites ( $\text{C}_3$  and CAM); BOX: E: grasses (predominantly  $\text{C}_4$ ); F: Cyperaceae ( $\text{C}_3$  and  $\text{C}_4$ ); G: *Tribulus* ( $\text{C}_4$ ).

Table 3.3. Biomarker data.

| Core        | Depth<br>(cm) | Age<br>(ka) | ACL <sub>27-33</sub> <sup>a</sup> | ACL <sub>22-32</sub> <sup>a</sup> | CPI <sub>27-33</sub> <sup>b</sup> | CPI <sub>22-32</sub> <sup>c</sup> | HPA <sup>d</sup> | MAR <sup>e</sup><br>C <sub>org</sub> | MAR <sup>e</sup><br>CaCO <sub>3</sub> | MAR <sup>e</sup><br>ALK <sup>f</sup> | MAR <sup>e</sup><br>-OH <sup>g</sup> |
|-------------|---------------|-------------|-----------------------------------|-----------------------------------|-----------------------------------|-----------------------------------|------------------|--------------------------------------|---------------------------------------|--------------------------------------|--------------------------------------|
| ODP 1075A   | 55            | 5.0         | 29.96                             | 26.59                             | 3.5                               | 3.9                               | 0.75             | 64                                   | 11                                    | 3.5                                  | 13.4                                 |
| GeoB 1008-3 | 13            | 2.0         | 29.92                             | 26.91                             | 4.8                               | 6.0                               | 0.67             | 44                                   | 17                                    | 5.3                                  | 13.2                                 |
| GeoB 1016-3 | 4             | 1.0         | 30.06                             | 27.76                             | 3.9                               | 5.2                               | 0.44             | 19                                   | 183                                   | 1.9                                  | 1.8                                  |
| ODP 1079A   | 77            | 3.0         | 30.28                             | 28.04                             | 4.9                               | 5.3                               | 0.75             | 800                                  | 2830                                  | 29                                   | 95.8                                 |
| GeoB 1028-5 | 20            | 4.0         | 30.55                             | 27.69                             | 4.5                               | 4.0                               | 0.62             | 21                                   | 3590                                  | 0.5                                  | 1.0                                  |
| ODP 1082A   | 37            | 3.8         | 30.68                             | 27.55                             | 4.3                               | 4.3                               | 0.72             | 170                                  | 3600                                  | 4.4                                  | 12.9                                 |
| GeoB 1710-3 | 3             | 1.0         | 30.54                             | 27.68                             | 4.1                               | 7.2                               | 0.60             | 39                                   | 1780                                  | 0.9                                  | 1.5                                  |
| ODP 1084A   | 55            | 2.5         | 30.83                             | 26.40                             | 5.4                               | 7.5                               | 0.69             | 400                                  | 9150                                  | 9.0                                  | 24.5                                 |
| GeoB 1722-1 | 8             | 6.8         | 30.45                             | 28.02                             | 4.0                               | 4.7                               | 0.49             | 1.1                                  | 1250                                  | 0.2                                  | 0.3                                  |

a) ACL<sub>27-33</sub>: ACL of *n*-alkanes (carbon numbers 27 to 33); ACL<sub>22-32</sub>: ACL of *n*-alkanols (carbon numbers 22 to 32)

b) Carbon preference index of *n*-alkanes

c) Carbon preference index of *n*-alkanols

d) HPA: Higher plant *n*-alkanol index (Poynter, 1989; Poynter and Eglinton, 1991)

e) MAR: mass accumulation rate (C<sub>org</sub>, CaCO<sub>3</sub>: mg cm<sup>-2</sup> kyr<sup>-1</sup>; biomarkers: µg cm<sup>-2</sup> kyr<sup>-1</sup>)

f) Sum of *n*-C<sub>27</sub>, *n*-C<sub>29</sub>, *n*-C<sub>31</sub> and *n*-C<sub>33</sub> alkanes

g) Sum of *n*-C<sub>22</sub>, *n*-C<sub>24</sub>, *n*-C<sub>26</sub>, *n*-C<sub>28</sub>, *n*-C<sub>30</sub> and *n*-C<sub>32</sub> alkanols

p. 275) at approximately 1°S, 7°E and 13°S, 12°E. There are probably many others active at the present time, and even more were active in the past (A. G. Judd, pers. commun., 2002).

Some of these mature hydrocarbons may be responsible for the unusual *n*-alkane distributions in the Southwest African continental margin sediments investigated by Hinrichs et al. (1999). However, mass spectral analysis for sterane and hopane biomarkers provided no evidence that mature fossil hydrocarbons were of any noticeable significance in the samples used in our study.

The compound-specific  $\delta^{13}\text{C}$  values for the individual *n*-alkanes (Table 3.4, Fig. 3.4) are consistent with an origin of these components from higher land plants and generally follow very similar trends for each carbon number, particularly for the abundant *n*-C<sub>29</sub> and *n*-C<sub>31</sub> homologues (Fig. 3.5). The  $\delta^{13}\text{C}$  values covary (Fig. 3.7c), a behaviour that was observed in a number of environmental studies (e.g., Huang et al., 2000; Hu et al., 2002; Zhao et al., 2000, 2003). Values for the three carbon number species (*n*-C<sub>27</sub>, *n*-C<sub>31</sub>, *n*-C<sub>33</sub>), when plotted against the *n*-C<sub>29</sub> homologue (Fig. 3.7c), simultaneously become less negative in the transect from North to South down to the position of ODP Site 1082, whereas there is a decrease to more negative values further south. This behaviour of the *n*-alkane homologues is ascribed to the effect of their biosynthetic origins (C<sub>3</sub>, C<sub>4</sub> and CAM plants) as leaf wax components of the continental vegetation. The *n*-C<sub>29</sub> homologue is commonly

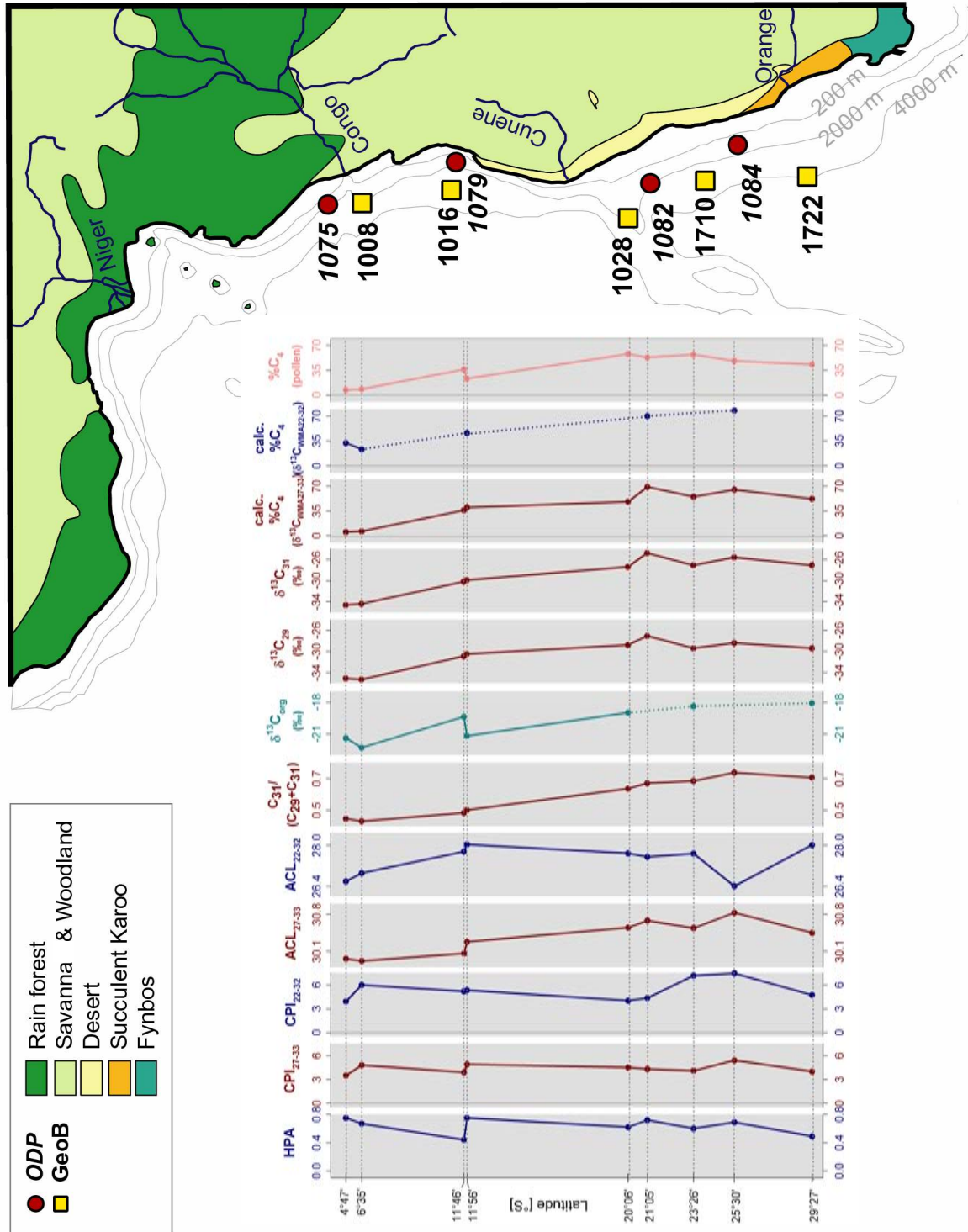


**Fig. 3.5.** N-S transects along the SW African continental margin of HPA, CPI, ACL data and individual *n*-alkane ratios,  $\delta^{13}\text{C}$  values (total organic carbon and individual *n*-alkanes), and  $\text{C}_4$  plant percentages (estimated from alkane and alkanol carbon isotope and pollen data). Colour coding of phytogeographic zones as in Fig. 3.2. Abbreviations and explanations: HPA: Higher plant *n*-alkanol index; CPI: Carbon preference index (CPI<sub>27-33</sub>: *n*-alkanes; CPI<sub>22-32</sub>: *n*-alkanols); ACL: Average chain length (ACL<sub>27-33</sub>: *n*-alkanes; ACL<sub>22-32</sub>: *n*-alkanols);  $n\text{-C}_{31}/(n\text{-C}_{29}+n\text{-C}_{31})$ : normalised content of the *n*-C<sub>31</sub> alkane;  $\delta^{13}\text{C}_{\text{org}}$  (‰ versus V-PDB); calc. %C<sub>4</sub> ( $\delta^{13}\text{C}_{\text{WMA27-33}}$  and  $\delta^{13}\text{C}_{\text{WMA22-32}}$ ): Estimate of percent C<sub>4</sub> plant contribution based on  $\delta^{13}\text{C}_{\text{WMA27-33}}$  and  $\delta^{13}\text{C}_{\text{WMA22-32}}$  values, respectively, key analytical data and a binary mixture model of C<sub>3</sub> and C<sub>4</sub> plants; %C<sub>4</sub> (pollen): Sum of C<sub>4</sub> species (grasses, predominantly C<sub>4</sub>, and *Tribulus*, C<sub>4</sub>).

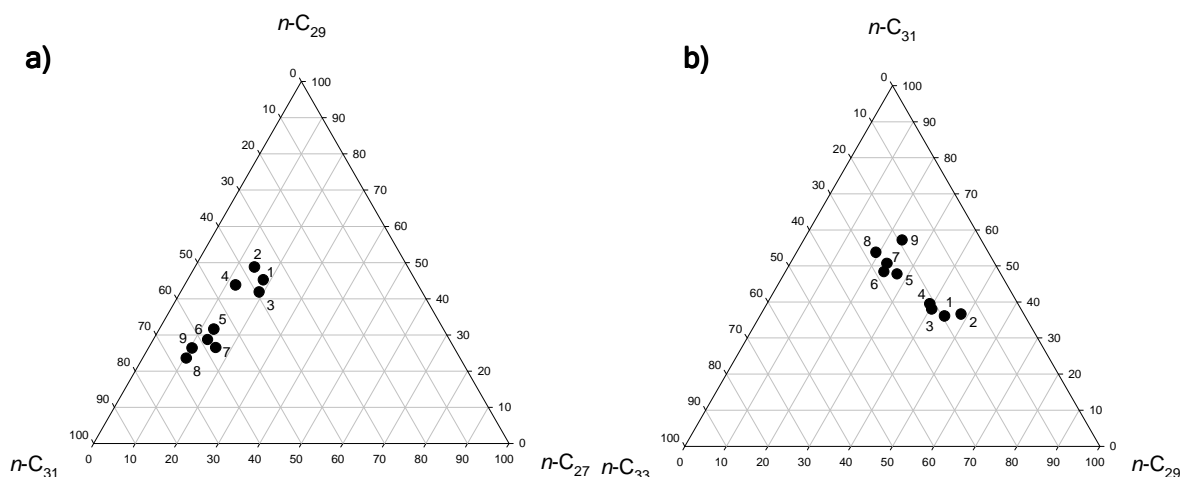


**Fig. 3.6.** Triangular diagram representations of percentages of three odd-carbon-numbered  $n$ -alkanes each. Sample codes: 1 - ODP 1075A; 2 - GeoB 1008-3; 3 - GeoB 1016-3; 4 - ODP 1079A; 5 - GeoB 1028-5; 6 - ODP 1082A; 7 - GeoB 1710-3; 8 - ODP 1084A; 9 - GeoB 1722-1.

the alkane most enriched in  $^{12}\text{C}$ , and in the present study the isotope values lie in the range  $-27.1\text{‰}$  to  $-35.3\text{‰}$  (Table 3.4).

There is a trend of less negative carbon isotope values for the  $n$ -alkanes with increasing chain length, expressed as  $\text{ACL}_{27-33}$ , over the N-S transect (Fig. 3.7a). This might be related to wax components from grasses which are particularly abundant according to the pollen data at ODP Sites 1079 and 1082 (Fig. 3.4, Table 3.5). The  $\delta^{13}\text{C}$  values are expressed as single weighted mean averages for the odd-numbered  $n\text{-C}_{27}$  to  $n\text{-C}_{33}$  alkanes in order to encompass the variability of data for individual homologues ( $\delta^{13}\text{C}_{\text{WMA27-33}}$ ; Fig. 3.4), but the  $\delta^{13}\text{C}$  values of the individual  $n\text{-C}_{29}$  and  $n\text{-C}_{31}$  homologues exhibit the same trend (Fig. 3.5). There is some indication of a positive displacement of  $\text{ACL}_{27-33}$  values with increasing water depth (or distance to the coast) of the sampling sites (Fig. 3.7a).

### 3.4.3 Carbon number distributions and molecular carbon isotope signatures of long-chain $n$ -alkanols

The distribution patterns of the long-chain alkanols ( $n\text{-C}_{21}$  to  $n\text{-C}_{33}$ ), normalised to the most abundant homologue, are shown for the samples from the nine sites in Fig. 3.4. The MAR data (Table 3.3) show a trend very similar to that of MAR for the  $n$ -alkanes (Table 3.3), with some relative differences from site to site, reflected in the HPA index values (Fig. 3.5), which vary in the range 0.44-0.75 (Table 3.3 and Fig. 3.4). There is no

Table 3.4. Isotope data.

| Core        | Depth (cm) | Age (ka) | $\delta^{13}\text{C}_{\text{org}}$ (‰) | <i>n</i> -Alkanes                |                                  |                                  |                                  |                                  |                                  |                        |                                  |                                  |                                  | <i>n</i> -Alkanols               |                                  |                                  |                                   |                        |                                  |                                  |                                  |                                  |                                  | $\text{C}_4$ (calc. %)           | $\text{C}_4$ (calc. %) |
|-------------|------------|----------|--|----------------------------------|----------------------------------|----------------------------------|----------------------------------|----------------------------------|----------------------------------|------------------------|----------------------------------|----------------------------------|----------------------------------|----------------------------------|----------------------------------|----------------------------------|-----------------------------------|------------------------|----------------------------------|----------------------------------|----------------------------------|----------------------------------|----------------------------------|----------------------------------|------------------------|
|             |            |          |  | $\delta^{13}\text{C}_{27}^a$ (‰) | $\delta^{13}\text{C}_{29}^a$ (‰) | $\delta^{13}\text{C}_{31}^a$ (‰) | $\delta^{13}\text{C}_{33}^a$ (‰) | $\delta^{13}\text{C}_{33}^b$ (‰) | $\text{C}_{\text{WMAZ7-33}}$ (‰) | $\text{C}_4$ (calc. %) | $\delta^{13}\text{C}_{22}^b$ (‰) | $\delta^{13}\text{C}_{24}^b$ (‰) | $\delta^{13}\text{C}_{26}^b$ (‰) | $\delta^{13}\text{C}_{28}^b$ (‰) | $\delta^{13}\text{C}_{30}^b$ (‰) | $\delta^{13}\text{C}_{32}^b$ (‰) | $\text{C}_{\text{WMAZ22-32}}$ (‰) | $\text{C}_4$ (calc. %) | $\delta^{13}\text{C}_{27}^a$ (‰) | $\delta^{13}\text{C}_{29}^a$ (‰) | $\delta^{13}\text{C}_{31}^a$ (‰) | $\delta^{13}\text{C}_{33}^a$ (‰) | $\delta^{13}\text{C}_{33}^b$ (‰) | $\text{C}_{\text{WMAZ7-33}}$ (‰) | $\text{C}_4$ (calc. %) |
| ODP 1075A   | 55         | 5.0      | -21.4                                  | -35.4                            | -35.1                            | -34.6                            | n.d.                             | n.d.                             | -35.0                            | 5                      | -28.6                            | -34.5                            | -31.0                            | -29.0                            | -29.3                            | -26.9                            | -30.2                             | 32                     |                                  |                                  |                                  |                                  |                                  |                                  |                        |
| GeoB 1008-3 | 13         | 2.0      | -22.3                                  | -34.5                            | -35.3                            | -34.4                            | n.d.                             | n.d.                             | -34.9                            | 6                      | -30.1                            | -34.0                            | -31.9                            | -33.6                            | -31.0                            | -29.5                            | -32.0                             | 23                     |                                  |                                  |                                  |                                  |                                  |                                  |                        |
| GeoB 1016-3 | 4          | 1.0      | -19.4                                  | n.d.                             | -30.9                            | -30.2                            | -30.5                            | -30.5                            | -30.5                            | 36                     | n.d.                             | n.d.                             | n.d.                             | n.d.                             | n.d.                             | n.d.                             | n.d.                              | n.d.                   | n.d.                             |                                  |                                  |                                  |                                  |                                  |                        |
| ODP 1079A   | 77         | 3.0      | -21.2                                  | -28.3                            | -30.5                            | -29.9                            | -29.8                            | -29.8                            | -29.9                            | 40                     | -26.0                            | -28.9                            | -29.6                            | -29.7                            | -28.9                            | -24.4                            | -28.1                             | 46                     |                                  |                                  |                                  |                                  |                                  |                                  |                        |
| GeoB 1028-5 | 20         | 4.0      | -19.0                                  | -32.7                            | -28.8                            | -27.4                            | -27.0                            | -27.0                            | -28.6                            | 48                     | n.d.                             | n.d.                             | n.d.                             | n.d.                             | n.d.                             | n.d.                             | n.d.                              | n.d.                   | n.d.                             |                                  |                                  |                                  |                                  |                                  |                        |
| ODP 1082A   | 37         | 3.8      | n.d.                                   | -24.9                            | -27.1                            | -24.8                            | -25.5                            | -25.5                            | -25.5                            | 69                     | -23.3                            | -24.4                            | -24.3                            | -26.6                            | -26.2                            | -22.9                            | -25.1                             | 70                     |                                  |                                  |                                  |                                  |                                  |                                  |                        |
| GeoB 1710-3 | 3          | 1.0      | -18.4                                  | -28.5                            | -29.4                            | -27.1                            | -26.4                            | -26.4                            | -27.6                            | 55                     | n.d.                             | n.d.                             | n.d.                             | n.d.                             | n.d.                             | n.d.                             | n.d.                              | n.d.                   | n.d.                             |                                  |                                  |                                  |                                  |                                  |                        |
| ODP 1084A   | 55         | 2.5      | n.d.                                   | -27.8                            | -28.4                            | -25.6                            | -24.8                            | -24.8                            | -26.1                            | 65                     | -23.1                            | -23.7                            | -23.1                            | -25.1                            | -25.7                            | -23.3                            | -24.1                             | 78                     |                                  |                                  |                                  |                                  |                                  |                                  |                        |
| GeoB 1722-1 | 8          | 6.8      | -18.1                                  | -30.1                            | -29.4                            | -27.1                            | -27.6                            | -27.6                            | -28.1                            | 52                     | n.d.                             | n.d.                             | n.d.                             | n.d.                             | n.d.                             | n.d.                             | n.d.                              | n.d.                   | n.d.                             |                                  |                                  |                                  |                                  |                                  |                        |

n.d. : not determined

a) *n*-alkanes

b) *n*-alkanol (corrected for TMS)

c) Estimates are based on 5%  $\text{C}_4$  plants in the Congo area and  $\delta^{13}\text{C}$  of  $\text{C}_4$  plants of -21‰

N-S trend, but HPA index values appear to be somewhat lower for those sites furthest from the coast and in deep water (GeoB Sites 1016, 1028, 1710, 1722). Selective degradation of the *n*-alkanols versus the *n*-alkanes was invoked to explain low HPA index values elsewhere (e.g., Poynter et al., 1989; Westerhausen et al., 1993; Cacho et al., 2001).

The distributions of homologues in the *n*-alkanol fraction ( $ACL_{22-32}$ ; Table 3.3, Fig. 3.4 and 3.5) do not show a simple N-S trend, unlike the *n*-alkanes. This different behaviour was likewise observed by Huang et al. (2000) in the mapping survey off Northwest Africa and also discussed by Eglinton et al. (2002). The distributions from *n*-C<sub>22</sub> to *n*-C<sub>32</sub> centre approximately around *n*-C<sub>26</sub>. They are not simply unimodal. The patterns give the appearance of being comprised of different assemblages of *n*-alkanol envelopes, corresponding to contributions from different groups of organisms. A lower-carbon-number distribution (approximately *n*-C<sub>20</sub> to *n*-C<sub>26</sub>) may be contributed by marine biota, such as copepods or algae (Mudge and Norris, 1997; Yunker et al., 1995). Overlapping with this assemblage are the long-chain wax alkanols from higher land plants.

The  $ACL_{22-32}$  values range from 26.40 to 28.04 (Table 3.3). In contrast, the *n*-alkanols in the Northwest African sediments ranged in ACL from 26.9 to 28.8, mainly 27.5, the most prominent carbon number representatives being the *n*-C<sub>28</sub> and *n*-C<sub>30</sub> homologues (Huang et al., 2000). The Gulf of Guinea sediments in that study contained *n*-alkanols with ACL values that centred around 27.5, different from the results at the nearest sites in our study (ODP 1075, GeoB 1008), where the  $ACL_{22-32}$  values of 26.6 and 26.9, respectively, indicate shorter average chain lengths (Table 3.3).

As with other studies involving long-chain alkanols, these compounds exhibit a marked carbon number dominance, even over odd ( $CPI_{22-32}$ ;  $CPI_{22-32}$  = 3.9 to 7.5; Table 3.3, Figs. 3.4 and 3.5). Thus, the carbon number distributions reported by Conte and Weber (2002a,b) were somewhat similar to those found in this transect study, the *n*-C<sub>26</sub>, *n*-C<sub>28</sub> or *n*-C<sub>30</sub> homologue being the dominant alkanol. The carbon number weighted isotopic values for the *n*-alkanols in their study were  $-29.7 \pm 0.9\text{‰}$ , values which they interpreted as being mainly due to an origin from C<sub>3</sub> plants. Specifically, Conte and Weber (2002b) interpreted the isotopic signal of leaf waxes in the Bermuda aerosols in terms of seasonal changes in source strengths of ecosystems at different latitudes within the North American biosphere. Their conclusions are based on the proposition that the waxes in the aerosols are mainly derived from the direct ablation of living vegetation. But there is a need to take into account the good evidence for significant contributions from aged material reaching collection points via aerosols derived from intermediate reservoirs such as soils and lake sediments (Eglinton et al., 2002).

Corresponding to the multimodal carbon number distribution of the *n*-alkanols in the present study, the molecular  $\delta^{13}\text{C}$  values do not follow a simple carbon number trend (Fig. 3.4; Table 3.4). This is illustrated by the absence of any correlation between  $\text{ACL}_{22-32}$  values and the weighted mean average stable carbon isotope values ( $\delta^{13}\text{C}_{\text{WMA22-32}}$ ) in Fig. 3.7b. Still, there is a pronounced N-S increase of the  $\delta^{13}\text{C}_{\text{WMA22-32}}$  values quite like the trend for the *n*-alkanes. The correlation coefficient ( $r^2$ ) of the two weighted mean average carbon isotope parameters is 0.94 (Fig. 3.7e), whereas that of the *n*-C<sub>28</sub> alkanol to the sum of all other homologues is 0.80 (Fig. 3.7d).

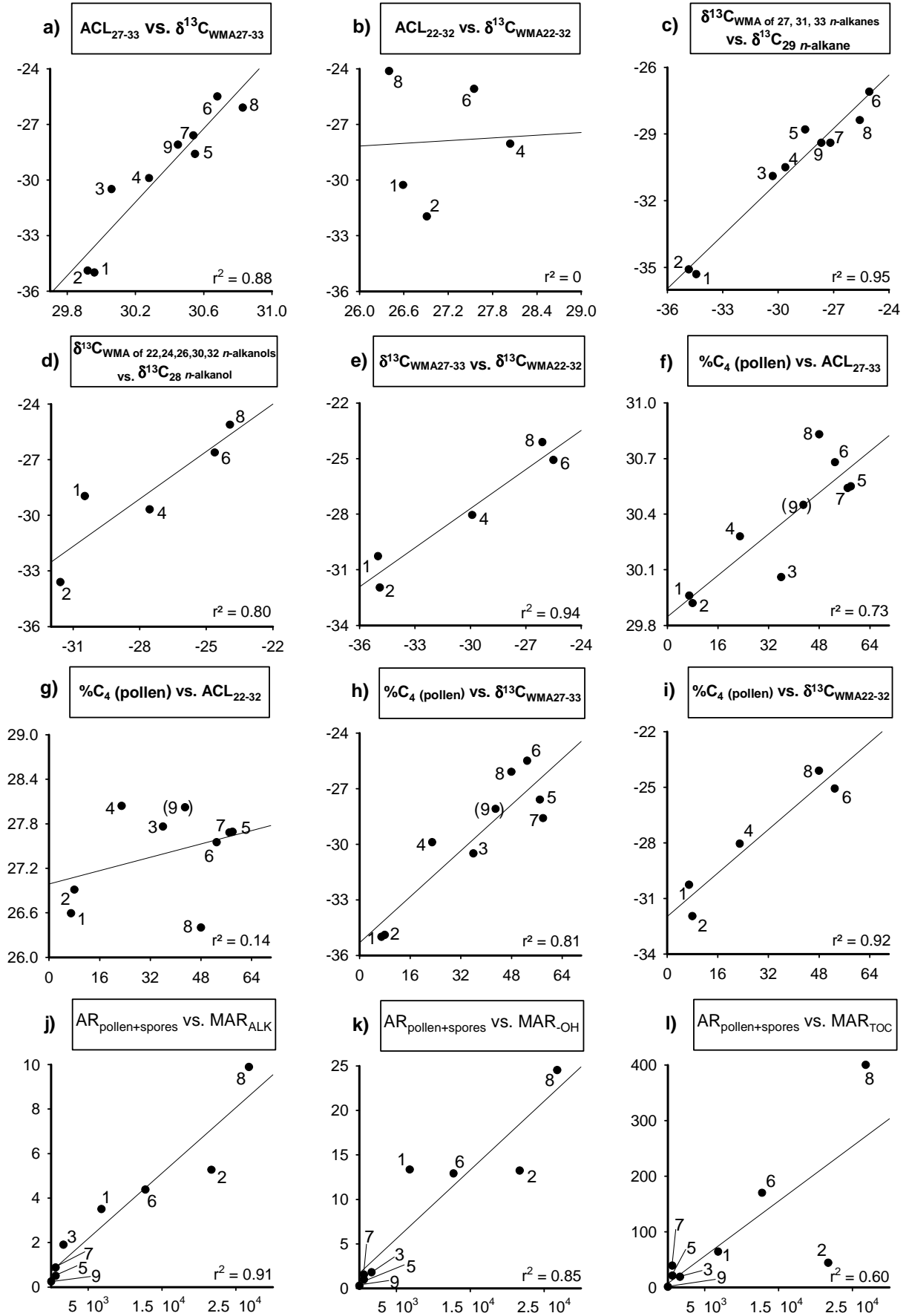
#### 3.4.4 Pollen distributions

Accumulation rates (in counts  $\text{cm}^{-2} \text{ka}^{-1}$ ; AR) of pollen and spores (Fig. 3.4, Table 3.5) for the sites of the N-S transect show the same trends as the MAR values of the *n*-alkanes and *n*-alkanols (Table 3.3), being highest close to the coast. Pollen AR values at GeoB Site 1722 are lowest and resulted in too small pollen counts to calculate meaningful percentages.

Fern spores and pollen of the sum of woody plants originate only from plants using C<sub>3</sub> metabolism. Relative abundance and accumulation rates indicate the importance of the C<sub>3</sub> plants within the vegetation. However, other pollen taxa originate partly from C<sub>3</sub> plants (but cannot be distinguished from the C<sub>4</sub> representatives). Therefore, the fern spores, woody plant pollen and cape reed pollen (see below) together only give a minimum indication for the proportion of 'C<sub>3</sub> pollen'. The two northern sites of our transect register 80-90% of 'C<sub>3</sub> pollen', recording very little 'C<sub>4</sub> pollen' in the marine sediments off the Congo river (Fig. 3.4 and 3.5, Table 3.5). Stepwise reduction of the C<sub>3</sub> plant proportion as recorded by pollen and spores is found for the rest of the N-S transect.

The partly wind-pollinated cape reeds are an important and typical constituent of the Cape flora. Cape reeds only use C<sub>3</sub> metabolism. At present, their distribution is restricted to the winter rainfall area of the Cape Province in South Africa (Fig. 3.2). Due to the northwards directed surface winds, low amounts of cape reed pollen are found in marine sediments as far north as ca. 20°S.

The Nama Karoo in Namibia and South Africa and the savannas in Namibia (western Kalahari; Fig. 3.2) are rich in composites. Among them are species that use the CAM metabolism (for instance *Scenecio* species). The increasing importance of composites in the vegetation of SW Africa is reflected in the higher pollen percentages found in the





southern sites of the N-S transect. Other important groups of CAM plants, such as the succulent Mesembryanthemaceae (Vijgjes), produce very little pollen and are palynologically almost silent.

Most important pollen groups indicating a C<sub>4</sub> plant origin are those of the grass (Poaceae) and sedge (Cyperaceae) families. The latter family includes C<sub>4</sub> species such as *Cyperus laevigatus* growing in halophytic swamps and *Cyperus papyrus* (papyrus) growing in freshwater swamps and around freshwater lakes. Except under closed canopies, grasses grow almost everywhere. Specifically, where the forest opens as a result of climatic or edaphic conditions, grasses are abundant. Most of the tropical grasses use the C<sub>4</sub> metabolism. Extratropical C<sub>3</sub> grasses are found in the winter rainfall area. Along the N-S transect, grass pollen is most abundant at the southern sites and declines towards values of less than 10% before the mouth of the Congo river. Additional information is given by the pollen record of *Tribulus*, a C<sub>4</sub> weed which grows in the desert. Contrary to the situation in Northwest Africa, pollen of halophytic plants from the families of Chenopodiaceae and Amaranthaceae are not well represented in Southwest Africa.

Parallel to the results for the *n*-alkanes and *n*-alkanols, the pollen reflect a strong southwards increase of the C<sub>4</sub> plant component in the vegetation. To facilitate comparison with the modelled C<sub>4</sub> plant supply using  $\delta^{13}\text{C}_{\text{WMA27-33}}$ , we summed the pollen percentages of Poaceae and *Tribulus* (Fig. 3.5). The Poaceae also contain some C<sub>3</sub> representatives; on the other hand, C<sub>4</sub> plant representation in other families like Cyperaceae are not included. The pollen-based estimates of the proportions of C<sub>4</sub> plants correlate well with the weighted mean average molecular carbon isotope values of *n*-alkanes ( $\delta^{13}\text{C}_{\text{WMA27-33}}$ ; Fig. 3.7h;  $r^2=0.79$ ) and *n*-alkanols ( $\delta^{13}\text{C}_{\text{WMA22-32}}$ ; Fig. 3.7i;  $r^2=0.92$ ), hence registering the effect of deposition of C<sub>4</sub> plant material: Whereas the *n*-alkane average chain length

**Fig. 3.7.** (opposite) Linear correlations of aliphatic biomarker and pollen parameters (x vs. y axis): a) ACL<sub>27-33</sub> versus  $\delta^{13}\text{C}_{\text{WMA27-33}}$ ; b) ACL<sub>22-32</sub> versus  $\delta^{13}\text{C}_{\text{WMA22-32}}$ ; c)  $\delta^{13}\text{C}_{\text{WMA}}$  of *n*-C<sub>27</sub>, *n*-C<sub>31</sub> and *n*-C<sub>33</sub> alkanes versus  $\delta^{13}\text{C}$  of *n*-C<sub>29</sub> alkane; d)  $\delta^{13}\text{C}_{\text{WMA}}$  of *n*-C<sub>22</sub>, *n*-C<sub>24</sub>, *n*-C<sub>26</sub>, *n*-C<sub>30</sub> and *n*-C<sub>32</sub> alkanols versus  $\delta^{13}\text{C}$  of *n*-C<sub>28</sub> alkanol; e)  $\delta^{13}\text{C}_{\text{WMA27-33}}$  versus  $\delta^{13}\text{C}_{\text{WMA22-32}}$  f) % C<sub>4</sub> pollen versus ACL<sub>27-33</sub>; g) % C<sub>4</sub> pollen versus ACL<sub>22-32</sub>; h) % C<sub>4</sub> pollen versus  $\delta^{13}\text{C}_{\text{WMA27-33}}$ ; i) % C<sub>4</sub> pollen versus  $\delta^{13}\text{C}_{\text{WMA22-32}}$ ; j) AR (pollen and spores) versus MAR (*n*-alkanes); k) AR (pollen and spores) versus MAR (*n*-alkanols); l) AR (pollen and spores) versus MAR (TOC). In diagrams j through l values for ODP 1079 (4) are not plotted for scaling reasons and not included in the calculation of the  $r^2$  values. Sample codes: 1 - ODP 1075A; 2 - GeoB 1008-3; 3 - GeoB 1016-3; 4 - ODP 1079A; 5 - GeoB 1028-5; 6 - ODP 1082A; 7 - GeoB 1710-3; 8 - ODP 1084A; 9 - GeoB 1722-1. Weighted mean average of carbon isotope values (‰ versus V-PDB):  $\delta^{13}\text{C}_{\text{WMA27-33}}$ : odd-carbon-numbered *n*-C<sub>27</sub> to *n*-C<sub>33</sub> alkanes;  $\delta^{13}\text{C}_{\text{WMA22-32}}$ : even-carbon-numbered *n*-C<sub>22</sub> to *n*-C<sub>32</sub> alkanols (note that mean average values for a given sample were only calculated of the alkane homologues for which carbon isotope ratios were available; cf. Table 3.4); ACL<sub>27-33</sub>/ACL<sub>22-32</sub>: Average chain length of *n*-alkanes (*n*-C<sub>27</sub> to *n*-C<sub>33</sub>) and *n*-alkanols (*n*-C<sub>22</sub> to *n*-C<sub>32</sub>), respectively; %C<sub>4</sub> (pollen): Sum of C<sub>4</sub>-species (grasses, predominantly C<sub>4</sub>, and *Tribulus*, C<sub>4</sub>).

Table 3.5. Pollen data.

| Core                  | Depth<br>(cm) | Age<br>(ka) | Accumulation rates                             |  |   |  |   |  |   |  |
|-----------------------|---------------|-------------|--|--|---|--|---|--|---|--|
|                       |               |             | Pollen<br>(cm <sup>-2</sup> ka <sup>-1</sup> ) | Spores<br>(cm <sup>-2</sup> ka <sup>-1</sup> ) | C <sub>3</sub> plants<br>(cm <sup>-2</sup> ka <sup>-1</sup> ) | Cape reeds<br>(cm <sup>-2</sup> ka <sup>-1</sup> ) | Grass<br>(cm <sup>-2</sup> ka <sup>-1</sup> ) | Cyperaceae<br>(cm <sup>-2</sup> ka <sup>-1</sup> ) | <i>Tribulus</i><br>(cm <sup>-2</sup> ka <sup>-1</sup> ) | Composites<br>(cm <sup>-2</sup> ka <sup>-1</sup> ) |
| Sequence <sup>a</sup> |               |             | A  | B  | C   | D  | E   | F  | G   | H  |
| ODP 1075A             | 65            | 6.1         | 5,809  | 1,004  | 5,109   | 0  | 456   | 122  | 0   | 0  |
| GeoB 1008-3           | 25            | 3.5         | 12,986   | 8,713  | 8,629   | 0  | 1,843   | 1,466  | 0   | 168  |
| GeoB 1016-3           | 10            | 2.1         | 1,604  | 61   | 823   | 0  | 593   | 92   | 0   | 26   |
| ODP 1079A             | 67            | 2.7         | 330,031  | 31,692   | 169,387   | 0  | 84,147  | 60,105   | 0   | 9,835  |
| GeoB 1028-5           | 20.5          | 3.7         | 628  | 9  | 151   | 0  | 348   | 75   | 0   | 35   |
| ODP 1082A             | 28            | 2.8         | 12,325   | 437  | 3,496   | 262  | 6,294   | 699  | 524   | 1,923  |
| GeoB 1710-3           | 3.5           | 0.9         | 585  | 25   | 137   | 21   | 319   | 46   | 0   | 74   |
| ODP 1084A             | 51            | 2.3         | 25,873   | 924  | 5,544   | 1,478  | 12,382  | 2,218  | 554   | 5,544  |
| GeoB 1722-1           | 4.5           | 2.2         | 18   | 2  | 4   | 1  | 6   | 1  | 0   | 3  |

| Core                  | Depth<br>(cm) | Age<br>(ka) | Percent of total pollen and spores |                   |                              |                   |                   |                   |                        |                   |
|-----------------------|---------------|-------------|------------------------------------|-------------------|------------------------------|-------------------|-------------------|-------------------|------------------------|-------------------|
|                       |               |             | Pollen<br>(%)                      | Spores<br>(%)     | C <sub>3</sub> plants<br>(%) | Cape reeds<br>(%) | Grass<br>(%)      | Cyperaceae<br>(%) | <i>Tribulus</i><br>(%) | Composites<br>(%) |
| Sequence <sup>a</sup> |               |             | A                                  | B                 | C                            | D                 | E                 | F                 | G                      | H                 |
| ODP 1075A             | 65            | 6.1         | 85                                 | 15                | 75                           | 0                 | 7                 | 2                 | 0                      | 0                 |
| GeoB 1008-3           | 25            | 3.5         | 60                                 | 40                | 40                           | 0                 | 8                 | 7                 | 0                      | 1                 |
| GeoB 1016-3           | 10            | 2.1         | 96                                 | 4                 | 49                           | 0                 | 36                | 6                 | 0                      | 2                 |
| ODP 1079A             | 67            | 2.7         | 91                                 | 9                 | 47                           | 0                 | 23                | 17                | 0                      | 3                 |
| GeoB 1028-5           | 20.5          | 3.7         | 99                                 | 1                 | 24                           | 0                 | 55                | 12                | 0                      | 5                 |
| ODP 1082A             | 28            | 2.8         | 97                                 | 3                 | 27                           | 2                 | 49                | 5                 | 4                      | 15                |
| GeoB 1710-3           | 3.5           | 0.9         | 96                                 | 4                 | 22                           | 3                 | 52                | 7                 | 0                      | 12                |
| ODP 1084A             | 51            | 2.3         | 97                                 | 3                 | 21                           | 6                 | 46                | 8                 | 2                      | 21                |
| GeoB 1722-1           | 4.5           | 2.2         | n.c. <sup>b</sup>                  | n.c. <sup>b</sup> | n.c. <sup>b</sup>            | n.c. <sup>b</sup> | n.c. <sup>b</sup> | n.c. <sup>b</sup> | n.c. <sup>b</sup>      | n.c. <sup>b</sup> |

a) Sequence refers to Figure 4, last column b) n.c. = not calculated due to low absolute counts

(ACL<sub>27-33</sub>) increases in parallel with the percentage of C<sub>4</sub> plant pollen (Fig. 3.7f;  $r^2=0.73$ ), thus suggesting that longer-chain *n*-alkanes are proportionally more C<sub>4</sub> plant in origin, a similar relationship was not observed for the ACL<sub>22-32</sub> values of the *n*-alkanols (Fig. 3.7g;  $r^2=0.08$ ).

#### 3.4.5 *Plant wax components of the transect sediments: biogeochemical and environmental considerations*

Plant waxes may be supplied by wind and particle abrasion of contemporary vegetation, smoke aerosols and by clay and other soil particles. Waxes are significant components of pollen but the mass flux is minute. Little is known of the direct shedding of plant wax crystallites into the wind, but plant waxes are released in smoke aerosols during vegetation burning (Swap et al., 1996b). Plant wax contents of aeolian dust can be several percent dry weight (Huang et al., 2000).

In the transect sediments, there is some proportionality seen in the fluxes of waxes (MAR of *n*-alkanes and of *n*-alkanols) and of pollen (AR of pollen) (Tables 3.3 and 3.5, Fig. 3.4 and 3.7j-k). This is to be expected, since both types of organic matter are transported by the wind systems, although they will differ in their source areas and fallout rates with distance carried. It is clear that AR of pollen correlates best with MAR of long-chain odd-carbon-numbered *n*-alkanes (almost exclusively of terrigenous higher plant origin; Fig. 3.7j), slightly less well with MAR of long-chain even-carbon-numbered *n*-alkanols (some marine contribution; Fig. 3.7k) and not significantly with MAR of TOC (strong influence of marine organic matter; Fig. 3.7l). A similar proportionality between accumulation rates of pollen and higher-plant wax lipids was reported for the Northwest African continental margin (Huang et al., 2000).

The varying proportions of marine and terrigenous organic matter in the sediments of the Southeast Atlantic Ocean have been quantitatively estimated in several studies. On the basis of stable carbon isotope ratios of the total organic matter ( $\delta^{13}\text{C}_{\text{org}}$ ) Westerhausen et al. (1993) calculated the proportion of terrigenous carbon as ranging from 20% to 60% in sediments of the eastern equatorial Atlantic, but a contribution from C<sub>4</sub> plants was neglected. In our study area, the C<sub>4</sub> plant contribution may, however, rise to 16% of total organic carbon, according to Wagner (2000). Also neglecting C<sub>4</sub> plant contribution, Schneider (1991) concluded that the marine organic carbon content in Late Quaternary sediments from the Congo deep-sea fan fluctuates between 0.5% and 3%, whereas the content of terrigenous organic carbon remains relatively constant at 0.5% to 1.0%.

In our study, the estimates of the percentage of C<sub>4</sub> plant contribution to the transect sites for the *n*-alkanes, based on  $\delta^{13}\text{C}_{\text{WMA27-33}}$ , the *n*-alkanols ( $\delta^{13}\text{C}_{\text{WMA22-32}}$ ) and the pollen

counts show reasonably parallel behaviour from North to South (Fig. 3.4, 3.5 and 3.7h,i), again as reported for the Northeast Atlantic Ocean (Huang et al., 2000). Close parallelism between  $\delta^{13}\text{C}$  values of *n*-alkanes, *n*-alkanols and pollen species distributions is not to be expected in view of the many differences in the operation of the relevant environmental processes. For example, Bird and Pousai (1997) provided evidence that  $\text{C}_4$  rather than  $\text{C}_3$  plant-derived carbon is preferentially contributed to the fine-sized fractions of aerosols, which are known to be subject to longer-range transport than the larger sizes. However, the observed parallelism is in accord with our concept of broadly similar perspectives of the source areas in terms of common phytogeographic origins. The pollen, dust and smoke emissions are averaged over large source regions by a variety of uplift and transporting wind systems (Table 3.2). Wagner (2000), in his study of ODP Sites 663 and 664 in the Gulf of Guinea, pointed out that enhanced aridity and stronger winds in Africa are reflected in the oceanic sediments in the form of greater  $\text{C}_4$  plant and inertinite contributions from increased dust lift-off from source areas such as the Chad Basin and from increased aerosols from vegetation fires in the savannas.

Of particular interest is the distinct parallelism in increasing *n*-alkane average chain length ( $\text{ACL}_{27-33}$ ) and more positive  $\delta^{13}\text{C}_{\text{WMA}27-33}$  values over the N-S transect.  $\text{ACL}_{27-33}$  increases by almost a full carbon number from 29.92 to 30.83 (Table 3.3), whereas  $\delta^{13}\text{C}_{\text{WMA}27-33}$  becomes more positive from -35.0‰ to -25.5‰ (Table 3.4). This relationship is also seen well in the x-y representation of these two parameters (Fig. 3.7a), expressing a latitudinal trend. A prior indication of such a relationship between carbon number and latitude was observed by Simoneit (1977) in lipids from aeolian dust trapped during ship transits in the South Atlantic Ocean. Collections in July and September revealed the typical wax patterns for the *n*-alkanes (high CPI values of long-chain homologues with carbon number maxima at *n*- $\text{C}_{29}$  and *n*- $\text{C}_{31}$ ) and for the *n*-alkanols (high even-carbon-number predominance with carbon number maximum at *n*- $\text{C}_{28}$ ). The data were very limited, but a N-S trend was noticeable in the *n*-alkane carbon number maximum from *n*- $\text{C}_{29}$  in the equatorial Atlantic to *n*- $\text{C}_{31}$  in the South Atlantic. Similar data are available for the Northwest African/Northeast Atlantic Ocean region (Simoneit, 1977; Huang et al., 2000; Eglinton et al., 2002; Schefuß et al., 2003b). One possibility is that we could relate the trend in the carbon number maximum of *n*- $\text{C}_{29}$  to *n*- $\text{C}_{31}$  in our data to increasing cover of grasses on the continent from the tropical jungle southwards, via the savanna areas of Angola, Zambia, Namibia and Botswana, to the Kalahari and the Nama Karoo in South Africa.

Conversely, Kawamura et al. (2003) remark that “higher plants growing in tropical regions biosynthesise higher molecular weight epicuticular waxes in response to higher ambient temperatures to maintain the hardness of leaf surfaces.” They adduce data for ten

species of broad-leaf trees growing at different latitudes. Thus, the ACL values for the *n*-alkanes were 28.9, 29.6 and 31.5 for 43°N, 27°N and 6°S, in effect for temperate, sub-tropical and tropical zones, respectively. These very limited data are, however, not for the same species growing at different latitudes and hence, because of the known variability of homologue distributions from one species to another, they can only be regarded as preliminary information. As the authors point out, larger surveys and also studies of single species growing in different temperature regimes are required.

Some basic phenomenon, operating continent-wide on a regional phytogeographic scale, would seem to lie behind these trends in carbon numbers and  $\delta^{13}\text{C}$  isotopic composition. Since we take the carbon stable isotopic composition as a measure of the percentage of  $\text{C}_4$  plant vegetation, increasingly less negative values corresponding to higher  $\text{C}_4$  plant proportions, then a possibility is that this relationship is also paralleled with a shift in carbon number distribution of *n*-alkanes to higher carbon numbers. However, there seems no a priori reason why  $\text{C}_4$  plant *n*-alkane biosynthesis should favour higher average chain length distributions. It may be that increased  $\text{C}_4$  plant competitiveness and increased ACL are independently related to specific environmental factors. Thus, longer carbon chains could be an evolutionary response to raised temperatures and/or aridity (cf. Schefuß et al., 2003a).

Overall, the N-S transect of oceanic sites parallels increased continental aridity but lower mean temperatures. White (1983), in his phytogeographic survey, uses Walter diagrams (Walter and Lieth, 1960-1967) to document the year-long situation for temperature and rainfall (Fig. 3.8). These diagrams graphically portray mean monthly temperatures and rainfall. In arid times the rainfall drops below the temperature curve, and thus much of the African continent below the equator is classified as “arid” for at least half the year. In contrast, the tropical forest region is classified as “humid” for almost all the year, with a mean annual temperature of about 25°C. Mean annual temperatures gradually fall from this high value to 17°C in southern South Africa, where aridity reaches high levels almost all year. Hence,  $\text{ACL}_{27-33}$  may be paralleling aridity but involving seasonality as another major factor. Aridity alone does not seem likely to be a factor which would determine ACL of *n*-alkanes in leaf waxes.

A related possibility is that leaf surface temperature may be the key factor. Leaf waxes are not generally present as smooth coatings of the leaf cuticle. Rather, they occur as carpets of microcrystallites in the micrometer range, varying greatly in size, shape and cuticular distribution from species to species (Martin and Juniper, 1970; Juniper and Southwood, 1986). Loss of this microstructure due to melting at raised temperatures is likely to be deleterious to the essential protective role of the waxy coating of leaves. Thus,

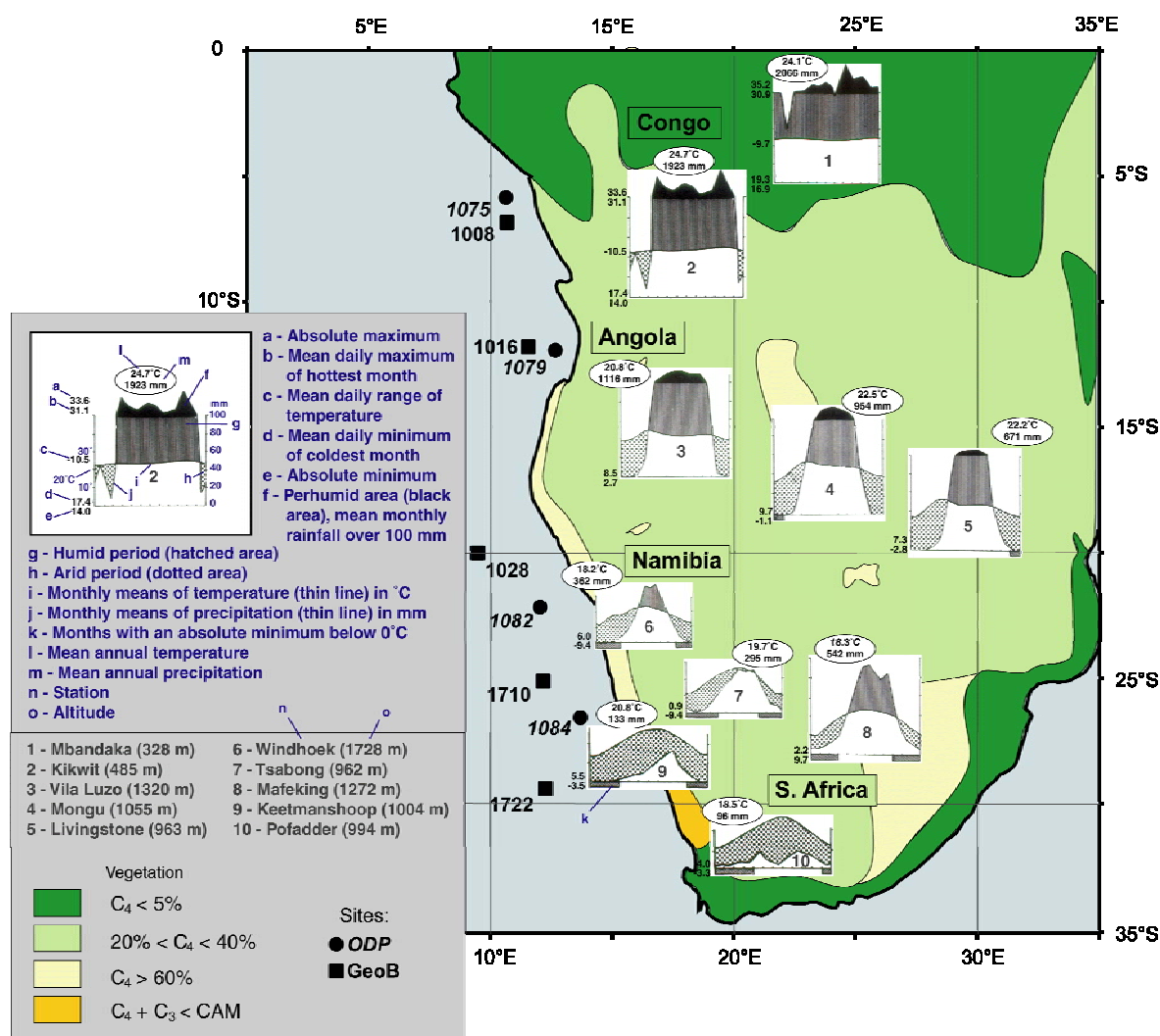


**Fig. 3.8.** Climatic classifications for Southern Africa (cf. Fig. 3.2 for phytogeographic zones). The figure is based on those presented by White (1983) using climatograms according to Walter and Lieth (1960-1967). A small number of climatograms was selected as being representative of the regions concerned. Arid periods prevail when the rainfall curve drops below the temperature curve. Details are given in White (1983, Chapter 2).

the melting points of the pure alkane homologues are reported as follows:  $n$ -C<sub>27</sub>, 59.5°C;  $n$ -C<sub>29</sub>, 63.7°C;  $n$ -C<sub>31</sub>, 67.9°C (Budavari, 1991), i.e. the melting point rises by ca. 4°C with an ACL increase of 2. The actual effect on the melting points of leaf waxes of increased ACL of the  $n$ -alkane components is presently not known but a slight increase seems a reasonable prediction.

One can anticipate, therefore, that a key parameter in relation to leaf wax protective behaviour may be the 'mean daily maximum temperature of the hottest month' or the 'absolute maximum temperature'. White (1983) lists a few such data (cf. Fig. 3.8) but none are given for important source areas such as the Central African pans in Botswana. Here, intense sunlight and persistent arid conditions must present plants with environmentally extreme situations. Such considerations describing actual leaf surface temperatures and

aridity would be of special interest in relation to the distributions of the C<sub>4</sub> tropical and sub-tropical long-leaved, tall grasses which likely contribute markedly to the aeolian wax signal registered for the southern portion of the transect. Associated factors may include wind velocity (wind burn) and dust abrasion. At the core of the present study is our interest in compound-specific  $\delta^{13}\text{C}$  biomarker data for leaf wax compounds extracted from oceanic sediments. We want to use the  $\delta^{13}\text{C}$  data to derive an understanding of the contributing continental vegetation in terms of C<sub>3</sub> versus C<sub>4</sub> photosynthetic pathways and then to use the resultant C<sub>3</sub> versus C<sub>4</sub> findings to infer the climatic regime pertaining in the source area. Unfortunately, the number of plant species examined for compound-specific stable carbon isotope measurements of their leaf waxes remains rather small (Rieley et al., 1993; Reddy et al., 2000). However, Boom et al. (2002) recently documented *n*-alkane distributions and compound-specific  $\delta^{13}\text{C}$  values for six species of grasses which are major contributors to the vegetation cover at 2-3 km altitude in the High Plains of the Colombian Andes. All six Poaceae species show high CPI values. The *n*-alkane distributions of the three C<sub>3</sub> species maximise at *n*-C<sub>25</sub> or *n*-C<sub>27</sub> and have an average  $\delta^{13}\text{C}$  value of approximately -35‰ for the *n*-alkanes, whereas the three C<sub>4</sub> plant *n*-alkanes maximise at *n*-C<sub>31</sub> or *n*-C<sub>33</sub> with  $\delta^{13}\text{C}$  values of about -21‰. For the purpose of establishing C<sub>3</sub> versus C<sub>4</sub> estimates they selected end member values for the *n*-C<sub>31</sub> alkanes of -35‰ and -20‰, respectively.

One problem for this approach and for the interpretation of the underlying processes are the present uncertainties in the relationships between the relevant environmental factors and the competition of C<sub>3</sub> versus C<sub>4</sub> (and CAM) plants. Teeri and Stowe (1976) demonstrated a good linear positive relationship between increasing relative abundance of C<sub>4</sub> versus C<sub>3</sub> grass species and increasing minimum temperature in the growing season in North America. However, Vogel et al. (1978) commented that this relationship did not hold for South Africa where the distribution map of C<sub>4</sub> versus C<sub>3</sub> grass cover seems to suggest higher temperatures and aridity as providing selective pressure for increases in C<sub>4</sub> grasses. Schultz (1995) summarised the situation underlying the larger proportions of C<sub>4</sub> plants found in warmer regions: "C<sub>4</sub> plants have higher temperature optimum (30-35°C compared with 10-25°C for the C<sub>3</sub> plants) and a higher water-use efficiency (transpiration ratio), no photorespiration losses, and they are capable of utilizing higher radiation intensities." Johnson et al. (1998) remarked that the distribution of C<sub>3</sub> versus C<sub>4</sub> grasses in Southern Africa depends on the seasonal rainfall patterns.

The C<sub>3</sub> plants include virtually all trees and many bushes and shrubs which, when given enough rainfall, nutrients and light, outcompete the less tall C<sub>4</sub> plants by simple exclusion through superior ground coverage (Lockheart et al., 1997). Wagner (1999) pointed out that "terrestrial C<sub>4</sub> plants include many grasses which exhibit optimum

photosynthesis at temperatures about 10°C higher than vascular C<sub>3</sub> plants and are thus common in warm tropical and dry to arid climates.” So, provided temperatures are not extreme, it is mainly under arid circumstances that C<sub>4</sub> plants outcompete C<sub>3</sub> plants through superior water control (Huang et al., 2001; Schefuß et al., 2003a,b). Hence, the subtropical and tropical grasses successfully maintain ground cover in the savanna and partial desert areas of the Southern African continent.

Clay fractions are known to carry much of the lipid load of a sediment through adsorption and absorption, which has implications for biomarker studies. Petschick et al. (1996) reported that simplified clay mineral provinces (kaolinite, smectite, illite, from N to S) can be distinguished in the Southeast Atlantic Ocean bottom sediments, which reflect different sources of wind-blown and riverine terrestrial material similar to those determining the pollen and  $\delta^{13}\text{C}$  differentiation observed in this study (Fig. 3.9). Dust plumes off Southwest Africa and their associated dust sources are described by Gingeles (1995) and Gingeles et al. (1998).

Clay mineral analyses of abyssal surface sediments in the eastern basin of the Southeast Atlantic Ocean revealed that the detrital clays are derived not only from Southwest and West Africa, but also, to a much smaller extent, from South America (e.g., Patagonia) and Antarctica. The clay assemblages north of 30°S are strongly influenced by the African sources, controlled by complex interaction of weathering regimes on land and also by wind, river and deep ocean current transport (Petschick et al., 1996). Hence, the mixed origin of the clays will have a parallel in a mixed origin of the biomarkers. However, these effects may be mitigated somewhat through mineralisation of the organic matter fraction during slow long-distance current transport of the clay particles.

The annual dust load carried by the wind systems from the South African continent into the Southeast Atlantic Ocean is much less than that encountered off Northwest Africa (Chester et al., 1972). However, this dust still contributes significantly to the sedimentary flux at the sites studied. The northern sites used for this study (GeoB 1008, ODP 1075, GeoB 1016) are on the northern fringe of the southern spring dust plume from the Kalahari and the Namib desert, but may also receive some dust from the northern winter plume coming from the Chad area (Gingeles, 1995).

The burning of savannas comprises 50% of all tropical biomass burning (Hao and Liu, 1994; Swap et al., 1996a). The burning grass liberates phytoliths and generates abundant microparticles of black carbon carrying adsorbed plant waxes. Aerosol emissions from savanna fires are rich in organic matter and black carbon (10-30% of aerosol mass; Andreae et al., 1998). Biomass burning in South Africa results in westwards-moving,



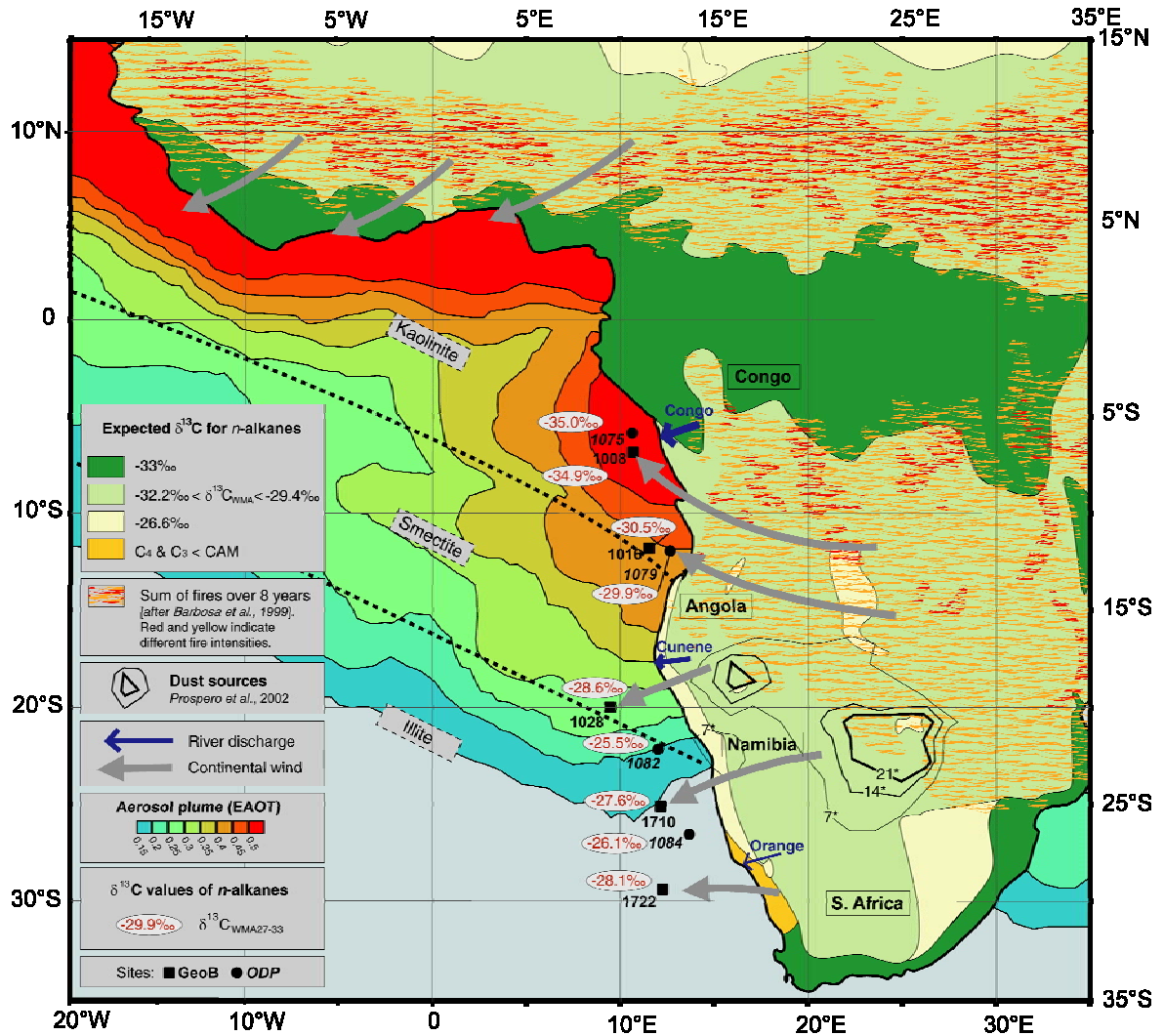


**Fig. 3.9.** Synoptic view of the N-S transect and terrestrial organic matter transport from the African continent. Displayed are: **Ocean:** Compound-specific  $\delta^{13}\text{C}$  isotope ratios for *n*-alkanes (weighted mean averages of odd-carbon-numbered *n*-C<sub>27</sub> to *n*-C<sub>33</sub> homologues at the coring sites;  $\delta^{13}\text{C}_{\text{WMA27-33}}$ ). Clay provinces from North to South are delineated by diagonal dashed lines (Petschick et al., 1996) approximately as follows: (1.) Kaolinite-rich. Eolian material from North Africa (Chad etc.) and West Africa; riverine material from the Congo. (2.) Smectite-rich. Eolian material from Angola and North Namibia; riverine material from the Cunene. (3.) Illite (and chlorite)-rich. Eolian material from Namib desert, Kalahari and South Africa; riverine material from the Orange. Also some current transport. Offshore aerosol plume areas were compiled by putting together Radiatively Equivalent Aerosol Optical Thickness (EAOT) information from Fig. 3.3b. **Rivers:** The arrows indicate the inflow points of the major rivers draining into the Atlantic Ocean. **Continent:** The *Sources of the Dust*. These are based on the general view that the most prolific sources of dust fine enough to travel long distances ( $10^2$ - $10^3$  km) are the seasonally wet/dry regions, such as pans, salt pans and old lake beds, and disturbed agricultural soils and the soils exposed in burnt-over areas. Southern African dust source: TOMS AAI frequency of occurrence distributions (days per month when the AAI equals or exceeds 0.7) are plotted from Prospero et al. (2002). Expected Weighted Mean Average  $\delta^{13}\text{C}$  Values of *n*-Alkanes calculated after assigned C<sub>4</sub> plant coverage (see Fig. 3.2). **Biomass Burning Areas:** Angola (west coast and hinterland, centred on 13°S; June to September with small peak in January transported south by Harmattan winds from 0-10°N, 15°W-20°E region), Central Africa (savannah and grassland, 0-10°S, mostly June) and Southern Africa (July to September; information from Barbosa et al., 1999; Andreae et al., 1994; Herman et al., 1997). Red areas: fires statistically every 1-1.6 years; orange areas: at least one fire over the 8-year period of observation. **Wind Directions:** Simplified after seasonal (austral winter and fall) clusters which are back-calculated to five of the sites for the austral fall and winter quarters (Fig. 5 in Dupont and Wyputta, 2003).

smoke-laden air exiting to the Atlantic Ocean over Angola and the Congo (cf. Fig. 3.3b). Most smoke over Africa and the South Atlantic Ocean results from man-induced burning. More than 50% of the African aerosol transported into the Southeast Atlantic Ocean is said to be from the region between 0 and 10°S. A dust collection off Northwest Africa (Eglinton et al., 2002) was found to have a high concentration of black carbon of presumed mainly C<sub>4</sub> plant origin on the basis of the  $\delta^{13}\text{C}$  values.

#### *3.4.6 Synoptic view of the North/South transect: Lipid biomarkers and pollen from the African continent*

Fig. 3.9 summarises the distributions of the various factors affecting the provision of material from the South African continent to the sediments of the Southeast Atlantic Ocean.

On the continent, the phytogeography is displayed in terms of 'ball park' estimates of  $\delta^{13}\text{C}$  values anticipated for the *n*-C<sub>29</sub> alkane in the leaf waxes of the vegetation. Thus, the tropical forests around the equator can be expected to provide a weighted mean average  $\delta^{13}\text{C}$  value for the long-chain *n*-alkanes of approximately -33‰. Values at ODP Site 1075 and Site GeoB 1008 are in accord with this concept when the wind arrows are considered. These winds will bring in not only leaf waxes but also pollen. Additionally, river drainage (Congo) contributes sediment containing clays, pollen and waxes from the forested region. Burning is not a major factor for this region, although there will be some material from the savanna belt to the North of the forest. The aerosol plume indicates that the  $\delta^{13}\text{C}$ -enriched Sahelian dust does not reach far south of the Equator.

South of the rain forest lie vast areas of savanna and scrubby grassland which have abundant C<sub>4</sub> grasses, although the C<sub>3</sub>/C<sub>4</sub> proportion varies and is assumed to range somewhat between 20% and 40% C<sub>4</sub> plants. Here we would anticipate weighted mean average  $\delta^{13}\text{C}$  values for the *n*-alkanes to lie between -32.2‰ and -29.4‰ (cf. Fig. 3.9). Once again, the austral fall and winter winds can be expected to carry the wax and pollen signals to the West and hence to contribute to the core sites in the middle and South of the transect. The savanna regions provide the main southern African smoke plumes due to anthropogenic burning of the grasslands. The plumes pass out over the Angolan coast into the Atlantic Ocean, carrying this C<sub>4</sub>-rich signal of plant waxes which will have much less negative  $\delta^{13}\text{C}$  values. In terms of dust, the southern part of this central region of southern Africa has many source areas of specialised vegetation often rich in C<sub>4</sub> plants in and around the areas of internal sporadic drainage - the pans, seasonally dry lake beds and semi-deserts within the Kalahari. This dust can be expected to contribute waxes enriched in  $^{13}\text{C}$  to the transect sites. Sites GeoB 1028 and ODP 1082 are just south of the

centre of this dust plume which carries illite and chlorite into the ocean during the southern spring (Fig. 3.9).

Further to the South and West, the Namib desert coastal strip acts as a source of dust which is carried west and northwest, reaching especially the southern sites of the transect. This dust can be expected to carry mainly C<sub>4</sub> and CAM plant signals, possibly with a  $\delta^{13}\text{C}_{\text{WMA}}$  value in the -26‰ range.

Finally, the main South African region with vegetation consisting of scrub and savanna grasses provides some pollen and smoke aerosol of a mixed C<sub>3</sub>/C<sub>4</sub> signal, mainly to the more southern sites. It is noteworthy that Tyson et al. (1996) stated that anticyclonal circulation of air parcels over South Africa takes place over thousands of kilometres, resulting in significant re-distribution and re-circulation of aerosols.

An additional outcome of the present work is the new light it throws on the quantification of terrestrial versus marine organic matter in sediments deposited at a given marine site. The assessment method employed in the past was based on <sup>13</sup>C data for total organic carbon, in which the binary model has one end member for terrigenous carbon and a second end member for marine carbon. It is now clear that such assessments will depend on the make-up of the terrigenous carbon component in terms of C<sub>4</sub> versus C<sub>3</sub> plant material. The present work shows that there can be quite a major shift, for example from a small percentage of C<sub>4</sub> plant material off the Congo to quite a high percentage off Namibia. New models will need to be set up to take account of such differences. Thus the <sup>13</sup>C data for TOC in the publication of Westerhausen et al. (1993) could now be reevaluated to provide more accurate calculations of terrigenous sediment fluxes, using estimates of C<sub>4</sub> versus C<sub>3</sub> plant material off North West Africa as documented by Huang et al. (2000).

## 3.5 Conclusions

The scope for mapping and profiling terrigenous biomarker transport and deposition into epicontinental areas is great. The actual mechanisms of transport - aeolian, riverine, coastal erosion, and currents - are, of course, important and need much further study in order to fully explain and interpret ocean sediment deposits. But mapping and profiling biomarker distributions and their isotopic compositions can already provide insights into the palaeophytogeography of the adjacent continental areas. This information can in turn be utilised to infer regional and continental-scale palaeoclimatic change.

The present study has made use of two types of biomarkers - the long-chain *n*-alkanes and *n*-alkanols - as homologous series of biosynthetically related compounds derived from terrigenous higher plant leaf waxes. Their relative abundances and  $\delta^{13}\text{C}$  values are interpretable on a compound-specific basis. The information that can be drawn at present is limited to a broad assessment of the extent of  $\text{C}_3$  versus  $\text{C}_4$  vegetation, which is not readily available in other ways. However, the large scale and the variable nature of the source areas and of the transport processes have a major averaging effect on the fluxes of the lipids and pollen and their areal distributions, resulting in broad aerosol plumes many hundreds of thousands of square kilometres in extent, with consequential extensive blurring and spreading of the original source signatures. Deep ocean current transport of the aeolian deposits once in the marine realm is a further factor but is probably of lesser importance in determining the observed sea floor distributions.

In effect, the present paper is a pilot study which employs pollen and spore counts, together with abundance and compound-specific  $\delta^{13}\text{C}$  measurements for the long-chain lipids extracted from sediments at nine sites on a 5-30° North to South latitudinal transect in the Southeast Atlantic Ocean. The lipid data, when interpreted in terms of leaf wax contributions of  $\text{C}_3$  versus  $\text{C}_4$  plants, broadly parallel the distribution of  $\text{C}_3$  and  $\text{C}_4$  vegetation on the South African continent, when taken in conjunction with the observed westerly and northwesterly paths of aerosol plumes, including smoke from vegetation fires and dust from arid regions, as observed by satellite and field measurements. Using the established wind trajectories for the austral winter as a guide, the principal source regions for the aerosols appear to include both heavily vegetated areas, such as the tropical jungle in the Congo (almost entirely  $\text{C}_3$  plants), the grasslands and savannas, and more sparsely vegetated areas and desert regions (mixture of  $\text{C}_3$  and  $\text{C}_4$  plants) of Southern Africa as a whole, such as the Kalahari, the Namib, and the Botswana salt pans. Our findings are in general accord with the data very recently reported by Schefuß et al. (2003b) for a survey of marine sediments in the same general area of the Southeast Atlantic Ocean.

Some salient conclusions are:

- ➔ Both *n*-alkanes and *n*-alkanols are present in similar abundances and possess similar compound-specific carbon isotope signatures. The hydrocarbon histograms show minor contributions from a smooth distribution of *n*-alkanes centred on the *n*- $\text{C}_{27}$  homologue which may be indicative of petroleum contributions. The long-chain *n*-alkanols have the advantage of not being influenced by contributions from petroleum or eroded mature organic matter.
- ➔ Fluxes or accumulation rates of *n*-alkanes, *n*-alkanols and pollen and spores are roughly proportional to one another, reflecting their common continental source regions and transport processes. Higher values are seen at the near-coastal sites

and at those sites in the path of the aerosol plumes born from the arid and semi-arid areas by the southeast trades and the offshore winds of the austral winter. River discharge is not a major feature except off the Congo river.

- ➔ For the *n*-alkanes the average chain length (ACL) essentially increases from North to South from 29.92 to 30.83 (the carbon number maximum moves from *n*-C<sub>29</sub> to *n*-C<sub>31</sub>). This trend is paralleled by more positive  $\delta^{13}\text{C}$  values, from -35‰ to -25‰. Similar trends are seen for the *n*-alkanols. This increase in ACL and the positive trend in  $\delta^{13}\text{C}$  values could possibly be explained by a contribution of C<sub>4</sub> plant waxes containing *n*-alkane distributions having a predominance of longer-chain homologues, e.g. higher proportions of *n*-C<sub>31</sub>, *n*-C<sub>33</sub>, *n*-C<sub>35</sub> alkanes, as well as more positive  $\delta^{13}\text{C}$  values. E.g., it was observed that the accumulation rate of the *n*-C<sub>31</sub> alkane relative to the other homologues increases with latitude. If tall subtropical grasses (C<sub>4</sub> type) biosynthesise predominantly the *n*-C<sub>31</sub> alkane, whereas trees etc. synthesise *n*-C<sub>27</sub> and *n*-C<sub>29</sub> alkanes (cf. Maffei, 1996, and literature quoted by Schwark et al., 2002), then this trend is in accord with the grass/herb pollen ratio increasing with increasing latitude as seen in our data set.
- ➔ The C<sub>4</sub> estimates based on  $\delta^{13}\text{C}$  values for individual *n*-alkanes and *n*-alkanols parallel each other and those afforded by pollen counts. All show a North to South trend, with the lowest values in the region of the Congo and the highest off Namibia at ca. 29°S. Both temperature and aridity are likely to be important factors in controlling the balance of C<sub>3</sub> versus C<sub>4</sub> vegetation, especially in relation to season.
- ➔ The increased C<sub>4</sub> plant contribution revealed by both the wax and pollen signals at the southern sediment sampling sites is probably related to the increased contributions reaching them from the tall grasses of the tropical and sub-tropical savanna regions and from the plant debris-rich dry soils of the desert areas of Southern Africa. The relative proportions of the contributions of waxes and of pollen spores provided directly from vegetation by ablation, by natural and anthropogenic burning, and indirectly by deflation of dusts from pans and semi-desert areas remain to be disentangled.

## 4 Glacial/interglacial changes in southern Africa: compound-specific $\delta^{13}\text{C}$ land plant biomarker and pollen records from Southeast Atlantic continental margin sediments

Florian Rommerskirchen, Geoffrey Eglinton, Lydie Dupont, Jürgen Rullkötter

This chapter was submitted to Geochemistry, Geophysics, Geosystems

### 4.1 Abstract

We examined Southwest African continental margin sediments from nine sites on a North-South transect from the Congo Fan (4°S) to the Cape Basin (30°S) representing two glacial (Marine Isotopic Stages, MIS, 2 and 6a) and two interglacial stages (MIS 1 and 5e) each. Contents, distribution patterns and molecular stable carbon isotope signatures of long-chain *n*-alkanes (*n*-C<sub>27</sub> - *n*-C<sub>33</sub>) and *n*-alkanols (*n*-C<sub>22</sub> - *n*-C<sub>32</sub>) as indicators of land plant vegetation of different biosynthetic types were correlated with concentrations and distributions of pollen taxa in sediments of the same time horizon. Selected single pollen type data reveal details of the vegetation changes, but the overall picture is best illustrated by summing the pollen known to predominantly derive from C<sub>4</sub> plants or C<sub>4</sub> plus CAM plants. The C<sub>4</sub> plant signals in the aliphatic biomarkers are recorded in the  $\delta^{13}\text{C}$  data and in the abundances of the *n*-C<sub>31</sub> and *n*-C<sub>33</sub> alkanes and the *n*-C<sub>32</sub> alkanol. Calculated clusters of wind trajectories for austral summer and winter situations for the Holocene (MIS 1) and the Last Glacial Maximum (MIS 2) afford information on the source areas for the lipids and pollen on land and their transport pathways to the ocean sites; these wind patterns appear to be applicable also to the earlier glacial and interglacial stages. This multidisciplinary approach on an almost continental scale provides clear evidence of latitudinal differences in leaf wax lipid and in pollen composition, with the Holocene sedimentary data paralleling the current major phytogeographic zonations on the adjacent continent. The northern sites (Congo Fan area and northern Angola Basin) get most of their terrestrial material from the Congo Basin and the Angolan highlands dominated by C<sub>3</sub> plants. Airborne particulates derived from the western and central South African hinterland dominated by deserts, semi-deserts and savanna regions are rich in organic matter from C<sub>4</sub> plants. Very little aerosol from the African continent is transported to the most southerly

sites in the Cape Basin. As can be expected from the present and glacial positions of the phytogeographic zones, the carbon isotopic signatures of the *n*-alkanes and *n*-alkanols both become isotopically more enriched in  $^{13}\text{C}$  from North to South. In the northern part of the transect the relative importance of the  $\text{C}_4$  plant indicators is higher during the glacials than in the interglacials, indicating a northward extension of arid zones favouring grass vegetation, but also an increase of open sedge swamps in areas of interglacial swamp forests. In the south, where grass-rich vegetation merges into semi-desert and desert, the difference in  $\text{C}_4$  plant indicators is small. The results of the study suggest that this combination of pollen data and compound-specific isotope vegetation proxies can be effectively applied in the reconstruction of past continental phytogeographic and palaeoclimatic changes.

## 4.2 Introduction

In the global organic carbon cycle the ocean is an important sink for terrigenous organic matter transported off shore by rivers and winds. Through this mechanism, marine sediments preserve a record of geographic and secular changes of continental climate and vegetation. Land-plant-derived organic particles may consist of microscopically recognisable spores, pollen and various kinds of plant fragments (e.g., Taylor et al., 1998). Land plant signatures are also displayed by specific biomarkers, such as long-chain *n*-alkanes and *n*-alkanols, and in bulk and molecular carbon isotopic signatures (e.g., Eglinton and Hamilton, 1967; Rieley et al., 1993).

Recent studies examined aeolian dusts, surface sediments and cores from continental margins for allochthonous terrigenous organic matter, using a combination of aliphatic biomarkers, carbon isotopic compositions and pollen distributions (e.g., Huang et al., 2000; Zhao et al., 2000, 2003; Eglinton et al., 2002; Schefuß et al., 2003a,b, 2004). The results comprise qualitative information concerning the phytogeography, soil conditions and the erosion and transport processes from land to ocean. The hinterland areas may be extensive, but the data provide an informative, integrated signal of the vegetation over a large, but broadly definable continental region.

In a previous pilot study, we employed pollen and spore counts, together with abundance and compound-specific  $\delta^{13}\text{C}$  measurements for the long-chain lipids extracted from Holocene near-surface sediments collected at nine sites on a 3000 km North to South latitudinal transect (5-30°S; Fig. 4.1) in the Southeast Atlantic Ocean (Rommerskirchen et al., 2003, Chapter 3). The Holocene lipid data, when interpreted

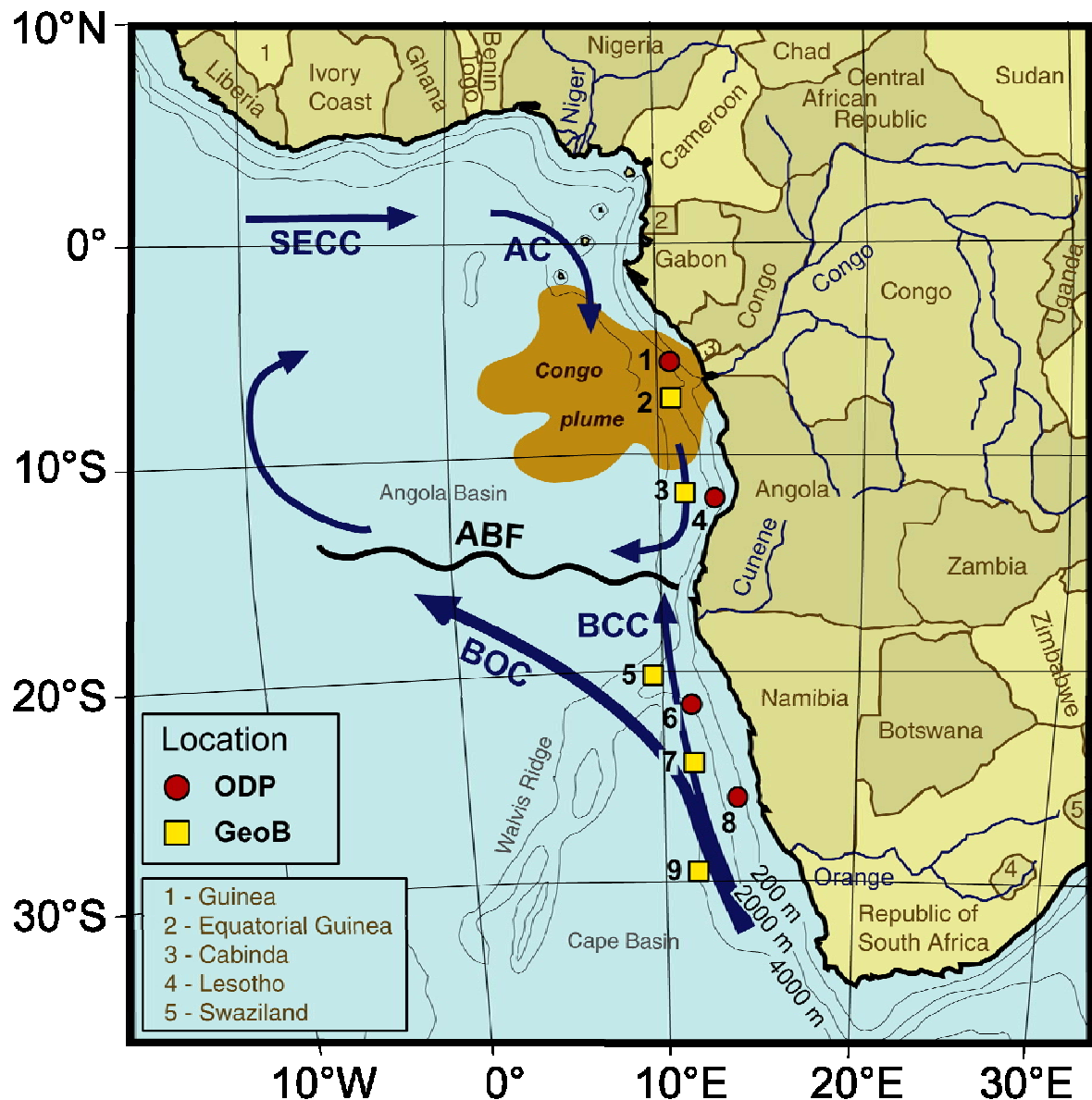


**Fig. 4.1.** Partial map of Africa showing site locations (see Table 4.1 for more details), major oceanic basins and currents in the Southeast Atlantic Ocean as well as political boundaries. ABF = Angola-Benguela Front, AC = Angola Current, BCC = Benguela Coastal Current, BOC = Benguela Ocean Current, SECC = South Equatorial Countercurrent; Congo Plume (after van Bennekom and Berger, 1984).

in terms of leaf wax contributions of  $C_3$  versus  $C_4$  plants, broadly paralleled the present-day distribution of  $C_3$  and  $C_4$  vegetation on the South African continent, when taken in conjunction with the observed westerly and northwesterly paths of aerosol plumes, including smoke from vegetation fires and dust from arid regions, as observed by satellite and field measurements. Using the established wind trajectories for the austral winter as a guide, the principal source regions for the aerosols appeared to include both heavily vegetated areas, such as the tropical jungle in the Congo (almost entirely  $C_3$  plants), the grasslands and savannas, and more sparsely vegetated areas and desert regions (mixture of  $C_3$  and  $C_4$  plants) of Southern Africa as a whole, such as the Kalahari, the Namib and



the Botswana salt pans. Our findings were in general accord with the data reported nearly synchronously by Schefuß et al. (2003b) for a survey of marine sediments in a similar area of the Southeast Atlantic Ocean.

The present study extends this approach back to about 140 ka by the investigation of additional sediment samples from the same nine sites off Southwest Africa representing two glacial (Marine Isotopic Stages, MIS 2 and 6a) and two interglacial stages (MIS 1 and 5e) each. The sediment material was recovered during Ocean Drilling Project (ODP) and *RV Meteor* cruises into the Southeast Atlantic Ocean (Table 4.1). The results of the molecular and microscopic analyses are discussed both along the transect for each time slice and as a time sequence at each sampling location in terms of the continental phytogeography related to the occurrence of C<sub>3</sub> and C<sub>4</sub> plants in warm and cold stages (cf. Fig. 4.2, page 105).

With the exception of the two northernmost sites, located in front of the Congo River, coring occurred at distances from the coast where aeolian (not riverine) contributions would be the dominant sources of terrigenous material. The length of the N-S transect, paralleled by a wide phytogeographic diversity on the continent, is an excellent test range for this type of multiproxy assessment. As with all proxies, pollen counts are biased records due to the differential effects of seasonal flowering, varying winds, amounts of pollen produced, transportability, different stabilities of pollen varieties, and ambiguities in the recognition of pollen species. However, wax components also have their problems, such as compositional variation with species in terms of amounts, compound and carbon isotope distributions and factors such as ease of abrasion, adsorption to soil particles and transport with dust.

## 4.3 Materials and methods

### 4.3.1 Sediment cores

Material for analysis was selected from five gravity cores collected during *Meteor* cruises M 6/6 (GeoB 1008, 1016 and 1028; February 1988) and M 20/2 (GeoB 1710 and 1722; January 1992) (Wefer et al. 1988; Schulz et al. 1992) and four drill cores from ODP Leg 175 (ODP 1075, 1079, 1082 and 1084; Wefer et al. 1998; Table 4.1). From each core and time slice, 5 to 10 mL sediment was taken. Stratigraphy and age models for *Meteor* cores are after Schneider et al. (1995, 1996), Shi et al. (1998) and Kirst et al. (1999), for

**Table 4.1.** Cores studied. Locations, sedimentation rates and age models.

| Site no. | Hole designation | Site location         | Latitude (°S) | Longitude (°E) | Water depth (m) | Distance to shore (km) | Distance to major river mouth (km) | Sedimentation rate (cm ka <sup>-1</sup> ) |       |        |        | Age model  |
|----------|------------------|-----------------------|---------------|----------------|-----------------|------------------------|------------------------------------|---|-------|--------|--------|--|
|          |                  |                       |               |                |                 |                        |                                    | MIS 1                                     | MIS 2 | MIS 5e | MIS 6a |  |
| 1        | ODP 1075A        | Congo Fan             | 4°47'         | 10°04'         | 2995            | 150                    | 280 (Congo)                        | 9   | 15    | 6      | 6      | Wefer et al. (1998), Dupont et al. (2001)                          |
| 2        | GeoB 1008-3      | Northern Angola Basin | 6°35'         | 10°19'         | 3124            | 270                    | 310 (Congo)                        | 7   | 9     | 5      | 6      | Schneider et al. (1995, 1996)                                      |
| 3        | GeoB 1016-3      | Southern Angola Basin | 11°46'        | 11°41'         | 3411            | 170                    | 630 (Cunene)                       | 5   | 8     | 3      | 4      | Schneider et al. (1995, 1996)                                      |
| 4        | ODP 1079A        | Southern Angola Basin | 11°56'        | 13°19'         | 738             | 60                     | 580 (Cunene)                       | 43  | 26    | 24     | 29     | Wefer et al. (1998)  |
| 5        | GeoB 1028-5      | Southern Angola Basin | 20°06'        | 9°11'          | 2209            | 320                    | 380 (Cunene)                       | 6   | 2     | 4      | 1      | Schneider et al. (1995, 1996)                                      |
| 6        | ODP 1082A        | Walvis Ridge          | 21°05'        | 11°49'         | 1279            | 150                    | 1000 (Orange)                      | 10  | 10    | 10     | 10     | Wefer et al. (1998)<br>B. Donner (pers. commun., 2002)             |
| 7        | GeoB 1710-3      | Walvis Basin          | 23°26'        | 11°42'         | 2987            | 270                    | 770 (Orange)                       | 4   | 7     | 4      | 6      | Kirst et al. (1999)  |
| 8        | ODP 1084A        | Northern Cape Basin   | 25°30'        | 13°01'         | 1992            | 175                    | 480 (Orange)                       | 22  | 21    | 11     | 21     | B. Donner (pers. commun., 2002),<br>J.-H. Kim (pers. commun, 2004) |
| 9        | GeoB 1722-1      | Cape Basin            | 29°27'        | 11°45'         | 3973            | 380                    | 450 (Orange)                       | 2   | 2     | 1      | 2      | T. Bickert (pers. commun., 2000)                                   |

ODP Site 1075 after Dupont et al. (2001), for ODP Site 1079 after Pérez and Berger (2000), for ODP Site 1082 after Bickert (pers. commun., 2000) and for ODP Site 1084 after Donner (pers. commun., 2002) and Kim (pers. commun., 2004). For comprehensive information on the oceanography of the Southeast Atlantic Ocean and the sedimentology and geochemistry of the sediments see Wefer et al. (1998, 2002).

A complete set of analytical data of this study will be made available through the PANGAEA database (<http://www.pangaea.de>).

#### 4.3.2 *Mass accumulation rates*

Organic carbon and biomarker mass accumulation rates (MAR,  $\text{mg cm}^{-2} \text{ kyr}^{-1}$ , total organic carbon, or  $\mu\text{g cm}^{-2} \text{ kyr}^{-1}$ , biomarkers) were calculated to eliminate any dilution effects by using the equation  $\text{MAR} = X \cdot \rho \cdot S_A$ , (van Andel et al., 1975; Lyle, 1988), where  $X$  = total organic carbon content ( $\text{mg g sed}^{-1}$ ) or content of a specific biomarker or group of biomarkers ( $\mu\text{g g sed}^{-1}$ ),  $\rho$  = dry bulk density ( $\text{g cm}^{-3}$ ; Wefer et al., 1998) and  $S_A$  = average sedimentation rate ( $\text{cm kyr}^{-1}$ ; Table 4.1).

#### 4.3.3 *Methods for lipid and pollen analysis*

For lipid analysis, sample aliquots of 2-15 g were extracted. The *n*-hexane-soluble fraction was separated by medium-pressure liquid chromatography (Radke et al., 1980) into fractions of aliphatic/alicyclic hydrocarbons, aromatic hydrocarbons and polar heterocomponents (NSO). Carboxylic acids were separated from the NSO fraction using a column with KOH-impregnated silica. *n*-Alkanols were isolated by urea adduction.

The compounds of interest were analysed by gas chromatography (GC), gas chromatography-mass spectrometry (GC-MS), GC coupled to a Finnigan MAT 252 isotope mass spectrometer for compound-specific carbon isotope analysis (GC-irm-MS) and a Carlo Erba CHNS 1108 analyser attached to a Finnigan MAT 252 isotope mass spectrometer for bulk carbon isotopic measurements of total organic matter.

Isotopic ratios are expressed as  $\delta^{13}\text{C}$  values in per mil relative to the V-PDB standard.  $\delta^{13}\text{C}$  values of alkanols are corrected for the contribution of the trimethylsilyl group from derivatisation. More details of the analytical procedures were described by Rommerskirchen et al. (2003, Chapter 3).

Procedures and palynological methods for the analysis of pollen and spores are described in Dupont and Wyputta (2003). Data here are given for total pollen, fern spores, sum of pollen from  $\text{C}_3$  plants (mainly woody plants), and the pollen taxa Restionaceae

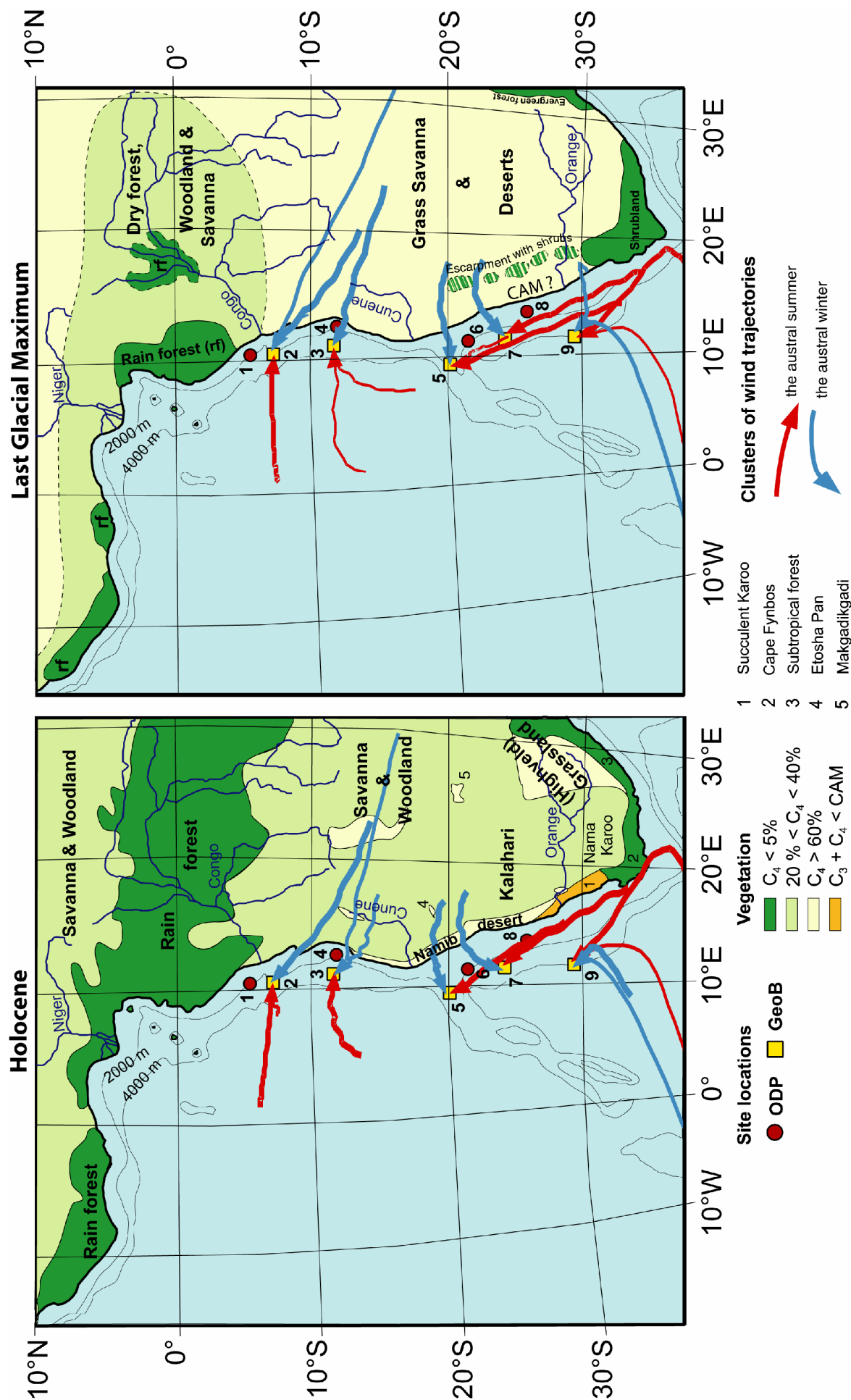
(cape reeds), Asteraceae (composites), Poaceae (grasses), Cyperaceae (sedges, rushes, papyrus etc.) and periporates (includes pollen of *Tribulus*, *Caryophyllaceae*, *Chenopodiaceae* and *Amaranthaceae*).

## 4.4 Results

### 4.4.1 *Simplified phytogeographical units of southwest Africa*

Modern phytogeography (White, 1983; Cowling et al., 1997) combined with isotope data of individual species (Dowton, 1975; Raghavendra and Das, 1978; Sage and Monson, 1999) formed the basis of our C<sub>3</sub>/C<sub>4</sub> plant distribution assessment for the Holocene (Rommerskirchen et al., 2003, Chapter 3). Werger and Ellis (1981) compiled floristic inventories along two transects (North-South and West-East) through the arid parts of South Africa. They showed that in deserts and semi-deserts the C<sub>4</sub> plant contribution to the vegetation may exceed 60%. Savanna vegetation comprising C<sub>4</sub> grasses and C<sub>3</sub> trees normally counts between 20 and 40% C<sub>4</sub> plant coverage.

In the extension of our broad brush assessment of Holocene C<sub>4</sub>/C<sub>3</sub> plant distribution to the period of the Last Glacial Maximum, we have used the vegetation reconstructions by Partridge et al. (1999) for southern Africa and by Dupont et al. (2000) and Ray and Adams (2001) for West and central Africa, respectively. These reconstructions assume that woodland and savanna dominated most of the Congo Basin and that rain forest only remained along the rivers and in the mountains west of the Congo Basin (Fig. 4.2). Rain forest refuges in West Africa are suggested by biogeography (Sosef, 1996) and marine pollen studies (Dupont et al., 2000). Most of southern Africa would have been covered by C<sub>4</sub>-rich grass savannas and deserts. Marine pollen studies suggest a shift of C<sub>3</sub> vegetation (depending on winter rainfall) northwards during the LGM (Shi et al., 2000, 2001). Also grain size distributions suggest more humid conditions in the southwestern part of the continent (Stuut et al., 2002, 2004). Stable oxygen isotope studies of the Stampriet aquifer indicate cooler conditions and a penetration of Atlantic moisture into the continent at 24°S and 19.5°E (Stute and Talma, 1998). Still, terrestrial pollen studies also indicate a cooler (and less evaporative) climate in the Western Cape Province (Parkington et al., 2000), a substantial northward extension of Cape vegetation could not be corroborated (Scott, 1989, 1994; Scott et al., 2004). Hence, we tentatively indicate the possibility of higher C<sub>3</sub> plant contributions on the Great Escarpment during the LGM. CAM vegetation as indicated



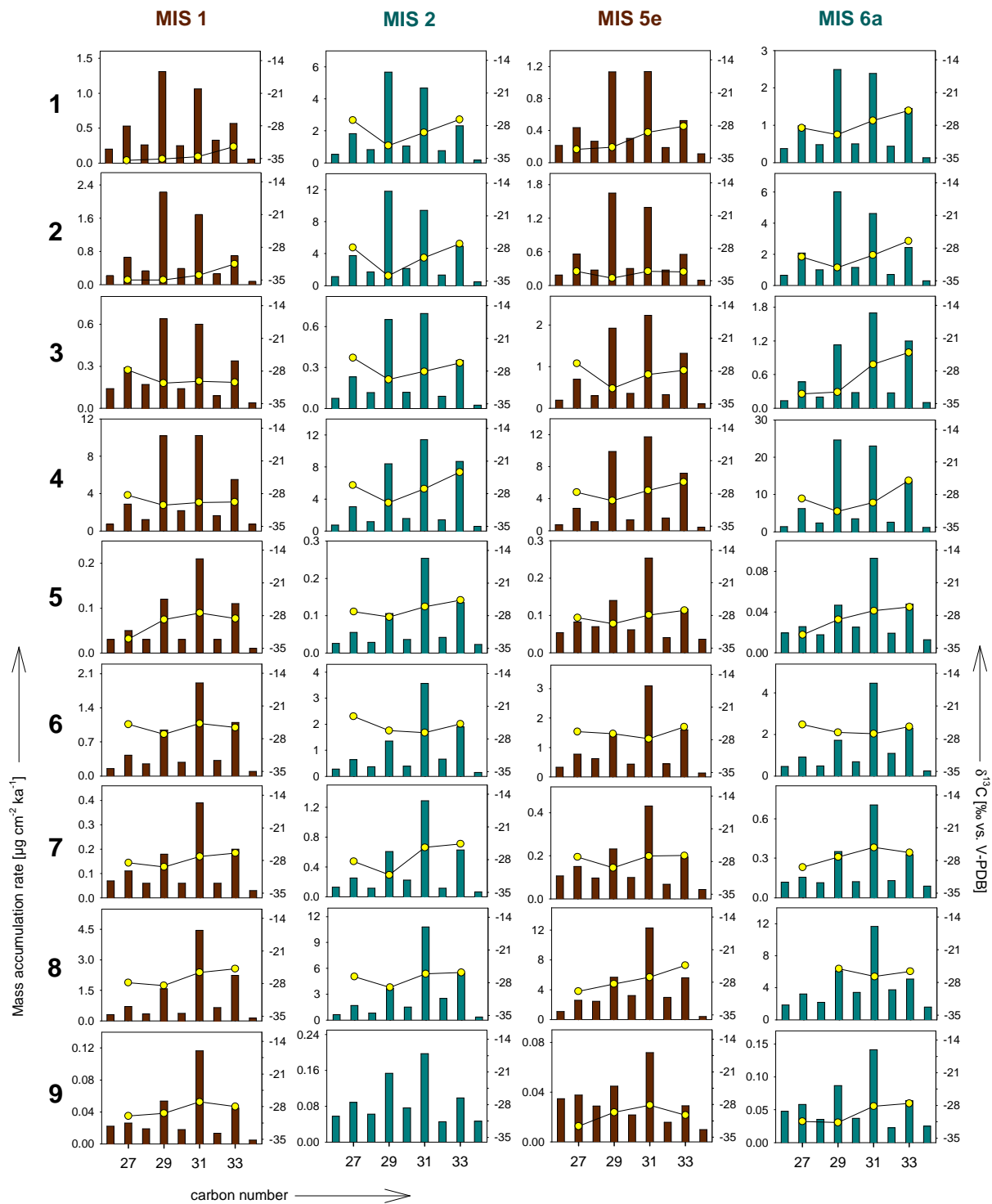
by pollen from succulents, with the possible exception of *Senecio* and other related composites, is rare in the LGM records. CAM plants may have been of secondary importance during the LGM (Scott, 1989, 1994; Scott et al., 2004).

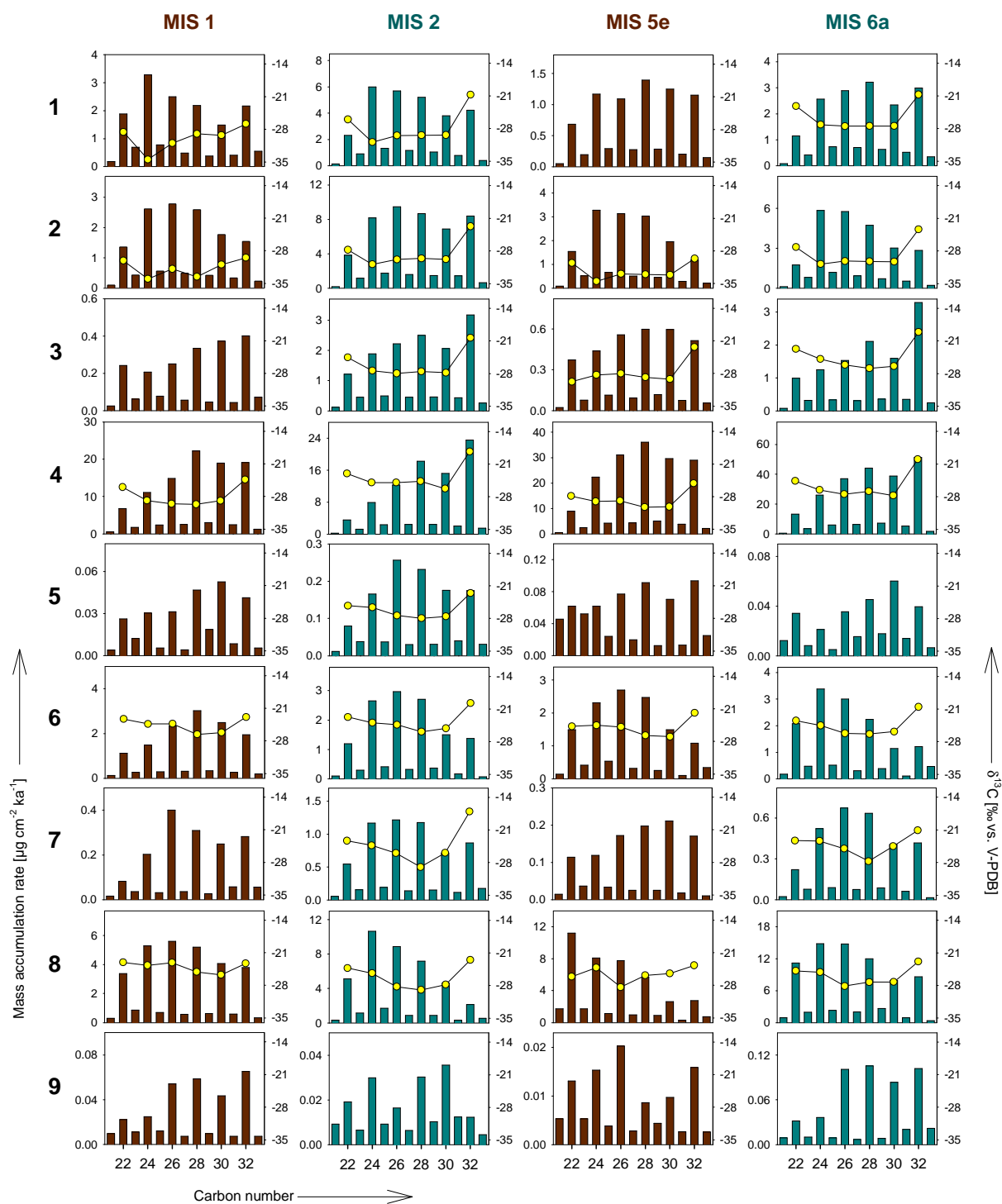
Mean aeolian transport directions in Fig. 4.2 are indicated after seasonal clusters (austral summer and austral winter) of 4-day back trajectories that were calculated on the 850 hPa standard pressure level using zonal and meridional wind components from two time slices (Present Day and LGM) of the ECHAM3 atmospheric circulation model (Dupont and Wyputta, 2003). The seasonally clustered trajectories average and highlight the aeolian routes at the low-tropospheric pressure level (850 hPa) for terrestrial particles to the location of marine sites. The trajectories modelled after two 10-year ECHAM3 model simulations show remarkably little differences between those of Present Day and of the LGM, which may be a result of insensitivities in the ECHAM3 atmospheric circulation model.

#### 4.4.2 Carbon number distributions and molecular carbon isotope signatures of long-chain *n*-alkanes

Fig. 4.3a shows the distribution patterns of long-chain *n*-alkanes (*n*-C<sub>26</sub> - *n*-C<sub>34</sub>) in the extractable lipids of sediments from nine sites and in four time slices at each site. The histograms are individually normalised to the most abundant homologue for each site and time slice. Numerical data are compiled in Table 4.3a-d (page 127). With the exception of the sites near the mouth of the Congo river (Sites 1 and 2), for almost all time slices the highest mass accumulation rate (MAR; Table 4.3a-d) values occur at the ODP sites (Sites 1, 4, 6, 8), which are closer to the coast and in shallower water than the GeoB sites (Sites 2, 3, 5, 7, 9). The highest MAR<sub>ALK</sub> values (29-67 µg cm<sup>-2</sup> kyr<sup>-1</sup>, sum of *n*-C<sub>27</sub> to *n*-C<sub>33</sub> odd-carbon-numbered homologues) were found at Site 4 in the Angola Basin, which is the closest site to the coast (60 km offshore) and has the shallowest water depth (738 m). All GeoB sites south of the Congo Fan exhibit low *n*-alkane accumulation rates in the order of 0.2 to 4.5 µg cm<sup>-2</sup> kyr<sup>-1</sup> in each time slice. Generally, glacial sediments have MAR<sub>ALK</sub> values higher by an averaged factor of two.

**Fig. 4.2.** (opposite) Simplified phytogeographical units of Holocene and Last Glacial Maximum (LGM) in Southwest Africa (colour codes according to C<sub>4</sub> plant occurrence) and clusters of wind trajectories of the austral summer (December, January, February; red arrows) and winter (June, July, August; blue arrows) to the GeoB core sites (cf. Table 4.1). The wind fields used are after a 10-year sample for climate simulation of ECHAM 3 at 850 hPa isobaric level (for more details see Dupont and Wyputta, 2003). The C<sub>4</sub> plant distribution for the Holocene is based on maps of White (1983) and Cowling et al. (1997) and that for the LGM is based on maps from Partridge et al. (1999), Dupont et al. (2000) and Ray and Adams (2001). C<sub>4</sub> plants are abundant in Southern Africa, although their occurrence is patchy and difficult to generalise in terms of proportions relative to C<sub>3</sub> plant abundance. Nevertheless, we suggest a tentative gross classification in four different areas (see explanation of colour codes at the bottom of the figure).

a) *n*-Alkane

b) *n*-Alkanol



## c) Pollen and spores

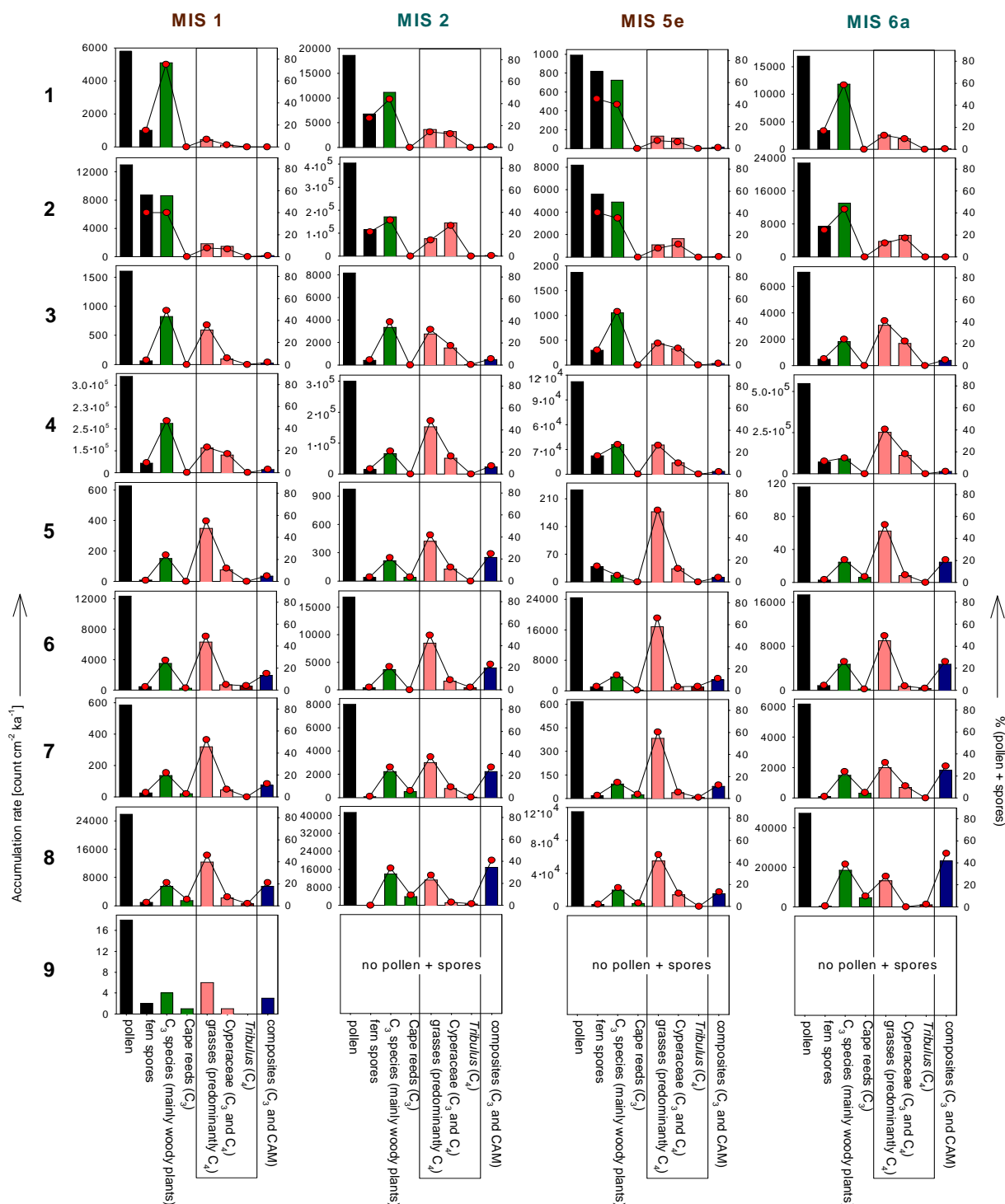


**Fig. 4.3.** North-South transect of histogram representations of a) the carbon number distributions, accumulation rates (MAR:  $\mu\text{g cm}^{-2} \text{ kyr}^{-1}$ ) and molecular carbon isotope signatures ( $\delta^{13}\text{C}$  in ‰ versus V-PDB) of long-chain  $n$ -alkanes, b) the carbon number distributions, accumulation rates (MAR:  $\mu\text{g cm}^{-2} \text{ kyr}^{-1}$ ) and molecular carbon isotope signatures ( $\delta^{13}\text{C}$  in ‰ versus V-PDB) of long-chain  $n$ -alkanols and c) pollen and spore accumulation rates (counts  $\text{cm}^{-2} \text{ kyr}^{-1}$ ; note very low abundance in Holocene data at site 9) and percentages in Holocene (MIS 1), Last Glacial Maximum (MIS 2), Eemian (MIS 5e) and penultimate glacial (MIS 6a) deep sea sediments from nine sampling locations in the Southeast Atlantic Ocean (cf. Fig. 4.1). Gaps in the data coverage of molecular isotope values are due to too low concentrations for reliable analysis.  $n$ -Alkanol distribution patterns with no molecular  $\delta^{13}\text{C}$  values were quantified from the alcohol fraction after liquid chromatography on KOH-impregnated silica column. All other  $n$ -alkanol distribution patterns were quantified from urea adducts of alkanol fractions.

The carbon number maximum of the *n*-alkane distributions moves from *n*-C<sub>29</sub> at the northernmost sites to *n*-C<sub>31</sub> further south for all time slices (Fig. 4.3a). In the Holocene, the transition occurs in the Angola Basin at Sites 3 and 4. In all other time slices, the transition is observed between the Congo Fan and Angola Basin sites. The values of the Average Chain Length (ACL) of odd-carbon-numbered *n*-C<sub>27</sub> to *n*-C<sub>31</sub> alkanes (ACL<sub>27-33</sub>) shows an analogous trend to longer chain lengths from North to South for each time slice (Fig. 4.4a). The ACL<sub>27-33</sub> values first increase southwards from about 30.0 at the Congo Fan to 30.8 in the Walvis Basin and decrease again further south to about 30.2 in the Northern Cape Basin. Generally, in the southern part of the transect we found higher ACL<sub>27-33</sub> values at ODP sites than for the adjacent GeoB sites. Compared to the interglacials Holocene and Eemian, the *n*-alkanes from the LGM and MIS 6a sediments have higher ACL<sub>27-33</sub> values. The transition from *n*-C<sub>29</sub>-dominated alkane distribution patterns in the North to those dominated by *n*-C<sub>31</sub> further south is also apparent in triangular plots both for the interglacials (Fig. 4.5a, page 114) and the glacials (Fig. 4.5b). The difference in the relative abundances of the two *n*-alkane homologues separates the transect sites into two groups. The *n*-C<sub>27</sub> and *n*-C<sub>33</sub> homologues do not contribute to this separation. Like previously reported for the Holocene data (Rommerskirchen et al., 2003, Chapter 3) the latitudinal succession from the northernmost to the southernmost sites is largely consistent for all four time slices. The offset between the group of the four northernmost sites (Sites 1-4) and the southern localities (Sites 5-9) corresponds to the latitudinal gap in sampling sites between Sites 4 and 5 (Fig. 4.2).

The Carbon Preference Index of the long-chain *n*-C<sub>27</sub> to *n*-C<sub>33</sub> alkanes (CPI<sub>27-33</sub>) of all samples in this study is significantly high. The CPI<sub>27-33</sub> values range from 2.3 to 6.8 and centre around 4.2; Table 4.3a-d). These values are typical for sedimentary hydrocarbons derived from higher plant waxes (Collister et al., 1994). Pollution by thermally mature hydrocarbons, which were generated in the past and then released into the environment (e.g. Hovland and Judd, 1988, p. 275) may have partly contributed to the *n*-alkanes studied. Especially at the southern sites, we found a trend to slightly lower CPI<sub>27-33</sub> values with increasing age of the sediments. However, mass spectral analysis provided no evidence of the presence of petroleum-type steranes and hopanes.

The stable carbon isotopic compositions ( $\delta^{13}\text{C}$ ) of the individual odd-carbon-numbered *n*-C<sub>27</sub> to *n*-C<sub>33</sub> alkanes are shown in Fig. 4.3a and listed in Table 4.4a-d (page 129). The values are consistent with an origin of these components from higher land plants. For all time slices we found a latitudinal trend of increasingly heavier  $\delta^{13}\text{C}$  values from the Congo Fan to the sites further south. Values for the three carbon number homologues *n*-C<sub>27</sub>, *n*-C<sub>31</sub> and *n*-C<sub>33</sub>, relative to those of the *n*-C<sub>29</sub> homologue, simultaneously become

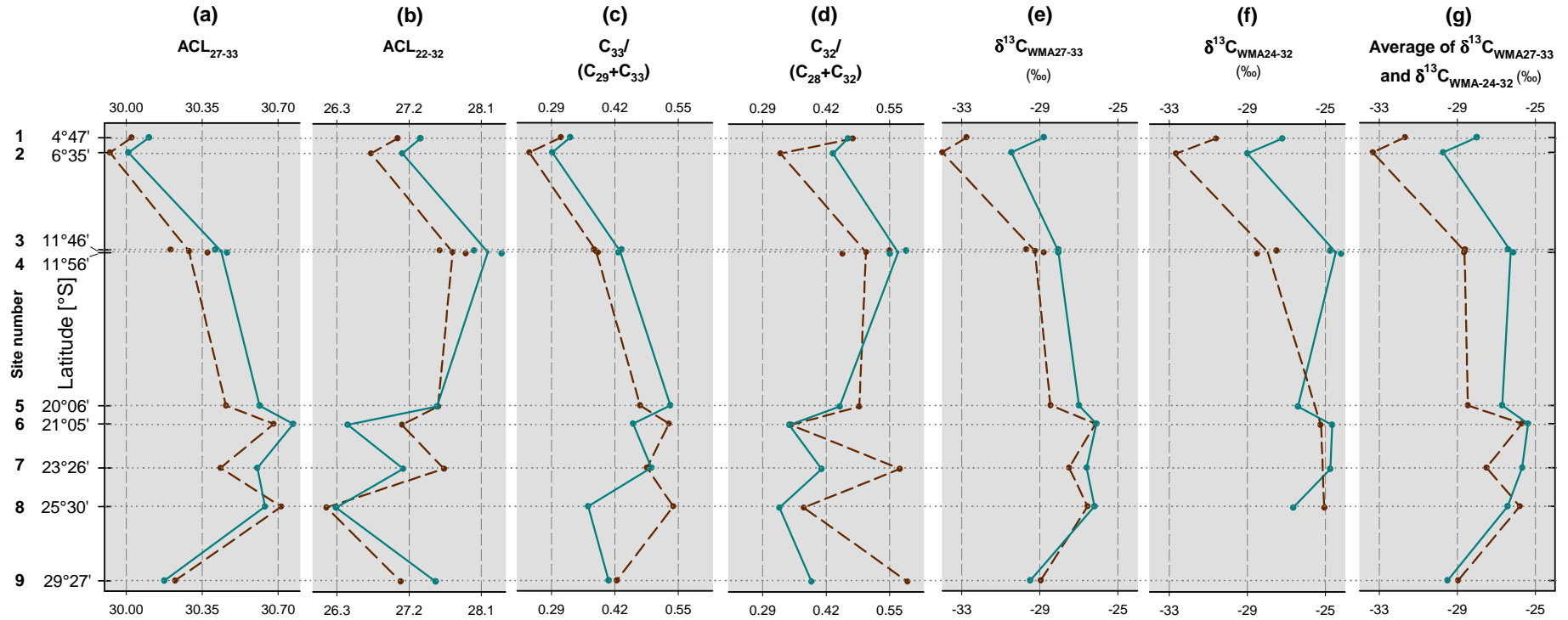


**Fig. 4.4.** Pairs of glacial and interglacial N-S transects along the SW African continental margin of a) ACL  $n$ -alkane data, b) ACL  $n$ -alkanol data, c) ratio of  $n$ -C<sub>33</sub> to  $n$ -C<sub>29</sub> plus  $n$ -C<sub>33</sub> alkane abundance, d) ratio of  $n$ -C<sub>32</sub> to  $n$ -C<sub>28</sub> plus  $n$ -C<sub>32</sub> alkanol abundance, e) weighted mean average  $\delta^{13}\text{C}$  data of  $n$ -alkanes, f) weighted mean average  $\delta^{13}\text{C}$  data of  $n$ -alkanols, g) average of  $\delta^{13}\text{C}_{\text{WMA27-33}}$  and  $\delta^{13}\text{C}_{\text{WMA24-32}}$ . For each proxy the pairs of averaged Holocene and Eemian and of averaged LGM and MIS 6a data are displayed. Solid blue and broken brown lines are used to connect glacial and interglacial data, respectively. For Sites 3 and 4, due to almost identical latitudes, averaged data were used for the trend lines, but the individual data points are shown as well.

Abbreviations and explanations: ACL: Average chain length (ACL<sub>27-33</sub>:  $n$ -alkanes; ACL<sub>22-32</sub>:  $n$ -alkanols);  $\delta^{13}\text{C}_{\text{WMA}}$  ( $\delta^{13}\text{C}_{\text{WMA27-33}}$  and  $\delta^{13}\text{C}_{\text{WMA24-32}}$ ): Averages of carbon isotope data of  $n$ -alkanes and  $n$ -alkanols (‰ versus V-PDB).

less negative in the transect from North to South down to the position of Site 6, whereas there are slightly more negative values further south (Table 4.4a-d). Both increasing  $ACL_{27-33}$  values and a positive trend in  $\delta^{13}C$  values over the N-S transect (Fig. 4.4a, Table 4.4a-d) can be explained by an increased contribution of  $C_4$  plant waxes. The  $n\text{-}C_{29}$  alkane is commonly most depleted in  $^{13}C$  (Fig. 4.3a). To encompass the variability of data for individual homologues we calculated the weighted mean averaged  $\delta^{13}C$  values of the odd-carbon-numbered  $n\text{-}C_{27}$  to  $n\text{-}C_{33}$  alkanes ( $\delta^{13}C_{WMA27-33}$ , cf. Table 4.4a-d). For all time slices we noted that heavier  $\delta^{13}C_{WMA27-33}$  values occur at sites of higher  $ACL_{27-33}$  values (Fig. 4.4a,e). Furthermore, glacial/interglacial changes in this study are illustrated by a  $\delta^{13}C_{WMA27-33}$  shift of up to 4‰ to lighter values for the northern sites (Fig. 4.4e). The difference becomes smaller at the southern sites and ultimately approaches 0‰.

#### 4.4.3 Carbon number distributions and molecular carbon isotope signatures of long-chain *n*-alkanols

The distribution patterns of long-chain *n*-alkanols ( $n\text{-}C_{20}$  to  $n\text{-}C_{34}$ ) are shown in Fig. 4.3b. The MAR data exhibit a trend similar to that of the *n*-alkanes (Table 4.3a-d). Except for the two sites at the Congo Fan the highest MAR values in each time slice were determined at the ODP sites, ranging from 12 to 211  $\mu\text{g cm}^{-2} \text{ kyr}^{-1}$  (sum of  $n\text{-}C_{22}$  to  $n\text{-}C_{32}$  even-carbon-numbered homologues) with the highest values occurring at Site 4 in the Angola Basin again. All GeoB sites south of the Congo Fan exhibit low *n*-alkanol accumulation rates in the range of 0.08 to 4.5  $\mu\text{g cm}^{-2} \text{ kyr}^{-1}$ . The MAR values are higher in glacial (MIS 2 and 6a) than in interglacial sediments (MIS 1 and 5e) at each site.

The Higher Plant Alkanol index (HPA, Poynter and Eglinton, 1991) relates to the expected preferential degradation of the *n*-alkanols compared to the more resistant *n*-alkanes during transport from the plant to the depositional site and during early diagenesis (Cacho et al., 2001; Poynter et al., 1989; Westerhausen et al., 1993). At interglacial times we found no N-S trend for the HPA index (Table 4.3a,c). But in glacial times (Table 4.3b,d) the index appears to be lower for those sites farthest from the coast and in deep water (Sites 5, 7, 9). It seems that the supply route of plant waxes into the ocean sediments (i.e. transport distance especially for sites with dominant aeolian supply of terrestrial organic matter) influences the sorting or the extent of preservation of the different wax components.

The *n*-alkanols show a high even-over-odd carbon number dominance ( $CPI_{22-32}$ ). The  $CPI_{22-32}$  values ( $n\text{-}C_{22}$  to  $n\text{-}C_{32}$  alkanols) range from 2.9 to 7.4 and centre at about 5.5 (Table 4.3a-d). The patterns are not simply unimodal, and some show a bimodal distribution (Fig. 4.3b). The main maxima vary between the  $n\text{-}C_{24}$  and  $n\text{-}C_{32}$  homologues

and centre around the  $n\text{-C}_{26}$  alkanol. Especially at the two glacial stages high amounts of the  $n\text{-C}_{32}$  alkanol give rise to a second maximum. The  $n$ -alkanol distributions appear to be envelopes of different overlapping patterns corresponding to contributions from different groups of organisms. Possibly marine biota (such as copepods or algae) contributed  $n$ -alkanols from approximately  $n\text{-C}_{20}$  to  $n\text{-C}_{26}$  (Yunker et al., 1995; Mudge and Norris, 1997) which overlap with long-chain wax alkanols from higher land plants. The  $\text{ACL}_{22-32}$  values of the alkanols (even  $n\text{-C}_{22}$  to  $n\text{-C}_{32}$ ) in Fig. 4.4b display a trend to longer chain length from the Congo Fan to the Angola Basin in all time slices (cf. Table 4.3a-d). Further south in the transect we do not find a consistent behaviour, except that the sediments from the near-shore ODP sites (6 and 8) have lower  $\text{ACL}_{22-32}$  values than those from the adjacent GeoB sites (5, 7, 9).

Like the  $\text{ACL}_{22-32}$  values, the molecular  $\delta^{13}\text{C}$  ratios of the  $n$ -alkanols do not follow a simple carbon number trend (Fig. 4.3b, Table 4.4a-d). The  $n\text{-C}_{22}$  and  $n\text{-C}_{32}$  alkanols are considerably more enriched in  $^{13}\text{C}$  than the adjacent alkanols. Accordingly, we conclude that the shorter-chain alkanols, particularly the isotopically relatively heavy  $n\text{-C}_{22}$  alkanol, originate from marine biota. Consequently, we left out the  $\delta^{13}\text{C}$  values of the  $n\text{-C}_{22}$  alkanol from the  $\text{C}_3/\text{C}_4$  plant assessment. The high  $\delta^{13}\text{C}$  values of the  $n\text{-C}_{32}$  alkanol can probably be attributed to dominant contributions from plants with the  $\text{C}_4$  photosynthetic pathway.  $\delta^{13}\text{C}$  values for the  $n\text{-C}_{28}$  alkanol, when correlated with the weighted mean average of those of the 24, 26, 30, and 32 carbon number homologues tend to become heavier in the transect from North to South in each time slice, but not as clearly and reliably expressed as the trend of the  $n$ -alkanes (cf. Tables 4.2 and 4.4a-d). The  $n\text{-C}_{28}$  alkanol is commonly most enriched in  $^{12}\text{C}$ . Heavier weighted mean averaged  $\delta^{13}\text{C}$  values of the even-carbon-numbered  $n\text{-C}_{24}$  to  $n\text{-C}_{32}$   $n$ -alkanols ( $\delta^{13}\text{C}_{\text{WMA24-32}}$ ; Table 4.4a-d) occur at sites of higher  $\text{ACL}_{22-32}$  values for all time slices, but in contrast to the  $n$ -alkanes only in the northern part of the transect (Fig. 4.4b,f). The same applies to the glacial/interglacial changes, where a shift to lighter values is only observed at the four northernmost sites (Fig. 4.4f). Further south there is no systematic difference between glacials and interglacials.

#### 4.4.4 Pollen distributions

In Fig. 4.3c a selection of pollen data for the four time slices is given (numerical data are listed in Table 4.5a-d, page 131). Accumulation rates of pollen and spores are highest at Site 4 which is located nearest to the coast. Relatively rich in pollen and spores are the sediments from Site 2 off the Congo River mouth receiving additional pollen and spore load with the river. Sediment recovered at Site 8, located under a high-productivity

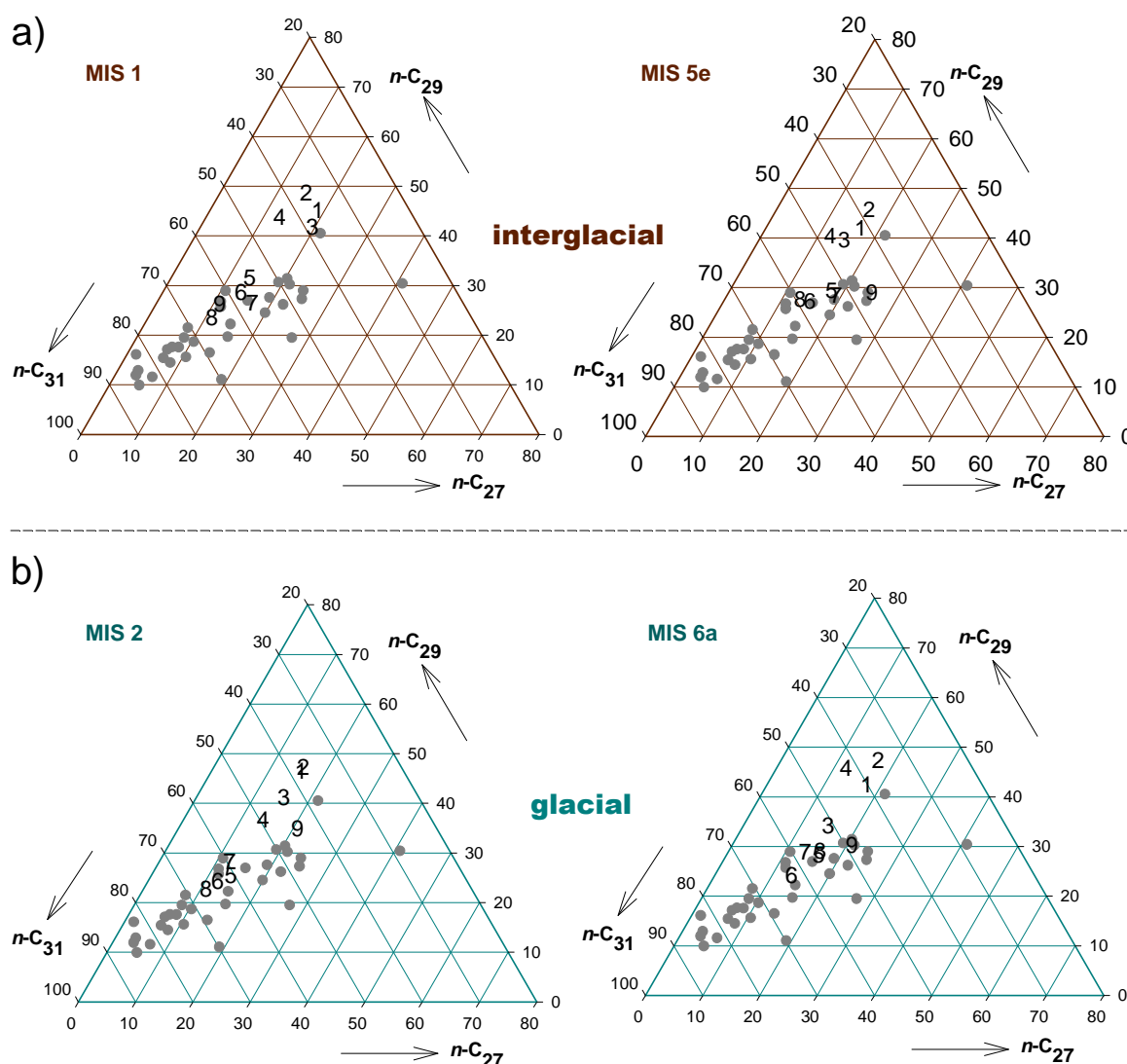


**Fig. 4.5.** Triangular diagram representations of percentages of three odd-carbon-numbered  $n$ -alkanes each for a) interglacial (MIS 1 and MIS 5e) and b) glacial (MIS 2 and MIS 6a) sediments. Sample codes 1-9 refer to site numbers (cf. Table 4.1). Also plotted are wax  $n$ -alkane compositions of some 35  $\text{C}_4$  grasses from South Africa (grey dots; after Rommerskirchen et al., in press, Chapter 2); the shaded area comprises the main cluster of these grass data.

upwelling area, is very rich in organic material. The high primary productivity resulting in high export productivity facilitates particle transport (including pollen) through the water column, and the efficient burial in the sediment guarantees that little post-depositional degradation of pollen occurs.

A high relative abundance of fern spores was only found at the two northern sites located closest to the fern-rich tropical rain forest. The absolute and relative abundance of pollen from woody plants ( $\text{C}_3$  plants, third bar in Fig. 4.3c) declines southwards with minimum relative values at Sites 5 ( $20^\circ\text{S}$ ) and 6 ( $21^\circ\text{S}$ ). The abundance of pollen from composites (last bar in Fig. 4.3c) increases both southwards and during the glacial stages (MIS 2 and MIS 6a). The family of composites includes both  $\text{C}_4$ ,  $\text{C}_3$  and CAM plants, and many representatives grow in arid and semi-arid areas. Within the family, species of

*Senecio* and related genera use the CAM metabolism. As far as is known,  $C_4$  representatives of the composites are not native in southern Africa. Cape Reed ( $C_3$ ) pollen occurs only at the southern sites (fourth bar in Fig. 4.3c), and its relative abundance is significantly higher during the glacial stages. Grass pollen percentages increase southwards until 20-21°S (Sites 5 and 6; Fig. 4.3c, 4.6b). These percentages decrease slightly again at 25°S (Site 8). Maximum relative values of grass pollen are higher during interglacial stages (MIS 1 and MIS 5e). Pollen of sedges (Cyperaceae) in the interglacial samples vary between 2 and 16% with little trend along the N-S transect (Fig. 4.3c, 4.6a). However, sedge pollen percentages are higher during glacial stages, up to 28%, at the northern sites (Sites 1-4). During glacial stages a clear N-S trend occurs for sedge pollen.

## 4.5 Discussion

This survey extends a previous study (Rommerskirchen et al., 2003, Chapter 3), which was restricted to the Holocene, by comparing four time slices comprising the Holocene (MIS 1), the Last Glacial Maximum (MIS 2), the Eemian (MIS 5e) and the penultimate glacial maximum (MIS 6a). We employed pollen and spore counts, together with abundance and compound-specific  $\delta^{13}C$  measurements for the long-chain lipids extracted from sediments at nine sites on a 5-30°S North to South latitudinal transect in the Southeast Atlantic Ocean.

### 4.5.1 *Temporal and latitudinal changes of aliphatic biomarker distributions and carbon isotope signatures*

The biomarker data in Tables 4.3a-d and 4.4a-d and in Fig. 4.3a,b and 4.4 show a significant amount of common trends, both as a function of geological time and latitude, but also some scatter. The inconsistencies appear to be related partly to the sampling sites having different distances to the continent (see, e.g., the data for Sites 5 and 7 versus 6 and 8 in several of the graphs in Fig. 4.4). In addition the various biases listed in the last paragraph of the Introduction will apply to the proxy parameters in this continent-wide approach. To overcome some of the effects caused by smaller-scale influences we have selected certain ratios and averages as outlined below.

Various plots of homologue ratios derived from the  $n$ -alkane distributions (Fig. 4.3a) have been tried, and we have chosen the  $C_{33}/(C_{29}+C_{33})$  ratio, for which the latitudinal trends are shown in Fig. 4.4c, as reflecting best the alkane homologue patterns in  $C_4$  grasses of southern Africa (Rommerskirchen et al., in press, Chapter 2). There is a N-S

trend of increasing chain length which levels off around Sites 5-8 and then decreases somewhat to Site 9. It is driven mainly by the decreasing dominance of the  $n\text{-C}_{29}$  in favour of the  $n\text{-C}_{33}$   $n$ -alkane. The  $\text{ACL}_{27-33}$  parameter for the  $n\text{-C}_{27}$  to  $n\text{-C}_{33}$   $n$ -alkanes (Fig. 4.4a) is probably the most representative measure of variations in the  $n$ -alkane distributions, with the values for glacial times being generally slightly larger than those for the interglacials, except for Sites 8 and 9. The shift of the  $\text{ACL}_{27-33}$  values from glacials to interglacials can be ascribed to significant changes in the  $\text{C}_3$ - versus  $\text{C}_4$ -dominated vegetation due to climate change.

The weighted mean  $\delta^{13}\text{C}$  values ( $\delta^{13}\text{C}_{\text{WMA27-33}}$ ; Fig. 4.4e) show a very similar profile to that of the  $\text{ACL}_{27-33}$  values (Fig. 4.4a), becoming increasingly less negative from North to South, steadying off at Sites 5 to 8 and then turning more negative at Site 9 for both glacials and interglacials. However, the northern part of the interglacial plot has more negative values (proportionally lower  $\text{C}_4$  plant coverage) than in the glacials. The

**Table 4.2.** Linear correlation coefficients ( $r^2$ ) of aliphatic biomarker and pollen parameters for Holocene (MIS 1), LGM (MIS 2), Eemian (MIS 5e) and penultimate glacial (MIS 6a) sediments from the South African continental margin. In all calculations values for Site 4 were not included due to the extremely high sedimentation rates (shallow water, near shore site; cf. Rommerskirchen et al., 2003, Chapter 3)

| Correlation parameters  | MIS 1 | MIS 2 | MIS 5e | MIS 6a |
|---|-------|-------|--------|--------|
| $\text{ACL}_{27-33}$ versus $\delta^{13}\text{C}_{\text{WMA27-33}}$   | 0.88  | 0.90  | 0.78   | 0.59   |
| $\text{ACL}_{22-32}$ versus $\delta^{13}\text{C}_{\text{WMA24-32}}$   | 0.35  | 0     | 0.06   | 0.17   |
| $\delta^{13}\text{C}_{\text{WMA}}$ of 27, 31, 33 $n$ -alkanes versus $\delta^{13}\text{C}_{29}$ $n$ -alkane       | 0.95  | 0.63  | 0.80   | 0.35   |
| $\delta^{13}\text{C}_{\text{WMA}}$ of 24, 26, 30, 32 $n$ -alkanols versus $\delta^{13}\text{C}_{28}$ $n$ -alkanol | 0.82  | 0.48  | 0.24   | 0.69   |
| $\delta^{13}\text{C}_{\text{WMA27-33}}$ versus $\delta^{13}\text{C}_{\text{WMA24-32}}$                            | 0.94  | 0.62  | 0.99   | 0.48   |
| % $\text{C}_4$ of pollen versus $\text{ACL}_{27-33}$  | 0.51  | 0.31  | 0.64   | 0.68   |
| % $\text{C}_4$ of pollen versus $\text{ACL}_{22-32}$  | 0.51  | 0.05  | 0.02   | 0.06   |
| % $\text{C}_4$ of pollen versus $\delta^{13}\text{C}_{\text{WMA27-33}}$   | 0.66  | 0.42  | 0.74   | 0.07   |
| % $\text{C}_4$ of pollen versus $\delta^{13}\text{C}_{\text{WMA24-32}}$   | 0.70  | 0.65  | 0.81   | 0.50   |
| % $\text{C}_4$ and CAM of pollen versus $\text{ACL}_{27-33}$  | 0.88  | 0.80  | 0.62   | 0.82   |
| % $\text{C}_4$ and CAM of pollen versus $\text{ACL}_{22-32}$  | 0.41  | 0.06  | 0.02   | 0      |
| % $\text{C}_4$ and CAM of pollen versus $\delta^{13}\text{C}_{\text{WMA27-33}}$                                   | 0.95  | 0.82  | 0.76   | 0.34   |
| % $\text{C}_4$ and CAM of pollen versus $\delta^{13}\text{C}_{\text{WMA24-32}}$                                   | 0.92  | 0.67  | 0.82   | 0.50   |



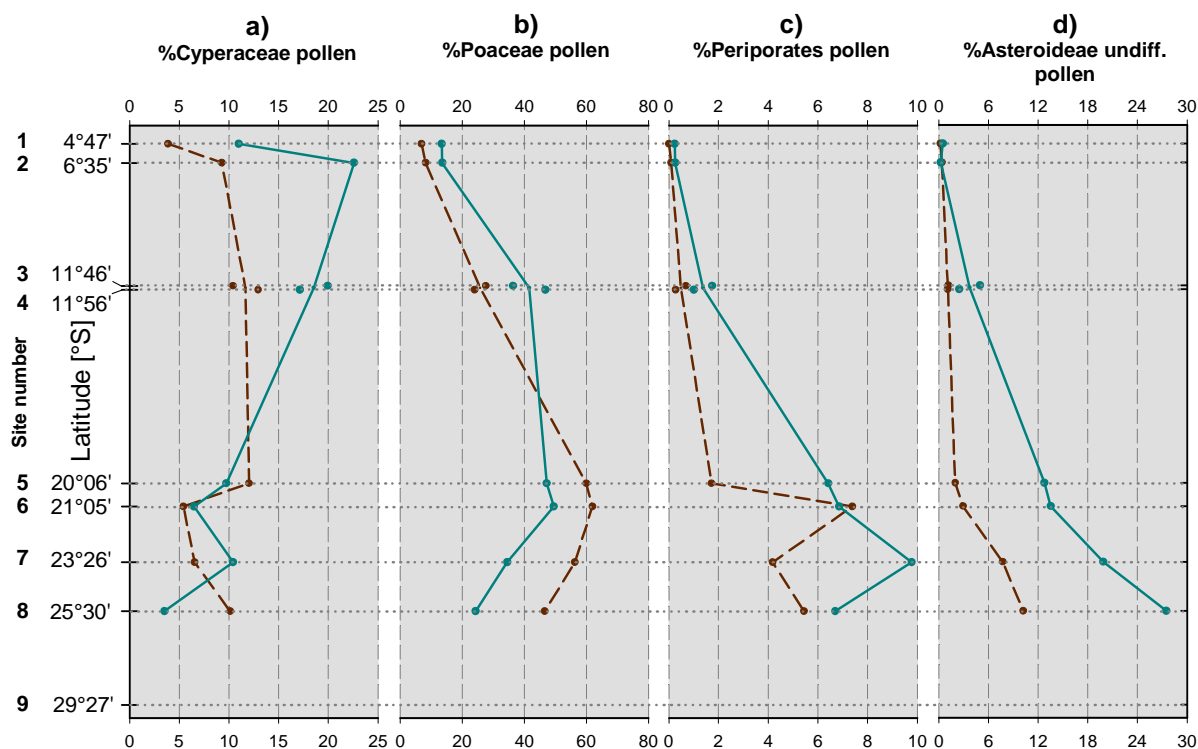


**Fig. 4.6.** Glacial and interglacial N-S transects of pollen percentages of a) Cyperaceae (sedges etc.), b) Poaceae (grass), c) periporates (sum of mostly desert plants such as *Tribulus*, Caryophyllaceae, Chenopodiaceae, Amaranthaceae), d) undifferentiated Asteroideae. C<sub>4</sub> plants are among the tropical sedges, grasses, and desert plants. For Sites 3 and 4, due to almost identical latitudes, averaged data were used for the trend lines, but the individual data points are shown as well.

correlation coefficients ( $r^2$ ) for these two parameters are high for each individual time horizon (Table 4.2). The behaviour of the individual homologues in terms of carbon isotope signatures is noticeably different, with the  $n$ -C<sub>33</sub> alkane showing more constantly a less negative value of about -26‰ throughout the sites for the glacials, although not for the interglacials (Fig. 4.3a, Table 4.4a-d). It is consistent with  $n$ -C<sub>33</sub> being mainly derived from the C<sub>4</sub> grasses (cf. Rommerskirchen et al., in press, Chapter 2). Our carbon isotope data of the  $n$ -C<sub>29</sub> alkane for the MIS 1 and 2 time horizons also compare well, i.e. within ca. 1‰, with those of Schefuß et al. (2005) for his site GeoB 6518, which is close to our Sites 1 and 2 though considerably nearer shore.

The differences in  $\delta^{13}\text{C}$  values ( $\Delta\delta^{13}\text{C}_{\text{No.}}$ ) between the  $n$ -C<sub>29</sub> alkane and the adjacent homologues are shown in Fig. 4.7a. Especially at glacial times (MIS 2 and 6a), the adjacent homologues are less  $^{13}\text{C}$ -depleted than in interglacial times. This is also reflected in higher correlation coefficients for interglacial times (MIS 1: 0.95, MIS 5e: 0.80) due to similar  $\delta^{13}\text{C}$  values of the adjacent alkanes (Table 4.2). This behaviour of  $n$ -alkane homologues can be ascribed to i) overlaying of different distribution patterns from different biosynthetic origins (C<sub>3</sub>, C<sub>4</sub> and CAM plants) of leaf wax components of the continental vegetation, where C<sub>4</sub> plant waxes contain  $n$ -alkanes with a predominance of longer-chain homologues, and ii) contributions of different types of vegetation on the adjacent continent

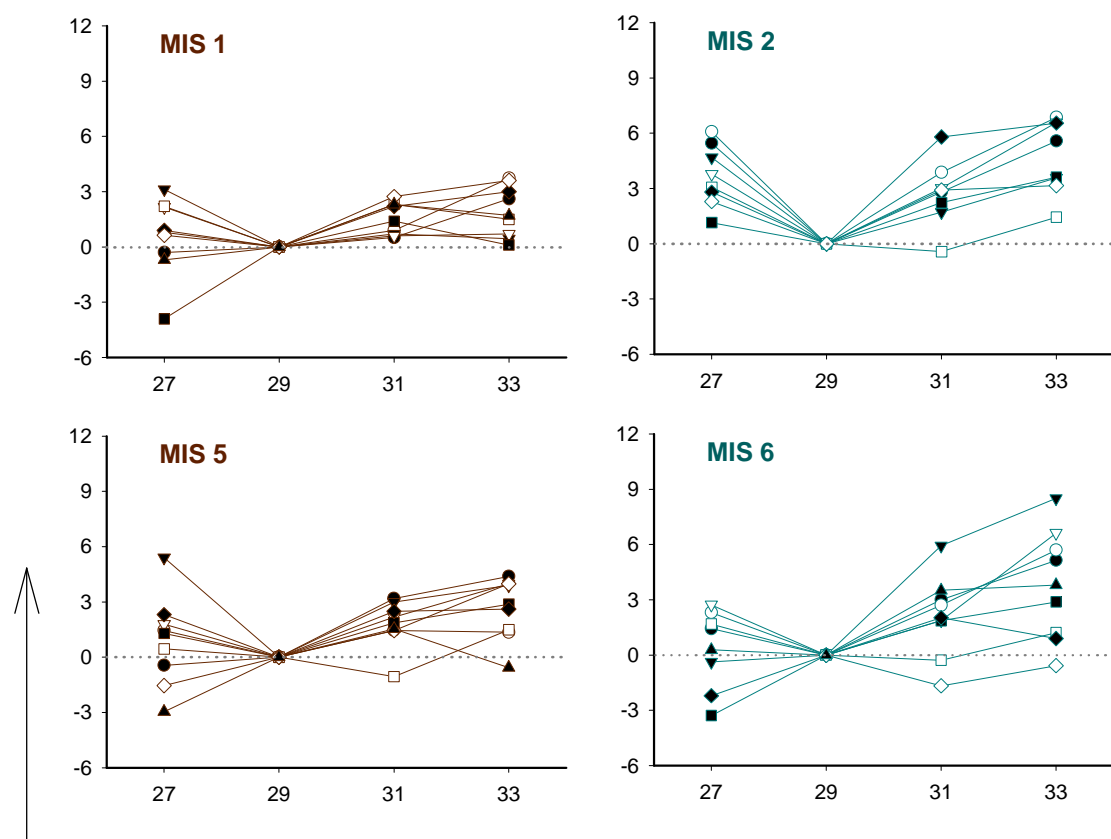
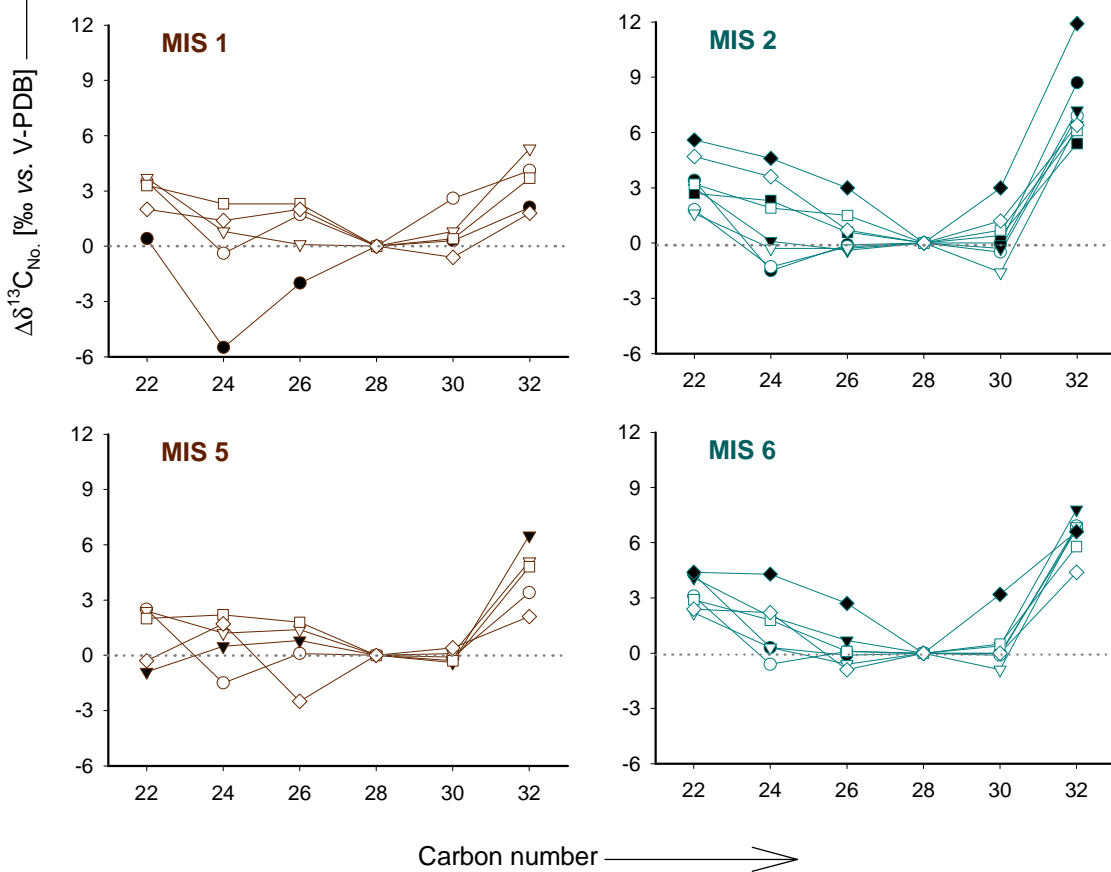
due to glacial/interglacial changes. The occurrence of heavier  $\delta^{13}\text{C}_{\text{WMA27-33}}$  values at sites of higher  $\text{ACL}_{27-33}$  values (Fig. 4.4a,c) can be ascribed to a N-S trend in the balance of vegetation types (cf. also Rommerskirchen et al., 2003, Chapter 3).

There is more variability in the distributions of the *n*-alkanols (Fig. 4.3b) as compared with those of the *n*-alkanes (Fig. 4.3a). One significant feature is the generally high contribution of the *n*-C<sub>32</sub> homologue (Figs. 4.3b, 4.4d). The  $\text{ACL}_{22-32}$  plots (Fig. 4.4b) reflect the variability of the distributions and are not easily interpreted in terms of N-S trends. However, the interglacial and glacial plots are rather similar, indicating that the *n*-alkanol chain length is certainly driven by phytogeographical characteristics which behave systematically in the same direction in all four time slices. The possible contributions from marine organisms are not readily identified within the carbon number range selected for calculation.

Sampling problems preclude  $\delta^{13}\text{C}$  data for the alkanols being available for every site (Fig. 4.3b), but, in principle, each even-numbered long-chain homologue in the range *n*-C<sub>24</sub> to *n*-C<sub>30</sub> seems to have much the same  $^{13}\text{C}$  content as the others in most samples (Table 4.4a-d). The difference in  $\delta^{13}\text{C}$  values between the *n*-C<sub>28</sub> alkanol and the adjacent homologues is shown in Fig. 4.7b. As found for the  $\delta^{13}\text{C}$  values of the *n*-C<sub>29</sub> alkane at glacial times (cf. Fig. 4.7a), the adjacent alkanol homologues are more  $^{12}\text{C}$  depleted than in interglacial times. Furthermore, the *n*-C<sub>32</sub> alkanol in most cases has the heaviest  $\delta^{13}\text{C}$  value. Presumably the *n*-C<sub>32</sub> homologue carries a strong contribution from the C<sub>4</sub> grasses since we know from our survey of the grasses in southern Africa that the *n*-C<sub>32</sub> homologue is a major component of their *n*-alkanol fractions (Rommerskirchen et al., in press, Chapter 2).

The absence of any correlation between the  $\text{ACL}_{22-32}$  values and the weighted mean average of the carbon isotopic values ( $\delta^{13}\text{C}_{\text{WMA24-32}}$ ; Table 4.2) illustrates the independent behaviour of these two parameters. But the  $\delta^{13}\text{C}_{\text{WMA24-32}}$  values become heavier from North to South, just like the  $\delta^{13}\text{C}_{\text{WMA27-33}}$  values of the *n*-alkanes (Fig. 4.4e,f). This corroborates the suggestion that the multimodal carbon number distributions are the result of multiple origins of the *n*-alkanols, e.g. from different types of biota (marine organisms and terrestrial CAM, C<sub>3</sub> and C<sub>4</sub> plants). Compared to the interglacials, we found more positive  $\delta^{13}\text{C}_{\text{WMA24-32}}$  values at glacial times in the northern part of our transect. Southwards there is a tendency of the difference to disappear as observed for the *n*-alkanes (cf. Fig. 4.4e,f).

Instead of having two separate molecular isotope parameters for the input of C<sub>3</sub> versus C<sub>4</sub> plant waxes to the oceanic sediments it is useful to have a single one. Thus, we averaged the  $\delta^{13}\text{C}_{\text{WMA27-33}}$  and  $\delta^{13}\text{C}_{\text{WMA24-32}}$  values separately for glacials and the

a) *n*-Alkaneb) *n*-Alkanol

interglacials (Fig. 4.4g). We were encouraged to do so by the high correlation coefficients of these parameters, particularly in the interglacials (Table 4.2). The resulting plots in Fig. 4.4g show the same general trends as described before for the separate sets of isotope data and compare well with the pollen data (see below).

#### 4.5.2 Pollen signals

Because most savanna and desert grasses are  $C_4$  plants, the grass pollen distribution is an indicator of  $C_4$  plant material which can be compared with that provided by the isotopic signature of terrestrial biomarkers. However, only part – albeit probably a most significant one – of the  $C_4$  signature is accounted for by the grass pollen. In the equatorial swamps, tropical sedges such as papyrus and others use the  $C_4$  metabolism. In desert and semi-desert areas numerous non-grassy herbs are  $C_4$  plants, like *Tribulus*, or members of the Chenopodiaceae and Amaranthaceae. In Fig. 4.6a-c, we distinguish three pollen types that contain pollen of mainly  $C_4$  plants: Cyperaceae (sedges), Poaceae (grass), periporates (Caryophyllaceae, Chenopodiaceae, Amaranthaceae, *Tribulus*).

CAM plants form an important part of the vegetation of south-western Africa. Pollen of the most common CAM plants (succulent species of the Aizoaceae and Crassulaceae), however, is rare, probably because they are not wind pollinators. CAM biosynthesis is also used by *Senecio* species and related genera (family of composites). Unfortunately, their pollen is not distinguishable from many other composites that belong to the subfamily of the Asteroideae. The representatives of this subfamily that can be palynologically distinguished use the  $C_3$  metabolism. They include the wild Camphor bush, which grows in a wide variety of habitats, the Renosterbos, which grows at present in the upland areas of the Cape provinces, and the colourful daisies of Namaqualand. Thus, within the group of composites pollen, only the taxon ‘Asteroideae undifferentiated’ (Fig. 4.6d) contains pollen from CAM species.

The Cyperaceae (sedge) pollen percentages along the N-S Transect are low at southern latitudes, both in glacial and interglacial stages (Fig. 4.6a, Table 4.5a,b). They are higher in the northern part during glacial times. The interglacial swamp forest of the Congo Basin, which has little sedges today, might have been replaced by open swamps with sedges and grasses during glacials. Poaceae (grass) pollen percentages are high at

**Fig. 4.7.** (opposite) Difference in  $\delta^{13}\text{C}$  values ( $\Delta\delta^{13}\text{C}_{\text{No.}}$ ) between a) the  $n\text{-C}_{29}$  alkane and its adjacent odd-carbon-numbered homologues and b) the  $n\text{-C}_{28}$  alkanol and its adjacent even-carbon-numbered homologues for Holocene, LGM, Eemian and penultimate glacial MIS 6a sediments. Values are given in ‰ versus V-PDB.

Symbols representing site numbers:

● - 1   ○ - 2   ▼ - 3   ▽ - 4   ■ - 5   □ - 6   ◆ - 7   ◇ - 8   ▲ - 9

latitudes between 10 and 20°S, they decline between 20 and 25°S, and they are very low around 5°S (Fig. 4.6b). The interglacial pattern nicely follows the modern latitudinal extension and position of the grass-rich savannas and open woodlands. A slight increase in the open grassy vegetation is indicated by slightly higher grass pollen percentages in the northern part of the transect during glacials. The southern part of the transect, however, shows a decline in relative grass pollen abundance during glacial stages. This decline, south of 20°S, probably reflects a retraction and/or northward shift of the savanna.

Significant expansion of desert and semi-desert vegetation particularly around 20°S and further south during glacial stages is indicated by the high relative abundance of periporate pollen (from *Tribulus*, Chenopodiaceae, Amaranthaceae, Caryophyllaceae; Fig. 4.6c). Composites (Asteraceae) pollen percentages are low during interglacial times, reaching maximum values around 25°S (Table 4.5a,b). Almost all composite pollen grains belong to the undifferentiated Asteroideae (Fig. 4.6d), which include pollen from *Senecio* and related CAM species. During glacials pollen of the undifferentiated Asteroideae become more abundant at all sites south of 10°S. Between 20 and 25°S, percentages for all composites rise, also those for C<sub>3</sub> plants in the composite family (Table 4.5a,b).

#### 4.5.3 Comparison of biomarker and pollen data

Stable isotopes indicate an increase in C<sub>4</sub> plant wax material during glacial stages for all transect sites with the exception of the southernmost one (ca. 30°S) while the pollen data indicate a differentiated response of the vegetation along the transect. Stable isotope data indicate the largest change toward more C<sub>4</sub> vegetation in the northern part. Here the grass pollen percentages increase slightly during the glacial stages, but those of sedges (Cyperaceae) increase markedly (Fig. 4.6b). This rise in the relative abundance of sedge pollen near the Congo mouth suggests an increase of open swamps at the cost of swamp forests in the Congo Basin rather than an increase of grass savanna. Grass pollen percentages suggest an increase of savanna around 12°S and a decrease of savanna at and south of 20°S. Thus, the increase of C<sub>4</sub> wax components around 12°S (Fig. 4.4g) can be attributed to a northward shift of the savanna. South of 20°S, the isotopic signature does not change between interglacials and glacials (Fig. 4.4g), but the pollen data indicate a shift to more desert and less savanna (Fig. 4.6). The strong glacial increase of the pollen percentages of composites, particularly those of the undifferentiated Asteroideae (Fig. 4.6d), might be attributed to CAM plants such as *Senecio*. Extension of the desert during glacial periods would explain both the high C<sub>4</sub> signature in the wax component stable isotope data (Fig. 4.4d) and the relative decline in grass pollen and the increase in

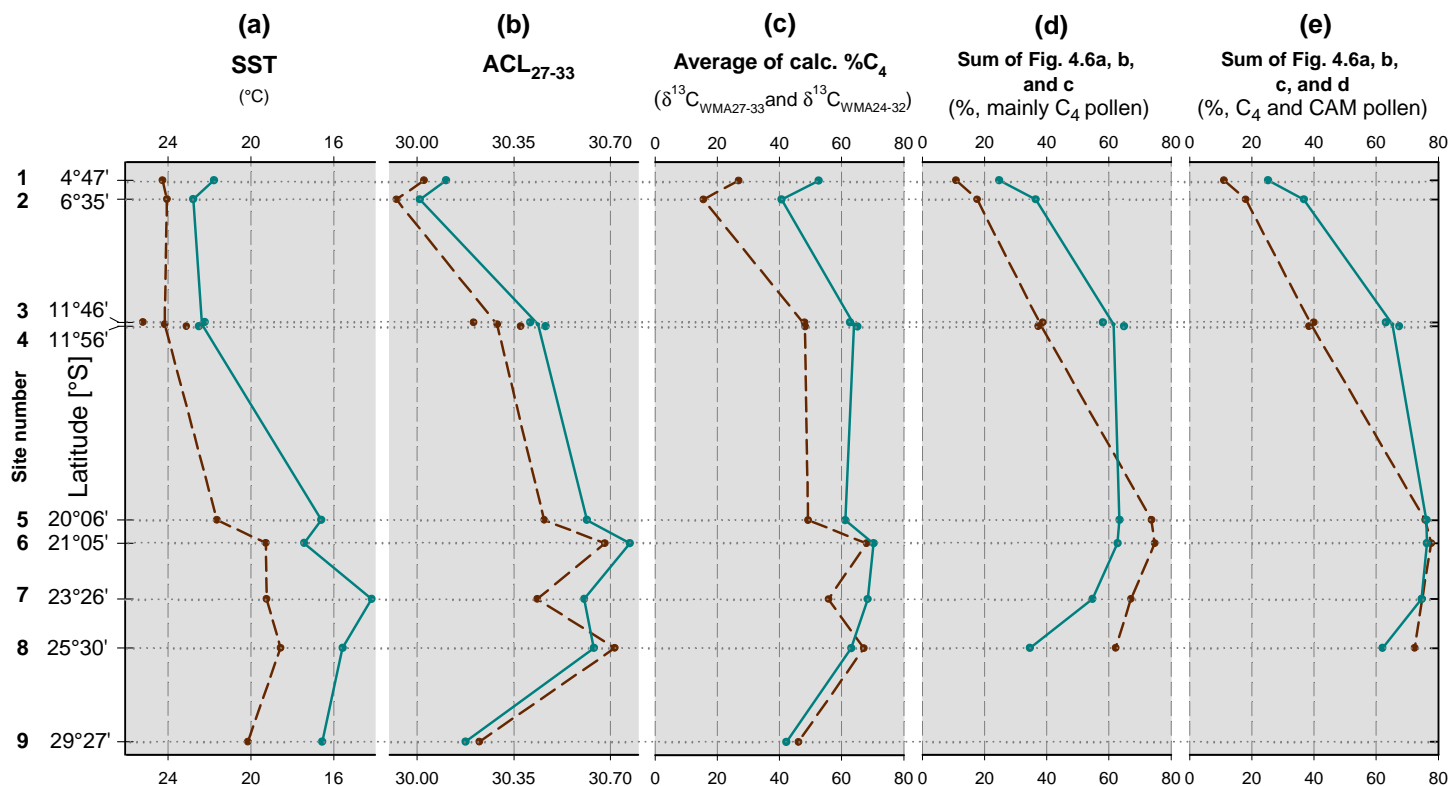


**Fig. 4.8.** Glacial and interglacial N-S transects of a) palaeo-sea surface temperature (SST), b)  $ACL_{27-33}$  values (cf. Fig. 4.4a), c) estimate of percent  $C_4$  plant contribution based on  $\delta^{13}C_{WMA27-33}$  and  $\delta^{13}C_{WMA24-32}$  values, respectively (cf. Rommerskirchen et al. (2003, Chapter 3) for way of calculation), d) sum of Cyperaceae, Poaceae and periporates pollen (cf. Fig. 4.6a-c), e) ibid. plus pollen of Asteroideae undifferentiated (cf. Fig. 4.6a-d). For Sites 3 and 4, due to almost identical latitudes, averaged data were used for the trend lines, but the individual data points are shown as well.

periporate pollen from composites (Fig. 4.6b,c). The isotope data, other than the pollen data in Figure 3c, do not support an expansion in C<sub>3</sub> or CAM vegetation from the Cape northwards related to a postulated shift in the winter rainfall area during glacial periods (Dupont and Wyputta, 2003).

A principal motivation for the present study has been our intention to derive an approach to the estimation of the phytogeographical extent of C<sub>4</sub> vegetation on a broad continental scale, because the competition between C<sub>3</sub> and C<sub>4</sub> plants mirrors important climatic factors such as solar irradiation, temperature, carbon dioxide concentration in the atmosphere as well as humidity and rainfall levels. Hence, assessing the percentage of C<sub>4</sub> vegetation from measurements conducted in ancient sediments has a direct relevance for palaeoclimate studies. From the organic geochemical and palynological data we derived a couple of proxies related to the percentage of C<sub>4</sub> plant material arriving at the sites of deposition. Using end member values of  $\delta^{13}\text{C}$  signatures of *n*-alkanes and *n*-alkanols in C<sub>3</sub> and C<sub>4</sub> plants (Rommerskirchen et al., in press, Chapter 2; cf. Rommerskirchen et al., 2003, Chapter 3, for methodological aspects) we converted the averaged  $\delta^{13}\text{C}_{\text{WMA27-33}}$  and  $\delta^{13}\text{C}_{\text{WMA24-32}}$  data in Fig. 4.4g into a percentage C<sub>4</sub> plants (Fig. 4.8c). Likewise, we added the pollen data of those taxa which essentially all comprise C<sub>4</sub> plants (Cyperaceae, Poaceae and periporates; Fig. 4.6a-c) and, additionally, the pollen of the same taxa plus those of the undifferentiated Asteroideae which essentially comprise CAM plants (Fig. 4.6d) to arrive at two different summed pollen parameters (Fig. 4.8e,f).

The pollen-derived sums compare well with the isotope-derived data (Fig. 4.8c-d). It is remarkable how much the values of the estimates based on totally different sources coincide. The pollen C<sub>4</sub> plant values must be an overestimate for the following reasons. Firstly, the C<sub>4</sub> plants produce more pollen than most C<sub>3</sub> plants in the area. Secondly, the groups that are used for the C<sub>4</sub>/CAM estimate contain C<sub>3</sub> species as well, but this problem is ignored in this summation. Thirdly, part of the isotope estimate relates to CAM plants, which should have an intermediate isotopic signature. Thus, as the pollen estimate for the C<sub>4</sub> and CAM part of the total vegetation is almost certainly too high, the isotope estimates must be also too high. One reason for a C<sub>4</sub> and CAM overestimate by the wax data may be the higher production of waxes by drought resistant C<sub>4</sub> and CAM plants. Supporting evidence for the validity of the approach, however, is the close similarity of the latitudinal and temporal trends in the  $\text{ACL}_{27-33}$  values based on the homologue distributions of the long-chain aliphatic wax components (Fig. 4.8b) and the average of the calculated C<sub>4</sub> plant percentages based on the isotope data (Fig. 4.8c); these plots, in turn, are not too different from the profiles of the C<sub>4</sub> percentages based on pollen data (Fig 4.8d,e).

Some systematic differences of pollen versus wax data at Sites 1 and 2 can be explained by the fact that more aeolian material is transported to Site 1 than to Site 2. This

includes an abundance of *Podocarpus* pollen from the Angolan highlands, but little grass pollen at Site 1, resulting in a higher  $C_3$  value based on the pollen data.

There is a close connection between oceanographic conditions and continental climate. Ocean surface temperatures have an influence on air temperatures and precipitation on the continent as well as on the strength of the wind systems (e.g., Camberlin et al., 2001; Lindzen and Nigam, 1987). Palaeo sea surface temperatures (SST) can be determined by measuring the ratios of long-chain alkenones with different degrees of unsaturation in marine sediments (e.g., Müller et al., 1998). The averaged values for interglacials and glacials for the nine sites of our transect are shown in Fig. 4.8a. There is the expected drop in temperature from North to South across the Angola-Benguela Front (ABF; Fig. 4.1) into the cold Benguela Current System driving the upwelling regime off South Africa (see the coast-parallel wind; Fig. 4.2a,b). The large sea surface temperature gradient over the Angola-Benguela Front is the result of strong SE trade winds driving upwelling of cool subsurface waters south of it, whereas north of it surface waters are heated by strong intrusion of warm equatorial waters (Kim et al., 2003, and references therein). The thermal gradient increases with increasing trade wind intensity. Also noteworthy is the systematic temperature difference between the interglacials and the glacials of about 4°C on average and slightly less in the very North than in the South. The plots quite obviously resemble those of the aliphatic wax biomarker and pollen diagrams both in terms of latitudinal trends and the offset between warm and cold stages.

In a recent publication, Schefuß et al. (2005) assessed the African continental climate in terms of aridity and wind regimes by determining a high-resolution SST profile and the isotopic composition of terrestrial plant lipids for the last 20,000 yrs at two near-shore sites in the eastern South Atlantic (5°35'S and 17°9'S). However, their investigation could not deal with some of the complexities of the system which have become obvious in this and our previous study (Rommerskirchen et al., 2003, Chapter 3). Even after investigating nine sites along the Southwest African continental margin we see the need for wider areal studies. This requires both a set of parameters which can be determined with an acceptable effort, like the combination of molecular and isotopic data of higher plant wax components in sediments, and a more solid taxonomic basis for the natural product chemistry of waxes of representative higher plants as we have recently documented for the grasses in southern Africa (Rommerskirchen et al., in press, Chapter 2).



## 4.6 Conclusions

Mapping and profiling biomarker distributions and their isotopic compositions in continental margin sediments can provide insights into the palaeophytogeography of the adjacent continental areas. This information can in turn be utilised to infer regional and continental-scale palaeoclimatic change. The present study has made use of two types of biomarkers - long-chain *n*-alkanes and *n*-alkanols - as homologous series of biosynthetic compounds derived from epicuticular leaf waxes of higher land plants. Their relative abundances and  $\delta^{13}\text{C}$  values are interpretable on a compound-specific basis. The information that can be drawn at present is limited to a broad assessment of the extent of  $\text{C}_3$  versus  $\text{C}_4$  vegetation, which is not readily available in other ways. This information can be strengthened by the interpretation of the distribution patterns and abundances of spores and pollen in the same sediments, relating plant taxa also to the  $\text{C}_3$  and  $\text{C}_4$  biosynthetic pathways. Our data provide a rather simplified view of the palaeophytogeographic development in southern Africa for four time slices over the last two glacial/interglacial cycles. This view is dominated by the large scale and variable nature of the source areas and of the transport processes, which have a major averaging effect on the fluxes of the lipids and pollen and their areal distributions. The aeolian input is mainly dependent on the prevailing austral winter winds blowing from the East and Southeast, which apparently operated in the glacials in the same way as at present.

Some salient conclusions are:

- ➔ For both glacial and interglacial times the latitudinal trends of *n*-alkane and *n*-alkanol distributions and their carbon isotopic signatures as well as pollen types display an increase in the relative proportion of  $\text{C}_4$  plant indicators from the latitude of the mouth of the Congo River ( $5^\circ\text{S}$ ) to about  $20\text{--}25^\circ\text{S}$  and then a decrease further south. This is true for the individual stages within the two pairs of glacial (MIS 2 and 6a) and interglacial (MIS 1 and 5e) sample sets; due to this the averages can conveniently be used to contrast cold and warm stages.
- ➔ The relative importance of the  $\text{C}_4$  plant indicators is higher during the glacials than in the interglacials in the northern part of the transect, indicating a northward extension of arid zones favouring grass vegetation together with an increase of open sedge swamps in areas of interglacial swamp forests. In the south, where grass-rich vegetation merges into semi-desert and desert, the difference in  $\text{C}_4$  plant indicators is comparatively small. Among the biomarker parameters this development is displayed by the chain length distribution of the *n*-alkanes ( $\text{ACL}_{27-33}$ ) in the same way as the

averaged carbon isotope data of *n*-alkanes and *n*-alkanols, whereas the *n*-alkanol chain lengths alone are less conclusive.

- Selected single pollen type data reveal details of the vegetation changes like the extension of the desert and savanna areas to the North in the glacials. The overall picture, however, is best illustrated by summing the pollen known to predominantly derive from C<sub>4</sub> plants or C<sub>4</sub> plus CAM plants.
- The C<sub>4</sub> plant signals in the aliphatic biomarkers are particularly controlled by the abundance of their *n*-C<sub>31</sub> and *n*-C<sub>33</sub> alkanes and their *n*-C<sub>32</sub> *n*-alkanol. The validity of this conclusion is strongly corroborated by a study of the wax composition of a variety of C<sub>4</sub> grass species from southern Africa (Rommerskirchen et al., in press, Chapter 2).
- The success of this approach warrants an areal extension of the study in order to validate and further strengthen the method, so that it can be routinely applied in palaeoclimatic assessments in this area and other epicontinental areas of the world oceans.

## 4.7 Appendix

**Table 4.3.** Biomarker data.

| Site                       | Code     | Depth<br>(cm) | Age<br>(ka) | SST <sup>a</sup><br>(°C) | ACL <sub>27-33</sub> <sup>b</sup> | ACL <sub>22-32</sub> <sup>b</sup> | CPI <sub>27-33</sub> <sup>c</sup> | CPI <sub>22-32</sub> <sup>c</sup> | HPA <sup>d</sup> | MAR <sup>e</sup><br>C <sub>org</sub> | MAR <sup>e</sup><br>CaCO <sub>3</sub> | MAR <sup>e</sup><br>ALK <sup>f</sup> | MAR <sup>e</sup><br>-OH <sup>g</sup> |
|----------------------------|----------|---------------|-------------|--------------------------|-----------------------------------|-----------------------------------|-----------------------------------|-----------------------------------|------------------|--------------------------------------|---------------------------------------|--------------------------------------|--------------------------------------|
| <i>a) Holocene (MIS 1)</i> |          |               |             |                          |                                   |                                   |                                   |                                   |                  |                                      |                                       |                                      |                                      |
| ODP 1075A                  | <b>1</b> | 55            | 5.0         | 23.9                     | 29.96                             | 26.68                             | 3.5                               | 4.2                               | 0.77             | 64                                   | 11                                    | 3.5                                  | 14                                   |
| GeoB 1008-3                | <b>2</b> | 13            | 2.0         | 24.0                     | 29.92                             | 26.86                             | 4.8                               | 5.0                               | 0.68             | 44                                   | 17                                    | 5.3                                  | 13                                   |
| GeoB 1016-3                | <b>3</b> | 4             | 1.0         | 24.5                     | 30.06                             | 27.76                             | 3.9                               | 5.2                               | 0.46             | 19                                   | 183                                   | 1.9                                  | 1.8                                  |
| ODP 1079A                  | <b>4</b> | 77            | 3.0         | 23.5                     | 30.28                             | 28.00                             | 4.9                               | 6.7                               | 0.75             | 800                                  | 2830                                  | 29                                   | 93                                   |
| GeoB 1028-5                | <b>5</b> | 20            | 4.0         | 22.2                     | 30.55                             | 27.69                             | 4.5                               | 4.0                               | 0.64             | 21                                   | 3590                                  | 0.5                                  | 1.0                                  |
| ODP 1082A                  | <b>6</b> | 37            | 3.8         | 18.4                     | 30.68                             | 27.63                             | 4.3                               | 7.4                               | 0.72             | 170                                  | 3600                                  | 4.4                                  | 12                                   |
| GeoB 1710-3                | <b>7</b> | 3             | 1.0         | 18.7                     | 30.54                             | 27.68                             | 4.1                               | 7.2                               | 0.49             | 39                                   | 1780                                  | 0.9                                  | 1.5                                  |
| ODP 1084A                  | <b>8</b> | 55            | 5.3         | 18.1                     | 30.83                             | 26.93                             | 5.4                               | 7.1                               | 0.74             | 400                                  | 9150                                  | 9.0                                  | 27                                   |
| GeoB 1722-1                | <b>9</b> | 8             | 6.8         | 18.4                     | 30.45                             | 28.02                             | 4.0                               | 4.7                               | 0.50             | 1.1                                  | 1250                                  | 0.2                                  | 0.3                                  |
| <i>b) LGM (MIS 2)</i>      |          |               |             |                          |                                   |                                   |                                   |                                   |                  |                                      |                                       |                                      |                                      |
| ODP 1075A                  | <b>1</b> | 355           | 23          | 20.1                     | 30.03                             | 27.09                             | 4.7                               | 4.6                               | 0.63             | 140                                  | 67                                    | 15                                   | 27                                   |
| GeoB 1008-3                | <b>2</b> | 220           | 19          | 21.5                     | 30.04                             | 27.40                             | 4.9                               | 5.3                               | 0.58             | 110                                  | 15                                    | 30                                   | 45                                   |
| GeoB 1016-3                | <b>3</b> | 112           | 18          | 21.1                     | 30.21                             | 27.81                             | 5.1                               | 4.7                               | 0.74             | 16                                   | 295                                   | 4.2                                  | 13                                   |
| ODP 1079A                  | <b>4</b> | 757           | 19          | 22.1                     | 30.63                             | 28.58                             | 6.2                               | 6.5                               | 0.70             | 510                                  | 4110                                  | 32                                   | 81                                   |
| GeoB 1028-5                | <b>5</b> | 95            | 20          | 15.9                     | 30.70                             | 27.44                             | 4.3                               | 5.4                               | 0.64             | 21                                   | 3590                                  | 0.5                                  | 1.1                                  |
| ODP 1082A                  | <b>6</b> | 237           | 21          | 15.9                     | 30.80                             | 26.77                             | 4.4                               | 7.0                               | 0.60             | 300                                  | 2550                                  | 7.5                                  | 12                                   |
| GeoB 1710-3                | <b>7</b> | 95            | 18          | 13.4                     | 30.65                             | 27.04                             | 5.1                               | 6.7                               | 0.65             | 84                                   | 1850                                  | 2.8                                  | 5.7                                  |
| ODP 1084A                  | <b>8</b> | 455           | 26          | 14.1                     | 30.85                             | 26.10                             | 3.7                               | 7.0                               | 0.36             | 800                                  | 3220                                  | 22                                   | 39                                   |
| GeoB 1722-1                | <b>9</b> | 24            | 17          | 17.0                     | 30.14                             | 26.98                             | 2.4                               | 2.9                               | 0.19             | 0.4                                  | 900                                   | 0.5                                  | 0.1                                  |

cont. Table 4.3. Biomarker data.

| Site                      | Code | Depth<br>(cm) | Age<br>(ka) | SST <sup>a</sup><br>(°C) | ACL <sub>27-33</sub> <sup>b</sup> | ACL <sub>22-32</sub> <sup>b</sup> | CPI <sub>27-33</sub> <sup>c</sup> | CPI <sub>22-32</sub> <sup>c</sup> | HPA <sup>d</sup> | MAR <sup>e</sup><br>C <sub>org</sub> | MAR <sup>e</sup><br>CaCO <sub>3</sub> | MAR <sup>e</sup><br>ALK <sup>f</sup> | MAR <sup>e</sup><br>-OH <sup>g</sup> |
|---------------------------|------|---------------|-------------|--------------------------|-----------------------------------|-----------------------------------|-----------------------------------|-----------------------------------|------------------|--------------------------------------|---------------------------------------|--------------------------------------|--------------------------------------|
| <i>c) Eemian (MIS 5e)</i> |      |               |             |                          |                                   |                                   |                                   |                                   |                  |                                      |                                       |                                      |                                      |
| ODP 1075A                 | 1    | 1879          | 126         | 24.6                     | 30.09                             | 27.43                             | 3.5                               | 4.7                               | 0.65             | 39                                   | 80                                    | 3.2                                  | 6.7                                  |
| GeoB 1008-3               | 2    | 820           | 123         | 24.1                     | 29.93                             | 26.59                             | 4.2                               | 5.3                               | 0.75             | 32                                   | 8.2                                   | 4.2                                  | 14                                   |
| GeoB 1016-3               | 3    | 603           | 122         | 25.9                     | 30.35                             | 27.40                             | 5.3                               | 5.5                               | 0.50             | 84                                   | 39                                    | 2.8                                  | 3.1                                  |
| ODP 1079A                 | 4    | 2943          | 127         | 22.7                     | 30.47                             | 27.81                             | 6.5                               | 6.9                               | 0.82             | 630                                  | 4120                                  | 32                                   | 160                                  |
| GeoB 1028-5               | 5    | 394           | 121         | 21.1                     | 30.37                             | 27.43                             | 2.9                               | 3.1                               | 0.41             | 22                                   | 3030                                  | 0.6                                  | 0.5                                  |
| ODP 1082A                 | 6    | 1286          | 127         | 20.1                     | 30.68                             | 26.59                             | 4.3                               | 6.3                               | 0.59             | 240                                  | 3730                                  | 6.9                                  | 12                                   |
| GeoB 1710-3               | 7    | 609           | 122         | 19.8                     | 30.33                             | 27.59                             | 3.2                               | 6.1                               | 0.44             | 14                                   | 2580                                  | 1.0                                  | 1.0                                  |
| ODP 1084A                 | 8    | 2633          | 124         | 19.0                     | 30.60                             | 25.41                             | 2.5                               | 6.2                               | 0.57             | 920                                  | 1200                                  | 26                                   | 38                                   |
| GeoB 1722-1               | 9    | 189           | 123         | 21.9                     | 30.00                             | 26.17                             | 2.6                               | 3.2                               | 0.25             | 2.5                                  | 820                                   | 0.2                                  | 0.1                                  |
| <i>d) MIS 6a</i>          |      |               |             |                          |                                   |                                   |                                   |                                   |                  |                                      |                                       |                                      |                                      |
| ODP 1075A                 | 1    | 1905          | 131         | 23.5                     | 30.18                             | 27.59                             | 4.3                               | 4.4                               | 0.65             | 63                                   | 260                                   | 7.3                                  | 15                                   |
| GeoB 1008-3               | 2    | 881           | 135         | 24.1                     | 29.98                             | 26.83                             | 4.5                               | 5.2                               | 0.58             | 46                                   | 22                                    | 15                                   | 24                                   |
| GeoB 1016-3               | 3    | 643           | 136         | 23.4                     | 30.61                             | 28.21                             | 4.9                               | 5.1                               | 0.69             | 62                                   | 86                                    | 4.5                                  | 11                                   |
| ODP 1079A                 | 4    | 3223          | 137         | 22.9                     | 30.30                             | 28.12                             | 6.8                               | 6.2                               | 0.75             | 690                                  | 4610                                  | 67                                   | 210                                  |
| GeoB 1028-5               | 5    | 454           | 136         | 17.3                     | 30.53                             | 27.65                             | 2.8                               | 3.3                               | 0.49             | 35                                   | 540                                   | 0.2                                  | 0.2                                  |
| ODP 1082A                 | 6    | 1376          | 136         | 18.9                     | 30.74                             | 26.10                             | 3.5                               | 6.4                               | 0.36             | 340                                  | 3350                                  | 9.4                                  | 13                                   |
| GeoB 1710-3               | 7    | 669           | 136         | 14.9                     | 30.56                             | 27.21                             | 3.5                               | 6.5                               | 0.61             | 38                                   | 2540                                  | 1.5                                  | 2.9                                  |
| ODP 1084A                 | 8    | 2949          | 139         | 17.1                     | 30.43                             | 26.48                             | 2.3                               | 6.0                               | 0.70             | 740                                  | 5630                                  | 26                                   | 69                                   |
| GeoB 1722-1               | 9    | 210           | 137         | 16.1                     | 30.21                             | 28.08                             | 3.0                               | 7.2                               | 0.50             | 0.8                                  | 770                                   | 0.4                                  | 0.5                                  |

<sup>a</sup>SST: Sea-surface temperature (based on long-chain alkenones)<sup>b</sup>ACL<sub>27-33</sub>: Averaged chain length of *n*-alkanes (carbon numbers 27 - 33); ACL<sub>22-32</sub>: Averaged chain length of *n*-alkanols (carbon numbers 22 - 32)<sup>c</sup>CPI<sub>27-33</sub>: Carbon preference index of *n*-alkanes (carbon numbers 27 - 33); CPI<sub>22-32</sub>: Carbon preference index of *n*-alkanols (carbon number 22 - 32)<sup>d</sup>HPA: Higher plant *n*-alkanol index (Poynter, 1989; Poynter and Eglinton, 1991)<sup>e</sup>MAR: Mass accumulation rate (C<sub>org</sub>, CaCO<sub>3</sub>: mg cm<sup>-2</sup> kyr<sup>-1</sup>; biomarkers: µg cm<sup>-2</sup> kyr<sup>-1</sup>)<sup>f</sup>ALK: Sum of *n*-C<sub>27</sub>, *n*-C<sub>29</sub>, *n*-C<sub>31</sub> and *n*-C<sub>33</sub> alkanes<sup>g</sup>-OH: Sum of *n*-C<sub>22</sub>, *n*-C<sub>24</sub>, *n*-C<sub>26</sub>, *n*-C<sub>28</sub>, *n*-C<sub>30</sub> and *n*-C<sub>32</sub> alkanols

Table 4.4. Isotope data.

| Site            | Depth (cm) | Age (ka) | $\delta^{13}C_{org}$ (‰) | $\delta^{13}C_{WMA27-33}$ (‰) | $\delta^{13}C_{WMA27-33}$ (‰) | calc. $\delta^{13}C_{WMA27-33}$ (‰) | $\delta^{13}C_{WMA27-33}$ (‰) | $\delta^{13}C_{27}$ (‰) | $\delta^{13}C_{29}$ (‰) | $\delta^{13}C_{31}$ (‰) | $\delta^{13}C_{33}$ (‰) | $\delta^{13}C_{WMA24-32}$ (‰) | calc. $\delta^{13}C_{WMA24-32}$ (‰) | $\delta^{13}C_{22}$ (‰) | $\delta^{13}C_{24}$ (‰) | $\delta^{13}C_{26}$ (‰) | $\delta^{13}C_{28}$ (‰) | $\delta^{13}C_{30}$ (‰) | $\delta^{13}C_{32}$ (‰) |
|-----------------|------------|----------|--------------------------|-------------------------------|-------------------------------|-------------------------------------|-------------------------------|-------------------------|-------------------------|-------------------------|-------------------------|-------------------------------|-------------------------------------|-------------------------|-------------------------|-------------------------|-------------------------|-------------------------|-------------------------|
| <i>a) MIS 1</i> |            |          |                          |                               |                               |                                     |                               |                         |                         |                         |                         |                               |                                     |                         |                         |                         |                         |                         |                         |
| 1               | 55         | 5.0      | -21.4                    | -34.6                         | -35.4                         | -35.1                               | -34.6                         | -32.5                   | -30.6                   | -30.6                   | -28.6                   | -34.5                         | -31.0                               | -29.0                   | -29.3                   | -26.9                   | -26.9                   | -26.9                   | -26.9                   |
| 2               | 13         | 2.0      | -22.3                    | -34.4                         | -34.5                         | -35.3                               | -34.4                         | -31.6                   | -32.2                   | -32.2                   | -30.1                   | -34.0                         | -31.9                               | -33.6                   | -31.0                   | -29.5                   | -29.5                   | -29.5                   | -29.5                   |
| 3               | 4          | 1.0      | -19.4                    | -30.1                         | -27.7                         | -30.9                               | -30.2                         | -30.5                   | -                       | -                       | -                       | -                             | -                                   | -                       | -                       | -                       | -                       | -                       | -                       |
| 4               | 77         | 3.0      | -21.2                    | -29.9                         | -28.3                         | -30.5                               | -29.9                         | -29.8                   | -28.2                   | -28.2                   | -26.0                   | -28.9                         | -29.6                               | -29.7                   | -28.9                   | -24.4                   | -24.4                   | -24.4                   | -24.4                   |
| 5               | 20         | 4.0      | -20.0                    | -28.6                         | -32.7                         | -28.8                               | -27.4                         | -27.0                   | -                       | -                       | -                       | -                             | -                                   | -                       | -                       | -                       | -                       | -                       | -                       |
| 6               | 37         | 3.8      | -20.2                    | -25.5                         | -24.9                         | -27.1                               | -24.8                         | -25.5                   | -25.3                   | -25.3                   | -23.3                   | -24.4                         | -24.3                               | -26.6                   | -26.2                   | -22.9                   | -22.9                   | -22.9                   | -22.9                   |
| 7               | 3          | 1.0      | -20.7                    | -27.6                         | -28.5                         | -29.4                               | -27.1                         | -26.4                   | -                       | -                       | -                       | -                             | -                                   | -                       | -                       | -                       | -                       | -                       | -                       |
| 8               | 55         | 5.3      | -20.3                    | -26.1                         | -27.8                         | -28.4                               | -25.6                         | -24.8                   | -24.3                   | -24.3                   | -23.1                   | -23.7                         | -23.1                               | -25.1                   | -25.7                   | -23.3                   | -23.3                   | -23.3                   | -23.3                   |
| 9               | 8          | 6.8      | -19.7                    | -28.1                         | -30.1                         | -29.4                               | -27.1                         | -27.6                   | -                       | -                       | -                       | -                             | -                                   | -                       | -                       | -                       | -                       | -                       | -                       |
| <i>b) MIS 2</i> |            |          |                          |                               |                               |                                     |                               |                         |                         |                         |                         |                               |                                     |                         |                         |                         |                         |                         |                         |
| 1               | 355        | 23       | -20.2                    | -29.8                         | -26.9                         | -32.3                               | -29.5                         | -26.7                   | -28.4                   | -28.4                   | -26.1                   | -30.9                         | -29.5                               | -29.4                   | -29.4                   | -20.8                   | -20.8                   | -20.8                   | -20.8                   |
| 2               | 220        | 19       | -20.2                    | -30.8                         | -27.8                         | -33.9                               | -30.0                         | -27.0                   | -28.5                   | -28.5                   | -27.8                   | -30.9                         | -29.8                               | -29.6                   | -29.8                   | -22.7                   | -22.7                   | -22.7                   | -22.7                   |
| 3               | 112        | 18       | -18.7                    | -28.0                         | -25.1                         | -29.8                               | -28.1                         | -26.2                   | -25.7                   | -25.7                   | -24.5                   | -27.4                         | -28.0                               | -27.5                   | -27.8                   | -20.4                   | -20.4                   | -20.4                   | -20.4                   |
| 4               | 757        | 19       | -19.6                    | -26.7                         | -26.2                         | -30.0                               | -27.0                         | -23.4                   | -23.1                   | -23.1                   | -23.0                   | -24.9                         | -25.0                               | -24.7                   | -26.3                   | -18.3                   | -18.3                   | -18.3                   | -18.3                   |
| 5               | 95         | 20       | -19.2                    | -26.2                         | -27.1                         | -28.3                               | -26.1                         | -24.7                   | -26.4                   | -26.4                   | -25.3                   | -25.7                         | -27.4                               | -28.0                   | -27.5                   | -22.6                   | -22.6                   | -22.6                   | -22.6                   |
| 6               | 237        | 21       | -20.1                    | -25.8                         | -23.2                         | -26.2                               | -26.7                         | -24.8                   | -24.2                   | -24.2                   | -22.7                   | -24.0                         | -24.4                               | -25.9                   | -25.2                   | -19.8                   | -19.8                   | -19.8                   | -19.8                   |
| 7               | 95         | 18       | -20.5                    | -26.8                         | -28.4                         | -31.2                               | -25.4                         | -24.7                   | -24.8                   | -24.8                   | -23.3                   | -24.3                         | -26.0                               | -29.0                   | -25.9                   | -17.1                   | -17.1                   | -17.1                   | -17.1                   |
| 8               | 455        | 26       | -19.5                    | -26.3                         | -26.7                         | -29.0                               | -26.1                         | -25.8                   | -27.0                   | -27.0                   | -24.3                   | -25.3                         | -28.2                               | -28.9                   | -27.8                   | -22.5                   | -22.5                   | -22.5                   | -22.5                   |
| 9               | 24         | 17       | -21.6                    | -                             | -                             | -                                   | -                             | -                       | -                       | -                       | -                       | -                             | -                                   | -                       | -                       | -                       | -                       | -                       | -                       |

cont. Table 4.4. Isotope data.

| Site             | Depth<br>(cm) | Age<br>(ka) | $\delta^{13}\text{C}_{\text{org}}$ <sup>a</sup><br>(‰) | $\delta^{12}\text{C}_{\text{WMA27-33}}$ <sup>b</sup><br>(‰) | calc. %C <sub>4</sub> <sup>e</sup><br>( $\delta^{13}\text{C}_{\text{WMA27-33}}$ ) | $\delta^{13}\text{C}_{27}$ <sup>c</sup><br>(‰) | $\delta^{13}\text{C}_{29}$ <sup>c</sup><br>(‰) | $\delta^{13}\text{C}_{31}$ <sup>c</sup><br>(‰) | $\delta^{13}\text{C}_{33}$ <sup>c</sup><br>(‰) | $\delta^{13}\text{C}_{\text{WMA24-32}}$ <sup>b</sup><br>(‰) | calc. %C <sub>4</sub> <sup>e</sup><br>( $\delta^{13}\text{C}_{\text{WMA24-32}}$ ) | $\delta^{13}\text{C}_{22}$ <sup>d</sup><br>(‰) | $\delta^{13}\text{C}_{24}$ <sup>d</sup><br>(‰) | $\delta^{13}\text{C}_{26}$ <sup>d</sup><br>(‰) | $\delta^{13}\text{C}_{28}$ <sup>d</sup><br>(‰) | $\delta^{13}\text{C}_{30}$ <sup>d</sup><br>(‰) | $\delta^{13}\text{C}_{32}$ <sup>d</sup><br>(‰) |
|------------------|---------------|-------------|--|---|---|--|--|--|--|---|---|--|--|--|--|--|--|
| <i>c) MIS 5e</i> |               |             |  |   |   |  |  |  |  |   |   |  |  |  |  |  |  |
| 1                | 1879          | 126         | -20.6  | -30.9   | 33  | -33.2  | -32.7  | -29.5  | -28.3  | -   | -   | -  | -  | -  | -  | -  | -  |
| 2                | 820           | 123         | -22.6  | -33.6   | 15  | -33.0  | -34.4  | -33.0  | -33.1  | -33.1   | 18  | -30.6  | -34.5  | -32.9  | -33.1  | -33.2  | -29.7  |
| 3                | 603           | 122         | -20.5  | -29.3   | 44  | -26.4  | -31.8  | -28.8  | -27.9  | -27.5   | 56  | -29.8  | -28.3  | -28.0  | -28.8  | -29.2  | -22.4  |
| 4                | 2943          | 127         | -21.1  | -27.7   | 55  | -27.8  | -29.6  | -27.4  | -25.6  | -28.8   | 47  | -27.9  | -29.1  | -28.9  | -30.3  | -30.2  | -25.2  |
| 5                | 394           | 121         | -22.3  | -28.3   | 51  | -28.5  | -29.8  | -27.9  | -26.9  | -   | -   | -  | -  | -  | -  | -  | -  |
| 6                | 1286          | 127         | -20.5  | -26.8   | 61  | -26.3  | -26.8  | -27.8  | -25.3  | -25.2   | 71  | -24.8  | -24.5  | -24.9  | -26.7  | -27.0  | -21.9  |
| 7                | 609           | 122         | -20.7  | -27.4   | 57  | -27.1  | -29.4  | -26.9  | -26.8  | -   | -   | -  | -  | -  | -  | -  | -  |
| 8                | 2633          | 124         | -19.9  | -27.0   | 59  | -31.0  | -28.4  | -26.9  | -24.4  | -25.8   | 67  | -26.1  | -24.2  | -28.4  | -25.9  | -25.5  | -23.7  |
| 9                | 189           | 123         | -20.1  | -29.8   | 40  | -32.7  | -29.7  | -28.2  | -30.3  | -   | -   | -  | -  | -  | -  | -  | -  |
| <i>d) MIS 6a</i> |               |             |  |   |   |  |  |  |  |   |   |  |  |  |  |  |  |
| 1                | 1905          | 131         | -19.9  | -27.8   | 54  | -29.6  | -30.0  | -27.0  | -24.9  | -26.0   | 66  | -23.2  | -27.2  | -27.5  | -27.5  | -27.5  | -20.7  |
| 2                | 881           | 135         | -20.4  | -30.1   | 38  | -29.9  | -32.2  | -29.5  | -26.5  | -29.5   | 42  | -27.2  | -30.8  | -30.2  | -30.3  | -30.3  | -23.4  |
| 3                | 643           | 136         | -19.6  | -28.1   | 49  | -33.0  | -32.6  | -26.6  | -24.1  | -23.8   | 81  | -22.7  | -24.9  | -26.2  | -26.9  | -26.4  | -19.1  |
| 4                | 3223          | 137         | -19.7  | -29.4   | 43  | -28.9  | -31.6  | -29.7  | -25.0  | -25.3   | 71  | -24.6  | -26.6  | -27.5  | -26.8  | -27.8  | -20.0  |
| 5                | 454           | 136         |  | -27.8   | 54  | -32.2  | -28.9  | -27.0  | -26.2  | -   | -   | -  | -  | -  | -  | -  | -  |
| 6                | 1376          | 136         | -20.4  | -26.4   | 63  | -25.0  | -26.7  | -27.0  | -25.5  | -25.1   | 72  | -23.5  | -24.5  | -26.2  | -26.4  | -25.9  | -20.6  |
| 7                | 669           | 136         | -20.2  | -26.4   | 63  | -29.5  | -27.3  | -25.2  | -26.4  | -24.7   | 75  | -23.3  | -23.4  | -25.0  | -27.7  | -24.5  | -21.1  |
| 8                | 2949          | 139         | -18.1  | -26.1   | 65  | -  | -25.1  | -26.8  | -25.7  | -26.3   | 64  | -24.9  | -25.2  | -28.2  | -27.3  | -27.3  | -22.9  |
| 9                | 210           | 137         | -20.8  | -29.5   | 42  | -31.4  | -31.7  | -28.2  | -27.9  | -   | -   | -  | -  | -  | -  | -  | -  |

- = no data due to low abundance

<sup>a</sup> $\delta^{13}\text{C}_{\text{org}}$ : Stable carbon isotopic composition of total organic carbon<sup>b</sup> $\delta^{13}\text{C}_{\text{WMA27-33}}$ : Weighted mean average of molecular stable carbon isotopic composition of odd-carbon-numbered *n*-alkanes (carbon number 27 - 33) in ‰ versus V-PDB; $\delta^{13}\text{C}_{\text{WMA24-32}}$ : Weighted mean average of molecular stable carbon isotopic composition of even-carbon-numbered *n*-alkanol (carbon number 27 - 33) in ‰ versus V-PDB<sup>c</sup> Molecular  $\delta^{13}\text{C}$  of *n*-alkanes in ‰ versus V-PDB<sup>d</sup> Molecular  $\delta^{13}\text{C}$  of *n*-alkanols in ‰ versus V-PDB (corrected for TMS)<sup>e</sup> calc. %C<sub>4</sub>: Estimates are based on 5% C<sub>4</sub> plants in the Congo area and a  $\delta^{13}\text{C}$  value of C<sub>4</sub> plants of -21‰

Table 4.5. Pollen data.

| Site            | Latitude<br>°S | Depth<br>cm | Age<br>ka | Pollen AR<br>cnts/cm <sup>2</sup> /kyr | Spore AR<br>cnts/cm <sup>2</sup> /kyr | Woody plants<br>(C <sub>3</sub> )<br>% | Cyperaceae<br>(sedges etc.)<br>% | Poaceae<br>(grass)<br>% | Tribulus<br>% | Asteraceae<br>(composites)<br>% | Restionaceae<br>(cape reeds)<br>% | Asteroidaeae<br>undiff.<br>% | Periporates <sup>a</sup><br>% | Sum 1 <sup>b</sup><br>% | Sum 2 <sup>c</sup><br>% |
|-----------------|----------------|-------------|-----------|--|---------------------------------------|--|----------------------------------|-------------------------|---------------|---------------------------------|-----------------------------------|------------------------------|-------------------------------|-------------------------|-------------------------|
| <i>a) MIS 1</i> |                |             |           |  |                                       |  |                                  |                         |               |                                 |                                   |                              |                               |                         |                         |
| 1               | -4.79          | 65          | 6.1       | 6,043                                  | 1,044                                 | 75.4                                   | 1.8                              | 6.7                     | 0.0           | 0.0                             | 0.0                               | 0.0                          | 0.0                           | 8.5                     | 8.5                     |
| 2               | -6.58          | 25          | 3.5       | 12,986                                 | 8,713                                 | 39.8                                   | 6.8                              | 8.5                     | 0.0           | 0.4                             | 0.0                               | 0.4                          | 0.0                           | 15.3                    | 15.6                    |
| 3               | -11.77         | 10          | 2.1       | 1,604                                  | 61                                    | 49.4                                   | 5.5                              | 35.6                    | 0.0           | 0.9                             | 0.0                               | 0.9                          | 0.0                           | 41.1                    | 42.0                    |
| 4               | -11.93         | 67          | 3.2       | 361,034                                | 32,515                                | 44.7                                   | 15.7                             | 21.9                    | 0.0           | 2.6                             | 0.0                               | 0.9                          | 0.3                           | 37.9                    | 38.8                    |
| 5               | -20.10         | 21          | 3.7       | 628                                    | 9                                     | 23.6                                   | 11.8                             | 54.7                    | 0.0           | 2.0                             | 0.0                               | 2.0                          | 3.4                           | 70.0                    | 71.9                    |
| 6               | -21.09         | 84          | 8.3       | 9,170                                  | 630                                   | 14.3                                   | 7.1                              | 57.9                    | 4.3           | 12.9                            | 1.4                               | 4.6                          | 7.6                           | 72.6                    | 77.2                    |
| 7               | -23.43         | 3.5         | 0.9       | 585                                    | 25                                    | 22.4                                   | 7.5                              | 52.3                    | 0.0           | 8.0                             | 3.4                               | 4.6                          | 4.6                           | 64.4                    | 69.0                    |
| 8               | -25.18         | 51          | 4.9       | 12,206                                 | 436                                   | 20.7                                   | 8.3                              | 46.2                    | 2.1           | 20.7                            | 5.5                               | 12.4                         | 6.9                           | 61.4                    | 73.8                    |
| 9               | -29,28         | 4.5         | 2.2       | 18                                     | 2                                     | -                                      | -                                | -                       | -             | -                               | -                                 | -                            | -                             | -                       | -                       |
| <i>b) MIS 2</i> |                |             |           |  |                                       |  |                                  |                         |               |                                 |                                   |                              |                               |                         |                         |
| 1               | -4.79          | 365         | 23.9      | 18,603                                 | 6,792                                 | 43.9                                   | 12.5                             | 14.2                    | 0.0           | 0.7                             | 0.0                               | 0.7                          | 0.5                           | 27.2                    | 28.0                    |
| 2               | -6.58          | 215         | 18.5      | 404,572                                | 115,012                               | 32.8                                   | 27.9                             | 14.6                    | 0.0           | 0.5                             | 0.0                               | 0.5                          | 0.5                           | 43.0                    | 43.5                    |
| 3               | -11.77         | 110         | 18.0      | 8,183                                  | 408                                   | 39.1                                   | 17.5                             | 32.1                    | 0.4           | 5.5                             | 0.0                               | 4.7                          | 2.2                           | 51.8                    | 56.6                    |
| 4               | -11.93         | 747         | 18.4      | 517,625                                | 25,286                                | 20.8                                   | 16.2                             | 48.5                    | 0.0           | 7.4                             | 0.0                               | 2.3                          | 1.7                           | 66.4                    | 68.7                    |
| 5               | -20.10         | 96          | 20.3      | 973                                    | 36                                    | 21.2                                   | 12.6                             | 41.9                    | 0.0           | 24.8                            | 3.6                               | 12.6                         | 7.7                           | 62.2                    | 74.8                    |
| 6               | -21.09         | 177         | 17.5      | 16,810                                 | 369                                   | 21.0                                   | 9.1                              | 49.5                    | 2.2           | 23.1                            | 0.0                               | 12.1                         | 7.1                           | 65.7                    | 77.8                    |
| 7               | -23.43         | 96          | 18.4      | 8,017                                  | 79                                    | 27.6                                   | 9.7                              | 37.0                    | 0.3           | 27.6                            | 6.2                               | 17.5                         | 8.8                           | 55.5                    | 73.1                    |
| 8               | -25.18         | 453         | 25.8      | 42,604                                 | 0                                     | 33.8                                   | 2.9                              | 27.3                    | 1.4           | 41.0                            | 9.4                               | 28.8                         | 7.2                           | 37.4                    | 66.2                    |
| 9               | -29,28         | 26          | ~18       | -                                      | -                                     | -                                      | -                                | -                       | -             | -                               | -                                 | -                            | -                             | -                       | -                       |

cont. Table 4.5. Pollen data.

| Site             | Latitude<br>°S | Depth<br>cm | Age<br>ka | Pollen AR<br>cnts/cm <sup>2</sup> /kyr | Spore AR<br>cnts/cm <sup>2</sup> /kyr | Woody plants<br>(C <sub>3</sub> )<br>% | Cyperaceae<br>(sedges etc.)<br>% | Poaceae<br>(grass)<br>% | Tribulus<br>% | Asteraceae<br>(composites)<br>% | Restionaceae<br>(cape reeds)<br>% | Asteroidaeae<br>undiff.<br>% | Periporates <sup>a</sup><br>% | Sum 1 <sup>b</sup><br>% | Sum 2 <sup>c</sup><br>% |
|------------------|----------------|-------------|-----------|--|---------------------------------------|--|----------------------------------|-------------------------|---------------|---------------------------------|-----------------------------------|------------------------------|-------------------------------|-------------------------|-------------------------|
| <i>c) MIS 5e</i> |                |             |           |  |                                       |  |                                  |                         |               |                                 |                                   |                              |                               |                         |                         |
| 1                | -4.79          | 1865        | 124       | 992                                    | 818                                   | 40.0                                   | 6.0                              | 7.2                     | 0.0           | 0.8                             | 0.0                               | 0.4                          | 0.0                           | 13.2                    | 13.6                    |
| 2                | -6.58          | 825         | 124       | 8,182                                  | 5,604                                 | 35.5                                   | 11.8                             | 8.0                     | 0.0           | 0.4                             | 0.0                               | 0.4                          | 0.2                           | 20.0                    | 20.4                    |
| 3                | -11.77         | 610         | 124       | 1,866                                  | 293                                   | 48.6                                   | 15.3                             | 19.8                    | 0.0           | 1.4                             | 0.0                               | 1.4                          | 1.4                           | 36.4                    | 37.8                    |
| 4                | -11.93         | 2803        | 121       | 112,532                                | 22,392                                | 26.8                                   | 10.2                             | 26.2                    | 0.0           | 2.3                             | 0.0                               | 1.3                          | 0.3                           | 36.6                    | 37.9                    |
| 5                | -20.10         | 395         | 121       | 232                                    | 39                                    | 6.1                                    | 12.2                             | 65.3                    | 0.0           | 4.1                             | 0.0                               | 2.0                          | 0.0                           | 77.6                    | 79.6                    |
| 6                | -21.09         | 1283        | 127       | 24,419                                 | 1,031                                 | 14.3                                   | 3.7                              | 66.0                    | 4.0           | 11.2                            | 0.6                               | 1.3                          | 7.1                           | 76.9                    | 78.2                    |
| 7                | -23.43         | 610         | 122       | 615                                    | 18                                    | 14.6                                   | 5.7                              | 60.4                    | 0.9           | 12.3                            | 3.8                               | 10.8                         | 3.8                           | 69.8                    | 80.7                    |
| 8                | -25.18         | 2632        | 124       | 237,216                                | 4,841                                 | 17.0                                   | 12.0                             | 47.0                    | 0.0           | 13.0                            | 3.0                               | 8.0                          | 4.0                           | 63.0                    | 71.0                    |
| 9                | -29.28         | 190         | 123       | -                                      | -                                     | -                                      | -                                | -                       | -             | -                               | -                                 | -                            | -                             | -                       | -                       |
| <i>d) MIS 6a</i> |                |             |           |  |                                       |  |                                  |                         |               |                                 |                                   |                              |                               |                         |                         |
| 1                | -4.79          | 1915        | 132       | 16,918                                 | 3,406                                 | 58.4                                   | 9.5                              | 12.7                    | 0.0           | 0.5                             | 0.0                               | 0.3                          | 0.0                           | 22.2                    | 22.4                    |
| 2                | -6.58          | 875         | 134       | 22,790                                 | 7,397                                 | 43.3                                   | 17.3                             | 12.6                    | 0.0           | 0.0                             | 0.0                               | 0.0                          | 0.0                           | 30.0                    | 30.0                    |
| 3                | -11.77         | 642         | 135       | 7,083                                  | 480                                   | 24.1                                   | 22.4                             | 40.7                    | 0.0           | 5.4                             | 0.0                               | 5.2                          | 1.3                           | 64.4                    | 69.6                    |
| 4                | -11.93         | 3413        | 147       | 354,882                                | 34,205                                | 14.3                                   | 18.1                             | 45.1                    | 0.3           | 3.0                             | 0.0                               | 2.7                          | 0.3                           | 63.5                    | 66.2                    |
| 5                | -20.10         | 456         | 137       | 116                                    | 3                                     | 20.7                                   | 6.9                              | 52.6                    | 0.0           | 20.7                            | 5.2                               | 12.9                         | 5.2                           | 64.7                    | 77.6                    |
| 6                | -21.09         | 1349        | 133       | 17,327                                 | 822                                   | 26.1                                   | 3.8                              | 49.5                    | 1.7           | 26.1                            | 1.0                               | 15.0                         | 6.6                           | 59.9                    | 74.8                    |
| 7                | -23.43         | 670         | 136       | 6,164                                  | 82                                    | 23.9                                   | 11.1                             | 32.0                    | 0.0           | 29.1                            | 4.9                               | 22.2                         | 10.8                          | 53.9                    | 76.1                    |
| 8                | -25.18         | 2951        | 139       | 52,446                                 | 364                                   | 40.7                                   | 4.1                              | 21.4                    | 0.0           | 47.6                            | 6.2                               | 26.2                         | 6.2                           | 31.7                    | 57.9                    |
| 9                | -29.28         | 211         | 137       | -                                      | -                                     | -                                      | -                                | -                       | -             | -                               | -                                 | -                            | -                             | -                       | -                       |

- = no data due to absence/low abundance of pollen.

<sup>a</sup> Sum of pollen of Caryophyllaceae, Chenopodiaceae, Amaranthaceae, Tribulus<sup>b</sup> Sum of periporates pollen and those of Cyperaceae, Poaceae<sup>c</sup> Ibid. plus pollen of Asteroideae undifferentiated



## 5 Summary and perspectives

In this thesis, the applicability of long-chain *n*-alkanes and *n*-alkan-1-ols as biomarkers to deduce the C<sub>4</sub> plant contribution to the vegetation was evaluated. As a first step, the plant waxes were analysed to validate the reliability of these components as C<sub>4</sub> plant proxies. Furthermore, the applicability was proven in Holocene sediment samples from a North to South transect along the southwest African continental margin. This transect parallels distinctive phytogeographic zones from C<sub>3</sub>-dominated vegetation types to C<sub>4</sub>-prevailing vegetation. In combination with pollen analyses of the same sediments, with known phytogeographic zones and known transport ways of organic material the biomarker signatures were checked on an almost continental scale. The proven reliability was then extended to reconstruct vegetation changes in the past during climatic variations of recent glacial/interglacial changes.

C<sub>4</sub> grasses appear to be the most important source of C<sub>4</sub> biomass in the geological record. Their distribution across the world in broad latitudinal belts is governed by climatic conditions of dry and arid tropical and subtropical areas. The C<sub>4</sub> grass subfamilial distribution is linked to the abundance of C<sub>4</sub> subtypes within them, which prefer different habitats of annual rainfall patterns (Schulze et al., 1996; Taub, 2000; Wan and Sage, 2001). Grasses of the subfamily Chloridoideae or grasses containing the C<sub>4</sub>-PCK or C<sub>4</sub>-NAD-ME subtypes thrive in extreme arid habitats. In such areas C<sub>3</sub> plants act with wide open stomata to counteract photorespiration. This reduces their water use efficiency dramatically. C<sub>4</sub> plants have more competitive success due to an adapted physiology, the CO<sub>2</sub> concentrating mechanism. Generally, the C<sub>3</sub> versus C<sub>4</sub> relationship in tropical and subtropical regions simply reflects the tree versus grass contribution to the vegetation. The extension or regression of tropical grasslands and savannas may hold important regional climatic information for the palaeoclimatic orientated scientist.

For validation, waxes of 35 C<sub>4</sub> grasses from the southern African grasslands and savannas and of three C<sub>3</sub> grasses from Peru and Australia were analysed for their carbon number distribution and stable carbon isotopic composition of long-chain *n*-alkanes (*n*-C<sub>27</sub> to *n*-C<sub>35</sub>) and *n*-alkanols (*n*-C<sub>22</sub> to *n*-C<sub>32</sub>). The investigated subspecies were chosen according to their abundance in southern Africa. Separated plant parts (flower, leaf, stem) of two grass species exhibit different homologue patterns, but the compound-specific isotopic composition seems to be unaffected. Significant amounts of shorter-chain *n*-alkanes in flower heads may have affected the whole-plant biomarker signature. *n*-Alkanol distribution patterns exhibited no systematics. The data are too limited to draw a

general conclusion and further investigations are required. The distinctive distribution patterns in plant parts may be the reason, why a chemotaxonomic relationship on a species level of whole grass samples was not successful.

The lipid data were separated in several groups by averaging on a photosynthetic, on a C<sub>4</sub>-subtype, and on a subfamilial level. At a preliminary state due to the limited number of samples, the C<sub>3</sub> grasses mainly contain the *n*-C<sub>29</sub> and *n*-C<sub>31</sub> alkanes and *n*-C<sub>26</sub> and *n*-C<sub>28</sub> alkanols. Their averaged weighted mean  $\delta^{13}\text{C}$  values are -33.8‰ and -26.7‰, respectively. For comparison, waxes of angiosperm C<sub>3</sub> trees collected in Japan and Thailand contain mainly the *n*-C<sub>29</sub> alkane (Chikaraishi and Naraoka, 2003). They may represent the second-most important group of biomarkers in the C<sub>3</sub> versus C<sub>4</sub> estimations. Wax signatures of C<sub>4</sub> grasses are distinguishable from those of C<sub>3</sub> species by high contents of *n*-C<sub>31</sub> and *n*-C<sub>33</sub> alkanes and the abundance of the *n*-C<sub>32</sub> alkanol, which is largely absent in C<sub>3</sub> grasses. The dominant *n*-alkanes and *n*-alkanols in the C<sub>4</sub> species are each characterised by consistently heavier  $\delta^{13}\text{C}$  values of circa -22‰. Especially chloridoid C<sub>4</sub> grasses or the species containing the NAD-ME or PCK C<sub>4</sub>-subtype, which thrive in extreme arid habitats, exhibited a longer averaged chain length of the wax homologues. This suggested that these C<sub>4</sub> species are adapted to warm and dry tropical environmental conditions by higher melting points of their waxes. Averaged bibliographic data of *n*-alkanes and *n*-alkanols of grass waxes substantiated the obtained results for C<sub>3</sub> and C<sub>4</sub> grass waxes. A hierarchical cluster analysis of bibliographic and the data of this study exhibit nearly the same subfamilial separation for *n*-alkanes compared to the postulated evolutionary sequence of grass subfamilies (Clayton and Renvoize, 1986). The *n*-alkanol clusters coincide with the phylogeny of grasses (Grass Phylogeny Working Group, 2001). An evolutionary adaptive role of leaf waxes appears to be certain but requires further investigations. Overall, in terms of palaeoenvironmental studies of soils, lake and marine sediments, the distribution and isotopic characteristics of *n*-alkanes and *n*-alkanols constitute useful biomarker proxies for the C<sub>4</sub>-dominated tropical and subtropical grasslands.

Wax lipids may be provided to ocean sediments directly from vegetation by wind- or river-transported plant detritus, by ablation, by natural and anthropogenic burning, and indirectly by deflation of dust particles from dry pans and semi-desert areas. Seasonal burning occurs in the investigation area, when savanna biomass, especially the grass layer, is turned into highly flammable material during senescence of plants in the dry season of the austral winter (e.g. Andreae et al., 1996; Barbosa et al., 1999). For palaeoclimatic studies this implies that seasonality and mode of transportation of plant material have to be considered. It has been reported that senescent grasses lose their flower heads and this affects the *n*-alkane signature of a whole plant (cf. Smith et al.,

2001). Hence, airborne organic matter originating from grasslands may be depleted in flower wax signatures. However, it is difficult to estimate the flower versus leaf biomarker ratio, which is transported to oceanic sediments. This calls for caution in palaeoclimatic assessments.

In southwestern Africa, offshore winds occurring during the austral winter season coincide in time with seasonal surface fires and dust storms abrading leaf waxes. The winds transport the generated aerosols and plant detritus to oceanic sediments. Hence, airborne particulate material derived from the western and central South African hinterland dominated by deserts, semi-deserts and savanna regions are rich in organic matter from  $C_4$  plants.

Near-surface, marine sediments of late Holocene age at nine core sites were recovered during ODP Leg 175 and METEOR M6/6 and M20/2 cruises along the southwest African continent from the Congo Fan to the Cape Basin. They were used to evaluate the land plant signatures in marine sediments. Compound-specific isotopic signatures of long-chain  $n$ -alkanes and  $n$ -alkanols can be correlated with concentrations and distributions of pollen and spores taxa in the same sediments. Fluxes or accumulation rates of lipid and pollen data are roughly proportional to each other and reflect common continental source regions and transport processes. Higher values are seen at sites off the Congo River, at near-coastal sites and at sites situated in the path of the aerosol plumes derived from the arid and semi-arid areas.

$n$ -Alkanes may be influenced by a contribution of petroleum hydrocarbons. The long-chain  $n$ -alkanols have the advantage of not being influenced. In the transect samples the ACL values of  $n$ -alkanes increase from 29.92 to 30.83 from North to South accompanied by a shift towards positive  $\delta^{13}C$  values from -35‰ to -25‰ and towards higher percentages of  $C_4$  plant pollen (approximately 7% to 60%). Similar trends are generally evident for the isotopic data of  $n$ -alkanols, but not for their ACL values. The alkanol patterns appear to be comprised of different assemblages of  $n$ -alkanol envelopes, corresponding to contributions from different groups of organisms ( $C_4$ ,  $C_3$ , and CAM land plants and marine biota). Generally, the molecular isotope signature of sedimentary lipids is not as constantly distributed among the homologues as found for the  $C_4$  and  $C_3$  grasses. This implies mixtures of  $C_3$  and  $C_4$  (CAM) plant wax signatures and a potential contribution of aquatic organisms.  $C_4$  plant estimates based on weighted mean  $\delta^{13}C$  values for  $n$ -alkanes and  $n$ -alkanols parallel each other and those afforded by pollen counts. All show a north to south trend. Lowest values were found in the region of the Congo, because today's Congo River catchment area is dominated by tropical rain forest (mainly  $C_3$  plants). The highest values occur off Namibia, where both temperature and aridity lead to a dominance of grasslands and savannas. The increased  $C_4$  plant contributions is

probably related in higher contribution of grasses. Hence, the transect data of oceanic sediments broadly parallel the present-day distribution of C<sub>3</sub> and C<sub>4</sub> vegetation of the source areas of the adjacent continent.

The information archived in the Holocene transect was extended to the recent geological history by investigation of sediment samples representing two glacial (Last Glacial Maximum, MIS 2, and penultimate glacial, MIS 6a) and two interglacial stages (Holocene, MIS 1, and Eemian, MIS 5e) from the same nine sites. Changes in continental phytogeographic zones relating to warm and cold stages were reconstructed using the same approach by lipid and pollen analyses. As it can be expected from the present and glacial positions of phytogeographic zones, the carbon isotopic signature of the *n*-alkanes and *n*-alkanol shows an enrichment of <sup>13</sup>C from North to South. Distinct differences were found in the patterns between glacials and interglacials. Generally, the latitudinal trends in the lipid and pollen data exhibit the same trends from North to South in all four time slices. The trends exhibit heavier δ<sup>13</sup>C values accompanied by longer-chain homologues and a higher C<sub>4</sub> pollen contribution. Glacial/interglacial changes are characterised by a shift of up to 25% to higher C<sub>4</sub> contribution in the northern part of the transect during glacial stages. Southward, the glacial/interglacial differences decrease and become negligible at the southernmost sites. Less Poaceae pollen and a higher contribution of C<sub>3</sub> pollen during glacial stages suggest a regional northward shift of the South African C<sub>3</sub> vegetation. It is inferred from these data that the open grass-rich vegetation on the southern African continent shifted northwards during glacial stages. Desert and semi-desert areas increased, and the winter rain vegetation occurred much further northward than during interglacial stages.

Uncertainties may occur in the interpretation of the results of the sediment data. The pollen assessments may be overestimated because C<sub>4</sub> plants produce more pollen than most C<sub>3</sub> plants. Furthermore, the taxa used for the C<sub>4</sub>/CAM estimate contain C<sub>3</sub> species as well. The interpretation of lipid data neglects the contribution of CAM plants, potential contribution of aquatic organisms as well as stable carbon isotopic variations of the plant signature due to interglacial/glacial cycles in δ<sup>13</sup>CO<sub>2</sub> and *p*CO<sub>2</sub>. Another reason may be the higher production of waxes by drought resistant C<sub>4</sub> and CAM plants. The potential contribution from aquatic organisms is unclear, although several studies have reported a low contribution of long-chain homologues to the investigated carbon-number range of *n*-alkanes and *n*-alkanols (e.g. Stránský et al., 1968; Davis, 1968; Blumer et al., 1971; Youngblood et al., 1971; Nishimoto, 1974b; Nichols et al., 1982; Nichols and Johns, 1985; Chikaraishi and Naraoka, 2003). In this project an endmember of molecular carbon isotopic composition of -35‰ for C<sub>3</sub> plants growing in a closed canopy and -20‰ for C<sub>4</sub> plants growing in open habitats is assumed in the assessment of C<sub>3</sub>/C<sub>4</sub> plant contribution

by the source vegetation. However, a difference of 3.3‰ to more negative values were reported within the same C<sub>3</sub> plant species when going from open to closed canopies (Ehleringer et al., 1987; Ehleringer and Monson, 1993). Therefore, typically isotopic key data for C<sub>3</sub> and C<sub>4</sub> plants growing in a savanna or forest vegetation are fundamentally important in palaeoclimatic assessments. Subsequent investigations should elaborate the mentioned lack of knowledge about source organisms contributing *n*-alkanes and *n*-alkanols to the sediments and factors affecting the biomarker signatures. The results of this project broadly suggest that a combination of lipid biomarker distribution, compound-specific isotope proxies, and pollen data can be applied in the reconstruction of past continental phytogeographic developments.

## 6 References

- Ali, H.A.M., 2003. The potential use of some plant wax compounds as faecal markers to measure the botanical composition of herbivore diets. PhD thesis, University of Aberdeen.
- Andreae, M. O., Anderson B. E., Blake D. R., Bradshaw, J. D., Collins, J. E., Gregory, G. L., Sachse, G. W., Shipham, M. C., 1994. Influence of plumes from biomass burning on atmospheric chemistry over the equatorial Atlantic during CITE-3. *Journal Geophysical Research* 99, 12,793-12,808.
- Andreae, M.O., Atlas, E., Cachier, H., Cofer III, W.R., Harris, G.W., Helas, G., Koppmann, R., Lacaux, J.-P., Ward, D.E., 1996. Trace gas and aerosol emissions from savannah fires. *Biomass Burning and Global Change* 1, 278-295.
- Andreae, M. O., Andreae, T. W., Annegarn, H., Beer, J., Cachier, H., le Canut, P., Elbert, W., Maenhaut, W., Salma, I., Wienhold, F. G., Zenker, T., 1998. Airborne studies of aerosol emissions from savanna fires in southern Africa: 2. Aerosol chemical composition. *Journal of Geophysical Research* 103, 32,119-32,128.
- Anhuf, D., 1997. Paleovegetation in West Africa for 18,000 B.P. and 8,500 B.P. *Eiszeitalter und Gegenwart* 47, 112-119.
- Arens, N.C., Jahren, A.H., Amundson, R., 2000. Can C<sub>3</sub> plants faithfully record the carbon isotopic composition of the atmospheric carbon dioxide? *Paleobiology* 26, 137-164.
- Avato, P., Bianchi, G., Salamini, F., 1987. Ontogenetic variations in the chemical composition of maize surface lipids. In: Stumpf, P.K., Mudd, J.B., Nes, W.D. (Eds.), *The Metabolism, Structure, and Function of Plant Lipids*. Plenum Press, New York, pp. 549-551.
- Avato, P., Bianchi, G., Pogna, N., 1990. Chemosystematics of surface lipids from maize and some related species. *Phytochemistry* 29, 1571-1576.
- Baker, E.A., 1974. The influence of environment on leaf wax development in *Brassica oleracea* var. *gemmifera*. *The New Phytologist* 73, 955-966.
- Baker, E.A., 1982. Chemistry and morphology of plant epicuticular waxes. In: Cutler, D.F., Alvin, K.L., Price, C.E., (Eds.), *The Plant Cuticle*. Linnean Society Symposium Series Vol. 10, London, pp. 139-165.
- Baker, E.A., Procopiou, J., 1980. Effect of soil moisture status on leaf surface wax yield of some drought resistant species. *Journal of Horticultural Science* 55, 85-87.
- Barbosa, P.M., Stroppiana, D., Grégoire, J.-M., Pereira, J.M.C., 1999. An assessment of vegetation fire in Africa (1981-1991): Burned areas, burned biomass, and atmospheric emissions. *Global Biogeochemical Cycles* 13, 933-950.
- Bayer, A.W., 1959. The ecology of grasslands. In: Meredith, D. (Ed.), *The Grasses and Pastures of South Africa*, Second Impression. Central News Agency, pp. 539-550.
- Beerling, D.J., Royer, D.L., 2002. Fossil plants as indicators of the Phanerozoic global carbon cycle. *Annual Review of Earth and Planetary Science* 30, 527-556.
- Bender, M., 1968. Mass spectrometric studies of carbon 13 variations in corn and other grasses. *Radiocarbon* 10, 469-472.
- Berger, A.L., 1978. Long-term variations of caloric insolation resulting from the Earth's orbital elements. *Quaternary Research* 9, 139-167.

- Berner, R.A., 1993. Paleozoic Atmospheric CO<sub>2</sub>: importance of solar radiation and plant evolution. *Science* 261, 68-70.
- Bianchi, G., 1995. Plant waxes. In: Hamilton, R.J. (Ed.), *Waxes: Chemistry, Molecular Biology and Functions*. The Oil Press, Dundee, 175-222.
- Bianchi, G., Avato, P., Scarpa, O., Murelli, C., Audisio, G., Rossini, A., 1989. Composition and structure of maize epicuticular wax esters. *Phytochemistry* 28, 167-171.
- Bird, M. I., Pousai, P., 1997.  $\delta^{13}\text{C}$  variations in the surface soil organic carbon pool. *Global Biogeochemical Cycles* 11, 313-322, 1997.
- Björkman, O., 1976. Adaptive and genetic aspects of C<sub>4</sub> photosynthesis. In: Burris, R.H., Black, C.C. (Eds.), *Metabolism and Plant Productivity*. University Park Press, Baltimore, pp. 287-309.
- Björkman, O., Berry, J., 1973. High-efficiency photosynthesis. *Scientific American* 229, 80-93.
- Blumer, M., Guillard, R.R.L., Chase, T., 1971. Hydrocarbons of marine phytoplankton. *Marine Biology* 8, 183-189.
- Boadi, D.A., Moshtaghi Nia, S.A., Wittenberg, K.M., McCaughey, W.P., 2002. The *n*-alkane profile of some native and cultivated forages in Canada. *Canadian Journal of Animal Science* 82, 465-469.
- Bond, W.J., van Wilgen, B.W., 1996. *Fire and Plants. Population and Community Biology Series 14*, Chapman and Hall, London.
- Bond, W.J., Midgley, G.F., Woodward, F.I., 2003. The importance of low atmospheric CO<sub>2</sub> and fire in promoting the spread of grasslands and savannas. *Global Change Biology* 9, 973-982.
- Boom, A., 2004. A geochemical study of lacustrine sediments: towards palaeo-climatic reconstructions of high Andean biomes in Colombia. PhD thesis, University of Amsterdam.
- Boom, A., Mora, G., Cleef, A.M., Hooghiemstra, H., 2001. High altitude C<sub>4</sub> grasslands in the northern Andes: relicts from glacial conditions? *Review of Palaeobotany and Palynology* 115, 147-160.
- Boom, A., Marchant, R., Hooghiemstra, H., Sinninghe Damsté, J.S., 2002. CO<sub>2</sub>- and temperature-controlled altitudinal shifts of C<sub>4</sub>- and C<sub>3</sub>-dominated grasslands allow reconstruction of palaeoatmospheric *p*CO<sub>2</sub>. *Palaeogeography, Palaeoclimatology, Palaeoecology* 177, 151-168.
- Bourliere, F., 1983. *Tropical Savannas*. Elsevier, Amsterdam.
- Bray, E.E., Evans, E.D., 1961. Distribution of *n*-paraffins as a clue to recognition of source beds. *Geochimica et Cosmochimica Acta* 22, 2-15.
- Budavari, S. (Ed.), 1991. *The Merck Index: An Encyclopedia of Chemicals, Drugs, and Biologicals*, 11th ed., 3rd print., Merck and Company, Rahway, NJ.
- Cacho, I., Grimalt, J. O., Canals, M., Sbaifi, L., Shackleton, N. J., Schönfeld, J., Zahn, R., 2001. Variability of the western Mediterranean Sea surface temperature during the last 25,000 years and its connection with the Northern Hemisphere climatic changes. *Paleoceanography* 16, 40-52.
- Camberlin, P., Janicot, S., Poccard, I., 2001. Seasonality and atmospheric dynamics of the teleconnection between African rainfall and tropical sea-surface temperature. Atlantic vs. ENSO. *International Journal of Climatology* 21, 973-1005.
- Cerling, T.E., Wang, Y., Quade, J., 1993. Expansion of C<sub>4</sub> ecosystems as an indicator of global ecological change in the late Miocene. *Nature* 361, 344-345.

- Cerling, T.E., Harris, J.M., MacFadden, B.J., Leakey, M.G., Quade, J., Eisenmann, V., Ehleringer, J.R., 1997. Global vegetation change through the Miocene/Pliocene boundary. *Nature* 389, 153-158.
- Chen, W., Lefroy, R.D.B., Scott, J.M., Blair, G.J., 1998. Field variations in alkane signatures among plant species in 'degraded' and perennial pastures on the Northern Tablelands of New South Wales. *Australian Journal of Agriculture Research* 49, 263-268.
- Chester, R., Elderfield, H., Griffin, J. J., Johnson, L. R., Padgham, R. C., 1972. Eolian dust along the eastern margins of the Atlantic Ocean. *Marine Geology* 13, 91-106.
- Chiapello, I., Bergametti, G., Chatenet, B., Dulac, F., Jankowiak, I., Liousse, C., Soares, E. S., 1999. Contribution of the different aerosol species to the aerosol mass load and optical depth over the northeastern tropical Atlantic. *Journal of Geophysical Research* 104, 4025-4035.
- Chibnall, A.C., Piper, S.H., Pollard, A., Williams, E.F., Sahai, P.N., 1934. The constitution of the primary alcohols, fatty acids and paraffins present in plant and insect waxes. *Biochemical Journal* 28, 2189-2208.
- Chikaraishi, Y., Naraoka, H., 2003. Compound-specific  $\delta D$ - $\delta^{13}C$  analyses of *n*-alkanes extracted from terrestrial and aquatic plants. *Phytochemistry* 63, 361-371.
- Clayton, W.D., Renvoize, S.A., 1986. *Genera Graminum – Grasses of the World*. Kew Bulletin Additional Series XIII, London: Her Majesty's Stationery Office.
- Collatz, G.J., 1977. Influence of certain environmental factors on photosynthesis and photorespiration in *Simmondsia chinensis*. *Planta* 134, 127-132.
- Collatz, G.J., Berry, J.A., Clark, J.S., 1998. Effects of climate and atmospheric CO<sub>2</sub> partial pressure on the global distribution of C<sub>4</sub> grasses: present, past, and future. *Oecologia* 114, 441-454.
- Collister, J.W., Rieley, G., Stern, B., Eglinton, G., Fry, B., 1994. Compound-specific  $\delta^{13}C$  analyses of leaf lipids from plants with differing carbon dioxide metabolisms. *Organic Geochemistry* 21, 619-627.
- Conte, M.H., Weber, J.C., 2002a. Long-range atmospheric transport of terrestrial biomarkers to the western North Atlantic. *Global Biogeochemical Cycles* 16, No. 4, 1142, doi:10.1029/2002GB001922.
- Conte, M.H., Weber, J.C., 2002b. Plant biomarkers in aerosol record isotopic discrimination of terrestrial photosynthesis. *Nature* 417, 639-641.
- Conte, M.H., Weber, J.C., Carlson, P.J., Flanagan, L.B., 2003. Molecular and carbon isotopic composition of leaf wax in vegetation and aerosols in a northern prairie ecosystem. *Oecologia* 135, 67-77.
- Coupland, R. T., 1992. Approach and generalizations. In: Coupland, R.T. (Ed.), *Ecosystems of the World 8A, Natural Grassland, Introduction and Western Hemisphere*. Elsevier, New York, pp. 1-6.
- Cowling, R.M., Richardson, D.M., Pierce, S.M. (Eds.), 1997. *Vegetation of Southern Africa*, Cambridge University Press, New York.
- Cranwell, P.A., 1973. Chain-length distribution of *n*-alkanes from lake sediments in relation to post-glacial environmental change. *Freshwater Biology* 3, 259-265.
- Cranwell, P.A., 1981. Diagenesis of free and bound lipids in terrestrial detritus deposited in a lacustrine sediment. *Organic Geochemistry* 3, 79-89.
- Cross, R.A., 1980. Distribution of subfamilies of Gramineae in the old world. *Kew Bulletin* 35, 279-289.



- Davis, J.B., 1968. Paraffinic hydrocarbons in the sulphate-reducing bacterium *Desulfovibrio desulfuricans*. *Chemical Geology* 3, 155-160.
- Dawson, L.A., Mayes, R.W., Elston, D.A., Smart, T.S., 2000. Root hydrocarbons as potential markers for determining species composition. *Plant, Cell and Environment* 23, 743-750.
- de la Harpe, A.C., Visser, J.H., Grobbelaar, N., 1981. Photosynthetic characteristics of some African parasitic flowering plants. *Zeitschrift für Pflanzenphysiologie* 103, 265-275.
- Delgado, D.C., Olivera, M.C., Navarro, A., 2000. Composition of cuticular *n*-alkanes in tropical plants. Their potential as markers to estimate consumption and selection of grazing ruminants. *Cuban Journal of Agricultural Science* 34, 147-152.
- DeLucia, E.H., Schlesinger, W.H., Billings, W.D., 1988. Water relation and the maintenance of Sierran conifers on hydrothermally altered rock. *Ecology* 69, 303-323.
- Dengler, N.G., Nelson, T., 1999. Leaf structure and development in C<sub>4</sub> plants. In: Sage, R.F., Monson, R.K. (Eds.), *C<sub>4</sub> Plant Biology*. Academic Press, San Diego, pp. 133-172.
- Dodd, R.S., Afzal-Rafii, Z., 2000. Habitat-related adaptive properties of plant cuticular lipids. *Evolution* 54, 1438-1444.
- Dove, H., 1992. Using the *n*-alkanes of plant cuticular wax to estimate the species composition of herbal mixtures. *Australian Journal of Agriculture Research* 43, 1711-1724.
- Dove, H., Mayes, R.W., 1991. The use of plant wax alkanes as marker substances in studies of the nutrition of herbivores: a review. *Australian Journal of Agriculture Research* 42, 913-952.
- Dove, H., Milne, J.A., Mayes, R.W., 1990. Comparison of herbage intakes estimated from in vitro or alkane-based digestibilities. *Proceedings of the New Zealand Society of Animal Production* 50, 457-459.
- Dove, H., Mayes, R.W., Freer, M., 1996. Effects of species, plant part, and plant age on the *n*-alkane concentrations in the cuticular wax of pasture plants. *Australian Journal of Agriculture Research* 47, 1333-1347.
- Downes, R.W., 1969. Differences in transpiration rate between tropical and temperate grasses under controlled conditions. *Planta* 88, 261-273.
- Downton, J.S., 1975. The occurrence of C<sub>4</sub> photosynthesis among plants. *Photosynthetica* 9, 96-105.
- Dupont, L. M., Wyputta, U., 2003. Reconstructing pathways of aeolian pollen transport to the marine sediments along the coastline of SW Africa. *Quaternary Science Reviews* 22, 157-174.
- Dupont, L., Jahns, S., Marret, F., Ning, S., 2000. Vegetation change in equatorial West Africa: time-slices for the last 150 ka. *Palaeogeography, Palaeoclimatology, Palaeoecology* 155, 95-122.
- Dupont, L. M., Donner, B., Schneider, R., Wefer, G., 2001. Mid-Pleistocene environmental change in tropical Africa began as early as 1.05 Ma. *Geology* 29, 195-198.
- Edwards, G.E., Nakamoto, H., Burnell, J.N., Hatch, M.D., 1985. Pyruvate, Pi dikinase and NADP-malate dehydrogenase in C<sub>4</sub> photosynthesis – properties and mechanism of light/dark regulation. *Annual Reviews of Plant Physiology* 36, 255-286.
- Eglinton, G., Hamilton, R., 1967. Leaf epicuticular waxes. *Science* 156, 1322-1335.

- Eglinton, T.I., Eglinton, G., Dupont, L., Sholkovitz, E.R., Montlucon, D., Reddy, C.M., 2002. Composition, age, and provenance of organic matter in NW African dust over the Atlantic Ocean. *Geochemistry, Geophysics, Geosystems* 3 (8), 1050, doi: 10.1029/2001GC000269
- Ehleringer, J.R., Monson, R.K., 1993. Evolutionary and ecological aspects of photosynthetic pathway variation. *Annual Review of Ecology and Systematics* 24, 411-439.
- Ehleringer, J.R., Lin, Z.F., Field, C.B., Sun, G.C., Kuo, C.Y., 1987. Leaf carbon isotope ratios of plants from a subtropical monsoon forest. *Oecologia* 72, 109-114.
- Ehleringer, J.R., Cerling, T.E., Helliker, B.R., 1997. C<sub>4</sub> photosynthesis, atmospheric CO<sub>2</sub>, and climate. *Oecologia* 112, 285-299.
- Ellis, R.P., 1977. Distribution of the Krantz syndrome in the southern African Eragrostoideae and Panicoideae. *Agroplanatae* 9, 73-110.
- Ellis, R.P., Vogel, J.C., Fuls, A., 1980. Photosynthetic pathways and the geographical distribution of grasses in South West Africa/Namibia. *South African Journal of Science* 76, 307-314.
- Elmore, C.D., Paul, R.N., 1983. Composite list of C<sub>4</sub> weeds. *Weed Science* 31, 686-692.
- Fairbanks, R.G., 1989. A 17,000-year glacio-eustatic sea level record: influence of glacial melting rates on the Younger Dryas event and deep-ocean circulation. *Nature* 342, 637-642.
- Farquhar, G.D., 1983. On the nature of carbon isotope discrimination in C<sub>4</sub> species. *Australian Journal of Plant Physiology* 10, 205-226.
- Farquhar, G.D., O'Leary, M.H., Berry, J.A., 1982. On the relationship between carbon isotope discrimination and the intercellular carbon dioxide concentration in leaves. *Australian Journal of Plant Physiology* 9, 121-137.
- Farquhar, G.D., Ehleringer, J.R., Hubick, K.T., 1989. Carbon isotope discrimination and photosynthesis. *Annual Review of Plant Physiology and Plant Molecular Biology* 40, 503-537.
- Faure, K., Dewit, M.J., Willis, J.P., 1995. Late Permian global coal hiatus linked to <sup>13</sup>C-depleted CO<sub>2</sub> flux into the atmosphere during the final consolidation of Pangea. *Geology* 23, 507-510.
- Ficken, K.J., Street-Perrott, R.A., Perrott, R.A., Swain, D.L., Olago, D.O., Eglinton, G., 1998. Glacial/interglacial variations in carbon cycling revealed by molecular and isotope stratigraphy of Lake Nkunga, Mt. Kenya, East Africa. *Organic Geochemistry* 5-7, 1701-1719.
- Fontugne, M.R., Duplessy, J.-C., 1981. Organic carbon isotopic fractionation by marine plankton in the temperature range -1 to 31°C. *Oceanologica Acta* 4, 85-90.
- Fredlund, G.G., Tieszen, L.L., 1997. Calibrating grass phytolith assemblages in climatic terms: Application to late Pleistocene assemblages from Kansas and Nebraska. *Palaeogeography, Palaeoclimatology, Palaeoecology* 136, 199-211.
- Friedli, H., Lotscher, H., Oeschger, H., Siegenthaler, U., Stauffer, B., 1986. Ice core record of the <sup>13</sup>C/<sup>12</sup>C of atmospheric CO<sub>2</sub> in the past two centuries. *Nature* 324, 237-238.
- Frost, P.G., Robertson, F., 1987. The ecological effects of fire in savannas. In: Walker, B.H. (Ed.), *Determinants of tropical savannas*. IRL Press, Oxford, pp. 93-140.
- Gagosian, R.B., Peltzer, E.T., 1986. The importance of atmospheric input of terrestrial organic matter to deep sea sediments. In: Leythaeuser, D., Rullkötter, J. (Eds.), *Advances in Organic Geochemistry 1985*. Pergamon Press, Oxford, pp. 661-669.

- Ghannoum, O., von Caemmerer, S., Conroy, J.P., 2001. Carbon and water economy of Australian NAD-ME and NADP-ME C<sub>4</sub> grasses. *Australian Journal of Plant Physiology* 28, 213-223.
- Gibbs, A., 1995. Physical properties of insect cuticular hydrocarbons: model mixtures and lipid interactions. *Comparative Biochemistry and Physiology B* 122, 667-672.
- Gibbs, A.G., 2002. Lipid melting and cuticular permeability: new insights into an old problem. *Journal of Insect Physiology* 48, 391-400.
- Gibbs Russell, G.E., 1988. Distribution of subfamilies and tribes of Poaceae in southern Africa. *Modern systematic studies in African botany. Monographs in Systematic Botany from the Missouri Botanical Garden* 25, 555-566.
- Gibbs Russell, G.E., Watson, L., Koekemoer, M., Smook, L., Barker, N.P., Anderson, M.J., Dallwitz, M.J., 1991. Grasses of Southern Africa. *Memoirs of the Botanical Survey No. 58*, Botanical Research Institute of South Africa.
- Gillon, D., 1983. The fire problem in tropical savannas. In: Bourlière, F. (Ed.), *Tropical Savannas*. Elsevier, Amsterdam, pp. 617-641.
- Gingele, F. X., 1995. Holocene climatic optimum in Southwest Africa - evidence from the marine clay mineral record. *Palaeogeography, Palaeoclimatology, Palaeoecology* 122, 77-87.
- Gingele, F. X., Müller, P. M., Schneider, R. R., 1998. Orbital forcing of freshwater input in the Zaire Fan area: clay mineral evidence from the last 200 kyr. *Palaeogeography, Palaeoclimatology, Palaeoecology* 138, 17-26.
- Giussani L.M., Cota-Sánchez, J.H., Zuloaga, F.O., Kellogg, E.A., 2001. A molecular phylogeny of the grass subfamily Panicoideae (Poaceae) shows multiple origins of C<sub>4</sub> photosynthesis. *American Journal of Botany* 88, 1993-2012.
- Grass Phylogeny Working Group, 2001. Phylogeny and subfamilial classification of the grasses (Poaceae). *Annals of the Missouri Botanical Garden* 88, 373-457.
- Grazzini, C.V., Saliège, J.F., Urrutiaguer, M.J., Iannace, A., 1990. Oxygen and carbon isotope stratigraphy of the ODP hole 653A and site 654: the Pliocene-Pleistocene glacial history recorded in the Tyrrhenian Basin (west Mediterranean). *Scientific Results of the Ocean Drilling Program* 107, 361-386.
- Gröcke, D.R., Price, G.D., Ruffel, A.H., Mutterlose, J., Baraboshkin, E., 2003. Isotopic evidence for Late Jurassic-Early cretaceous climate change. *Palaeogeography, Palaeoclimatology, Palaeoecology* 202, 97-118.
- Guilderson, T.P., Fairbanks, R.G., Rubenstone, J.L., 1994. Tropical temperature variations since 20,000 years ago: modulating interhemispheric climate change. *Science* 263, 663-665.
- Gülz, P.-G., 1994. Epicuticular leaf waxes in the evolution of the plant kingdom. *Journal of Plant Physiology* 143, 453-464.
- Güntner, U., 2000. Geochemische Signale in Tiefseesedimenten des südwestafrikanischen Kontinentalrands: Indikatoren für paläoklimatische und paläoozeanographische Bedingungen. Dissertation, University of Oldenburg.
- Hao, W.M., Liu, M.-H., 1994. Spatial and temporal distribution of tropical biomass burning. *Global Biogeochemical Cycles* 8, 495-503.
- Hartly, W., 1950. The global distribution of tribes of the Gramineae in relation to historical and environmental factors. *Australian Journal of Agriculture Research* 1, 355-373.
- Hatch, M.D., 1987. C<sub>4</sub> photosynthesis: a unique blend of modified biochemistry, anatomy and ultra structure. *Biochimica et Biophysica Acta* 895, 81-106.

- Hatch, M.D., Slack, C.R., 1966. Photosynthesis by sugarcane leaves. A new carboxylation reaction and the pathway of sugar formation. *Biochemical Journal* 101, 103-111.
- Hatch, M.D., Slack, C.R., Johnson, H.S., 1967. Further studies on a new pathway of photosynthetic carbon dioxide fixation in Sugar-Cane and its occurrence in other plant species. *Biochemical Journal* 102, 417-422.
- Hatch, M.D., Kagawa, T., Craig, S., 1975. Subdivision of C<sub>4</sub> pathway species based on differing C<sub>4</sub> acid decarboxylating systems and ultrastructural features. *Australian Journal of Plant Physiology* 2, 111-128.
- Hattersley, P.W., 1982.  $\delta^{13}\text{C}$  values of C<sub>4</sub> types of grasses. *Australian Journal of Agriculture Research* 9, 139-154.
- Hattersley, P.W., 1987. Variations in photosynthetic pathway. In: Soderstrom, T.R., Hilu, K.W., Campbell, C.D.S., Barkworth, M. E. (Eds.), *Grass Systematics and Evolution*. Smithsonian Institution Press, Washington, DC, pp. 49-64.
- Hattersley, P.W., Watson, L., 1992. Diversification of photosynthesis. In: Chapman, G.P. (Ed.), *Grass Evolution and Domestication*. Cambridge University Press, Cambridge, pp. 38-116.
- Hayes, J.M., 1993. Factors controlling  $^{13}\text{C}$  contents of sedimentary organic compounds: Principles and evidence. *Marine Geology* 113, 111-125.
- Herman, J. R., Bhartia, P. K., Torres, O., Hsu, N. C., Seftor, C. J., Celarier, E., 1997. Global distribution of UV-absorbing aerosols. *Journal of Geophysical Research* 102, 16,911-16,922.
- Hinrichs, K.-U., Rinna, J., Rullkötter, J., 1997. Late Quaternary palaeoenvironmental conditions indicated by marine and terrestrial molecular biomarkers in sediments from the Santa Barbara basin. In: Wilson, R.C., Tharp, V.L. (Eds.), *Proceedings of the Fourteenth Annual Pacific Climate (PACLIM) Workshop*, Interagency Ecology Program, Technical Report no. 57, California Department of Water Resources, Sacramento (CA), pp. 125-134.
- Hinrichs, K.-U., Schneider, R. R., Müller, P. J., Rullkötter, J., 1999. A biomarker perspective on paleoproductivity variations in two Late Quaternary sediment sections from the Southeast Atlantic Ocean. *Organic Geochemistry* 30, 341-366.
- Hovland, M., Judd, A. G., 1988. *Seabed Pockmarks - Impact on Geology, Biology and Marine Environment*. Graham & Trotman, London.
- Hsu, N. C., Herman, J. R., Bhartia, P. K., Seftor, C. J., Thompson, A. M., Gleason, J. F., Eck, T. F., Holben, B. N., 1996. Detection of biomass burning smoke from TOMS measurements. *Geophysical Research Letters* 23, 745-748.
- Hu, J., Peng, P., Jia, G., Fang, D., Zhang, G., Fu, J., Wang, P., 2002. Biological markers and their carbon isotopes as an approach to the paleoenvironmental reconstruction of Nansha area, South China Sea, during the last 30 ka. *Organic Geochemistry* 33, 1197-1204.
- Huang, Y., Dupont, L.M., Sarnthein, M., Hayes, J.M., Eglinton, G., 2000. Mapping of C<sub>4</sub> plant input from North West Africa into North East Atlantic sediments. *Geochimica et Cosmochimica Acta* 64, 3505-3513.
- Huang, Y., Street-Perrott, F. A., Metcalfe, S. E., Brenner, M., Moreland, M., Freeman K. H., 2001. Climate change as the dominant control on glacial-interglacial variations in C<sub>3</sub> and C<sub>4</sub> plant abundance. *Science* 293, 1647-1651.
- Husar, R. B., Prospero, J. M., Stowe, L. L., 1997. Characterization of tropospheric aerosols over the oceans with the NOAA advanced very high resolution radiometer optical thickness operational product. *Journal of Geophysical Research* 102, 16,889-16,909.

- Huntley, B.J., Walker, B.H., 1982. *Ecology of Tropical Savannas*. Springer, Berlin.
- Imbrie, J., Hays, J.D., Martinson, D.G., McIntyre, A., Mix, A.C., Morley, J.J., Pisias, N.G., Prell, W.L., Shackleton, N.J., 1984. The orbital theory of Pleistocene climate: support from a revised chronology of marine  $\delta^{18}\text{O}$  record. In: Berger, A.L., Imbrie, J., Hays, J., et al. (Eds.), *Milankovitch and Climate Part 1. Series C: Mathematical and Physical Science*. Reidel Publishing Company, Dordrecht, pp. 269-305.
- Jacobs, B.F., Kingston, J.D., Jacobs, L.L., 1999. The origin of grass-dominated ecosystems. *Annals of the Missouri Botanical Garden* 86, 590-643.
- Jansen, J.H.F., van Weering, T.C.E., Gieles, R., van Iperen, J., 1984. Middle and Late Quaternary oceanography and climatology of the Zaire-Congo fan and the adjacent Angola basin. *Netherlands Journal of Sea Research* 17, 201-249.
- Johnson, B. J., Fogel, M., Miller, G. H., 1998. Stable isotopes in modern ostrich eggshell: a calibration for paleoenvironmental applications in semi-arid regions of southern Africa. *Geochimica et Cosmochimica Acta* 62, 2451-2461.
- Jolly, D., Haxeltine, A., 1997. Effect of low glacial atmospheric  $\text{CO}_2$  on tropical African montane vegetation. *Science* 276, 786-788.
- Jones, M.B., 1987. The photosynthetic characteristics of papyrus in a tropical swamp. *Oecologia* 71, 355-359.
- Jouzel, J., Lorius, C., Petit, J.R., Genthon, C., Barkov, N.I., Kotlyakov, V.M., Petrov, V.M., 1987. Vostok ice core: a continuous isotope temperature record over the last climatic cycle (160,00 years). *Nature* 329, 403-408.
- Juniper, D., Southwood, R. (Eds.), 1986. *Insects and plant surfaces*, Edward Arnold, London, 360 pp.
- Justice, C. O., Kendall, J. D., Dowty, P. R., Scholes, R. J., 1996. Satellite remote sensing of fires during the SAFARI campaign using NOAA advanced very high resolution radiometer data. *Journal of Geophysical Research* 101, 23,851-23,864.
- Kaufman, L., Rousseeuw, P.J., 1990. *Finding Groups in Data. An Introduction to Cluster Analyses*, Wiley, New York, 368 pp.
- Kawamura, K., Ishimura, Y., Yamazaki, K., 2003. Four years' observation of terrestrial lipid class compounds on marine aerosols from the western North Pacific. *Global Biogeochemical Cycles* 17, 1-19.
- Keeley, J.E., Rundel, P.W., 2003. Evolution of CAM and  $\text{C}_4$  carbon-concentrating mechanisms. *International Journal of Plant Science* 164, S55-S77.
- Keeling, C.D., Mook, W.G., Tans, P., 1979. Recent trends in the  $^{13}\text{C}/^{12}\text{C}$  ratio of atmospheric carbon dioxide. *Nature* 277, 121-123.
- Kellogg, E.A., 1999. Phylogenetic aspects of the evolution of  $\text{C}_4$  photosynthesis. In: Sage, F., Monson, R.K. (Eds.),  *$\text{C}_4$  Plant Biology*. Academic Press, London, pp. 411-444.
- Kellogg, E.A., 2001. Evolutionary history of the grasses. *Plant Physiology* 125, 1198-1205.
- Kim, J.-H., Schneider, R. R., Mulitza, S., Müller, P. J., 2003. Reconstruction of SE trade-wind intensity based on sea-surface temperature gradients in the Southeast Atlantic over the last 25 kyr. *Geophysical Research Letters* 30, 2144-2147, doi: 10.1029/2003GL017557.
- Kirst, G. J., Schneider, R. R., Müller, P. J., von Storch, I., Wefer, G., 1999. Late Quaternary temperature variability in the Benguela Current system derived from alkenones. *Quaternary Research* 52, 92-103.
- Koch P.L., Behrensmeyer, A.K., Fogel, M.L., 1991. The isotopic ecology of plants and animals in Amboseli National Park, Kenya. *Carnegie Institution Year Book: The President's report*, 163-171.

- Kolattukudy, P.E., 1976. Introduction to natural waxes. In: Kolattukudy, P.E. (Ed.), *Chemistry and Biochemistry of Natural Waxes*, 1st Edition. Elsevier, Amsterdam, pp. 1-17.
- Kolattukudy, P.E., 1980. III. Biosynthesis of waxes, cutin, and suberin. In: Stumpf, P.K., Conn, E.E. (Eds.), *The Biochemistry of Plants*, Volume 4, *Lipids: Structure and Function*. Academic Press, New York, pp. 600-617.
- Kolattukudy, P.E., 1996. Biosynthetic pathways of cutin and waxes, and their sensitivity to environmental stresses. In: Kerstiens, G. (Ed.), *Plant Cuticles, an Integrated Functional Approach*, 1st Edition. BIOS Scientific Publishers Ltd, Oxford, pp. 83-108.
- Laetsch, W.M., 1969. Relationship between chloroplast structure and photosynthetic carbonfixation pathways. *Science Progress* 57, 323-351.
- Laing, W.A., Ogren, W.L., Hageman, R.H., 1974. Regulation of soybean net photosynthetic CO<sub>2</sub> fixation by interaction of CO<sub>2</sub>, O<sub>2</sub> and ribose 1,5-bisphosphate carboxylase. *Plant Physiology* 54, 678-685.
- Laredo, M.A., Simpson, G.D., Minson, D.J., Orpin, C.G., 1991. The potential for using *n*-alkanes in tropical forages as a marker for the determination of dry matter by grazing ruminants. *Journal of Agricultural Science* 117, 355-361.
- Leegood, R.C., 1999a. Photosynthesis in C<sub>3</sub> plants: The Benson-Calvin Cycle and photorespiration. In: Lea, P.J., Leegood, R.C. (Eds.), *Plant Biochemistry and Molecular Biology*. Wiley, West Sussex, pp. 29-50.
- Leegood, R.C., 1999b. Carbon dioxide-concentrating mechanisms: C<sub>4</sub> photosynthesis and crassulacean acid metabolism. In: Lea, P.J., Leegood, R.C. (Eds.), *Plant Biochemistry and Molecular Biology*. Wiley, West Sussex, pp. 51-79.
- Legendre, P., Legendre, L., 1998. *Numerical Ecology*, Elsevier, Amsterdam.
- Leistner, O.A., 1967. The plant ecology of the southern Kalahari. *Botanical Survey of South Africa* 38, 11-73.
- Leuenberger, M., Siegenthaler, U., Langway, C.C., 1992. Carbon isotopic composition of atmospheric CO<sub>2</sub> during the last ice age from an Antarctic ice core. *Nature* 357, 488-490.
- Libbert, E., 1991. *Allgemeine Biologie*, Fischer-Verlag, Stuttgart.
- Lichtfouse, É., Derenne, S., Mariotti, A., Largeau, C., 1994. Possible algal origin of long chain odd *n*-alkanes in immature sediments as revealed by distributions and carbon isotopic ratios. *Organic Geochemistry* 22, 1023-1027.
- Lide, D.R., 2004. *CRC-Handbook of Chemistry and Physics*. CRC-Press, London.
- Lindzen, R. S., Nigam, S., 1987. On the role of sea surface temperature gradients in forcing low level winds and convergence in the tropics. *Journal of Atmosphere Science* 44, 2418-2436.
- Lockheart, M. J., van Bergen, P. F., Evershed, R. P., 1997. Variation in the stable carbon isotope compositions of individual lipids from the leaves of modern angiosperms: Implications for the study of higher land plant-derived sedimentary organic matter. *Organic Geochemistry* 26, 137-153.
- Loveland, T. R., Zhu, Z., Ohlen, D. O., Brown, J. F., Reed, B. C., Yang, L., 1999. An analysis of the IGBP global land-cover characterization process, *Photogrammetric Engineering Remote Sensing* 65, 1021-1032.
- Loveland, T.R., Reed, B.C., Brown, J.F., Ohlen, D.O., Zhu, J., Yang, L., Merchant, J.W., 2000. Development of a global land cover characteristics database and IGBP DISCover from 1-km AVHRR data. *International Journal of Remote Sensing* 21, 1303-1330.

- Lutjeharms, J.R.L., Meeuwis, J.M., 1987. The extent and variability of south-east Atlantic upwelling. *South African Journal of Marine Science* 5, 51-62.
- Lutjeharms, J.R.L., Stockton, P.L., 1987. Kinematics of the upwelling front of southern Africa. The Benguela and comparable ecosystems. *South African Journal of marine Science* 5, 35-49.
- Lüttge, U., 2002. CO<sub>2</sub>-concentrating:consequences in Crassulacean acid metabolism. *Journal of Experimental Botany* 53, 2131-2142.
- Lyle, M., 1988. Climatically forced organic carbon burial in equatorial Atlantic and Pacific Oceans. *Nature* 335, 529-532.
- Maffei, M., 1996. Chemotaxonomic significance of leaf wax alkanes in the Gramineae. *Biochemical Systematics and Ecology* 24, 53-64.
- Malossini, F., Piasentier, E., Bovolenta, S., 1990. *n*-Alkane content of some forages. *Journal of the Science of Food and Agriculture* 53, 405-409.
- Mangelsdorf, K., Güntner, U., Rullkötter, J., 2000. Climatic and oceanographic variations on the California continental margin during the last 160 kyr. *Organic Geochemistry* 31, 829-846.
- Marino, B.D., McElroy, M.B., Salawitch, R.J., Spaulding, W.G., 1992. Glacial-to-interglacial variations in the carbon isotopic composition of atmospheric CO<sub>2</sub>. *Nature* 357, 461-466.
- Mariotti, A., Gadel, F., Giresse, P., Kinga-Mouzeo, 1991. Carbon isotope composition and geochemistry of particulate organic matter in the Congo River (Central Africa): Application to the study of Quaternary sediments off the mouth of the river. *Chemical Geology (Isotope Geoscience Section)* 86, 345-357.
- Martin, J.T., Juniper, B.E., 1970. *The Cuticles of Plants*, Edward Arnold, London.
- Mayes, R.W., Lamb, C.S., Colgrove, P.M., 1986. The use of dosed and herbage *n*-alkanes as markers for the determination of herbage intake. *Journal of Agricultural Science* 107, 161-170.
- Mayes, R.W., Beresford, N.A., Lamb, C.S., Barnett, C.L., Howard, B.J., Jones, B.-E.V., Eriksson, O., Hove, K., Pederson, Ø., Staines, B.W., 1994. Novel approaches to the estimation of intake and bioavailability of radiocaesium in ruminant grazing forested areas. *Science of the Total Environment* 157, 289-300.
- McDuffee, K.E., Eglinton, T.I., Sessions, A.L., Sylva, S., Wagner, T., Hayes, J.M., 2004. Rapid analysis of <sup>13</sup>C in plant-wax *n*-alkanes for reconstruction of terrestrial vegetation signals from aquatic sediments. *Geochemistry, Geophysics, Geosystems* 5 (10), 10004, doi: 10.1029/2004GC000772.
- McLean, B., Scott, L., 1999. Phytoliths in sediments of the Pretorian Saltpan (Tswaing Crater) and their potential as indicators of environmental history at the site. In: Patridge, T.C. (Ed.), *Tswaing-Investigations into the Origin, Age and Palaeoenvironments of the Pretoria Saltpan*. Council for Geoscience, Pretoria, pp. 167-171.
- Medina, E., Minchin, P., 1980. Stratification of δ<sup>13</sup>C values of leaves in Amazonian rain forest. *Oecologia* 45, 377-378.
- Milankovitch, M., 1930. *Mathematische Klimalehre und astronomische Theorie der Klimaschwankungen*. Gebrüder Bornträger, Berlin.
- Mook, W.G., Bommerson, J.C., Staverman, W.H., 1974. Carbon isotope fractionation between dissolved bicarbonate and gaseous carbon dioxide. *Earth Planetary Science Letters* 22, 169-176.
- Moore, P.D., Webb, J.A., Collinson, M.E., 1991. *Pollen analysis*. Blackwell, Oxford.

- Mudge, S. M., Norris, C. E., 1997. Lipid biomarkers in the Conwy Estuary (North Wales, U.K.): a comparison between fatty alcohols and sterols. *Marine Chemistry* 57, 61-84.
- Muzuka, A.N.N., 1999. Isotopic composition of tropical East African flora and their potential as source indicators of organic matter in coastal marine sediments. *Journal of African Earth Sciences* 28, 757-766.
- Neftel, A., Oeschger, H., Staffelbach, T., Stauffer, B., 1988. CO<sub>2</sub> record in the Byrd ice core 50,000-5,000 years BP. *Nature* 331, 609-611.
- New, M., Hulme, M., Jones, P., 1999. Representing twentieth-century space-time climate variability. Part I: Development of a 1961-90 mean monthly terrestrial climatology. *Journal of Climate* 12, 829-856.
- Nichols, P.D., Klumpp, D.W., Johns, R.B., 1982. Lipid components of the seagrasses *Posidonia australis* and *Heterozostera tasmanica* as indicators of carbon source. *Phytochemistry* 21, 1613-1621.
- Nichols, P.D., Johns, R.B., 1985. Lipids of the tropical seagrass *Thalassia hemprichii*. *Phytochemistry* 24, 81-84.
- Nishimoto, S., 1974a. A chemotaxonomic study of *n*-alkanes in leaf surface waxes of terrestrial plants. *Journal of Science of Hiroshima University* 38, 151-158.
- Nishimoto, S., 1974b. A chemotaxonomic study of *n*-alkanes in aquatic plants. *Journal of Science of Hiroshima University* 38, 159-163.
- Norton-Griffiths, M., 1979. The influence of grazing, browsing, and fire on the vegetation dynamics of the Serengeti. In: Sinclair, A.R.E., Norton-Griffiths, M. (Eds.), *Serengeti: Dynamics of an Ecosystem*. University of Chicago Press, Chicago, pp. 310-352.
- O'Connor, T.G., Bredenkamp, G.J., 1997. Grassland. In: Cowling, R.M., Richardson, D.M., Pierce, S.M. (Eds.), *Vegetation of Southern Africa*. Cambridge University Press, New York, 215-257.
- O'Leary, M.H., 1981. Carbon isotope fractionation in plants. *Phytochemistry* 20, 553-567.
- Osmond, C.B., Winter, K., Ziegler, H., 1980. Functional significance of different pathways of CO<sub>2</sub> fixation of photosynthesis. *Encyclopedia of Plant Physiology* 12A, 480-547.
- Pancost, R.D., Boot, C.S., 2004. The palaeoclimatic utility of terrestrial biomarkers in marine sediments. *Marine Chemistry* 92, 239-261.
- Parkington, J., Cartwright, C., Cowling, R.M., Baxter, A., Meadows, M., 2000. Palaeovegetation at the last glacial maximum in the western Cape, South Africa: wood charcoal and pollen evidence from Elands Bay Cave. *South African Journal of Science* 96, 543-546.
- Partridge, T.C., Scott, L., Hamilton, J.E., 1999. Synthetic reconstructions of southern African environments during the Last Glacial Maximum (21-18 kyr) and the Holocene Altithermal (8-6 kyr). *Quaternary Research* 57/58, 207-214.
- Patel, S., Nelson, D.R., Gibbs, A.G., 2001. Chemical and physical analyses of wax ester properties. *Journal of Insect Science* 1 (4), 7 pp.
- Pérez, M. E., Berger, W. H., 2000. Late Quaternary productivity fluctuations in the Mid-Angola Basin: Evidence from benthic foraminifera (Poster). Workshop on Quaternary Evolution of the Benguela Upwelling System, 19<sup>th</sup>-21<sup>st</sup> May, Carcans, France.
- Petschick, R., Kuhn, G., and Gingele, F., 1996. Clay mineral distribution in surface sediments of the South Atlantic: sources, transport, and relation to oceanography. *Marine Geology* 130, 203-229.



- Petit, J.R., Jouzel, J., Raynaud, D., Barkov, N.I., Barnola, J.-M., Basile, I., Benders, M., Chappellaz, J., Davis, M., Delaygue, G., Delmotte, M., Kotlyakov, V.M., Legrand, M., Lipenkov, V.Y., Lorius, C., Pépin, L., Ritz, C., Saltzman, E., Stievenard, M., 1999. Climate and atmospheric history of the past 420,000 years from the Vostok ice core, Antarctica. *Nature* 399, 429-436.
- Pierce, S., Winter, K., Griffiths, H., 2002. Carbon isotope ratio and the extent of daily CAM use by Bromeliaceae. *New Phytologist* 156, 75-83.
- Poynter, J. G., 1989. Molecular Stratigraphy: The Recognition of Palaeoclimatic Signals in Organic Geochemical Data. Ph.D. thesis, University of Bristol, Bristol.
- Poynter, J., and Eglinton, G., 1991. The biomarker concept - strengths and weaknesses. *Fresenius' Zeitschrift für analytische Chemie* 339, 725-731.
- Poynter, J.G., Farrimond, P., Robinson, N., Eglinton, G., 1989. Aeolian-derived higher plant lipids in the marine sedimentary records: Links with paleoclimate. In: Leinen, M., Sarnthein, M. (Eds.), *Paleoclimatology and Paleometeorology: Modern and Past Patterns of Global Atmospheric Transport*. Kluwer Academy, Norwell, Massachusetts, pp. 435-462.
- Prospero, J. M., Ginoux, P., Torres, O., Nicholson, S., Gill, T., 2002. Environmental characterization of global sources of atmospheric soil dust identified with the NIMBUS 7 Total Ozone Mapping Spectrometer (TOMS) absorbing aerosol product. *Reviews of Geophysics* 40(1), 1002, doi:10.1029/2000RG000095.
- Radke, M., Willsch, H., Welte, D., 1980. Preparative hydrocarbon group type determination by automated medium pressure liquid chromatography. *Analytical Chemistry* 52, 406-411.
- Raghavendra, A.S., Das, V.S.R., 1978. The occurrence of C<sub>4</sub>-photosynthesis: A supplementary list of C<sub>4</sub> plants reported during late 1974-mid 1977. *Photosynthetica* 12, 200-208.
- Ray, N., Adams, J.M., 2001. A GIS-based vegetation map of the world at the Last Glacial Maximum (25,000-15,000 BP). *Internet Archaeology* 11, 1-44.
- Reddy, Christopher M., Eglinton, T. I., Palic, R., Benitez-Nelson, B. C., Stojanovic, G., Palic, I., Djordjevic, S., Eglinton, G., 2000. Even carbon number predominance of plant wax *n*-alkanes: a correction. *Organic Geochemistry* 31, 331-336.
- Renvoize, S.A., Clayton, W.D., 1992. Classification and evolution of the grasses. In: Chapman, G.P. (Ed.), *Grass Evolution and Domestication*. University Press, Cambridge, pp. 3-37.
- Riederer, M., Schreiber, L., 1995. Waxes – The transport barriers of plant cuticles. In: Hamilton, R.J. (Ed.), *Waxes: Chemistry, Molecular Biology and Functions*. The Oil Press, Dundee, pp. 131-156.
- Rieley, G., Collier, R.J., Jones, D.M., Eglinton, G., Eakin, P.A., Fallick, A.E., 1991. Sources of sedimentary lipids deduced from stable carbon isotopic analyses of individual compounds. *Nature* 352, 425-427.
- Rieley, G., Collister, J.W., Stern, B., Eglinton, G., 1993. Gas chromatography/isotope ratio mass spectrometry of leaf wax *n*-alkanes from plants of differing carbon dioxide metabolisms. *Rapid Communications in Mass Spectrometry* 7, 488-491.
- Ries, S.K., Wert, V., Sweeley, C.C., Leavitt, R.A., 1977. Triacntanol: A new naturally occurring plant growth regulator. *Science* 195, 1339-1341.
- Rinna, J., Güntner, U., Hinrichs, K.-U., Mangelsdorf, K., van der Smissen, J.H., Rullkötter, J., 2000. Temperature-related molecular proxies: Degree of alkenone unsaturation and average chain length of *n*-alkanes. In: *Proceedings of the 16th Annual Pacific Climate (PACLIM) Workshop* (West G.J., Buffaloe, L., Eds.). Interagency Ecology

- Program, Technical Report, State of California, Department of Water Resources, Sacramento (CA), pp. 183-192.
- Rommerskirchen, F., Eglinton, G., Dupont, L., Güntner, U., Wenzel, C., Rullkötter, J., 2003. A north to south transect of Holocene southeast Atlantic continental margin sediments: Relationship between aerosol transport and compound-specific  $\delta^{13}\text{C}$  plant biomarker and pollen records. *Geochemistry, Geophysics, Geosystems* 4 (12), 1101, doi:10.1029/2003GC000541.
- Sackett, W.M., 1989. Stable carbon isotope studies on organic matter in the marine environment. In: Fritz, P., Fontes, J.C. (Eds.), *Handbook of Environmental Isotope Geochemistry*. Elsevier, Amsterdam, pp. 139-169.
- Sage, R.F., 1999. Why  $\text{C}_4$  photosynthesis? In: Sage, R.F., Monson, R.K. (Eds.),  *$\text{C}_4$  Plant Biology*. Academic Press, London, pp. 3-16.
- Sage, R.F., 2001.  $\text{C}_4$  plants. In: Levin, S.A. (Ed.), *Encyclopedia of Biodiversity*, Volume 1. Academic Press, London, pp. 575-598.
- Sage, R. F., 2004. The evolution of  $\text{C}_4$  photosynthesis. *New Phytologist* 161, 341-370.
- Sage, R. F., Monson, R. K., 1999.  *$\text{C}_4$  Plant Biology*, Academic Press, San Diego.
- Sage, R.F., Li, M.R., Monson, R.K., 1999a. The taxonomic distribution of  $\text{C}_4$  photosynthesis. In: Sage, R.F., Monson, R.K. (Eds.),  *$\text{C}_4$  Plant Biology*. Academic Press, London, pp. 551-584.
- Sage, R.F., Wedin, D.A., Li, M.R., 1999b. The biogeography of  $\text{C}_4$  photosynthesis: Patterns and controlling factors. In: Sage, R.F., Monson, R.K. (Eds.),  *$\text{C}_4$  Plant Biology*. Academic Press, London, pp. 313-373.
- Sala, O.E., Austin, A.T., Vivanco, L., 2001. Temperate grassland and shrubland ecosystems. In: Levin, S.A. (Ed.), *Encyclopedia of Biodiversity*, Volume 5, Academic Press, London, pp. 627-635.
- Sauvaire, Y., Tal, B., Heupel, R.C., England, R., Hanners, P.K., Nes, W.D., Mudd, J.B., 1987. A comparison of sterol and long chain fatty alcohol biosynthesis in *Sorghum bicolor*. In: Stumpf, P.K., Mudd, J.B., Nes, W.D. (Eds.), *The Metabolism, Structure, and Function of Plant Lipids*. Plenum Press, New York, pp. 107-110.
- Schefuß, E., Schouten, S., Jansen, J.H.F., Sinninghe Damsté, J.S., 2003a. African vegetation controlled by tropical sea surface temperatures in the mid-Pleistocene period. *Nature* 422, 418-421.
- Schefuß, E., Rathmeyer, V., Stuut, J.-B.W., Jansen, J.H.F., Sinninghe Damsté, J.S., 2003b. Carbon isotope analyses of  $n$ -alkanes in dust from the lower atmosphere over the central eastern Atlantic. *Geochimica et Cosmochimica Acta* 67, 1757-1767.
- Schefuß, E., Versteegh, G. J. M., Jansen, J. H., F., Sinninghe Damsté, J. S., 2004. Lipid biomarkers as major source and preservation indicators in SE Atlantic surface sediments. *Deep-Sea Research I* 51, 1199-1228.
- Schefuß, E., Schouten, S., Schneider, R.R., 2005. Climatic controls on central African hydrology during the past 20,000 years. *Nature* 437, 1003-1006.
- Schidlowski, M., 1987. Application of stable carbon isotopes to early biochemical evolution on earth. *Annual Review of Earth and Planetary Sciences* 15, 47-72.
- Schleser, G.H., Jayasekera, R., 1985.  $\delta^{13}\text{C}$ -Variations of leaves in forests as an indication of reassimilated  $\text{CO}_2$  from the soil. *Oecologia* 65, 536-542.
- Schlesinger, W.H., 1997. *Biogeochemistry*, Academic Press, San Diego.

- Schneider, R., 1991. Spätquartäre Produktivitätsänderungen im östlichen Angola-Becken: Reaktion auf Variationen im Passat-Monsun-Windsystem und in der Advektion des Benguela-Küstenstroms, Dissertation, University of Bremen.
- Schneider, R. R., Müller, P. J., Ruhland, G., 1995. Late Quaternary surface circulation in the east equatorial South Atlantic: evidence from alkenone sea surface temperatures. *Paleoceanography* 10, 197-219.
- Schneider, R.R., Müller, P.J., Ruhland, G., Meinecke, G., Schmidt, H., Wefer, G., 1996. Late Quaternary surface temperatures and productivity in the east-equatorial South Atlantic: response to changes in trade/monsoon wind forcing and surface water advection. In: Wefer, G., Berger, W.H., Siedler, G., Webb, D.J. (Eds.), *The South Atlantic: Present and Past Circulation*, Springer, Berlin, pp. 527-551.
- Schultz, J., 1995. *The Ecozones of the World*. Springer, Heidelberg.
- Schulz, H. D., and cruise participants, 1992. Report and preliminary results of Meteor cruise M20/2 Abidjan - Dakar, 27.12.1991 - 3.2.1992, *Berichte des Fachbereichs Geowissenschaften, Universität Bremen*, 25.
- Schulze, E.-D., Ellis, R., Schulze, W., Trimborn, P., Ziegler, H., 1996. Diversity, metabolic types and  $\delta^{13}\text{C}$  carbon isotope ratios in the grass flora of Namibia in relation to growth form, precipitation and habitat conditions. *Oecologia* 106, 352-369.
- Schwark, L., Zink, K., Lechterbeck, J., 2002. Reconstruction of postglacial to early Holocene vegetation history in terrestrial Central Europe via cuticular lipid biomarkers and pollen records from lake sediments. *Geology* 30, 463-466.
- Schwartz, D., Mariotti, A., Glanfranchi, R., Guillet, B., 1986.  $^{12}\text{C}/^{13}\text{C}$  ratios of soil organic matter as indicators of vegetation changes in the Congo. *Geoderma* 39, 97-103.
- Scott, L., 1989. Climatic conditions in Southern Africa since the last glacial maximum, inferred from pollen analysis. *Palaeogeography. Palaeoclimatology. Palaeoecology* 70, 345-353.
- Scott, L., 1994. Palynology of Late Pleistocene Hyrax middens, southwestern Cape Province, South Africa: a preliminary report. *Historical Biology* 9, 71-81.
- Scott, L., Marais, E., Brook, G. A., 2004. Fossil Hyrax dung and evidence of Late Pleistocene and Holocene vegetation types in the Namib Desert. *Journal of Quaternary Science* 19, 829-832.
- Sellers, P. J., Randall, D. A., Collatz, G. J., Berry, J. A., Field, C. B., Dazlich, D. A., Zhang, C., Collelo, G. D., Bounoua L., 1996. A revised land surface parameterization (SiB2) for atmospheric GCMs. Part I: Model formulation. *Journal of Climate* 9, 676-705.
- Shackleton, N.J., 1977. Tropical rainforest history and the equatorial Pacific carbonate dissolution cycles. In: Anderson, N.R., Malahoff, A. (Eds.), *The Fate of Fossil Fuel  $\text{CO}_2$  in the Oceans*. Plenum Press, New York, pp. 401-428.
- Shackleton, N.J., Hall, M.A., 1984. Oxygen and carbon isotope stratigraphy of deep sea drilling project hole 552A: Plio-Pleistocene glacial history. *Initial Reports of the Deep Sea Drilling Project* 81, 599-609.
- Shannon, L.V., Nelson, G., 1996. The Benguela: large scale features and processes and system variability. In: Wefer, G., Berger, W.H., Siedler, G., Webb, D.J. (Eds.), *The South Atlantic: Present and Past circulation*. Springer, Berlin, pp. 162-210.
- Shi, N., Dupont, L. M., Beug, H.-J., Schneider, R., 1998. Vegetation and climate changes during the last 22000 yr in SW Africa - evidence from a high resolution marine palynological record. *Vegetation History and Archaeobotany* 7, 127-140.

- Shi, N., Dupont, L. M., Beug, H.-J., Schneider, R., 2000. Correlation between vegetation in southwestern Africa and oceanic upwelling in the past 21,000 years. *Quaternary Research* 54, 72-80.
- Shi, N., Schneider, R., Beug, H.-J., Dupont, L. M., 2001. Southeast trade wind variations during the last 135 kyr: Evidence from pollen spectra in eastern South Atlantic. *Earth Planetary Science Letters* 187, 311-321.
- Simoneit, B. R. T., 1977. Organic matter in eolian dusts over the Atlantic Ocean. *Marine Chemistry* 5, 443-464.
- Smith, B.N., Epstein, S., 1971. Two categories of  $^{13}\text{C}/^{12}\text{C}$  ratios for higher plants. *Plant Physiology* 47, 380-384.
- Smith, R.M., Martin-Smith, M., 1978. Hydrocarbons in leaf waxes of *Saccharum* and related genera. *Phytochemistry* 17, 1293-1296.
- Smith, J.Y.C., Winter, K., 1996. Taxonomic distribution of Crassulacean Acid Metabolism. In: Winter, K., Smith, J.A.C. (Eds.), *Crassulacean Acid Metabolism: Biochemistry, Ecophysiology and Evolution, Ecological Studies, Volume 114*, Springer, New York, pp. 427-436.
- Smith, H.J., Fischer, H., Wahlen, M., Mastroianni, D., Deck, B., 1999. Dual modes of the carbon cycle since the Last Glacial Maximum. *Nature* 400, 248-250.
- Smith, D.G., Mayes, R.W., Raats, J.G., 2001. Effect of species, plant part and season of harvest on *n*-alkane concentrations in the cuticular wax of common rangeland grasses from southern Africa. *Australian Journal of Agriculture Research* 52, 875-882.
- Soderstrom, T.R., 1981. Some evolutionary trends in the Bambusoideae (Poaceae). *Annals of the Missouri Botanical Garden* 68, 15-47.
- Sosef, M. S. M., 1996. Begonias and African rain forest refuges: General aspects and recent progress. In: van der Maesen, L.J.G., van der Burgt, X.M., van Medenbach de Rooy, J.M. (Eds.), *The Biodiversity of African Plants*. Kluwer Academic Press, Dordrecht, pp. 602-611.
- Spencer, R.R., Chapman, W., 1985. Surface wax of coastal Bermuda grass. *Journal of Agricultural and Food Chemistry* 33/4, 654-656.
- Stránský, K., Streibl, M., Sorm, F., 1968. On natural waxes. VII. Lipid hydrocarbons of the alga. *Collection of Czechoslovak Chemical Communications* 33, 416-424.
- Street-Perrott, F.A., Perrott, R.A., 1993. Holocene vegetation, lake levels, and climate of Africa. In: Wright, H.E., Jr. (Ed.) *Global Climates since the Last Glacial Maximum*. University of Minnesota Press, London, pp. 318-356.
- Street-Perrott, F.A., Huang, Y., Perrott, R.A., Eglinton, G., Barker, P., Khelifa, L.B., Harkness, D.D., Olago, D.O., 1997. Impact of lower atmospheric carbon dioxide on tropical mountain ecosystems. *Science* 278, 1422-1426.
- Stute, M., Talma, A. S., 1998. Glacial temperatures and moisture transport regimes reconstructed from noble gases and  $\delta^{18}\text{O}$ , Stampriet Aquifer, Namibia. *Isotope Techniques in the Study of Environmental Change, Proceedings series, IAEA, Vienna*, pp. 307-318.
- Stuut, J.-B., Prins, M. A., Schneider, R. R., Weltje, G. J., Jansen, J. H. F., Postma, G., 2002. A 300-kyr record of aridity and wind strength in southwestern Africa: inferences from grain-size distributions of sediments on Walvis Ridge, SE Atlantic. *Marine Geology* 180, 221-233.
- Stuut, J.-B., Crosta, X., van der Borg, K., Schneider, R., 2004. Relationship between Antarctic sea ice and southwest African climate during the late Quaternary. *Geology* 32, 909-912.

- Swap, R., Garstang, M., Macko, S.A., Tyson, P.D., Maenhaut, W., Artaxo, P., Kållberg, P., Talbot, R., 1996a. The long-range transport of southern African aerosols to the tropical South Atlantic. *Journal of Geophysical Research* 101, 23,777-23,791.
- Swap, R. J., Garstang, M., Macko, S. A., Tyson, P. D., Kållberg, P., 1996b. Comparisons of biomass burning emissions and biogenic emissions to the tropical South Atlantic. In: Levine, J.S. (Ed.), *Biomass Burning and Global Change*, Vol. 1, MIT Press, Cambridge, MA, pp. 396-401.
- Tajika, E., 1998. Climate change during the last 150 million years: reconstruction from a carbon cycle model. *Earth and Planetary Science Letters* 160, 695-707.
- Takahashi, T., Olafsson, J., Goddard, J.G., Chipman, D.W., Sutherland, S.C., 1993. Seasonal variation of CO<sub>2</sub> and nutrients in the high-latitude surface oceans: a comparative study. *Global Biogeochemical Cycles* 7, 843-878.
- Taub, D.R., 2000. Climate and the US distribution of C<sub>4</sub> grass subfamilies and decarboxylation variants of C<sub>4</sub> photosynthesis. *American Journal of Botany* 87, 1211-1215.
- Taylor, G.H., Teichmüller, M., Davis, A., Diessel, C. F. K., Littke, R., Robert, P., 1998. *Organic Petrology*, Gebrüder Borntraeger, Berlin-Stuttgart.
- Teeri, J. A., Stowe, L. G., 1976. Climatic patterns and the distribution of C<sub>4</sub> grasses in North America. *Oecologia* 23, 1-12.
- Tulloch, A.P., 1973. Composition of leaf surface waxes of *Triticum* species: variation with age and tissue. *Phytochemistry* 12, 2225-2232.
- Tulloch, A.P., 1976. Chemistry of waxes of higher plants. In: Kolattukudy, P.E. (Ed.), *Chemistry and Biochemistry of Natural Waxes*. Elsevier, Amsterdam, pp. 236-289.
- Tulloch, A.P., 1981. Composition of epicuticular waxes from 28 genera of Graminaea: differences between subfamilies. *Canadian Journal of Botany* 59, 1213-1221.
- Tulloch, A.P., 1982. Epicuticular wax of *Eragrostis curvula*. *Phytochemistry* 21, 661-664.
- Tulloch, A.P., 1984. Epicuticular waxes of four eragrostoid grasses. *Phytochemistry* 23, 1619-1623.
- Tulloch, A.P., Hoffmann, L.L., 1976. Epicuticular wax of *Agropyron intermedium*. *Phytochemistry* 15, 1145-1151.
- Tulloch, A.P., Baum, B.R., Hoffman, L.L., 1980. A survey of epicuticular waxes among genera of Triticeae. 2. Chemistry. *Canadian Journal of Botany* 58, 2602-2615.
- Tyson, P. D., Garstang, M., Swap, R., 1996. Large-scale recirculation of air over Southern Africa. *Journal of Applied Meteorology* 35, 2218-2236.
- van Andel, T. H., Heath, G. R., Moore Jr, T. C., 1975. Cenozoic history and paleoceanography of the central equatorial Pacific Ocean. *Geological Society of American Memoir* 143.
- van Bennekom, A. J., Berger, G. W., 1984. Hydrography and silica budget of the Angola basin. *Netherlands Journal of Sea Research* 17, 149-200.
- van der Merwe, J.H., 1983. *National Atlas of South West Africa (Namibia)*. National Book Printers, Capetown.
- van der Merwe, N.J., Medina, E., 1989. Photosynthesis and <sup>13</sup>C/<sup>12</sup>C ratios in Amazonian rain forests. *Geochimica et Cosmochimica Acta* 53, 1091-1094.
- van Oudtshoorn, F., 1999. *Guide to Grasses of Southern Africa*. Briza Publication, Pretoria.

- Voznesenskaya, E.V., Chuong, S.D.X., Koteyeva, N.K., Edwards, G.E., Franceschi, V.R., 2005. Functional compartmentation of C<sub>4</sub> photosynthesis in the triple layered chlorenchyma of *Aristida* (Poaceae). *Functional Plant Biology* 32, 67-77.
- Vogel, J.C., 1978. Recycling of carbon in a forest environment. *Oecologia Plantarum* 13, 89-94.
- Vogel, J.C., Fuls, A., Ellis, R.P., 1978. The geographical distribution of Kranz grasses in South Africa. *South African Journal of Science* 74, 209-215.
- Wagner, T., 1998. Pliocene-Pleistocene deposition of carbonate and organic carbon at Site 959: Paleoenviromental implications for the eastern equatorial Atlantic off the Ivory Coast/Ghana. *Proceedings in the Ocean Drilling Program, Ocean Drilling Program College Station, Texas, Scientific Results* 159, 557-574.
- Wagner, T., 1999. Petrology of organic matter in modern and late Quaternary deposits of the equatorial Atlantic: Climatic and oceanographic links. *International Journal of Coal Geology* 39, 155-184.
- Wagner, T., 2000. Control of organic carbon accumulation in the late Quaternary equatorial Atlantic (Ocean Drilling Program Sites 664 and 663): Productivity versus terrigenous supply. *Paleoceanography* 15, 181-199.
- Wagner, T., Dupont, L.M., 1999. Terrestrial organic matter in marine sediments: analytical approaches and eolian-marine records in the central equatorial Atlantic. In: Fischer, G., Wefer, G. (Eds.), *Use of Proxies in Paleoceanography: Examples from the South Atlantic*, Springer, Berlin, pp. 547-574.
- Walker, B.H., Ludwig, D., Holling, C.S., Peterman, R.M., 1981. Stability of semi-arid savanna grazing systems. *Journal of Ecology* 69, 473-498.
- Walker, B.H., Noy-Meir, I., 1982. Aspects of the stability and resilience of savanna ecosystems. In: Huntley, B.J., Walker, B.H. (Eds.), *Ecology of tropical savannas*. Springer, Berlin, pp. 556-590.
- Walter, H., 1971. *Ecology of Tropical and Subtropical Vegetation*. Oliver and Boyd, Edinburgh.
- Walter, H., Lieth, H., 1960-1967. *Klimadiagramm-Weltatlas*, Fischer, Jena.
- Walter, H., Harnickell, E., Mueller-Dombois, D., 1975. *Climate-diagram Maps of the Individual Continents and the Ecological Climatic Regions of the Earth*. Springer, Berlin.
- Wan, C.S.M., Sage, R.F., 2001. Climate and the distribution of C<sub>4</sub> grasses along the Atlantic and Pacific coasts of North America. *Canadian Journal of Botany* 79, 474-486.
- Watson, L., Dallwitz, M.J., 1992a. *The Grass Genera of the World*. University Press, Cambridge.
- Watson, L., Dallwitz, M.J., 1992b onwards. *Grass Genera of the World: Descriptions, Illustrations, Identification and Information Retrieval; Including Synonyms, Morphology, Anatomy, Physiology, Phytochemistry, Cytology, Classification, Pathogens, World and Local Distribution, and References*. <http://biodiversity.uno.edu/delta/>, Version: 18<sup>th</sup> August 1999.
- Wefer, G., and cruise participants, 1988. Bericht über die METEOR-Fahrt M6/6 Libreville-Las Palmas, 18.2.-23.3.1988, *Berichte des Fachbereichs Geowissenschaften Universität Bremen* 3.
- Wefer, G., Berger, W., Richter, C., and Shipboard Scientific Party, 1998, *Proceedings of the ODP, Initial Reports* 175, Ocean Drilling Program College Station (Texas).

- Wefer, G., Berger, W.H., Richter, C. (Eds.), 2002. Proceedings of the ODP, Scientific Results 175 [CD-ROM], available from Ocean Drilling Program, Texas A&M University, College Station TX 77845-9547, USA.
- Weiss, R.F., 1974. Carbon dioxide in water and seawater: the solubility of a non-ideal gas. *Marine Chemistry* 2, 203-215.
- Werger, M.J.A., Ellis, R.P., 1981. Photosynthetic pathways in the arid regions of South Africa. *Flora* 171, 64-75.
- Werner, P.A., 1991. *Savannah Ecology and Management: Australian Perspectives and Intercontinental Comparisons*. Blackwell Science, London.
- Westerhausen, L., Poynter, J., Eglinton, G., Erlenkeuser, H., Sarnthein, M., 1993. Marine and terrigenous origin of organic matter in modern sediments of the east Atlantic: the  $\delta^{13}\text{C}$  and molecular record. *Deep-Sea Research I* 40, 1087-1121.
- White, F., 1983. *The Vegetation of Africa. A descriptive Memoir to Accompany the UNESCO/AETFAT/UNSO Vegetation Map of Africa*. UNESCO, Paris.
- Whitecross, M.I., Armstrong, D.J., 1972. Environmental effects on epicuticular waxes of *Brassica napus* L. *Australian Journal of Botany* 20, 87-95.
- Whitman, J.M., Berger, W.H., 1994. Pliocene-Pleistocene carbon isotopic record, site 586, Ontong Java Plateau. *Scientific Results of the Ocean Drilling Program* 130, 333-348.
- Whittaker, R.H., 1975. *Communities and Ecosystems*. Macmillan, New York.
- Williams, G.J., 1974. Photosynthetic adaptation to temperature in  $\text{C}_3$  and  $\text{C}_4$  grasses. A possible ecological role in the shortgrass prairie. *Plant Physiology* 54, 709-711.
- Winslow, J.C., Hunt Jr., E.R., Piper, S.C., 2003. The influence of seasonal water availability on global  $\text{C}_3$  versus  $\text{C}_4$  grassland biomass and its implications for climate change research. *Ecological Modelling* 163, 153-173.
- Youngblood, W.W., Blumer, M., Guillard, R.R.L., Fiore, F., 1971. Saturated and unsaturated hydrocarbons in marine benthic algae. *Marine Biology* 8, 190-201.
- Yunker, M. B., Macdonald, R. W., Velthkamp, D. J., Cretney, W. J., 1995. Terrestrial and marine biomarkers in a seasonally ice-covered Arctic estuary-integration of multivariate and biomarker approaches. *Marine Chemistry* 49, 1-50 *n*-alkane.
- Zhang, Z., Zhao, M., Lu, H., Faiia, A.M., 2003. Lower temperature as the main cause of  $\text{C}_4$  plant declines during the glacial periods on the Chinese Loess Plateau. *Earth and Planetary Science Letters* 214, 467-481.
- Zhang, Y., Togamura, Y., Otsuki, K., 2004. Study on the *n*-alkane patterns in some grasses and factors affecting the *n*-alkane patterns. *Journal of Agricultural Science* 142, 469-475.
- Zhang, Z., Zhao, M., Eglinton, G., Lu, H., in press. Leaf wax lipids as paleovegetational and paleoenvironmental proxies for the Chinese Loess Plateau. *Quaternary Science Reviews*.
- Zhao, M., Eglinton, G., Haslett, S.K., Jordan, R.W., Sarnthein, M., Zhang, Z., 2000. Marine and terrestrial biomarker records for the last 35,000 years at ODP site 685C off NW Africa. *Organic Geochemistry* 31, 919-930.
- Zhao, M., Dupont, L., Eglinton, G., Teece, M., 2003. *n*-Alkane and pollen reconstruction of terrestrial climate and vegetation for N.W. Africa over the last 160 kyr. *Organic Geochemistry* 34, 131-143.

## 7 Appendix

### 7.1 Supplementary data

**Table 7.1.** Mean annual temperature and precipitation data of selected stations in southwest Africa (gathered from climatograms presented by Walter et al., 1975). The code refers to numbers used in Fig. 1.6, page 13, Fig. 1.7, page 16, and Fig. 3.8, page 90)

| Code | Station      | Country            | Latitude/<br>longitude | Mean annual<br>temperature<br>(°C) | Mean annual<br>precipitation<br>(mm) |
|------|--------------|--------------------|------------------------|------------------------------------|--------------------------------------|
| 1    | Mbandaka     | Dem. Rep.<br>Congo | 0.1°N/17.1°E           | 24.1                               | 2066                                 |
| 2    | Kikwit       | Dem. Rep.<br>Congo | 5.1°S/18.9°E           | 24.7                               | 1923                                 |
| 3    | Vila Luzo    | Angola             | 11.8°S/19.9°E          | 20.8                               | 1116                                 |
| 4    | Mongu        | Zambia             | 15.3°S/23.1°E          | 22.5                               | 954                                  |
| 5    | Livingstone  | Zambia             | 17.9°S/25.9°E          | 22.2                               | 671                                  |
| 6    | Windhoek     | Namibia            | 22.6°S/17.1°E          | 18.2                               | 362                                  |
| 7    | Tsabong      | Botswana           | 26.1°S/22.5°E          | 19.7                               | 295                                  |
| 8    | Mafeking     | South Africa       | 25.9°S/25.7°E          | 18.3                               | 542                                  |
| 9    | Keetmanshoop | Namibia            | 26.5°S/18.1°E          | 20.8                               | 133                                  |
| 10   | Pofadder     | South Africa       | 29.1°S/19.4°E          | 18.5                               | 95                                   |



**Table 7.2.** *n*-Alkane data of sediment samples studied: Location, depth, age, MIS, individual *n*-alkane mass accumulation rates in  $\mu\text{g cm}^{-2} \text{ kyr}^{-1}$  and TCOC<sub>27-35</sub> values in  $\mu\text{g cm}^{-2} \text{ kyr}^{-1}$ .

| Location     | Depth<br>(cmcd <sup>a</sup> ) | Age<br>(ka) | MIS <sup>b</sup> | <i>n</i> -Alkane mass accumulation rate <sup>c</sup> (μg cm <sup>-2</sup> kyr <sup>-1</sup> ) |      |      |       |      |       |      |       |      |      |      |      | TCOC <sub>27-35</sub> <sup>d</sup> |
|--------------|-------------------------------|-------------|------------------|---|------|------|-------|------|-------|------|-------|------|------|------|------|------------------------------------|
|              |                               |             |                  | 26  | 27   | 28   | 29    | 30   | 31    | 32   | 33    | 34   | 35   | 36   |      |                                    |
| ODP 1075A    | 55                            | 5           | 1                | 0.20  | 0.53 | 0.26 | 1.31  | 0.25 | 1.06  | 0.33 | 0.57  | 0.06 | 0.28 | -    | 3.8  |                                    |
|              | 355                           | 23          | 2                | 0.54  | 1.83 | 0.82 | 5.67  | 1.05 | 4.67  | 0.76 | 2.32  | 0.17 | 0.57 | -    | 81.8 |                                    |
|              | 1879                          | 126         | 5e               | 0.21  | 0.44 | 0.27 | 1.14  | 0.30 | 1.14  | 0.19 | 0.53  | 0.11 | 0.31 | -    | 3.5  |                                    |
|              | 1905                          | 131         | 6a               | 0.37  | 0.99 | 0.48 | 2.49  | 0.50 | 2.39  | 0.44 | 1.45  | 0.13 | 0.39 | -    | 7.7  |                                    |
| GeoB 1008-3  | 13                            | 2           | 1                | 0.22  | 0.66 | 0.33 | 2.23  | 0.39 | 1.69  | 0.26 | 0.70  | 0.08 | 0.25 | 0.04 | 5.5  |                                    |
|              | 220                           | 19          | 2                | 1.14  | 3.76 | 1.73 | 11.82 | 2.16 | 9.42  | 1.32 | 4.95  | 0.48 | 1.71 | 0.20 | 31.7 |                                    |
|              | 820                           | 123         | 5e               | 0.19  | 0.56 | 0.27 | 1.65  | 0.30 | 1.39  | 0.28 | 0.56  | 0.09 | 0.20 | 0.05 | 4.4  |                                    |
|              | 881                           | 135         | 6a               | 0.66  | 2.09 | 1.01 | 6.02  | 1.15 | 4.61  | 0.70 | 2.44  | 0.29 | 0.75 | 0.11 | 15.9 |                                    |
| GeoB 1016 -3 | 4                             | 1           | 1                | 0.14  | 0.29 | 0.17 | 0.64  | 0.14 | 0.60  | 0.09 | 0.34  | 0.04 | 0.11 | 0.02 | 2.0  |                                    |
|              | 112                           | 18          | 2                | 0.16  | 0.51 | 0.25 | 1.43  | 0.26 | 1.52  | 0.19 | 0.77  | 0.05 | 0.20 | 0.03 | 4.4  |                                    |
|              | 603                           | 122         | 5e               | 0.09  | 0.32 | 0.14 | 0.88  | 0.16 | 1.02  | 0.15 | 0.60  | 0.05 | 0.21 | 0.01 | 3.0  |                                    |
|              | 643                           | 136         | 6a               | 0.13  | 0.47 | 0.20 | 1.13  | 0.28 | 1.70  | 0.27 | 1.20  | 0.10 | 0.45 | 0.03 | 49   |                                    |
| ODP 1079A    | 77                            | 3           | 1                | 0.71  | 2.86 | 1.21 | 10.19 | 2.16 | 10.23 | 1.64 | 5.51  | 0.72 | 2.11 | -    | 30.9 |                                    |
|              | 757                           | 19          | 2                | 0.73  | 3.05 | 1.18 | 8.42  | 1.58 | 11.43 | 1.40 | 8.71  | 0.59 | 3.23 | -    | 34.8 |                                    |
|              | 2943                          | 127         | 5e               | 0.74  | 2.80 | 1.13 | 9.92  | 1.36 | 11.75 | 1.60 | 7.19  | 0.47 | 3.21 | -    | 34.9 |                                    |
|              | 3223                          | 137         | 6a               | 1.26  | 6.13 | 2.33 | 26.14 | 2.85 | 22.82 | 2.49 | 13.82 | 0.89 | 5.00 | -    | 73.9 |                                    |
| GeoB 1028-5  | 20                            | 4           | 1                | 0.03  | 0.05 | 0.03 | 0.12  | 0.03 | 0.21  | 0.03 | 0.11  | 0.01 | 0.03 | -    | 0.5  |                                    |
|              | 95                            | 20          | 2                | 0.03  | 0.06 | 0.03 | 0.11  | 0.04 | 0.25  | 0.04 | 0.13  | 0.02 | 0.04 | 0.01 | 0.6  |                                    |
|              | 394                           | 121         | 5e               | 0.05  | 0.08 | 0.07 | 0.14  | 0.06 | 0.25  | 0.04 | 0.12  | 0.04 | 0.07 | 0.01 | 0.7  |                                    |
|              | 454                           | 136         | 6a               | 0.02  | 0.03 | 0.02 | 0.05  | 0.03 | 0.09  | 0.02 | 0.05  | 0.01 | 0.01 | -    | 0.2  |                                    |

cont. Table 7.2. *n*-Alkane data of sediment samples studied.

| Site        | Depth<br>(cmcd <sup>a</sup> ) | Age<br>(ka) | MIS <sup>b</sup> | <i>n</i> -Alkane mass accumulation rate <sup>c</sup> (µg cm <sup>-2</sup> kyr <sup>-1</sup> ) |      |       |       |       |       |      |      |      |      |      |      | TCOC <sub>27-35</sub> <sup>d</sup> |
|-------------|-------------------------------|-------------|------------------|---|------|-------|-------|-------|-------|------|------|------|------|------|------|------------------------------------|
|             |                               |             |                  | 26  | 27   | 28    | 29    | 30    | 31    | 32   | 33   | 34   | 35   | 36   |      |                                    |
| ODP 1082A   | 37                            | 4           | 1                | 0.15  | 0.43 | 0.25  | 0.94  | 0.28  | 1.91  | 0.32 | 1.10 | 0.09 | 0.28 | -    | 4.7  |                                    |
|             | 237                           | 21          | 2                | 0.27  | 0.64 | 0.37  | 1.35  | 0.38  | 3.56  | 0.66 | 1.89 | 0.15 | 0.45 | 0.07 | 7.9  |                                    |
|             | 1286                          | 127         | 5e               | 0.33  | 0.77 | 0.62  | 1.45  | 0.44  | 3.10  | 0.45 | 1.60 | 0.13 | 0.47 | -    | 7.4  |                                    |
|             | 1376                          | 136         | 6a               | 1.39  | 2.78 | 4.31  | 6.85  | 5.83  | 8.02  | 4.00 | 3.39 | 0.52 | 0.91 | 0.17 | 21.9 |                                    |
| GeoB 1710-3 | 3                             | 1           | 1                | 0.07  | 0.11 | 0.06  | 0.18  | 0.06  | 0.39  | 0.06 | 0.20 | 0.03 | 0.05 | 0.01 | 0.9  |                                    |
|             | 95                            | 18          | 2                | 0.13  | 0.25 | 0.12  | 0.61  | 0.22  | 1.29  | 0.12 | 0.63 | 0.07 | 0.14 | -    | 2.9  |                                    |
|             | 609                           | 122         | 5e               | 0.11  | 0.15 | 0.10  | 0.23  | 0.10  | 0.43  | 0.07 | 0.19 | 0.04 | 0.08 | -    | 1.1  |                                    |
|             | 669                           | 136         | 6a               | 0.12  | 0.16 | 0.11  | 0.35  | 0.12  | 0.70  | 0.13 | 0.33 | 0.09 | 0.14 | -    | 1.7  |                                    |
| ODP 1084A   | 55                            | 5           | 1                | 0.31  | 0.71 | 0.35  | 1.59  | 0.37  | 4.45  | 0.66 | 2.24 | 0.14 | 0.53 | 0.07 | 9.5  |                                    |
|             | 455                           | 26          | 2                | 5.03  | 9.40 | 14.88 | 21.81 | 17.14 | 22.11 | 9.59 | 8.30 | 1.02 | 1.36 | 0.27 | 63.0 |                                    |
|             | 2633                          | 124         | 5e               | 1.10  | 2.59 | 2.46  | 5.69  | 3.23  | 12.29 | 3.00 | 5.60 | 0.41 | 1.32 | 0.12 | 27.5 |                                    |
|             | 2949                          | 139         | 6a               | 1.85  | 3.23 | 2.17  | 6.09  | 3.42  | 11.65 | 3.76 | 5.09 | 1.57 | -    | -    | 26.1 |                                    |
| GeoB 1722-1 | 8                             | 7           | 1                | 0.02  | 0.03 | 0.02  | 0.05  | 0.02  | 0.12  | 0.01 | 0.04 | -    | 0.01 | -    | 0.3  |                                    |
|             | 24                            | 17          | 2                | 0.06  | 0.09 | 0.06  | 0.15  | 0.08  | 0.20  | 0.05 | 0.10 | 0.05 | 0.03 | -    | 0.6  |                                    |
|             | 189                           | 123         | 5e               | 0.03  | 0.04 | 0.03  | 0.04  | 0.02  | 0.07  | 0.02 | 0.03 | 0.01 | 0.02 | -    | 0.2  |                                    |
|             | 210                           | 1378        | 6a               | 0.05  | 0.06 | 0.04  | 0.09  | 0.04  | 0.14  | 0.02 | 0.06 | 0.03 | 0.03 | -    | 0.4  |                                    |

<sup>a</sup>cmcd: Centimetres composite depth

<sup>b</sup>MIS: Marine isotopic stage

<sup>c</sup>Numbers according to individual *n*-alkane carbon numbers

<sup>d</sup>TCOC<sub>27-35</sub>: Total content of odd-carbon-numbered *n*-C<sub>27</sub> to *n*-C<sub>35</sub> alkanes in µg cm<sup>-2</sup> kyr<sup>-1</sup>

**Table 7.3.** *n*-Alkanol data of sediment samples studied: Location, depth, age, MIS, individual *n*-alkanol mass accumulation rates in  $\mu\text{g cm}^{-2} \text{ kyr}^{-1}$  and TCEC<sub>22-32</sub> values in  $\mu\text{g cm}^{-2} \text{ kyr}^{-1}$ .

| Location     | Depth<br>(cmcd <sup>a</sup> ) | Age<br>(ka) | MIS <sup>b</sup> | <i>n</i> -Alkanol mass accumulation rate <sup>c</sup> (μg cm <sup>-2</sup> kyr <sup>-1</sup> ) |       |      |       |      |       |      |       |      |       |      |       |      |       | TCEC <sub>22-32</sub> <sup>d</sup> |
|--------------|-------------------------------|-------------|------------------|--|-------|------|-------|------|-------|------|-------|------|-------|------|-------|------|-------|------------------------------------|
|              |                               |             |                  | 21   | 22    | 23   | 24    | 25   | 26    | 27   | 28    | 29   | 30    | 31   | 32    | 33   |       |                                    |
| ODP 1075A    | 55                            | 5           | 1                | 0.18   | 1.89  | 0.69 | 3.28  | 0.78 | 2.50  | 0.48 | 2.19  | 0.38 | 1.48  | 0.41 | 2.17  | 0.55 | 13.5  |                                    |
|              | 355                           | 23          | 2                | 0.14   | 2.31  | 0.90 | 5.99  | 1.32 | 5.69  | 1.16 | 5.20  | 1.05 | 3.79  | 0.79 | 4.22  | 0.41 | 27.2  |                                    |
|              | 1879                          | 126         | 5e               | 0.05   | 0.69  | 0.19 | 1.17  | 0.29 | 1.09  | 0.28 | 1.39  | 0.29 | 1.25  | 0.20 | 1.15  | 0.15 | 6.7   |                                    |
|              | 1905                          | 131         | 6a               | 0.08   | 1.15  | 0.42 | 2.56  | 0.73 | 2.89  | 0.70 | 3.22  | 0.63 | 2.34  | 0.52 | 2.99  | 0.35 | 15.1  |                                    |
| GeoB 1008-3  | 13                            | 2           | 1                | 0.10   | 1.36  | 0.43 | 2.62  | 0.56 | 2.78  | 0.49 | 2.60  | 0.43 | 1.77  | 0.34 | 1.54  | 0.23 | 12.7  |                                    |
|              | 220                           | 19          | 2                | 0.19   | 3.85  | 1.18 | 8.18  | 1.78 | 9.46  | 1.59 | 8.66  | 1.49 | 6.89  | 1.44 | 8.41  | 0.65 | 45.5  |                                    |
|              | 820                           | 123         | 5e               | 0.08   | 1.54  | 0.52 | 3.28  | 0.67 | 3.13  | 0.51 | 3.03  | 0.45 | 1.95  | 0.29 | 1.18  | 0.21 | 14.1  |                                    |
|              | 881                           | 135         | 6a               | 0.12   | 1.75  | 0.81 | 5.83  | 1.19 | 5.75  | 0.93 | 4.72  | 0.71 | 3.02  | 0.53 | 2.84  | 0.22 | 23.9  |                                    |
| GeoB 1016 -3 | 4                             | 1           | 1                | 0.03   | 0.19  | 0.15 | 0.21  | 0.05 | 0.28  | 0.06 | 0.46  | 0.09 | 0.53  | 0.14 | 0.82  | 0.20 | 2.5   |                                    |
|              | 112                           | 18          | 2                | 0.12   | 1.22  | 0.45 | 1.88  | 0.50 | 2.22  | 0.46 | 2.50  | 0.46 | 2.06  | 0.43 | 3.17  | 0.26 | 13.0  |                                    |
|              | 603                           | 122         | 5e               | 0.02   | 0.37  | 0.08 | 0.44  | 0.11 | 0.56  | 0.09 | 0.60  | 0.12 | 0.60  | 0.08 | 0.51  | 0.06 | 3.1   |                                    |
|              | 643                           | 136         | 6a               | 0.08   | 1.00  | 0.32 | 1.26  | 0.33 | 1.53  | 0.32 | 2.11  | 0.36 | 1.60  | 0.35 | 3.29  | 0.24 | 10.8  |                                    |
| ODP 1079A    | 77                            | 3           | 1                | 0.47   | 6.74  | 1.72 | 11.07 | 2.32 | 14.87 | 2.47 | 22.22 | 2.98 | 19.00 | 2.45 | 19.08 | 1.21 | 93.0  |                                    |
|              | 757                           | 19          | 2                | 0.26   | 3.56  | 1.25 | 7.89  | 2.35 | 12.31 | 2.37 | 18.23 | 2.44 | 15.18 | 1.98 | 23.57 | 1.50 | 80.7  |                                    |
|              | 2943                          | 127         | 5e               | 0.50   | 8.96  | 2.46 | 22.37 | 4.23 | 31.06 | 4.36 | 36.07 | 5.04 | 29.56 | 3.89 | 28.98 | 2.17 | 157.0 |                                    |
|              | 3223                          | 137         | 6a               | 0.60   | 13.30 | 3.52 | 26.09 | 6.10 | 36.99 | 6.48 | 44.13 | 7.36 | 38.88 | 5.37 | 51.25 | 1.72 | 210.6 |                                    |
| GeoB 1028-5  | 20                            | 4           | 1                | 0.02   | 0.11  | 0.05 | 0.13  | 0.02 | 0.13  | 0.02 | 0.20  | 0.08 | 0.22  | 0.04 | 0.18  | 0.02 | 1.0   |                                    |
|              | 95                            | 20          | 2                | 0.01   | 0.08  | 0.04 | 0.17  | 0.04 | 0.26  | 0.03 | 0.23  | 0.03 | 0.18  | 0.04 | 0.17  | 0.03 | 1.1   |                                    |
|              | 394                           | 121         | 5e               | 0.05   | 0.06  | 0.05 | 0.06  | 0.02 | 0.08  | 0.02 | 0.09  | 0.01 | 0.07  | 0.01 | 0.09  | 0.03 | 0.5   |                                    |
|              | 454                           | 136         | 6a               | 0.01   | 0.03  | 0.01 | 0.02  | 0.01 | 0.04  | 0.02 | 0.05  | 0.02 | 0.06  | 0.01 | 0.04  | 0.01 | 0.2   |                                    |

cont. **Table 7.3.** *n*-Alkanol data of sediment samples studied.

| Site        | Depth<br>(cmcd <sup>a</sup> ) | Age<br>(ka) | MIS <sup>b</sup> | <i>n</i> -Alkanol mass accumulation rate <sup>c</sup> (µg cm <sup>-2</sup> kyr <sup>-1</sup> ) |       |      |       |      |       |      |       |      |      |      |      |      |                                    |
|-------------|-------------------------------|-------------|------------------|--|-------|------|-------|------|-------|------|-------|------|------|------|------|------|------------------------------------|
|             |                               |             |                  | 21   | 22    | 23   | 24    | 25   | 26    | 27   | 28    | 29   | 30   | 31   | 32   | 33   | TCEC <sub>22-32</sub> <sup>d</sup> |
| ODP 1082A   | 37                            | 4           | 1                | 0.12   | 1.11  | 0.26 | 1.48  | 0.29 | 2.34  | 0.32 | 3.02  | 0.34 | 2.49 | 0.26 | 1.94 | 0.20 | 12.4                               |
|             | 237                           | 21          | 2                | 0.10   | 1.20  | 0.30 | 2.65  | 0.41 | 2.96  | 0.33 | 2.71  | 0.37 | 1.50 | 0.17 | 1.38 | 0.07 | 12.4                               |
|             | 1286                          | 127         | 5e               | 0.14   | 1.49  | 0.42 | 2.31  | 0.53 | 2.70  | 0.32 | 2.47  | 0.25 | 1.49 | 0.10 | 1.08 | 0.34 | 11.5                               |
|             | 1376                          | 136         | 6a               | 0.18   | 2.08  | 0.47 | 3.38  | 0.52 | 3.00  | 0.31 | 2.23  | 0.39 | 1.14 | 0.11 | 1.22 | 0.47 | 13.0                               |
| GeoB 1710-3 | 3                             | 1           | 1                | 0.01   | 0.09  | 0.05 | 0.20  | 0.04 | 0.23  | 0.02 | 0.11  | 0.01 | 0.11 | 0.01 | 0.22 | 0.01 | 1.0                                |
|             | 95                            | 18          | 2                | 0.06   | 0.54  | 0.15 | 1.17  | 0.19 | 1.22  | 0.14 | 1.17  | 0.15 | 0.71 | 0.11 | 0.87 | 0.17 | 5.7                                |
|             | 609                           | 122         | 5e               | 0.01   | 0.11  | 0.04 | 0.12  | 0.03 | 0.17  | 0.03 | 0.20  | 0.03 | 0.21 | 0.02 | 0.17 | 0.01 | 1.0                                |
|             | 669                           | 136         | 6a               | 0.02   | 0.22  | 0.08 | 0.52  | 0.09 | 0.67  | 0.08 | 0.63  | 0.09 | 0.41 | 0.06 | 0.42 | 0.02 | 2.9                                |
| ODP 1084A   | 55                            | 5           | 1                | 0.30   | 3.38  | 0.86 | 5.29  | 0.69 | 5.59  | 0.57 | 5.20  | 0.63 | 4.07 | 0.59 | 3.78 | 0.33 | 27.3                               |
|             | 455                           | 26          | 2                | 0.34   | 5.12  | 1.16 | 10.65 | 1.71 | 8.88  | 0.87 | 7.17  | 0.89 | 4.61 | 0.33 | 2.15 | 0.56 | 38.6                               |
|             | 2633                          | 124         | 5e               | 1.74   | 11.20 | 1.74 | 8.09  | 1.13 | 7.77  | 0.96 | 5.69  | 0.91 | 2.61 | 0.31 | 2.77 | 0.73 | 38.1                               |
|             | 2949                          | 139         | 6a               | 0.91   | 11.21 | 1.98 | 14.82 | 2.33 | 14.81 | 2.00 | 12.03 | 2.66 | 7.92 | 0.93 | 8.65 | 0.39 | 69.4                               |
| GeoB 1722-1 | 8                             | 7           | 1                | 0.01   | 0.02  | 0.01 | 0.02  | 0.01 | 0.05  | 0.01 | 0.06  | 0.01 | 0.04 | 0.01 | 0.07 | 0.01 | 0.3                                |
|             | 24                            | 17          | 2                | 0.01   | 0.02  | 0.01 | 0.03  | 0.01 | 0.02  | 0.01 | 0.03  | 0.01 | 0.04 | 0.01 | 0.01 | -    | 0.1                                |
|             | 189                           | 123         | 5e               | 0.01   | 0.01  | 0.01 | 0.02  | -    | 0.02  | -    | 0.01  | -    | 0.01 | -    | 0.02 | -    | 0.1                                |
|             | 210                           | 1378        | 6a               | 0.01   | 0.03  | 0.01 | 0.04  | 0.01 | 0.10  | 0.01 | 0.11  | 0.01 | 0.08 | 0.02 | 0.10 | 0.02 | 0.5                                |

<sup>a</sup>cmcd: Centimetres composite depth<sup>b</sup>MIS: Marine isotopic stage<sup>c</sup>Numbers according to individual *n*-alkanol carbon numbers<sup>d</sup>TCEC<sub>22-32</sub>: Total content of odd-carbon-numbered *n*-C<sub>27</sub> to *n*-C<sub>35</sub> alkanols in µg cm<sup>-2</sup> kyr<sup>-1</sup>

## 7.2 Photographs



**Figure 7.1.** Woody terrace of the Cunene River. [photo: Paul de Wilt, Namibia, April 2005]



**Figure 7.2.** Savanna/dry forest at the Baobab corner in Kaokoland ( $18^{\circ}29'S$   $13^{\circ}46'E$ ). (left) Eugene Marais, National Museum of Namibia, and (right) Lydie Dupont, Geosciences, University of Bremen, Germany. [photo: Paul de Wilt, Namibia, April 2005]





**Figure 7.3.** Savanna at Omatjenni ( $20^{\circ}25'S$   $16^{\circ}19'E$ ). [photo: Paul de Wilt, Namibia, April 2005]



**Figure 7.4.** Kori Bustard in the mopane savanna of the Etosha National Park ( $18^{\circ}45'S$   $16^{\circ}56'E$ ). [photo: Paul de Wilt, Namibia, April 2005]





**Figure 7.5.** Dunes with *Stipagrostis sabulicola* (C<sub>4</sub> grass). Namib Desert near Sesriem (24°29'S 15°48'E). [photo: Paul de Wilt, Namibia, April 2005]

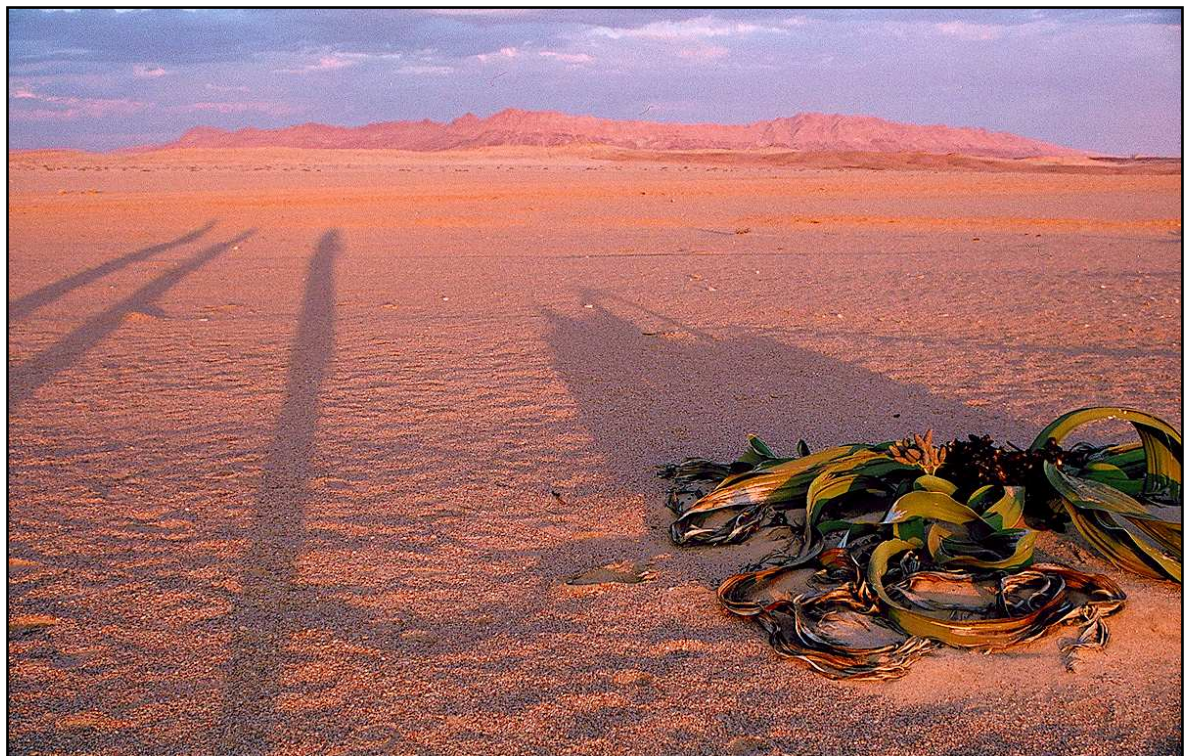


**Figure 7.6.** *Welwitschia mirabilis* in the Welwitschia Plain, Namib Desert (22°42'S 14°57'E). [photo: Paul de Wilt, Namibia, April 2005]





**Figure 7.7.** Namib Desert near Mirrabib (approx. 23°S 15°E). [photo: Paul de Wilt, Namibia, April 2005]



**Figure 7.8.** One of the very productive “Transect Crew” meetings at the Hanse-Wissenschaftskolleg in Delmenhorst (Germany; 29<sup>th</sup> April 2004). From left to right: Geoffrey Eglinton, Lydie Dupont, Jürgen Rullkötter and Florian Rommerskirchen.



# Acknowledgements (Danksagung)

Bei Herrn Prof. Dr. Jürgen Rullkötter möchte ich mich für die interessante, interdisziplinäre Themenstellung, das mir entgegengebrachte Vertrauen und die Unterstützung bedanken. Sein Verständnis und seine wertvolle Hilfe bei der Erstellung von Publikationen und Tagungsbeiträgen sowie Unterstützung bei der Anfertigung dieser Arbeit machten ihn zu einem wirklichen Doktorvater für mich. „Großvater“ bzw. „Großmutter“ dieser Doktorarbeit sind Prof. Geoffrey Eglinton (University of Bristol, UK) und Dr. Lydie Dupont (Universität Bremen), denen ich für den unerschöpflichen Ideenreichtum und ihre ständige Diskussionsbereitschaft ganz herzlich danken möchte. Insbesondere möchte ich Geoffrey für die Übernahme des Korreferates und Lydie für die Bereitstellung von Pflanzenproben und Fotos (fotografiert von Paul de Wilt) von einer Exkursion in Namibia (April 2005) danken.

*Many thanks for the inspiration and the endearing personality!*

Herrn Prof. Dr. Hans-Jürgen Brumsack danke ich ganz herzlich für die Übernahme des Korreferats. Außerdem gilt mein ganz besonderer Dank Dr. Robert W. Mayes (Macaulay Institute, Aberdeen, UK), Prof. Dr. Ernst-Detlef Schulze (Max-Planck-Institut für Biogeochemie, Jena), Dr. Albrecht Gerlach (Universität Oldenburg) und Andrea Gerecht (Universität Oldenburg), die für dieses Projekt Pflanzenproben bereitgestellt haben, und Anna Plader und Angela Vogts für die sehr gute Zusammenarbeit während der Anfertigung ihrer Diplomarbeiten in diesem Projekt.

Auf fachlicher Ebene bedanke ich mich bei

- Dr. Yoshito Chikaraishi (Japan Agency for Marine-Earth Science and Technology, Yokosuka, Japan) für sein Vertrauen bei der Bereitstellung von unveröffentlichten analytischen Daten,
  - Dr. Elizabeth Kellogg (University of Missouri-St. Louis, USA) für die fachliche Beratung in der Grasphylogenetik,
  - Dr. Hans-Peter Bäumer (Universität Oldenburg) für die Hilfe bei der Clusteranalyse,
  - Dr. Jérémy Jacob (Institut des Sciences de la Terre d'Orléans, France) für die Bereitstellung von pentazyklischen Triterpenoidether-Standards,
  - Dr. Maureen Conte (Woods Hole Oceanographic Institution, USA) für die Details der Harnstoffadduktion
- und bei
- Dr. Arnoud Boom (University of Leicester, UK),
  - Dr. Thomas Wagner (University of Newcastle-upon-Tyne),
  - Dr. Jens Holtvoeth (Woods Hole Oceanographic Institution, USA), und
  - Dr. Jung-Hyun Kim (Université de Perpignan, France) für ihre vielen Anregungen und wertvolle Diskussionen.

Des Weiteren möchte ich mich herzlich bei der AG Organische Geochemie bedanken für das persönliche Arbeitsumfeld und die vielen Aktivitäten außerhalb des Instituts. Besonders bedanken möchte ich mich bei Bernd Kopke, Barbara Scholz-Böttcher, Ralf Wöstmann und Jochen Maurer für die ausdauernde Unterstützung bei GC-MS- und GC-irm-MS-Analysen, Claus Köller für die Einweisungen und Hilfe bei der Auseinandersetzung mit der EDV, Gesine Schmidt, Matthias Macke, Andrea Gerecht, Mirja Bardenhagen, Sonja Scholz, Anke Schneider und Dirk Brouwer für die analytische Unterstützung, Annka Scherf für das Grasbestimmungsbuch und Almut Hetzel, Jörg Fichtel und Verena Reineke für das gute Klima im „angebauten Büro“. Ute Güntner danke ich für ihre wissenschaftliche „Vorarbeit“, durch die für mich ein Zugang zur Organischen Geochemie erleichtert wurde. Jürgen Köster, Ursel Gerken und Wiebke Hillebrecht danke ich für die Korrekturen.

Der Deutschen Forschungsgemeinschaft gilt mein Dank für die finanzielle Unterstützung im Rahmen des Ocean Drilling Program.

# Curriculum vitae (Lebenslauf)

**Name:** Florian Rommerskirchen  
**Geburtsdatum:** 30. Mai 1974  
**Geburtsort:** Nordenham  
**Staatsangehörigkeit:** deutsch  
**Familienstand:** ledig

## Schulbildung:

|           |  |
|-----------|--|
| 1980-1985 | Grundschule Süd, Nordenham                         |
| 1985-1987 | Orientierungsstufe Süd, Nordenham                  |
| 1987-1991 | Realschule der Zinzendorfschule in Tossens         |
| 1991-1994 | Gymnasium der Zinzendorfschule in Tossens (Abitur) |

## Berufsausbildung:

|                       |   |
|-----------------------|---|
| Jul. 1994 - Sep. 1995 | Zivildienst in der Jugendherberge Nordenham   |
| WS 1995/96 - SS 2001  | <p>Studium Diplom Chemie an der Carl von Ossietzky Universität Oldenburg:</p> <p>Vordiplom: 18. Dezember 1997</p> <p>Jan. - Sep. 2000 studentische Hilfskraft am Institut für Chemie und Biologie des Meeres (ICBM)</p> <p>Diplomarbeit (ICBM): „Verteilungsmuster und Kohlenstoff-isotopenzusammensetzung langkettiger <i>n</i>-Alkohole in Tiefseesedimenten des südwestafrikanischen Kontinentalrands“</p> <p>Diplom: 24. September 2001</p> |
| seit Okt. 2001        | wiss. Angestellter am ICBM, Carl von Ossietzky Universität Oldenburg  |

## **Erklärung**

Hiermit versichere ich, dass ich die vorliegende Arbeit selbständig angefertigt und keine anderen als die angegebenen Quellen und Hilfsmittel verwendet habe. Zusätzlich erkläre ich, dass diese Dissertation weder in ihrer Gesamtheit noch in Teilen einer anderen wissenschaftlichen Hochschule zur Begutachtung in einem Promotionsverfahren vorliegt oder vorgelegen hat.

Oldenburg, 21. Dezember 2005

(Florian Rommerskirchen)

## Parts of this thesis were presented at meetings and conferences:

(oral and poster presentations; presenter underlined)

Rommerskirchen, F., Wenzel, C., Rullkötter, J., 2002. Klimasignale in den Sedimenten des südwestafrikanischen Kontinentalrands (ODP Leg 175, Sites 1075A, 1079A und 1082A). DFG ICDP-ODP Colloquium (6<sup>th</sup> - 8<sup>th</sup> June), Potsdam, Germany. (poster)

Rommerskirchen, F., Eglinton, G., Dupont, L., Rullkötter, J., 2003. Land plant biomarkers as indicators of prevalent vegetation: A study of Holocene Southeast Atlantic continental margin sediments. DFG ICDP-ODP Colloquium (26<sup>th</sup> - 28<sup>th</sup> March), Mainz, Germany. (poster)

Rullkötter, J., Rommerskirchen, F., Eglinton, G., Dupont, L., 2003. Land plant biomarkers as indicators of prevalent vegetation: A study of Holocene Southeast Atlantic continental margin sediments. Organic Geochemistry Symposium (11<sup>th</sup> - 13<sup>th</sup> May), Stockholm, Sweden. (poster)

Rommerskirchen, F., Eglinton, G., Dupont, L., Rullkötter, J., 2003. Land plant biomarkers as indicators of prevalent vegetation: A study of Holocene Southeast Atlantic continental margin sediments. 18<sup>th</sup> Meeting of Sedimentologists 'Sediment 2003' (10<sup>th</sup> - 14<sup>th</sup> June), Wilhelmshaven, Germany. (poster)

Rommerskirchen, F., Eglinton, G., Dupont, L., Rullkötter, J., 2003. Land plant biomarkers as indicators of prevalent vegetation: A study of Holocene Southeast Atlantic continental margin sediments. 21<sup>th</sup> International Meeting on Organic Geochemistry (8<sup>th</sup> - 12<sup>th</sup> September), Krakow, Poland. (poster)

Rommerskirchen, F., Eglinton, G., Dupont, L., Rullkötter, J., 2004. Land plant biomarkers as indicators of prevalent vegetation: A study of Holocene Southeast Atlantic continental margin sediments. Lecture at the Max-Planck Institute of Biogeochemistry (26<sup>th</sup> February), Jena, Germany. (oral)

Rommerskirchen, F., Eglinton, G., Dupont, L., Rullkötter, J., 2004. Evidence of vegetation change due to glacial/interglacial changes: A study of land plant biomarker and pollen record in Southeast Atlantic continental margin sediments. IODP/ICDP Euroforum (17<sup>th</sup> - 19<sup>th</sup> March), Bremen, Germany. (poster)

Rommerskirchen, F., Eglinton, G., Dupont, L., Güntner, U., Wenzel, C., Rullkötter, J., 2004. A north to south transect of Holocene Southeast Atlantic continental margin sediments: Relationship between aerosol transport and compound-specific  $\delta^{13}\text{C}$  land plant biomarker and pollen records. IODP/ICDP Euroforum (17<sup>th</sup> - 19<sup>th</sup> March), Bremen, Germany. (poster)

Rommerskirchen, F., Eglinton, G., Dupont, L., Rullkötter, J., 2005. Marine sedimentary record of the phytogeographic competition of  $\text{C}_3$  and  $\text{C}_4$  plants due to climatic glacial/interglacial changes in Southern Africa. 1<sup>st</sup> Northern German Organic Geochemistry Workshop (17<sup>th</sup> June), Bremen, Germany. (oral)

## **The following parts of this thesis have been published or submitted for publication:**

### **Chapter 2**

Rommerskirchen, F., Plader, A., Eglinton, G., Chikaraishi, Y., Rullkötter, J., 2006. Chemotaxonomic significance of distribution and stable carbon isotopic composition of long-chain alkanes and alkan-1-ols in C<sub>4</sub> grass waxes. *Organic Geochemistry*, in press.

### **Chapter 3**

Rommerskirchen, F., Eglinton, G., Dupont, L., Güntner, U., Wenzel, C., Rullkötter J., 2003. A north to south transect of Holocene Southeast Atlantic continental margin sediments: Relationship between aerosol transport and compound-specific  $\delta^{13}\text{C}$  land plant biomarker and pollen records. *Geochemistry, Geophysics, Geosystems*, 4(12), 1101, doi: 10.1029/2003GC00541.

### **Chapter 4**

Rommerskirchen, F., Eglinton, G., Dupont, L., Rullkötter, J., 2005. Glacial/interglacial changes in Southern Africa: compound-specific  $\delta^{13}\text{C}$  land plant biomarker and pollen records from Southeast Atlantic continental margin sediments. *Geochemistry, Geophysics, Geosystems*, submitted.